
THE UNIVERSITY OF QUEENSLAND

# DIVISION OF CIVIL ENGINEERING

**REPORT CH59/06**

# AIR-WATER TIME AND LENGTH SCALES IN SKIMMING FLOWS ON A STEPPED SPILLWAY. APPLICATION TO THE SPRAY CHARACTERISATION

AUTHORS: Giovanna CAROSI and Hubert CHANSON

HYDRAULIC MODEL REPORTS

This report is published by the Division of Civil Engineering at the University of Queensland. Lists of recently-published titles of this series and of other publications are provided at the end of this report. Requests for copies of any of these documents should be addressed to the Civil Engineering Secretary.



Division of Civil Engineering
The University of Queensland
Brisbane QLD 4072
AUSTRALIA

Telephone: (61 7) 3365 3619
Fax: (61 7) 3365 4599

URL: http://www.eng.uq.edu.au/civil/

First published in 2006 by
Division of Civil Engineering
The University of Queensland, Brisbane QLD 4072, Australia



ISBN No. 1864998601

The University of Queensland, St Lucia QLD

# AIR-WATER TIME AND LENGTH SCALES IN SKIMMING FLOWS ON A STEPPED SPILLWAY. APPLICATION TO THE SPRAY CHARACTERISATION

by

Giovanna CAROSI

Visiting Research Fellow, Division of Civil Engineering, School of Engineering,

The University of Queensland, Brisbane QLD 4072, Australia

and

Hubert CHANSON

Reader, Division of Civil Engineering, School of Engineering,

The University of Queensland, Brisbane QLD 4072, Australia

Ph.: (61 7) 3365 3619, Fax: (61 7) 3365 4599, Email: h.chanson@uq.edu.au

Url: http://www.uq.edu.au/~e2hchans/

REPORT No. CH 59/06

ISBN 1864998601

Division of Civil Engineering, The University of Queensland

July 2006

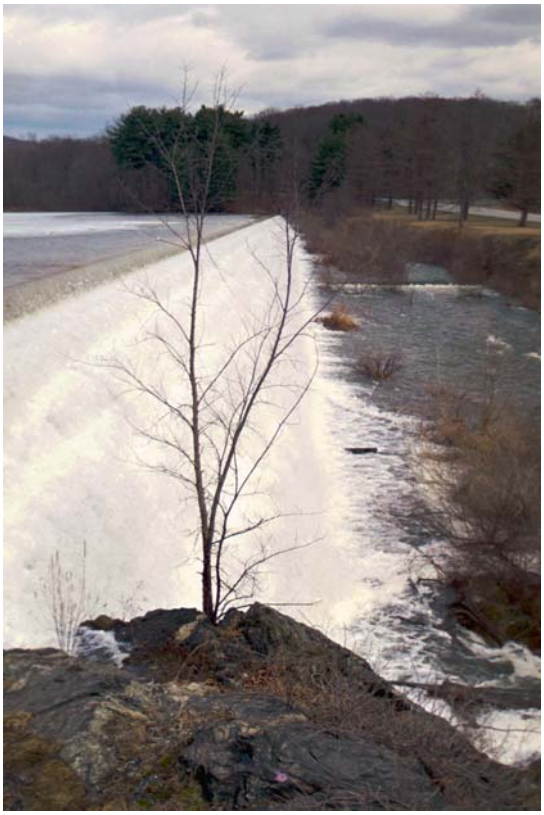

Skimming flow on Croton Falls stepped spillway in March 2001 (Courtesy of Mrs Jenny HACKER)

## ABSTRACT

Modern stepped spillways are typically designed for large discharge capacities corresponding to a skimming flow regime. Skimming flows are characterised by large amounts of entrained air and very-strong interactions between main stream turbulence, step cavity recirculation and free-surface. The present study is focused on new measurements of air-water turbulent time and length scales in air-water flow using several phase-detection intrusive probes. A new signal processing method and some correlation analyses were developed and applied.

The air water flow properties presented basic characteristics that were qualitatively and quantitatively comparable to previous studies in skimming flows. Some self-similarity was observed systematically at both macroscopic and microscopic levels. This included the distributions of void fraction, bubble count rate, interfacial velocity and turbulence level at a macroscopic scale, and the bubble/droplet chord distributions, and the auto- and cross-correlation functions at a microscopic level. Self-similarity is closely linked with dynamic similarity, and present results demonstrated a number of self-similar relationships that remain invariant under changes of scale which led in turn to remarkable application at prototype scales. The present findings are significant because they provide a picture general enough to be used as a first approximation to characterise the air-water flow field in similar stepped spillway structures.

The correlation analyses yielded a characterisation of the large eddies advecting the bubbles. The basic results included the transverse and streamwise integral turbulent length scales, the transverse and streamwise integral turbulent time scales, and the advection length scale. The turbulent length scales characterised a measure of the size of large vortical structures advecting air bubbles in the skimming flows. Both streamwise and transverse air-water length scales were closely related to the characteristic air-water depth $Y_{90}$ : i.e., $L_{xy}/Y_{90}$ = 0.05 to 0.2. The result was irrespective of the Reynolds numbers within the range of the experiments. Detailed measurements in the spray region highlighted the existence of an upper spray region for C > 0.95 to 0.97. In this upper spray, the distributions of droplet chord sizes and the distributions of advection length scales presented some marked difference with the rest of the flow. It is suggested that this highlighted a change in spray structure, where the upper spray region consisted primarily of ejected droplets interacting little with the rest of the flow until they re-attached.

Keywords : Air-water turbulent shear flow, Stepped spillways, Integral turbulence time scales, Integral turbulence length scales, Turbulent length and time scales, Spray, Physical modelling, Signal processing, Correlation analyses, Self-similarity, Phase-detection intrusive probes, Air bubble entrainment, Skimming flows, Bubble and droplet chord distributions.

**SCALA DELLE LUNGHEZZE E DEI TEMPI ARIA-ACQUA NELLE CORRENTI AREATE SU UNO SFIORATORE A GRADINI. UN'APPLICAZIONE PER LA CARATTERIZZAZIONE DELLO SPRAY**

*Sommario*

I moderni sfioratori a gradini sono tipicamente progettati per elevate portate corrispondenti ad un regime di corrente areata (skimming flow). In condizioni di skimming flow la corrente è caratterizzata da una grande quantità di aria e forti interazioni tra la turbolenza della corrente principale, le zone di ricircolo nella cavità del gradino e la superficie libera. I meccanismi di dissipazione di energia comprendono il ricircolo nelle cavità, lo scambio di quantità di moto e le interazioni tra la superficie libera e la turbolenza della corrente principale. Questo studio focalizza l'attenzione su nuove misurazioni delle scale delle lunghezze e dei tempi turbolenti nella corrente aria-acqua usando diverse sonde intrusive in grado di rilevare le due fasi. È stato inoltre sviluppato un nuovo metodo di elaborazione del segnale ed i dati sono stati analizzati attraverso il metodo della correlazione.

Le proprietà del fluido acqua-aria sia qualitativamente che quantitativamente hanno mostrato caratteristiche di base simili ai precedenti studi sulle correnti areate. Alcune auto-similitudini (self-similarity) sono state osservate sistematicamente a livello sia macroscopico che microscopico. A livello macroscopico si includono la distribuzione della frazione di vuoto, della frequenza di conteggio delle bolle, della velocità interfacciale e del livello di turbolenza; a livello microscopico la distribuzione della dimensione delle bolle/gocce, di auto-correlazione e correlazione. Le auto-similitudini sono strettamente legate alle analogie dinamiche ed i risultati hanno dimostrato che alcune rimangono invariate anche sotto i cambiamenti di scala. Questo può portare ad alcune interessanti osservazioni per le applicazioni alle scale dei prototipi. I risultati ottenuti sono inoltre significativi perché forniscono una rappresentazione sufficientemente generale per essere usata in prima approssimazione per caratterizzare la corrente aria-acqua nel campo delle strutture di sfioratori a gradini. Le analisi dei dati effettuati attraverso il metodo della correlazione, hanno fornito una caratterizzazione dei grandi vortici che trasportano per avvezione le bolle. I risultati di base comprendono le scale delle lunghezze integrali in direzione longitudinale e trasversale, le scale dei tempi integrali in direzione longitudinale e trasversale e la scala delle lunghezze di Taylor. La scala delle lunghezze turbolente è una misura della dimensione delle grandi strutture vorticose che trasportano per avvezione le bolle nella corrente areata. La scala delle lunghezze in direzione trasversale e longitudinale è strettamente legata alla profondità caratteristica dell'acqua-aria, $Y_{90}$: per esempio $L_{xy}/Y_{90}$ = 0.1 a 0.2. Il risultato non è funzione del numero di Reynolds nella gamma degli esperimenti eseguiti. Le misurazioni dettagliate effettuate nella regione dello spray, hanno messo in luce l'esistenza di una regione superiore per valori dell'indice dei vuoti maggiori di 0.95-0.97. Nella regione superiore dello spray, le distribuzioni delle dimensioni delle gocce e delle scale integrali di Taylor hanno mostrato alcune differenze rispetto al resto della corrente. Questo fa ritenere che vi sia un cambiamento nella struttura dello spray, dove la zona superiore consiste fondamentalmente in gocce che poco interagiscono con la corrente dalla quale fuoriescono, fino a che non vi rientrano.

Parole chiave: ingresso di bolle d’aria, corrente areata, sfioratori a gradini, scala integrale dei tempi, scala integrale delle lunghezze, scala dei tempi e delle lunghezze turbolente, spray, modelli fisici, elaborazione del segnale, correlazioni, corrente aria-acqua tangenziale turbolenta, auto-similitudini, sonde intrusive rivelatrici di fase, distribuzione della dimensione delle bolle e delle gocce.

## TABLE OF CONTENTS

## NOTATION

The following symbols are used in this report :

| | |
|---|---|
| $A_w$ | water flow cross-section area ($m^2$); |
| a | constant; |
| b | constant; |
| C | void fraction defined as the volume of air per unit volume of air and water; it is also called air concentration or local air content; |
| c | instantaneous void fraction; c = 0 or 1; |
| $C_{mean}$ | depth-average void fraction defined in terms of $Y_{90}$ : $C_{mean} = 1 - d/Y_{90}$; |
| ch | chord size (m); |
| $D_H$ | hydraulic diameter (m) also called equivalent pipe diameter; |
| $D_t$ | turbulent diffusivity ($m^2/s$) of air bubbles in air-water flow; |
| $D_o$ | dimensionless constant |
| D' | dimensionless air bubble diffusivity; |
| d | equivalent clear water flow depth defined as: $d = \int_{C=0}^{C=0.90} (1 - C) * dy$ ; |
| $d_{ab}$ | air bubble size (m); |
| $d_c$ | critical flow depth (m); |
| F | air bubble count rate (Hz) or bubble frequency defined as the number of detected air bubbles per unit time; |
| $F_{max}$ | maximum bubble count rate (Hz) at a given cross-section; |
| Fr | Froude number; |
| $F_{scan}$ | scanning frequency (Hz) or scan rate; |
| $F_*$ | Froude number defined in terms of the step height : $F_* = \frac{q_w}{\sqrt{g * \sin\theta * (h * \cos\theta)^3}}$ |
| f | Darcy-Weisbach friction factor; |
| $f_d$ | equivalent Darcy-Weisbach friction factor of form drag process; |
| $f_e$ | equivalent Darcy-Weisbach friction factor in air-water skimming flows; |
| g | gravity constant: g = 9.80 $m/s^2$ in Brisbane, Australia; |
| H | total head (m); |
| $H_{max}$ | maximum upstream head (m) above chute toe; |
| $H_{res}$ | residual head (m); |
| $H_1$ | upstream head (m) above weir crest; |
| h | vertical step height (m); |
| K | inverse of the dimensionless expansion rate of a developing shear layer; |
| K' | dimensionless integration constant; |
| $K^*$ | dimensionless constant; |
| $k_s$ | step cavity roughness height (m) : $k_s = h*\cos\theta$; |

$k_s'$ step surface equivalent sand roughness height (m);

L length (m);

**L** turbulent length scale (m);

$L_I$ longitudinal distance (m) measured from the weir crest where the inception of free-surface aeration takes place;

$L_r$ geometric scaling ratio defined as the prototype to model dimensions: e.g., $L_r = 2$ when the model is half the prototype size;

$L_{xx}$ air-water advection integral length scale (m) :

$$L_{xx} = V * T_{xx}$$

$L_{xy}$ transverse/streamwise air-water integral turbulent length scale (m) :

$$L_{xy} = \int_{Y=0}^{Y_{max}} (R_{xy})_{max} * dY$$

$(L_{xx})_{max}$ maximum advection air-water length scale (m) in a cross-section;

$(L_{xy})_{max}$ maximum transverse/streamwise air-water integral turbulent length scale (m) in a cross-section;

l horizontal step length (m);

Mo Morton number defined as : $Mo = g*\mu_w^4/(\rho_w*\sigma^3)$;

N power law exponent;

$N_{ab}$ number of air bubbles per record;

$P_w$ wetter perimeter (m);

$Q_w$ water discharge ($m^3/s$);

$q_w$ water discharge per unit width ($m^2/s$);

Re Reynolds number defined in terms of the hydraulic diameter;

$R_{xx}$ normalised auto-correlation function (reference probe);

$R_{xy}$ normalised cross-correlation function between two probe output signals;

$(R_{xy})_{max}$ maximum cross-correlation between two probe output signals;

T time lag (s) for which $R_{xy} = (R_{xy})_{max}$;

**T** turbulent time scale (m);

**T** integral turbulent time scale (s) characterising the large eddies advecting the air bubbles;

Tu turbulence intensity defined as: $Tu = u'/V$;

$T_{scan}$ scan duration (Hz) or sampling period;

$T_{xx}$ auto-correlation time scale (s) :

$$T_{xx} = \int_{\tau=0}^{\tau=\tau(R_{xx}=0)} R_{xx}(\tau) * d\tau$$

$T_{xy}$ cross-correlation time scale (s) :

$$T_{xy} = \int_{\tau=\tau(R_{xy}=(R_{xy})_{max})}^{\tau=\tau(R_{xy}=0)} R_{xy}(\tau) * d\tau$$

$T_{0.5}$ characteristic time lag $\tau$ for which $R_{xx} = 0.5$;

$\mathbf{T}_{max}$ maximum integral time scale (s) in a cross-section;

| | |
|---|---|
| $t$ | time (s); |
| $t_{ch}$ | chord time (s); |
| $U_w$ | flow velocity (m/s) : $U_w = q_w/d$; |
| $u'$ | root mean square of longitudinal component of turbulent velocity (m/s); |
| $V$ | interfacial velocity (m/s); |
| $V_c$ | critical flow velocity (m/s); |
| $W$ | channel width (m); |
| $x$ | distance along the channel bottom (m); |
| $Y$ | separation distance (m) between two phase-detection probe sensors; |
| $Y_{90}$ | characteristic depth (m) where the void fraction is 90%; |
| $y$ | distance (m) measured normal to the invert (or channel bed); |
| $y'$ | dimensionless distance (m) normal to the invert (or channel bed) : $y' = y/Y_{90}$; |
| $z$ | transverse distance (m) from the channel centreline; |
| $\Delta x$ | streamwise separation distance (m) between sensor; |
| $\Delta z$ | transverse separation distance (m) between sensor; |
| $\mu$ | dynamic viscosity (Pa.s); |
| $\mu_w$ | water dynamic viscosity (Pa.s); |
| $\theta$ | angle between the pseudo-bottom formed by the step edges and the horizontal; |
| $\rho$ | density (kg/m$^3$); |
| $\rho_w$ | water density (kg/m$^3$); |
| $\sigma$ | surface tension between air and water (N/m); |
| $\tau$ | time lag (s); |
| $\tau_{0.5}$ | characteristic time lag $\tau$ for which $R_{xy} = 0.5 * (R_{xy})_{max}$; |
| $\varnothing$ | - diameter (m); |
| | - probe sensor size (m); |

*Subscript*

| | |
|---|---|
| air | air flow; |
| c | critical flow conditions; |
| w | water flow; |
| xx | auto-correlation of reference probe signal; |
| xy | cross-correlation; |
| 90 | flow conditions where C = 0.90; |

*Abbreviations*

| | |
|---|---|
| F/D | fully-developed inflow conditions; |
| P/D | partially-developed inflow conditions; |
| Std | standard deviation. |

# 1. INTRODUCTION

## 1.1 Presentation

Stepped spillways have been used for many centuries (Fig. 1-1). The stepped design increases the rate of energy dissipation on the chute and reduces the size of the downstream energy dissipation system. For the last ten years, the research in the hydraulics of stepped spillways has been active (CHANSON 1995a, 2001a). On a stepped spillway, the waters flow as a succession of free-falling nappes (nappe flow regime) at small discharges (CHAMANI and RAJARATNAM 1994, CHANSON 1994a, TOOMBES 2002, EL-KAMASH et al. 2005). For a range of intermediate flow rates, a transition flow regime is observed (CHANSON 2001b, CHANSON and TOOMBES 2004). Modern stepped spillways are typically designed for large discharge capacities corresponding to a skimming flow regime (RAJARATNAM 1990, CHANSON 1994b, CHAMANI and RAJARATNAM 1999). In a skimming flow, the flow is non-aerated at the upstream end of the chute. Free-surface aeration occurs when the turbulent shear next to the free-surface becomes larger than the bubble resistance offered by surface tension and buoyancy. Downstream of the inception point of free-surface aeration, some strong air-water mixing takes place (Fig. 1-1A). Large amounts of air are entrained, and very-strong interactions between main stream turbulence, step cavity recirculation zones and free-surface are observed (e.g. CHANSON and TOOMBES 2003, GONZALEZ 2005, GONZALEZ et al. 2005).

The flow resistance is primarily a form drag in skimming flows. At each step, the cavity flow is driven by the developing shear layer and the transfer of momentum across it (Fig. 1-2) (GONZALEZ and CHANSON 2004). The energy dissipation mechanisms include cavity recirculation, momentum exchange with the free stream, and interactions between free-surface and mainstream turbulence. The interactions between mixing layer and horizontal step face, and the skin friction at the step faces may contribute to further energy dissipation, in particular on moderate slopes. At each step edge, highly coherent small-scale vortices are formed abruptly at the step corner because of the large gradient of vorticity at the corner (Fig. 1-2). The initial region of the mixing layer is dominated by a train of sequential small-scale vortices which eventually pair to form large scale vortical structures that are advected downstream. It is argued that the distance from the step edge to the impingement of the shear layer onto the step face is an important length because some feedback might occur nearly instantaneously from the impingement to the singularity region of the shear layer in the vicinity of the step edge (e.g. LIN and ROCKWELL 2001). Experimental studies of turbulent flows past two-dimensional cavities showed that cavity resonance is primarily a function of the ratio of boundary layer thickness to cavity length. That is, $Y_{90}*\sin\theta/h$ for a stepped chute where $Y_{90}$ is the characteristic air-water depth where the void fraction is 90%, h is the vertical step height, $\theta$ is the slope between the pseudo-bottom formed by the step edges and the horizontal. OHTSU et al. (2004) showed that the flow resistance appeared to be maximum for a slope $\theta$ of around 18° to 22°. GONZALEZ and CHANSON (2006) hypothesised that some maximum in flow resistance must be related to some flow instability. The three dimensional nature of recirculating vortices is believed to play a role to further the rate of energy dissipation (ANDRE et al. 2004, CHANSON and GONZALEZ 2004). GONZALEZ (2005) demonstrated quantitatively the means to enhance the flow resistance with turbulence manipulation.

Fig. 1-1 - Photographs of stepped spillways

(A) Skimming flow on Camp Dyer diversion dam spillway (Courtesy of John LABOON and US Bureau of Reclamation) - The clear-water flow at the upstream end and the inception point of free-surface aeration are clearly seen

(B) Croton Falls stepped spillway in operation in March 2001 (Courtesy of Mrs Jenny HACKER) - Completed in 1911, the spillway is equipped with 0.61 m high rounded steps (WEGMANN 1911, CHANSON 1995a)

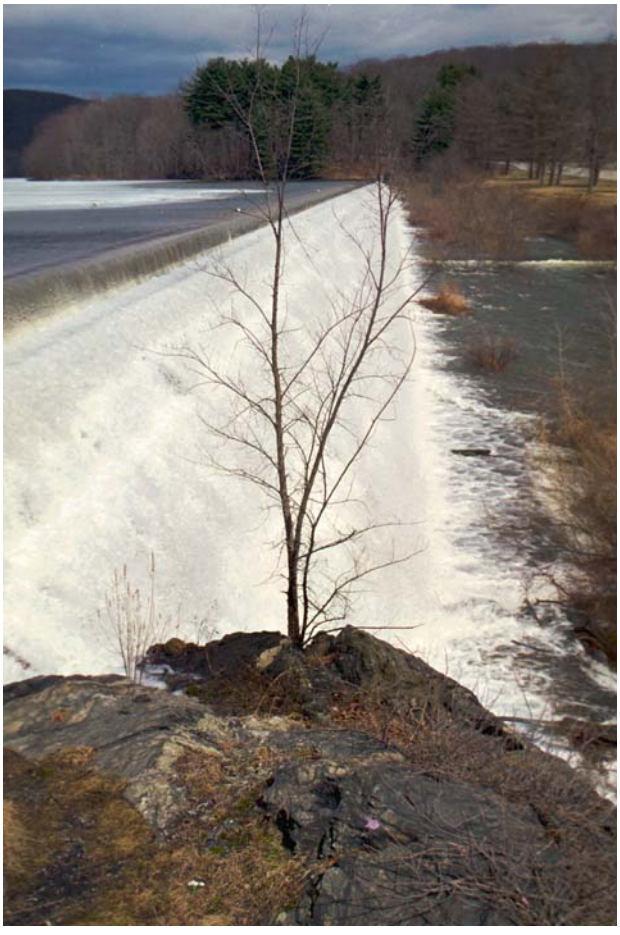

Fig. 1-2 - Cavity recirculation in skimming flow

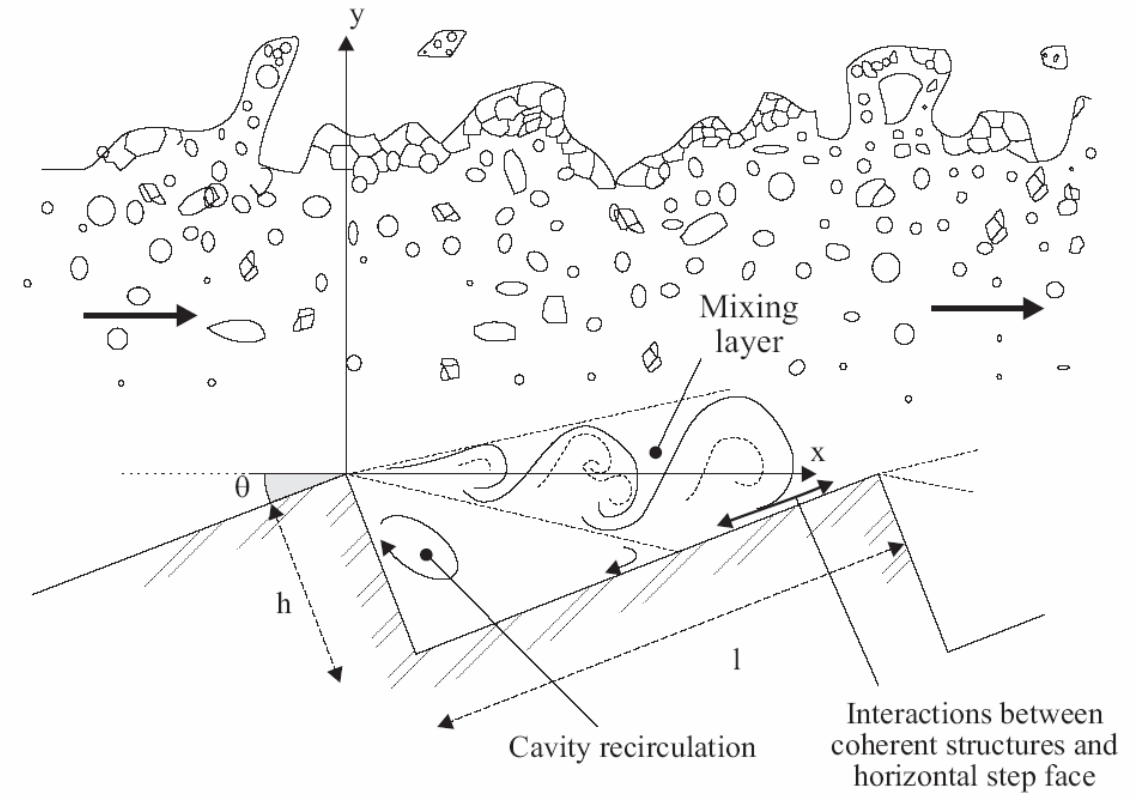


It is the purpose of this study to investigate thoroughly the air-water turbulent time and length scales in skimming flows, with a focus on the spray region and its specific features. New measurements were conducted in a large-size facility ($\theta$ = 22º, h = 0.1 m) with several phase-detection intrusive probes. An advanced signal processing method was developed and some new correlation analyses were conducted. Detailed air-water flow properties were recorded systematically for several flow rates. The results provide a new understanding of the turbulence structure, the spray properties and the energy dissipation mechanisms. In the next paragraphs (1.2 and 1.3), the turbulence and spray generation in skimming flows are reviewed. The Section 2 develops a basic dimensional analysis. Section 3 describes the experimental setup and instrumentation. The experimental results are presented in Sections 4, 5 and 6, and they are discussed in Section 7. The full experimental data sets are presented in Appendices D, E and F.

## 1.2 Skimming flow turbulence

In skimming flows, the turbulence levels are markedly higher than in monophase flows on a smooth invert (e.g. OHTSU and YASUDA 1997, CHANSON and TOOMBES 2002a, AMADOR et al. 2004a). OHTSU and YASUDA (1997) and AMADOR et al. (2004a,b) measured turbulence intensities upstream of the inception point of air entrainment. OHTSU and YASUDA observed turbulence levels of about 15-25%, while AMADOR et al. obtained turbulence intensities between 20 to 100%. Downstream of the inception point of air entrainment, experimental results showed further enhanced turbulence levels for $0.1 < C < 0.9$ with turbulence intensities between 50 to 150% where C is the void fraction (e.g. CHANSON and TOOMBES 2002a, GONZALEZ 2005, GONZALEZ et al. 2005).

In a skimming flow, the high turbulence levels are generated by the form drag at each step. The resulting turbulent fluctuations acting next to the free surface contribute to a drastic air entrapment, advective dispersion and spray generation. At the "pseudo-free-surface", air is continuously entrained and released. Interfacial aeration involves both entrainment of air bubbles and formation of water droplets, and the exact location of the "pseudo-free-surface" becomes undetermined (Fig. 1-3). For $0.05 < C < 0.95$, the air-water flow structure is dominated by collisions between particles (bubbles, droplets, packets) and by interactions between particles and turbulence. Such dynamic processes are associated with continuous bubble/droplet break-up, coalescence and interfacial deformations, all of which contribute to large fluctuations in air-water interfacial velocities and high levels of turbulence.

## 1.3 Air-water exchanges and spray generation

In the spray region, the drop formation results from some surface distortion, tip-streaming of ligaments and interactions between eddies and free-surface (e.g. HOYT and TAYLOR 1977, REIN 1998). The formation and ejection of a water droplet must be associated with a transfer of turbulent kinetic energy from the main flow. Figure 1-3 shows some high-speed photographs of spray droplets viewed from upstream. Once a droplet is ejected, the history/memory of its ejection process has a dominant effect because the droplet response time is nearly two orders of magnitude larger than the air flow response time. The energy of each droplet is a combination of its potential and kinetic energies, although NIELSEN (2004, *Pers. Comm.*) suggested that surface tension effects could increase the pressure work.

Today the study of spray and splashing remains limited in high-velocity water flows. Some researchers used visual techniques ([1]), while others used intrusive phase detection probes ([2]). Some studies suggested that the spray region, defined as $C > 0.7$, may be sub-divided into several sub-zones (TOOMBES 2002, CHANSON and GONZALEZ 2004). Despite limited data sets, most studies ([3]) showed a wide range of droplet chord lengths at each sampling location. The chord length distributions were skewed with a preponderance of small chord sizes relative to the mean, with decreasing numbers of droplets and decreasing droplet sizes with increasing heights y and decreasing liquid fractions (1-C).

[1]Experimental techniques included photography (HOYT and TAYLOR 1976,1977), infra-red sensors (AUGIER 1996, KADEM 2005) and video-observations (WU and FAETH 1995, WU et al. 1995).

[2]For example, CHANSON (1999b), TOOMBES (2002), HONG et al. (2004).

[3]These data sets included CHANSON (1999b), TOOMBES (2002), CHANSON and GONZALEZ (2004), GONZALEZ (2005), GONZALEZ et al. (2005) in supercritical open channel flows, HONG et al. (2004) in high-velocity water jets and CHANSON (2006a) in hydraulic jumps.

Fig. 1-3 - High-speed photographs of water droplet ejections and spray above a skimming flow on a stepped chute (h = 0.1 m, l = 0.25 m) - Looking downstream from the weir crest - Most droplets were about 0.20 to 0.3 m above the pseudo-bottom formed by the step edges

(A) $d_c/h$ = 1.33, Re = 5.7 E+5, shutter speed: 1/320 s, probe located at step edge 7

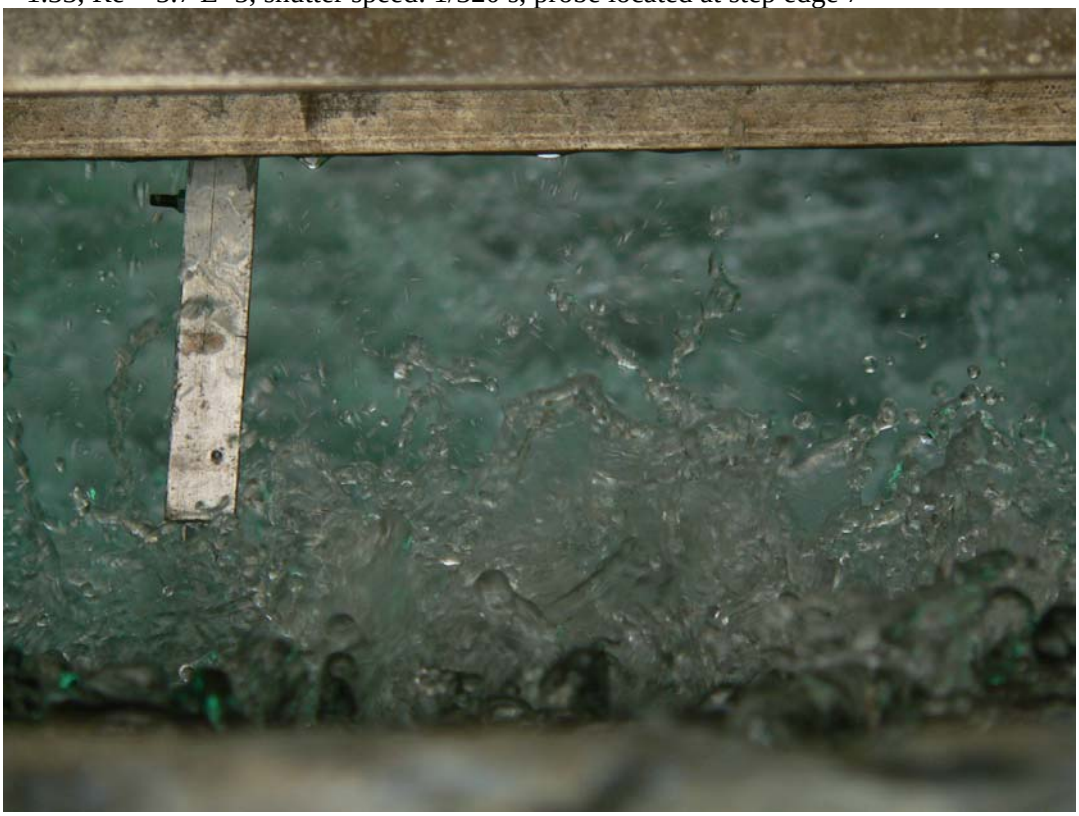

(B) $d_c/h$ = 1.57, Re = 7.1 E+5, shutter speed: 1/320 s, probe located at step edge 7

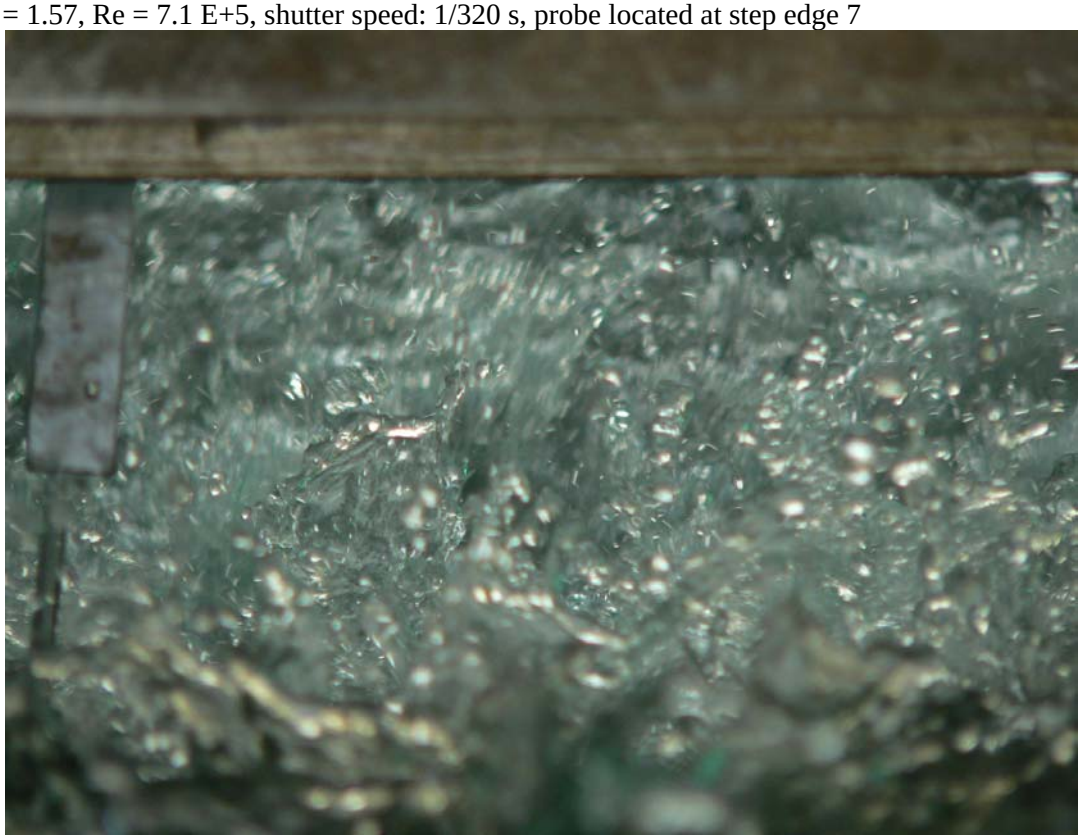

## 2. DIMENSIONAL ANALYSIS AND SIMILITUDE

### 2.1 Basic considerations

A key feature of skimming flow on a stepped chute is the strong free-surface aeration and air-water flow turbulence (Fig. 1-1 and 1-3). Physical modelling and experimental investigations may be performed if a suitable dynamic similarity is achievable (Table 2-1). With geometrically similar models, the geometric scaling ratio $L_r$ is defined as the ratio of prototype to model dimensions.

In a dimensional analysis, the relevant parameters include the fluid properties and physical constants, the chute geometry and inflow conditions, the air-water flow properties and the geometry of the steps. Considering a skimming flow at uniform equilibrium down a stepped chute with flat horizontal steps and for a prismatic rectangular channel. At uniform equilibrium, the gravity force component in the flow direction counteracts exactly the flow resistance. A complete dimensional analysis yields a relationship between the local air-water flow properties, and the fluid properties, physical constants, flow conditions and step geometry :

$$C, \frac{V}{\sqrt{g * h}}, \frac{u'}{V}, \mathbf{T} * \sqrt{\frac{g}{h}}, \frac{\mathbf{L}}{h}, \frac{d_{ab}}{h}, ... = F_1\left(\frac{x}{h}; \frac{y}{h}; \frac{q_w}{\sqrt{g * h^3}}; \rho_w * \frac{q_w}{\mu_w}; \frac{g * \mu_w^4}{\rho_w * \sigma^3}; \frac{W}{h}; \theta; \frac{k_s'}{h}; ...\right) \quad (2\text{-}1)$$

where C is the local void fraction, V is the local velocity, g is the gravity acceleration, d is the equivalent water depth at uniform equilibrium, u' is a characteristic turbulent velocity, $\mathbf{T}$ is a turbulent time scale, $\mathbf{L}$ is a turbulent length scale, $d_{ab}$ is a characteristic size of entrained bubble, x is the coordinate in the flow direction measured from the step edge, y is the distance normal from the pseudo-bottom formed by the step edges, $q_w$ is the water discharge per unit width, $\rho_w$ and $\mu_w$ are the water density and dynamic viscosity respectively, $\sigma$ is the surface tension between air and water, W is the chute width, h is the step height, $\theta$ is the angle between the pseudo-bottom and the horizontal, and $k_s'$ is the skin roughness height (Fig. 1-2). In the left handside of Equation (2-1), the 3rd, 4th and 5th terms are dimensionless turbulence properties. In the right handside, the 3rd, 4th and 5th dimensionless terms are the Froude, Reynolds and Morton numbers respectively, and the last three terms characterise the step cavity shape and the skin friction effects on the cavity wall.

Note that any combination of dimensionless numbers may replace one of these dimensionless numbers. For example, one parameter among the Froude, Reynolds and Weber numbers may be replaced by the Morton number $Mo = (g*\mu_w^4)/(\rho_w*\sigma^3)$ as seen in Equation (2-1) where the Weber number was replaced by the Morton number.

Lastly a characteristic water depth in air-water flows is the equivalent clear water depth which may be deduced from the void fraction distribution :

$$d = \int_{y=0}^{y=Y_{90}} (1 - C) * dy \quad (2\text{-}2)$$

where $Y_{90}$ is the depth where C = 0.9.

## 2.2 Discussion

In free-surface flows, laboratory studies are typically based upon an undistorted Froude similitude (e.g. HENDERSON 1966, CHANSON 2004a). The same applies to stepped spillway studies (e.g. BOES 2000b, CHANSON 2004b, CHANSON and GONZALEZ 2005, GONZALEZ et al. 2005). However cavity recirculation and momentum exchanges between the cavity and stream flows are dominated by viscous effects. At the same time, the entrapment/detrainment of air bubbles and the mechanisms of air bubble breakup and coalescence are dominated by surface tension effects. With some assumptions, Equation (2-1) shows that a dynamic similarity of skimming flow on stepped spillway is impossible to achieve using geometrically similar models unless working at full-scale. In small size models ($L_r >> 1$), the air entrainment process is adversely affected by significant scale effects (KOBUS 1984, WOOD 1991, CHANSON 1997a).

In the present study, the same fluids (air and water) were used in model and prototype, and the Morton number becomes an invariant. Similarly, the chute slope θ, the step height h, the channel width W and the step roughness $k_s'$ were constant. For a Froude similitude, Equation (2-1) may be rewritten :

$$C \text{ , } \frac{V}{\sqrt{g * d_c}} \text{ , } \frac{u'}{V} \text{ , } \mathbf{T} * \sqrt{\frac{g}{d_c}} \text{ , } \frac{\mathbf{L}}{d_c} \text{ , } \frac{d_{ab}}{d_c} \text{ , ... } = F_2\left(\frac{x}{d_c}; \frac{y}{d_c}; \frac{d_c}{h}; Re\right) \quad (2\text{-}3)$$

where $d_c$ is the critical depth ($d_c = \sqrt[3]{q_w^2/g}$) and Re is the Reynolds number defined in terms of the equivalent pipe diameter $D_H$ ($Re = \rho_w * V * D_H / \mu_w$). Equation (2-3) gives a dimensionless expression of the local air-water turbulent flow properties as functions of independent parameters that include both Froude and Reynolds numbers.

The validity of the Froude similitude itself was rarely tested in stepped chutes but in a few studies (see review by CHANSON and GONZALEZ 2005). Recently, detailed studies of local air-water flow properties yielded stringent conditions to minimise scale effects suggesting the impossibility to achieve true dynamic similarity even in large-size models (BOES 2000b, GONZALEZ and CHANSON 2004, CHANSON and GONZALEZ 2005, TAKAHASHI et al. 2005). In the present study, a Froude similitude was used as for most open channel flow studies. The experiments were conducted in a large size facility operating at large Reynolds numbers. These conditions may be representative of a full-scale storm waterway.

Table 2-1 - Experimental investigations of stepped chute flows on flat slopes ($\theta < 30^o$)

| Reference | $\theta$ deg. | Step geometry | Flow conditions | Instrumentation | Remarks |
|---|---|---|---|---|---|
| (1) | (2) | (3) | (4) | (5) | (6) |
| CHANSON and TOOMBES (2001,2002c) | 22 | Smooth horizontal steps (h = 0.1 m, l = 0.25 m). | | | W = 1 m. $k_s'$ = 0.5 mm. |
| Series 1 | | | $q_w$ = 0.046 to 0.182 $m^2/s$, Re = 1.8 to 7.3 E+5. | Single-tip conductivity probe (Ø = 0.35 mm). | Experiments EV200. |
| Series 2 | | | $q_w$ = 0.058 to 0.182 $m^2/s$, Re = 2.3 to 7.3 E+5. | Double-tip conductivity probe (Ø = 0.025 mm). | Experiments TC200. |
| CHANSON and TOOMBES (2002a) | | | | | |
| Series 1 | 16 | Smooth horizontal steps (h = 0.1 m, l = 0.25 m). | | | W = 1 m. $k_s'$ = 0.5 mm. |
| Series 2 | 22 | Smooth horizontal steps (h = 0.1 m, l = 0.35 m). | | | W = 1 m. $k_s'$ = 0.5 mm. |
| CHANSON and TOOMBES (2002b) | | | | Single-tip conductivity probe (Ø = 0.35 mm). | W = 0.5 m, $k_s'$ = 0.5 mm. |
| Series 1 | 3.4 | Smooth horizontal steps (h = 0.143 m, l = 2.4 m). | | | L = 24 m, 10 steps. |
| series 2 | 3.4 | Smooth horizontal steps (h = 0.0715 m, l = 1.2 m). | | | L = 24 m, 180 steps. |
| TOOMBES (2002) | | Smooth horizontal steps (h = 0.143 m, l = 2.4 m). | | | $k_s'$ = 0.5 mm. |
| Stepped cascade | 3.4 | L = 24 m, 10 steps | | Single-tip conductivity probe (Ø = 0.35 mm). | W = 0.5 m. |
| Single-step | 3.4 | L = 3.2 m, 1 step | | Double-tip conductivity probe (Ø = 0.025 mm). | W = 0.25 m. |
| YASUDA and CHANSON (2003) | 16 | Smooth horizontal steps (h = 0.05 m). | $q_w$ = 0.0776 $m^2/s$ Re = 3.1 E+5 | Double-tip conductivity probe (Ø = 0.025 mm) | W = 0.5 m. $k_s'$ = 0.5 mm. |
| OHTSU et al. (2004) | 5.7, 8.5, 11.3, 19, 23, 30 | h = 0.006 to 0.05 m | $q_w$ = 0.02 to 0.08 $m^2/s$, Re = 8 E+4 to 3.2 E+5. | Single-tip conductivity probe (Ø = 0.1 mm). | W = 0.4 m. |
| GONZALEZ (2005) | | | | Double-tip conductivity probe (Ø = 0.025 mm). | W = 1 m. $k_s'$ = 0.5 mm. |
| | 16 | Smooth horizontal steps (h = 0.05 m, l = 0.175 m). | | | |
| | 16 | Smooth horizontal steps (h = 0.1 m, l = 0.35 m). | | | |
| | 22 | Smooth horizontal steps (h = 0.1 m, l = 0.25 m). | | | Turbulence manipulation with triangular vanes. |
| GONZALEZ et al. (2005) | 22 | Horizontal steps (h = 0.1 m, l = 0.25 m). | $q_w$ = 0.01 to 0.219 $m^2/s$, Re = 4 E+4 to 9 E+5. | Double-tip conductivity probe (Ø = 0.025 mm). | Experiments CMH_05. W = 1 m. |
| Configuration A | 22 | Rough step faces: 8-mm thick screens on both vertical and horizontal step faces | | | k = 8 mm ($k_s'$ ≈ 6.6 mm). |
| Configuration B | 22 | 8-mm thick screens on each vertical step face | | | k = 8 mm ($k_s'$ ≈ 6.6 mm). |
| Configuration C | 22 | 8-mm thick screens on each horizontal step face | | | k = 8 mm ($k_s'$ ≈ 6.6 mm). |
| Configuration S (smooth steps) | 22 | Smooth horizontal steps | | | $k_s'$ = 0.5 mm. |

| Reference | $\theta$ deg. | Step geometry | Flow conditions | Instrumentation | Remarks |
|---|---|---|---|---|---|
| (1) | (2) | (3) | (4) | (5) | (6) |
| MURILLO (2006) | | Smooth horizontal steps (h = 0.15 m) | | Conical hot-film probe (Dantec 55R42) | W = 0.4 m, $k_S'$ = 0.5 mm. |
| Model I | 16 | h = 0.15 m, l = 0.525 m | $q_W$ = 0.06 to 0.13 $m^2/s$, Re = 2.4 E+5 to 5.5 E+5. | | |
| Model II | 11.3 | h = 0.15 m, l = 0.75 | $q_W$ = 0.06 to 0.14 $m^2/s$, Re = 2.4 E+5 to 5.8 E+5. | | |
| Model III | 5.7 | h = 0.15 m, l = 1.5 m | $q_W$ = 0.06 to 0.15 $m^2/s$, Re = 2.4 E+5 to 6.2 E+5. | | |
| Present study | 22 | Smooth horizontal steps (h = 0.1 m, l = 0.25 m). | | | Experiments GH_06. W = 1 m. $k_S'$ = 0.5 mm. |
| Series 1 | 22 | | $q_W$ = 0.095 to 0.18 $m^2/s$, Re = 3.8 E+5 to 7.1 E+5 | Single-tip conductivity probes (Ø = 0.35 mm) | |
| Series 2 | 22 | | $q_W$ = 0.12 to 0.16 $m^2/s$, Re = 4.6 E+5 to 6.4 E+5 | Double-tip conductivity probes (Ø = 0.25 mm) | |

Notes : $k_S'$ : step surface roughness height; Re : flow Reynolds number defined in terms of hydraulic diameter.

## 3. EXPERIMENTAL CHANNEL AND INSTRUMENTATION

### 3.1 Experimental channel

Several series of new experiments were performed in the Gordon McKAY Hydraulics Laboratory at the University of Queensland (Table 3-1). The experimental channel was previously used by CHANSON and TOOMBES (2001,2002a,2003) and GONZALEZ (2005) with smooth step faces, and by GONZALEZ et al. (2005) (Table 1-1). Waters were supplied from a large feeding basin (1.5 m deep, surface area 6.8 m × 4.8 m) leading to a sidewall convergent with a 4.8:1 contraction ratio. The test section consisted of a broad-crested weir (1 m wide, 0.6 m long, with upstream rounded corner (0.057 m radius)) followed by ten identical steps (h = 0.1 m, l = 0.25 m) made of marine ply (Fig. 3-1). The stepped chute was 1 m wide with perspex sidewalls followed by a horizontal concrete-invert canal ending in a dissipation pit.

The pump, delivering the flow rate, was controlled with an adjustable frequency AC motor drive which enabled an accurate discharge adjustment in the closed-circuit system.

Table 3-1 - Summary of experimental flow conditions (Present study)

| Ref. | $q_W$ $m^2/s$ | $\frac{d_c}{h}$ | Re | Instrumentation | Comments |
|---|---|---|---|---|---|
| (1) | (2) | (3) | (4) | (5) | (6) |
| Present study | | | | | W = 1 m, h = 0.1 m, l = 0.25 m. |
| | 0.008 to 0.17 | 0.19 to 1.48 | 3.2 E+4 to 6.6 E+5 | Visual observations | |
| | 0.095 | 1.0 | 3.8 E+5 | One single-tip probe | |
| | 0.116 | 1.15 | 4.6 E+5 | Two single-tip probes | $\Delta z$ = 3.6 to 40.3 mm. |
| | 0.143 | 1.33 | 5.7 E+5 | One single-tip probe | |
| | 0.161 | 1.45 | 6.4 E+5 | Two single-tip probes | $\Delta z$ = 3.6 to 55.7 mm. |
| | 0.180 | 1.57 | 7.1 E+5 | One single-tip probe | |
| | 0.116 | 1.15 | 4.6 E+5 | One dual-tip probe | $\Delta x$ = 7.0 & 9.6 mm. |
| | 0.143 | 1.33 | 5.7 E+5 | One dual-tip probe | $\Delta x$ = 7.0 mm. |
| | 0.161 | 1.45 | 6.4 E+5 | One dual-tip probe | $\Delta x$ = 7.0 & 9.6 mm. |

Notes : $d_C$ : critical flow depth; h : step height; l : step length; Re : Reynolds number defined in terms of the hydraulic diameter; W : channel width.

Fig. 3-1 - Photographs of the experimental channel

(A) General view - $d_C/h$ 1.0, Re = 3.8 E+5

(B) Looking downstream at the trolley system supporting a double-tip conductivity probe - $d_C/h$ 1.33, Re = 4.7 E+5

## 3.2 Instrumentation

Clear-water flow depths were measured with a point gauge. The discharge was measured from the upstream head above the crest with an accuracy of about 2% ([4]).

Air-water flow properties were measured with two types of probes : single-tip conductivity and double-tip conductivity probes (Table 3-2). Basic air-water flow measurements were performed with two single-tip conductivity probes (needle probe design) (Fig. 3-2). Each probe consisted of a sharpened rod (platinum wire ∅ = 0.35 mm) coated with non-conductive epoxy set into a stainless steel surgical needle (∅ = 1.42 mm) acting as the second electrode as sketched in Figure 3-2. Additional measurements were performed with some double-tip conductivity probes (Fig. 3-3). Each sensor consisted of a sharpened rod (platinum wire ∅ = 0.25 mm) which was insulated except for its tip and set into a metal supporting tube (stainless steel surgical needle ∅ = 0.5 mm (internal) and 0.8 mm (external)). The stainless steel tube acted as the second electrode and it was separated from the inner wire by insulating epoxy. The longitudinal spacing between probe sensors was measured with a microscope and this yielded $\Delta x$ = 7.0, 9.6, and 12.2 mm for each of the three double-tip probes, although most measurements were conducted with $\Delta x$ = 7.0 and 9.6 mm.

All the probes were excited by an electronic system (Ref. UQ82.518) designed with a response time less than 10 μs and calibrated with a square wave generator. A summary of the probe characteristics is presented in Table 3-2. Further details on probe design and electronic system were reported by CHANSON (1995b) and CUMMINGS (1996).

Table 3-2 - Comparative summary of conductivity probe characteristics

| Reference : | CHANSON and TOOMBES (2002a), TOOMBES (2002), GONZALEZ (2005) | CHANSON and TOOMBES (2002c) | | Present study | |
|---|---|---|---|---|---|
| Design : | Double-tip | Single-tip | Double-tip | Single-tip | Double-tip |
| Probe sensor | | | | | |
| Inner electrode diameter (Pt): | 0.025 mm | 0.35 mm | 0.025 mm | 0.35 mm | 0.25 mm |
| Outer electrode inner diameter: | -- | -- | -- | -- | 0.5 mm |
| Outer electrode outer diameter: | 0.200 mm | 1.42 mm | 0.200 mm | 1.42 mm | 0.8 mm |
| Probe sensor spacing | | | | | |
| $\Delta x$ = | 7.5-10 mm | N/A | 8 mm | N/A | 7.0 mm<br>9.6 mm<br>12.2 mm |
| $\Delta z$ = | 0.5-1.5 mm | 3.6 to 54.7 mm | 1.33 mm | 3.6 to 54.7 mm | 1.4 mm |

[4]The discharge measurements were based upon GONZALEZ' (2005) detailed velocity distribution measurements on the broad-crested weir. The discharge estimates were based upon the analysis of his results which yielded the resulting calibration curve :

$$\frac{Q_W}{W} = \left(1.013 - 0.37 * \frac{H_1}{W}\right) * \sqrt{g * \left(\frac{2}{3} * H_1\right)^3}$$

where $H_1$ is the upstream total head above the weir crest elevation and W is the channel width. The above relationship was derived for $0.05 \leq H_1/W \leq 0.22$

All measurements were conducted on the channel centreline (z = 0). For some experiments, the second, identical probe was placed beside the first one with the probe sensors at the same vertical and streamwise distances y and x respectively (Fig. 3-4A). The reference probe was located on the channel centreline (z = 0) while the second probe was separated in the transverse direction by a known separation Δz. Photographs of the probes are shown in Figure 3-4.

Fig. 3-2 - Sketch of two single-tip conductivity probes placed side-by-side

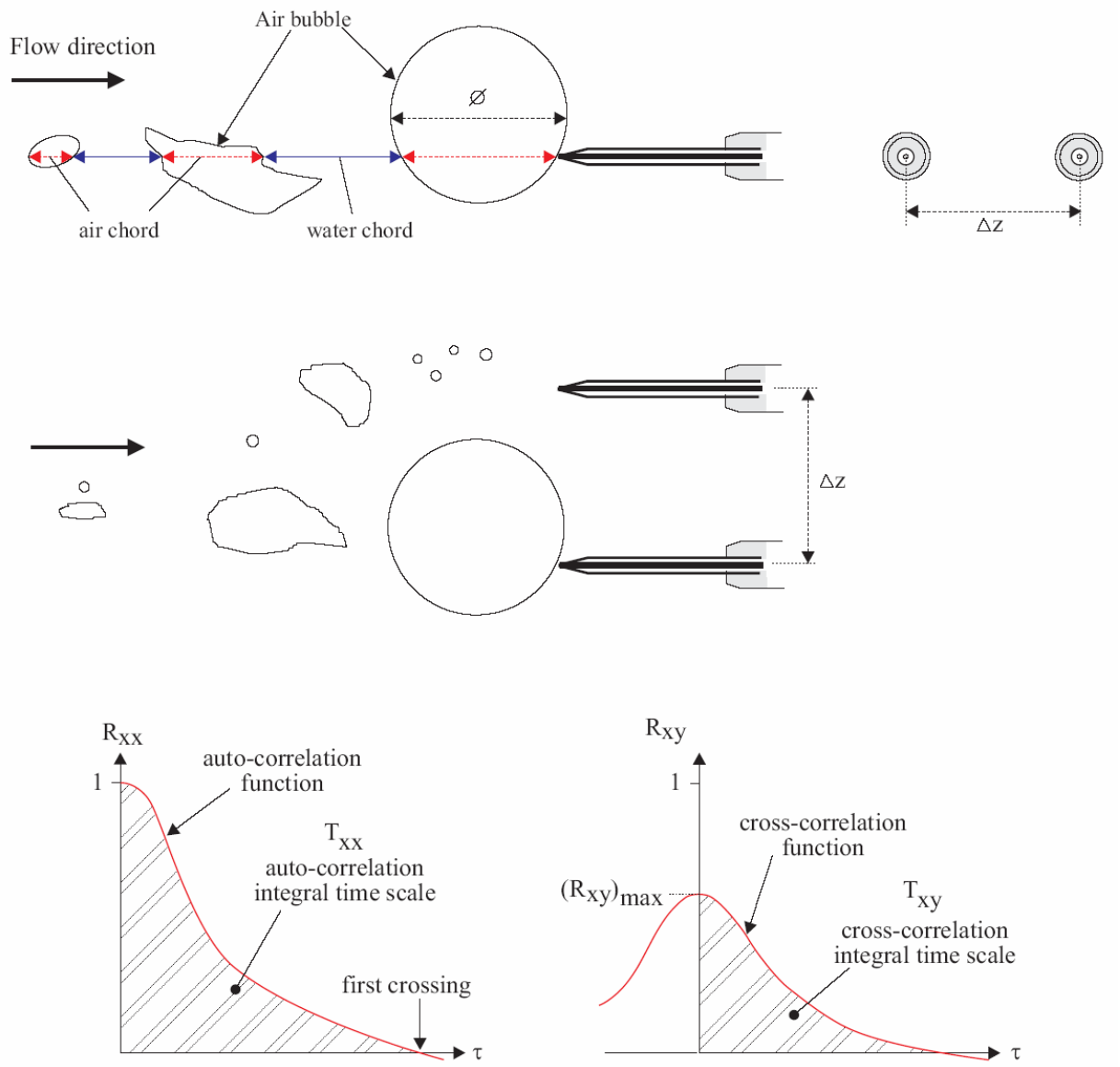

Fig. 3-3 - Sketch of the double-tip conductivity probe

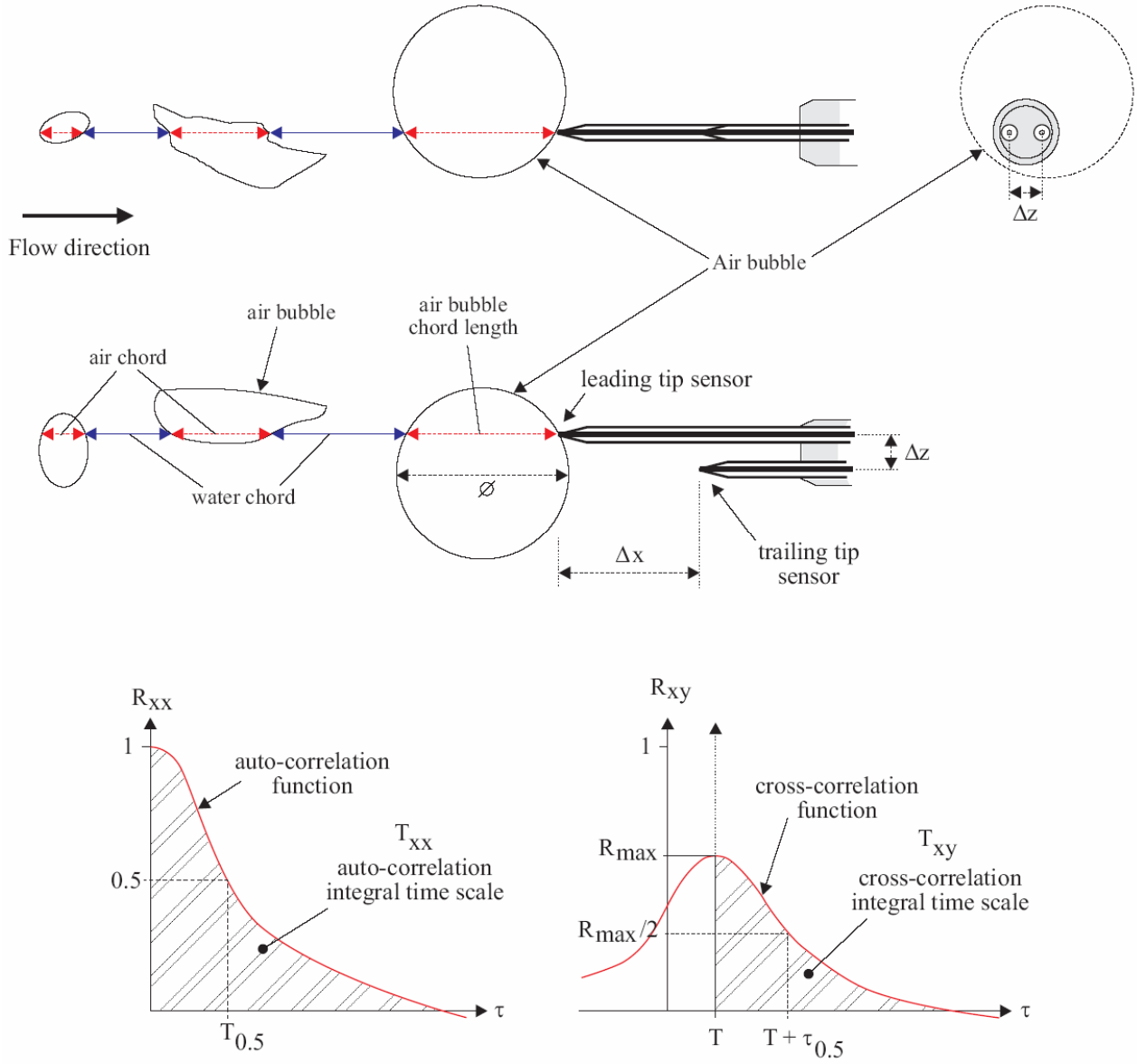


## 3.3 Data processing

The measurement principle of conductivity probes is based upon the difference in electrical resistivity between air and water. The resistance of water is one thousand times lower than the resistance of air. When the probe tip is in contact with water, current will flow between the tip and the supporting metal; when it is in contact with air no current will flow. A sketch of the single-tip conductivity probe is presented in Figure 3-2. Figure 3-5 shows some typical signal outputs. Figure 3-5A presents the signals of two single-tip probes side-by-side separated by $\Delta z = 3.6$ mm, and Figure 3-5B shows the signal outputs of a dual-tip probe. The time-variation of the voltage output has a "square-wave" shape. Each steep drop of the signal corresponds to an air bubble pierced by the probe tip. Although the signal is theoretically rectangular, the probe response is not square because of the finite size of the tip, the wetting/drying time of the interface covering the tip and the response time of the probe and electronics.

In the present study, the air-water flow properties were calculated using a single threshold technique and the threshold was set at about 45 to 55% of the air-water voltage range. A sensitivity analysis was conducted

with thresholds between 40 and 60% of the voltage range (TOOMBES 2002, pp. 55-56). The results showed little effect of threshold on the air-water flow properties. HERRINGE and DAVIS (1974) obtained a similar result for threshold between 20% and 70% of the air-water voltage range.

The air concentration or void fraction C is the proportion of time that the probe tip is in the air. Past experience showed that the probe orientation with the flow direction had little effect on the void fraction accuracy provided that the probe support does not affect the flow past the tip (e.g. SENE 1984, CHANSON 1988). In the present study, the probe tip was aligned with the main flow direction as shown in Figures 3-2 and 3-3. This configuration allowed the best conditions for bubble piercing by the probe sensor and hence a better quality signal.

The bubble count rate F is the number of bubbles impacting the probe tip per second. The measurement is sensitive to the probe tip size, bubble sizes, velocity and discrimination technique, particularly when the sensor size is larger than the smallest bubbles.

Fig. 3-4 - Photographs of the conductivity probes

(A) Two single-tip conductivity probes ($\Delta z$ = 21.7 mm) in the lower spray region - $d_C/h$ = 1.45, Re = 6.4 E+5, flow from left to right, shutter speed: 1/80 s

(B) Double-tip conductivity probe ($\Delta x$ = 12.2 mm) in the upper spray region, looking downstream - $d_c/h$ = 1.15, Re = 6.6 E+5, shutter speed: 1/1,000 s

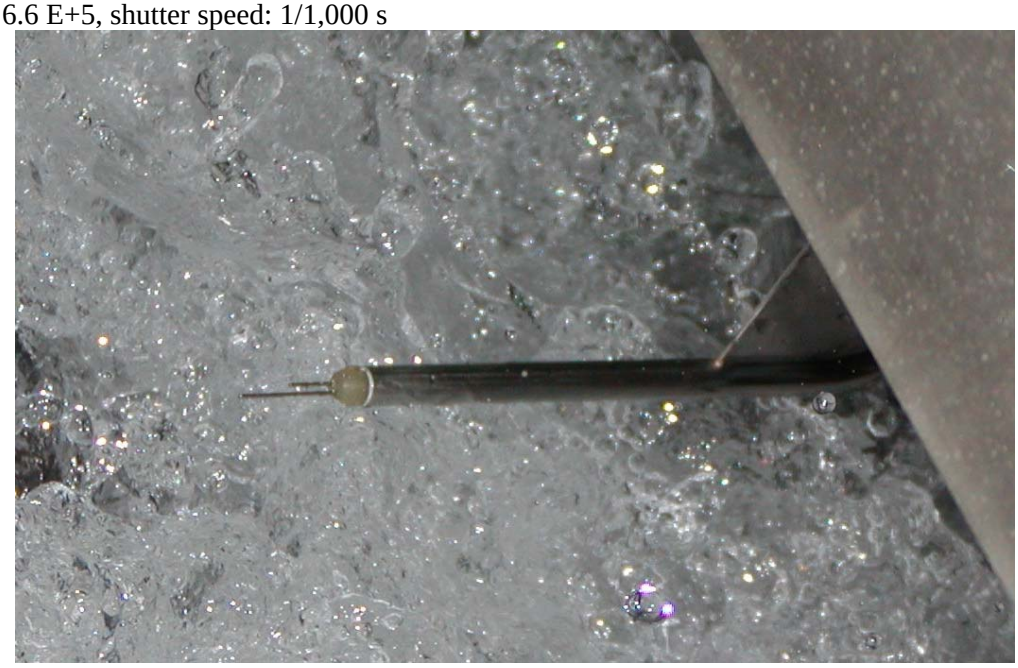

Figure 3-5 - Signal outputs of conductivity probes

(A) Signals of two single-tip conductivity probes side-by-side ($\Delta z$ = 3.6 mm) - $d_c/h$ = 1.15, Re = 4.6 E+5, Step edge 10, y = 0.022 m, C = 0.114, F = 117 Hz, $(R_{xy})_{max}$ = 0.41

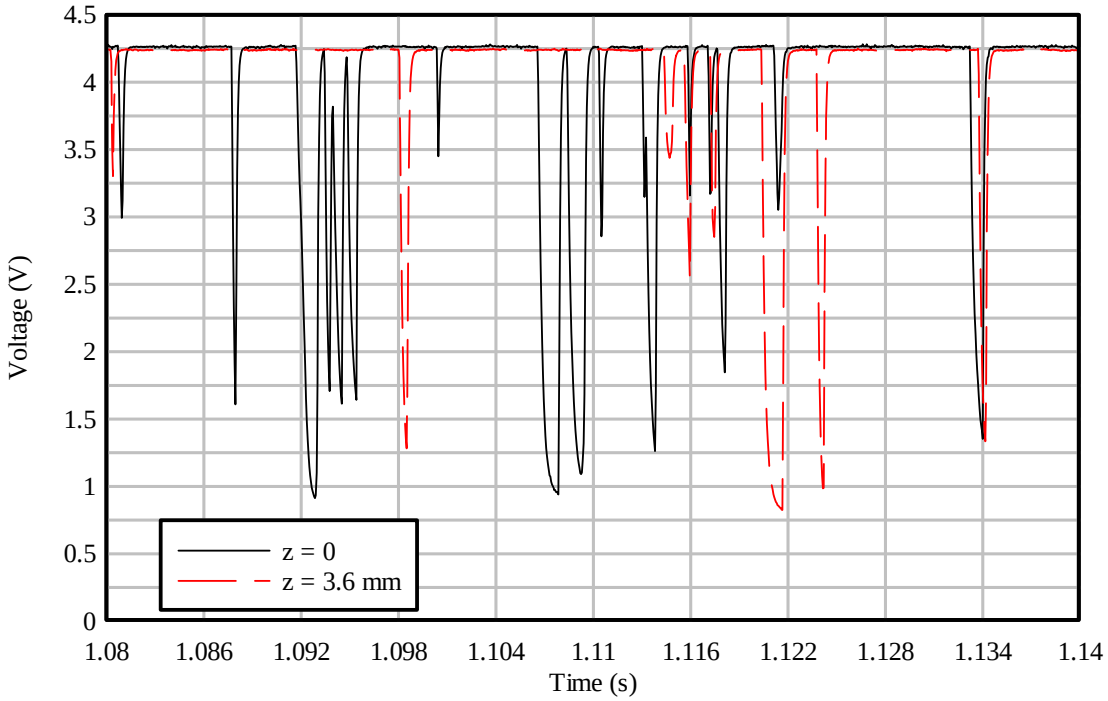

(B) Dual-tip conductivity probe signals ($\Delta x$ = 7.0 mm) - $d_C/h$ = 1.33, Re = 5.7 E+5, Step edge 10, y = 0.0365 m, C = 0.187, F = 167 Hz, V = 3.4 m/s, $(R_{xy})_{max}$ = 0.602

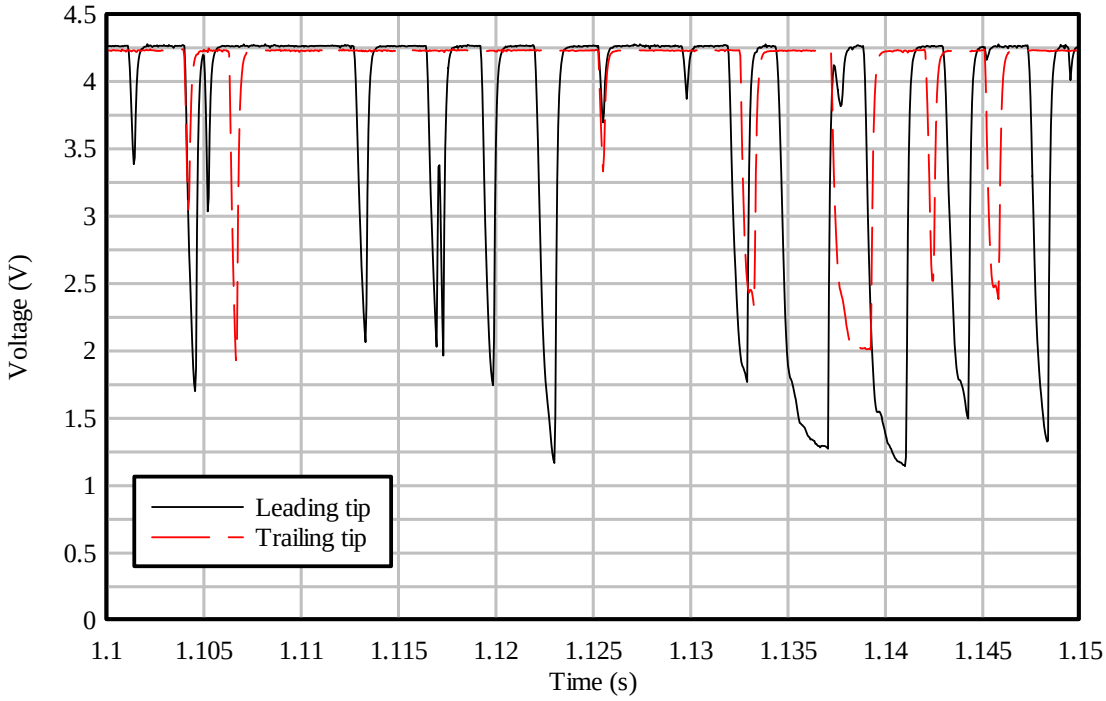


## 3.4 Correlation analyses

When two probe sensors are simultaneously sampled, a correlation analysis may provide additional air-water flow properties.

In the present study, the air-water interfacial velocities were deduced from a correlation analysis between the two sensors of the double-tip probe. The cross-correlation technique is commonly used with large void fractions (C > 0.10) (CHANSON 1997, CROWE et al. 1998, CHANSON 2002). The time averaged velocity equals :

$$V = \frac{\Delta x}{T} \qquad (3\text{-}1)$$

where T is the air-water interfacial travel time for which the cross-correlation function is maximum and $\Delta x$ is the longitudinal distance between probe sensors (Fig. 3-3). Turbulence levels may be derived from the relative width of the cross-correlation function :

$$Tu = 0.851 * \frac{\sqrt{\tau_{0.5}^2 - T_{0.5}^2}}{T} \qquad (3\text{-}2)$$

where $\tau_{0.5}$ is the time scale for which the cross-correlation function is half of its maximum value such as: $R_{xy}(T+\tau_{0.5}) = 0.5*R_{xy}(T)$, $R_{xy}$ is the normalised cross-correlation function, and $T_{0.5}$ is the characteristic time for which the normalised auto-correlation function equals : $R_{xx}(T_{0.5}) = 0.5$ (Fig. 3-3). Equation (3-2) was derived first by CHANSON and TOOMBES (2001,2002a). Physically, a thin narrow cross-correlation function ($(\tau_{0.5}-T_{0.5})/T << 1$) must correspond to little fluctuations in the interfacial velocity, hence a small turbulence level Tu. While Equation (3-2) might not be equal to the turbulence intensity u'/V, it is an expression of some turbulence level and average velocity fluctuations.

More generally, when two probe sensors are separated by a transverse or streamwise distance Y, their signals may be analysed in terms of auto-correlation and cross-correlation functions $R_{xx}$ and $R_{xy}$ respectively. Herein the original data of 900,000 samples were segmented because the periodogram resolution is inversely proportional to the number of samples and it could be biased with large data sets (HAYES 1996, GONZALEZ 2005). All data signals were sub-divided into fifteen non-overlapping segments of 60,000 samples. Further the correlation analyses were conducted on the raw probe output signals. With a single-threshold technique, the analysis based upon thresholded signals tends to ignore the contributions of the smallest air-water particles.

Following CHANSON (2006a), the basic correlation analysis results included the maximum cross-correlation coefficient $(R_{xy})_{max}$, and the correlation time scales $T_{xx}$ and $T_{xy}$ where :

$$T_{xx} = \int_{\tau=0}^{\tau=\tau(R_{xx}=0)} R_{xx}(\tau) * d\tau \quad (3\text{-}3)$$

$$T_{xy} = \int_{\tau=\tau(R_{xy}=(R_{xy})_{max})}^{\tau=\tau(R_{xy}=0)} R_{xy}(\tau) * d\tau \quad (3\text{-}4)$$

where $R_{xx}$ is the normalised auto-correlation function, $\tau$ is the time lag, and $R_{xy}$ is the normalised cross-correlation function between the two probe output signals (Fig. 3-2 & 3-3). $T_{xx}$ is the auto-correlation integral time scale which characterises the longitudinal bubbly flow structure and the eddies advecting the air-water interfaces in the streamwise direction. $T_{xy}$ is the cross-correlation integral time scale. It is a characteristic time of the large vortices with a length scale Y advecting the air-water flow structures, where the length scale Y is the probe separation distance ([5]).

When identical experiments were repeated with different separation distances Y (Y = $\Delta z$ or $\Delta x$), an integral turbulent length scale was calculated as :

$$L_{xy} = \int_{Y=0}^{Y=Y((R_{xy})_{max}=0)} (R_{xy})_{max} * dY \quad (3\text{-}5)$$

The integral turbulent length scale $L_{xy}$ is a function of the inflow conditions, streamwise position $x/d_c$ and normal distance $y/d_c$. MOUAZE et al. (2005) introduced a similar definition to characterise some free-surface fluctuation length scale. Herein, the length scale $L_{xy}$ represents a measure of the transverse/streamwise turbulent length scale of the large vortical structures advecting air bubbles and air-water packets.

An advection integral length scale is :

$$L_{xx} = V * T_{xx} \quad (3\text{-}6)$$

where V is the advective velocity magnitude. $L_{xx}$ is a characteristic longitudinal size of the eddies advecting air bubbles based upon the hypothesis of "frozen turbulence".

A turbulence integral time scale is :

---

[5]The probe separation distance Y is also denoted $\Delta z$ for the transverse separation distance or $\Delta x$ for the streamwise separation.

$$\mathbf{T} = \frac{\int_{Y=0} (R_{xy})_{max} * T_{xy} * dY}{L_{xy}} \quad (3\text{-}7)$$

$\mathbf{T}$ represents the transverse/streamwise integral time scale of the large eddies advecting air bubbles.

## 3.5 Bubble chord calculations

With the single-tip conductivity probes, a basic signal processing yields the air/water chord times and their distribution. The air/water chord times are defined as the time spent by the air/water phase on the probe sensor. Bubble chord times were calculated from the raw probe signal using the single threshold technique (described above). Statistical analyses of chord time distributions yielded the median chord time, standard deviation, skewness and kurtosis of both air and water chord times. Interparticle arrival times ([6]) were also calculated and analysed (e.g. CHANSON 2006a).

With the single-tip conductivity probe, the chord time results are presented herein in terms of pseudo-bubble/droplet chord sizes ch defined as :

$$ch = U_W * t_{ch} \quad (3\text{-}8)$$

where $t_{ch}$ is the air/water chord time, $U_W$ is the mean flow velocity defined as : $U_W = q_W/d$, $q_W$ is the flow rate per unit width and d is the equivalent clear-water depth. The pseudo chord size ch is not equal to the air/water chord length because the local interfacial velocity V may differ from the mean flow velocity $U_W$.

The writers re-analysed some chord size data of GONZALEZ et al. (2005) obtained in the same chute with smooth steps (App. A). The data were recorded with a 0.025 mm sensor scanned at 20 kHz for 20 s. The comparative analysis showed that Equation (3-8) overestimated the air/water chord sizes by 2% in average for $0 \leq C \leq 0.97$. For $C > 0.97$, the error was larger but the droplet populations were small and not statistically representative. The air/water chord time data will be presented in terms of pseudo-chord sizes because the results are easier to comprehend and to compare with dual-tip probe data, visual observations, high-speed photographs and movies. Figure 3-6 shows some normalised chord length probability distribution functions where each data point represents the probability of a bubble/droplet chord in 0.5 mm intervals : e.g., the probability of a chord between 1.0 and 1.5 mm is represented by the data point labelled 1.25. The probability of bubble chord lengths greater than 15 mm is not shown for clarity. In Figure 3-6, the thick solid line is the measured bubble chord length distribution and the thin dashed line is the pseudo-chord size distribution calculated using Equation (3-8).

With the double-tip probe, the signal processing yielded the air/water chord sizes. The chord size measurement is not a bubble/droplet diameter, but a characteristic streamwise air/water size as sketched in Figure 3-3.

[6]The interparticle arrival time is defined as the time between the arrival of two successive particles. It is the time between two consecutive water-to-air interfaces.

Fig. 3-6 - Chord size distributions in skimming flows : comparison between measured chord lengths and Equation (3-8) - Experimental data by GONZALEZ et al. (2005), $d_C/h$ = 1.18, Re = 5 E+5, Step 10

(A) Air bubble chords, $y/Y_{90}$ = 0.29, C = 0.107, F = 177.5 Hz, V = 3.1 m/s, 3550 bubbles

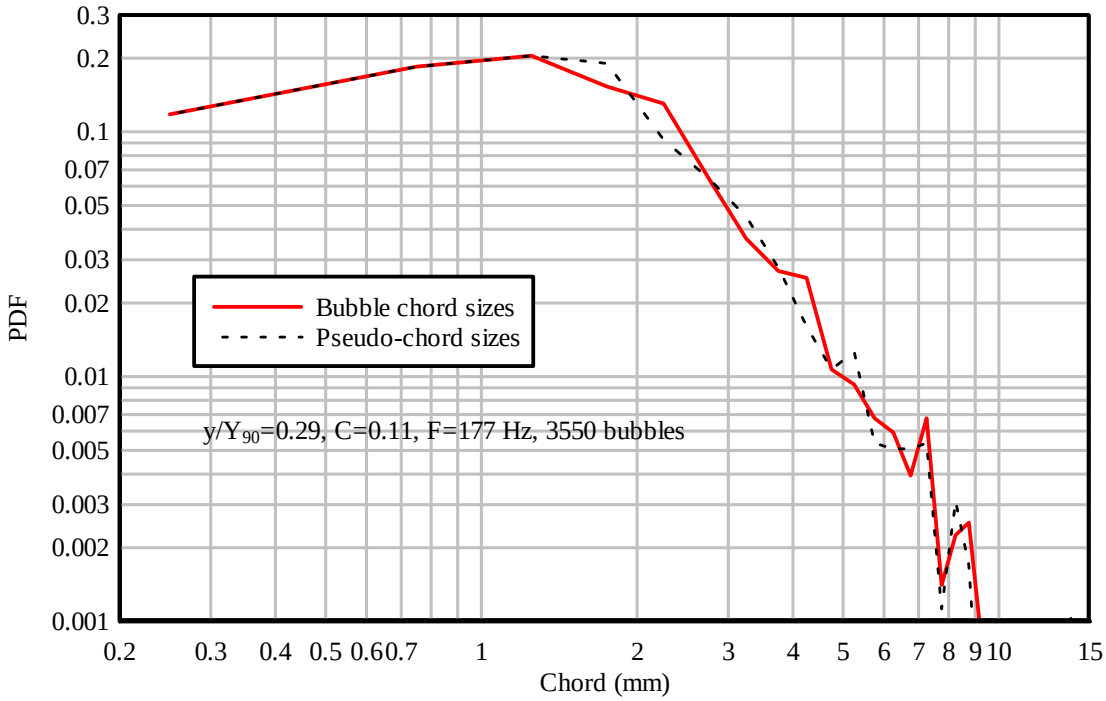


(B) Droplet chords, $y/Y_{90}$ = 0.87, C = 0.82, F = 170 Hz, V = 3.52 m/s, 3397 droplets

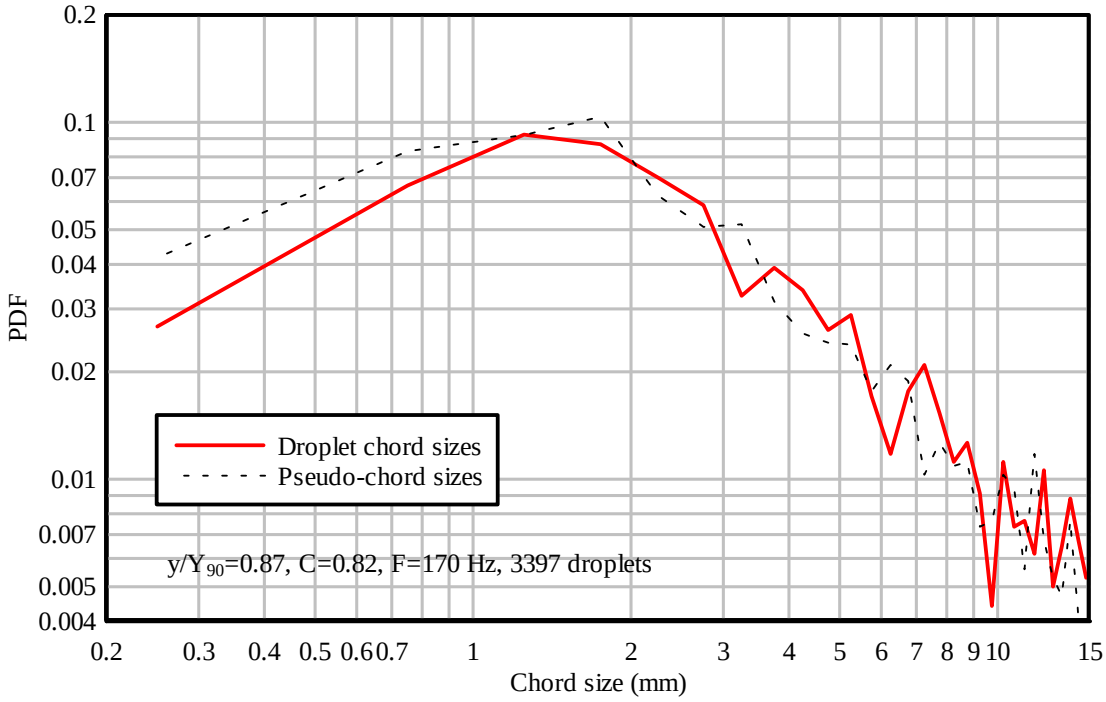

## 3.6 Quality control, scan frequency and scan duration

Phase-detection probes are very sensitive devices and they are susceptible to a number of problems. In the present study, the quality control procedure developed by TOOMBES (2002, pp. 70-72) was applied thoroughly. Specifically, the probe signals were checked systematically for long-term signal decays often induced by probe tip contamination, short-term signal fluctuations caused by debris and water impurities, electrical noise and non-representative samples. Although most quality control procedures can be automatised, it must be stressed that human supervision and intervention are essential to validate each quality control step.

Based upon past experiences (CHANSON and TOOMBES 2002a, TOOMBES 2002, GONZALEZ 2005), a sampling rate of 20 kHz per sensor was used for all the study, and the sampling duration was set at 45 seconds.

## 3.7 Data accuracy

The water discharge was measured with an accuracy of about 2% ([7]). The translation of the conductivity probes in the direction normal to the channel invert was controlled with an error of less than 0. 5 mm. The accuracy on the longitudinal probe position was estimated as $\Delta x$ < +/- 0.5 cm. The error on the transverse position of the probe was less than 0.1 mm.

With both single- and double-tip conductivity probes, the error on the air concentration (void fraction) measurements was estimated as : $\Delta C/C = 4$ % for $0.05 < C < 0.95$, $\Delta C/C \sim 0.002/(1 - C)$ for $C > 0.95$, and $\Delta C/C \sim 0.005/C$ for $C < 0.05$. The minimum detectable bubble chord time was about 0.05 ms for a data acquisition frequency of 20 kHz per channel (Eq. (3-8)).

The scan frequency determines the resolution of the intrusive phase-detection probe, in particular the accuracy of chord size measurement, minimum detectable air/water chord length, and the accuracy of the interfacial velocity. The minimum measurable chord size is the smallest of the probe sensor size and :

$$\Delta ch = \frac{V}{F_{scan}} \quad (3\text{-}9)$$

where ch is the chord size, V is the velocity, and $F_{scan}$ is the scan rate frequency. Conversely the minimum detectable chord time is $1/F_{scan}$ provided that the particles are larger than the sensor size.

The error on the interfacial velocity was :

$$\Delta V = 1 - \frac{1}{1 + \frac{V}{F_{scan} * \Delta x}} \quad (3\text{-}10)$$

where $\Delta x$ is the streamwise distance between probe sensors. Herein the scan frequency was 20 kHz per sensor and the streamwise distance between probe sensor was : $\Delta x$ = 7.0, 9.6 or 12.2 mm.

With the double-tip conductivity probe, the analysis of the velocity field and chord length distributions implied no slip between the air and water phases. The error on the mean air-water velocity measurements

[7]GONZALEZ (2005) performed detailed velocity distribution measurements on the broad-crest for a range of flow rates. Measurements were conducted in clear-water flows with a Prandtl-Pitot tube (∅ = 3.3 mm). Present discharge estimates are based upon the re-analysis of his results.

was estimated as : $\Delta V/V = 5$ %. for $0.05 < C < 0.95$ , $\Delta V/V = 10$ %. for $0.01 < C < 0.05$ and $0.95 < C < 0.99$ (CHANSON and BRATTBERG 1997). The guidelines are consistent with Equation (3-10). With the two-tip conductivity probe, the minimum detectable bubble chord length was about 0.15 mm in a 3 m/s flow based upon a data acquisition frequency of 20 kHz per channel (Eq. (3-9)).

*Effect of probe sensor size on chord size data*

The effect of probe sensor on chord size data were tested for one flow rate ($d_C/h = 1.15$). Present chord data obtained with a 0.35 mm sensor probe were compared with some experimental results obtained by GONZALEZ et al. (2005) for $d_C/h = 1.18$ with a 0.025 mm probe sensor. CHANSON and TOOMBES (2002c) performed a similar comparison between two probe sensors sizes (0.025 and 0.35 mm) in skimming flows. Their data indicated larger measured count rates with the smaller 0.025 mm sensor probe.

Fig. 3-7 - Normalised probability distribution functions of bubble/droplet pseudo-chord sizes : comparison between 0.025 mm and 0.35 mm sensor probes

(A) Bubbly flow region

| Probe sensor size (mm) | $d_C/h$ | Step number | C | F (Hz) | Reference | Run |
|---|---|---|---|---|---|---|
| 0.025 | 1.18 | 10 | 0.107 | 177.5 | GONZALEZ et al. (2005) | Sm13S10_05 |
| 0.35 | 1.15 | 10 | 0.106 | 118.1 | Present study | 060411S10_04 |

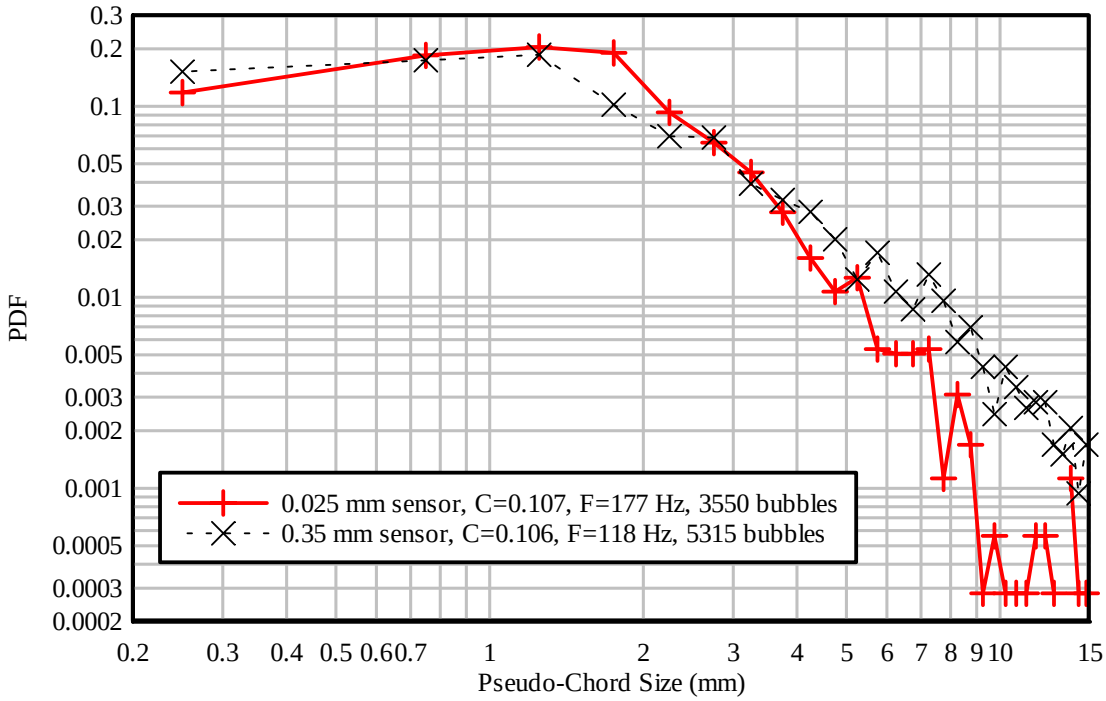

(B) Spray region

| Probe sensor size (mm) | $d_C/h$ | Step number | C | F (Hz) | Reference | Run |
|---|---|---|---|---|---|---|
| 0.025 | 1.18 | 10 | 0.893 | 102.9 | GONZALEZ et al. (2005) | Sm13S10_19 |
| 0.35 | 1.15 | 10 | 0.874 | 82.3 | Present study | 060411S10_14 |

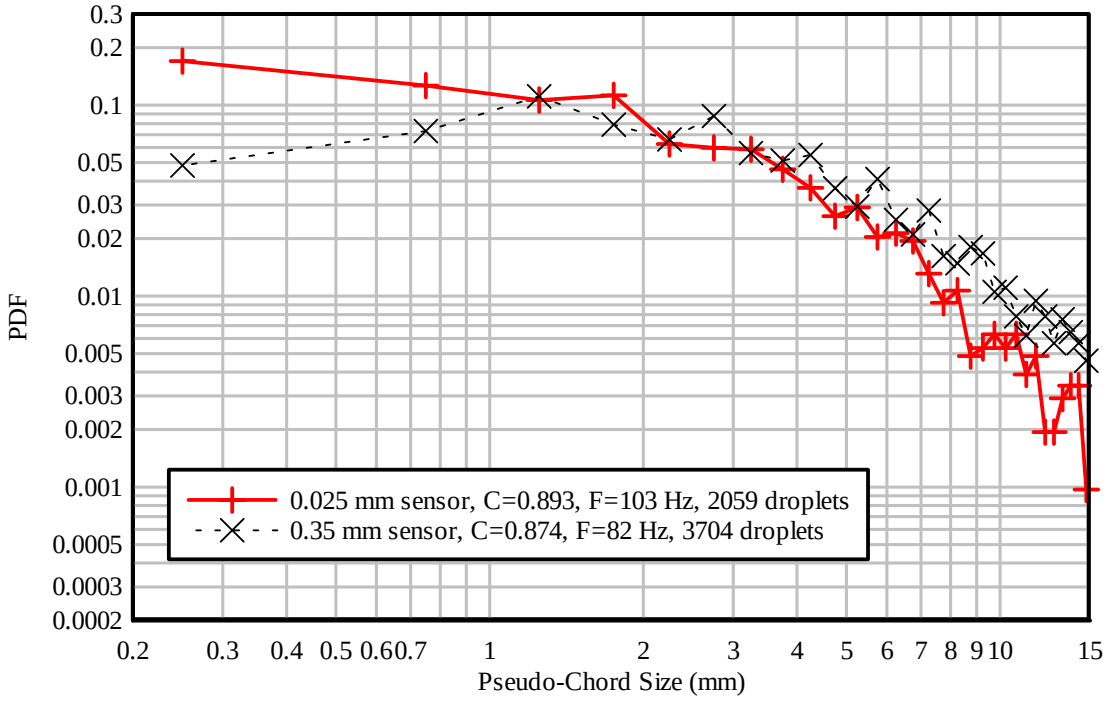


The present data showed consistently larger measured count rates and a broader range of bubble/droplet sizes with the 0.025 mm sensor probe than with the 0.35 mm sensor probe (App. A). The pseudo chord sizes measured with the 0.35 mm sensor were typically 18 to 50% larger (average: 28%) than the chord lengths measured with the 0.025 mm sensor. This suggested the existence of a significant proportion of small bubbles/droplets with sizes ranging from 0.025 to 0.35 mm. However, in the upper spray/splashing region (i.e. C > 0.97), the pseudo-chords were close implying that most water droplets were larger than 0.35 mm.

A typical comparison is shown in Figure 3-7. The figure caption and legend list the air-water flow conditions including local void fraction, count rates and the total number of bubbles/particles ([8]). Figure 3-7 shows some pseudo-chord size probability distribution functions where each data point represents the probability of a chord length in 0.5 mm intervals. In Figure 3-7, the measurements with the 0.025 mm sensor probe are drawn with the thick solid line while the thin dashed line shows the data obtained with the 0.35 mm sensor probe.

[8]Both probes were scanned at 20 kHz per sensor. The scan duration was 20 and 45 s for the 0.025 and 0.35 mm sensor probes respectively.

## 3.8 Experimental procedure and inflow conditions

Experiments were conducted for a range of flow rates although the focus was on the highly aerated skimming flows (Table 3-1). Detailed air-water flow measurements were performed for flow rates between 0.09 and 0.18 $m^3/s$ corresponding to dimensionless discharges $d_c/h$ = 1.0 to 1.57 and flow Reynolds numbers $\rho_W*U_W*D_H/\mu_W$ between 3.8 E+5 and 7.1 E+5, where $d_c$ is the critical flow depth, h is the step height, $U_W$ is the depth-averaged velocity, $D_H$ is the hydraulic diameter, and $\rho_W$ and $\mu_W$ are the water density and dynamic viscosity respectively.

Present measurements were performed systematically at step edges downstream of the inception point of free-surface aeration (Fig. 3-8). For each flow rate, measurements were repeated systematically with several transverse probe spacing Δz and with several dual-tip probe designs (streamwise sensor separation Δx). A total of more than 41 vertical profiles were recorded with a minimum of 30 measurement points per profile. At each measurement point, the data acquisition yielded 900,000 data per probe sensor. (Altogether the present data set encompassed over 1.2 billion samples.) Note that uniform equilibrium flow conditions were not achieved at the downstream end of the chute because the flume was relatively short.

Fig. 3-8 - Skimming flow on a stepped chute

(A) Definition sketch of step edge numbering

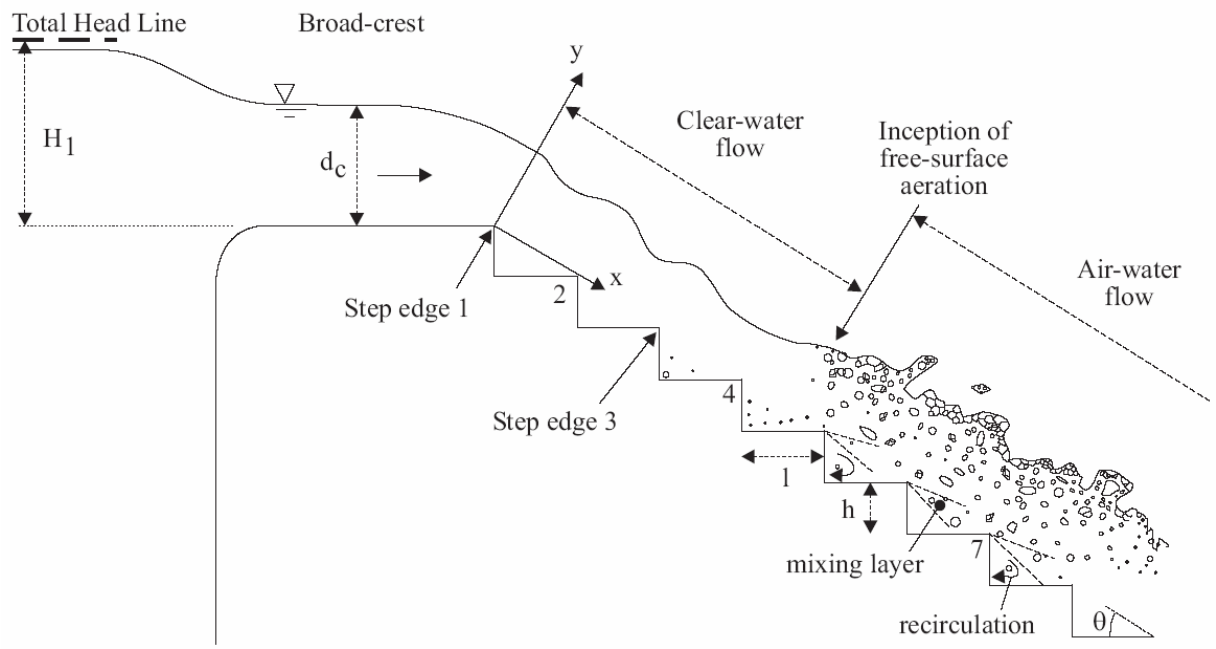

(B) Typical void fraction and velocity distributions at a step edge

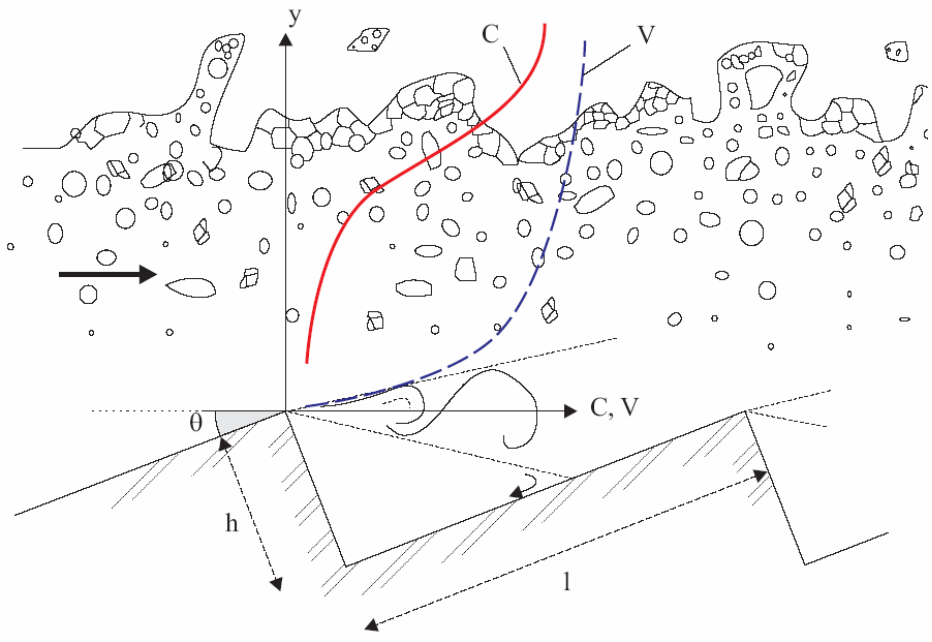

## 4. AIR-WATER FLOW PATTERNS

### 4.1 Flow regimes

The basic flow regimes were inspected in a series of preliminary experiments with discharges ranging from 0.008 to 0.180 $m^3/s$. Visual observations were complemented by photographic informations (Fig. 3-1 and 4-1).

For small flow rates ($d_C/h < 0.5$), the waters flowed as a succession of free-falling jets that was typical of a nappe flow regime. For some intermediate discharges ($0.5 < d_C/h < 0.95$), the flow had a chaotic behaviour characterised by strong splashing and droplet projections downstream of the inception point of free-surface aeration. That was a transition flow regime (Fig. 4-1A). For larger flows ($d_C/h > 0.95$), the waters skimmed above the pseudo-bottom formed by the step edges (Fig. 4-1B). The skimming flows were characterised by strong cavity recirculation with three-dimensional vortical patterns. These were best seen next to the inception point of free-surface aeration. Overall the results in terms of flow regimes and changes between flow regimes were very close to the observations of CHANSON and TOOMBES (2001), GONZALEZ (2005) and GONZALEZ et al. (2005) in the same chute with the same slope and step height.

Fig. 4-1 - Photographs of transition and skimming flows
(A) Transition flow - $d_C/h = 0.70$, Re = 2.3E+5

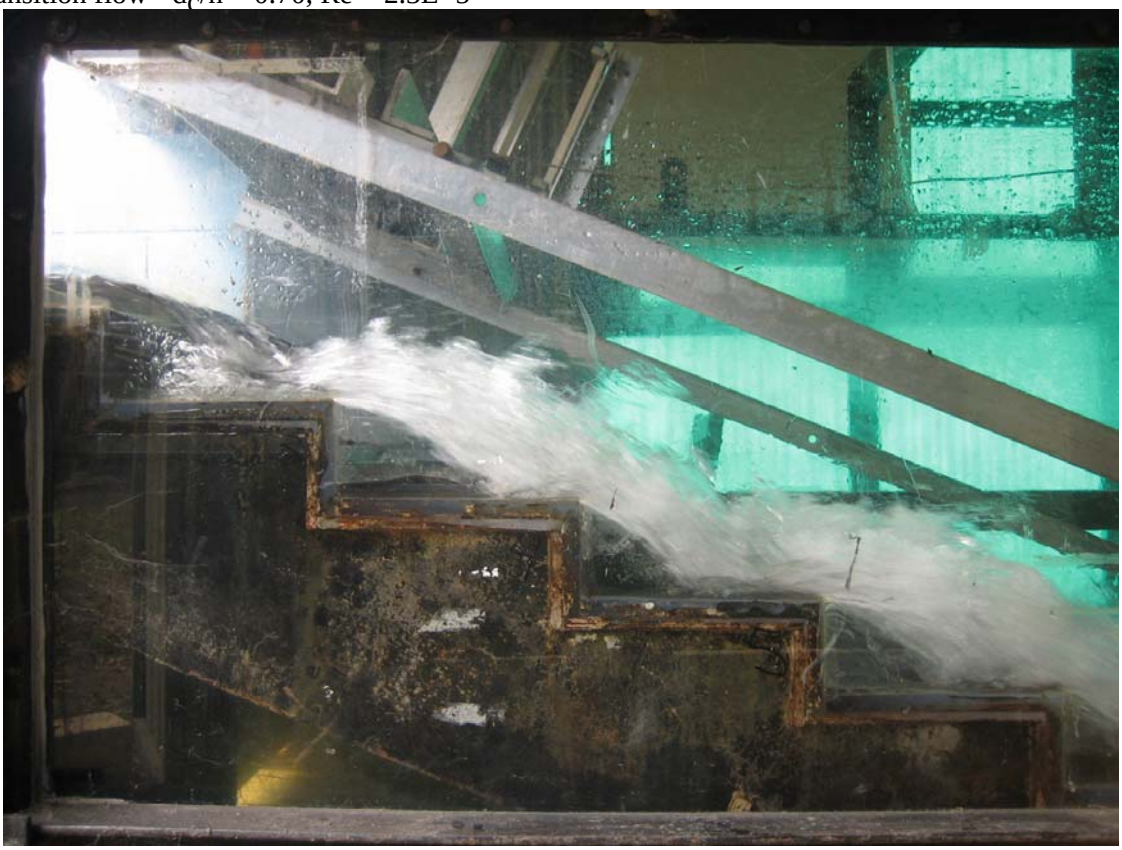

(B) Skimming flow (flow from left to right) - $d_c/h = 1.45$, Re = 6.4 E+5

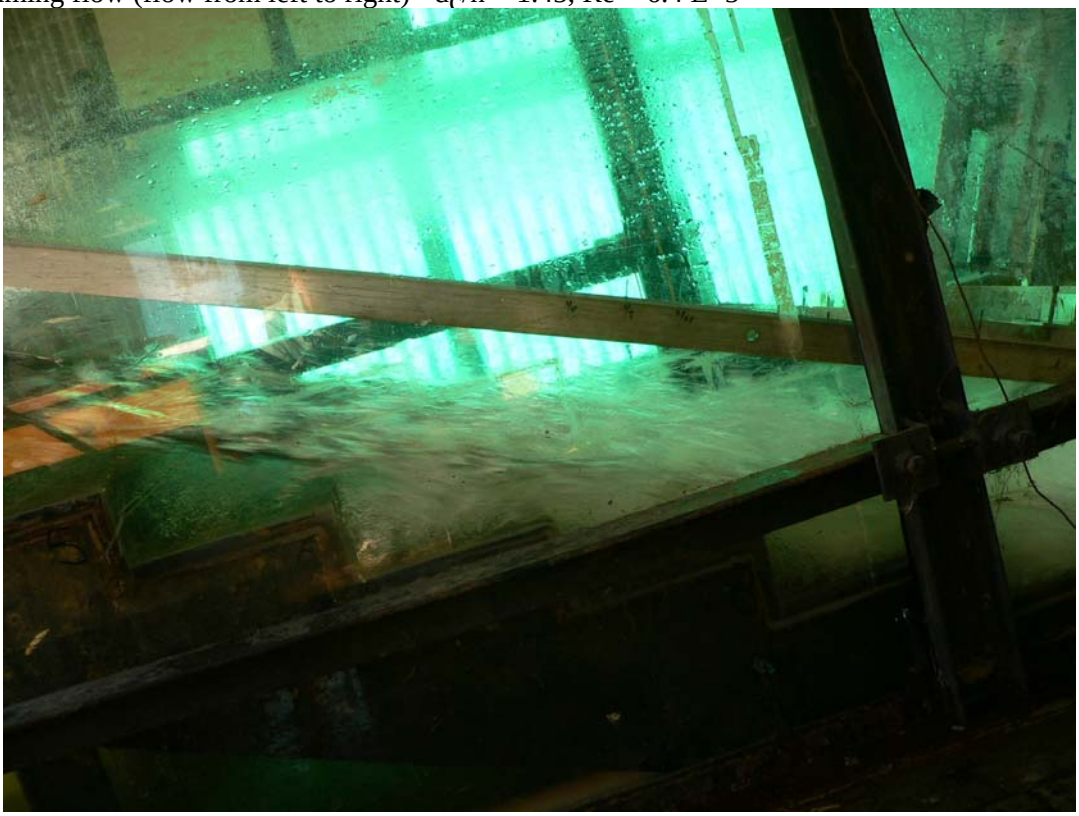

## 4.2 Inception point of free-surface aeration

In transition and skimmings flows, the location of the inception point of free-surface aeration was recorded with discharges per unit width ranging from 0.034 to 0.18 $m^2/s$. The results are reported in Table 4-1 and summarised in Figure 4-2. In Figure 4-2, the data are presented as $L_I/k_S$ as a function of $F_*$, where $L_I$ is the streamwise distance from the downstream end of the crest ([1]), and $k_S$ is the step cavity height normal to the flow direction $k_S = h*\cos\theta$. $F_*$ is a Froude number defined in terms of the step roughness :

$$F_* = \frac{q_W}{\sqrt{g * \sin\theta * (h * \cos\theta)^3}} \quad (4\text{-}1)$$

where $q_W$ is the water discharge per unit width, g is the gravity acceleration and $\theta$ is the angle between the pseudo-bottom and the horizontal.

The present data are compared in Figure 4-2 with some earlier data with smooth steps (CHANSON and TOOMBES 2001, GONZALEZ et al. 2005) and a study with rough steps (GONZALEZ et al. 2005), as well as with the empirical correlation of CHANSON (1994b,1995a) :

$$\frac{L_I}{h * \cos\theta} = 9.719 * (\sin\theta)^{0.0796} * F_*^{0.713} \quad (4\text{-}2)$$

The agreement between all the data with smooth steps is good. For the present study, the results were best correlated by :

$$\frac{L_I}{h * \cos\theta} = 1.05 + 5.11 * F_* \qquad 0.45 < \frac{d_c}{h} < 1.6 \quad (4\text{-}3)$$

[1]That is, the longitudinal distance measured from the step edge 1 (Fig. 3-8).

with a normalised correlation coefficient of 0.95. Equation (4-3) is valid for transition and skimming flows on a 22º stepped chute with $0.45 < d_c/h < 1.6$.

Table 4-1 - Experimental observations of the inception point of free-surface aeration (Present study, $\theta$ = 21.8º)

| $Q_w$ | $d_c/h$ | Location of inception point of free-surface aeration | Flow regime |
|---|---|---|---|
| $m^3/s$ | | step edge | |
| (1) | (2) | (3) | (4) |
| 0.180 | 1.57 | 7 to 8 | Skimming flow |
| 0.166 | 1.48 | 6 to 7 | |
| 0.161 | 1.45 | 7 to 8 | |
| 0.160 | 1.44 | 6 | |
| 0.146 | 1.35 | 5 to 6 | |
| 0.143 | 1.33 | 6 to 7 (almost 6) | |
| 0.143 | 1.33 | 6 to 7 (almost 6) | |
| 0.143 | 1.33 | 6 to 7 (almost 6) | |
| 0.137 | 1.29 | 5 to 6 | |
| 0.136 | 1.29 | 6 | |
| 0.133 | 1.27 | 5 to 6 | |
| 0.125 | 1.21 | 5 | |
| 0.122 | 1.19 | 5 to 6 | |
| 0.117 | 1.16 | 4 to 5 | |
| 0.116 | 1.15 | 6 to 7 | |
| 0.116 | 1.15 | 6 to 7 | |
| 0.113 | 1.13 | 5 | |
| 0.109 | 1.10 | 4 to 5 | |
| 0.108 | 1.09 | 4 to 5 | |
| 0.099 | 1.03 | 4 to 5 | |
| 0.098 | 1.03 | 4 | |
| 0.090 | 0.97 | 4 to 5 | |
| 0.083 | 0.91 | 4 | Transition flow |
| 0.077 | 0.87 | 4 | |
| 0.073 | 0.83 | 3 to 4 | |
| 0.072 | 0.83 | 3 to 4 | |
| 0.070 | 0.81 | 3 to 4 | |
| 0.068 | 0.79 | 3 | |
| 0.067 | 0.79 | 3 to 4 | |
| 0.061 | 0.74 | 3 to 4 | |
| 0.060 | 0.73 | 3 | |
| 0.056 | 0.70 | 3 to 4 | |
| 0.054 | 0.68 | 3 to 4 | |
| 0.052 | 0.66 | 3 to 4 | |
| 0.047 | 0.61 | 3 | |
| 0.046 | 0.61 | 3 | |
| 0.042 | 0.57 | 2 to 3 | |
| 0.041 | 0.56 | 2 to 3 (almost 3) | |
| 0.035 | 0.51 | 2 to 3 | |
| 0.034 | 0.49 | 2 to 3 | |
| 0.034 | 0.49 | 2 to 3 | |

Note : $L_I$ : streamwise distance from the downstream end of the crest (Fig. 3-8).

Fig. 4-2 - Dimensionless location of the inception point of free-surface aeration - Comparison between the present observations, the data of CHANSON and TOOMBES (2001) and GONZALEZ et al. (2005) (Series CMH_05), the correlation of CHANSON (1994b) (Eq. (4-2)) and Equation (4-3)

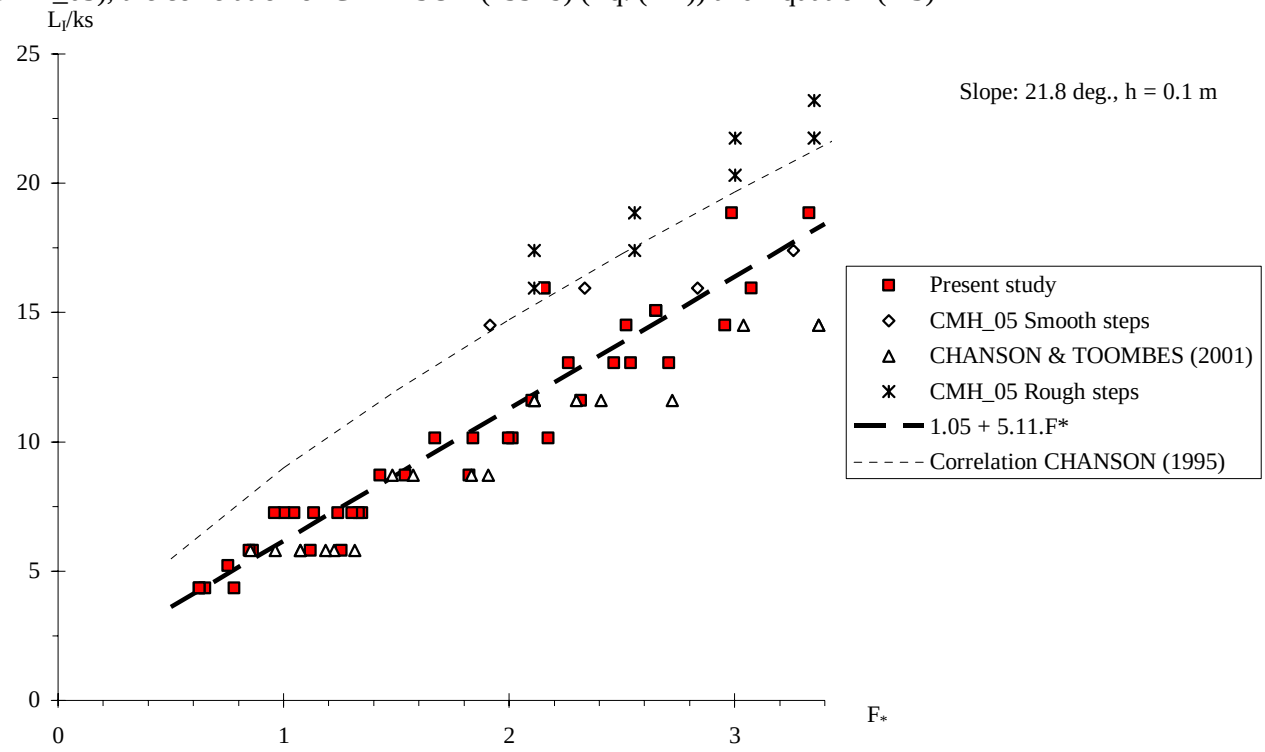

## 5. BASIC AIR-WATER FLOW PROPERTIES

### 5.1 Void fraction and bubble count rate distributions

*5.1.1 Void fraction profiles*

Experimental observations demonstrated substantial free-surface aeration immediately downstream of the inception point of free-surface aeration and some sustained flow aeration was observed downstream. This is illustrated in Figure 5-1 where the dimensionless distributions for void fraction C and bubble count rate $F^* d_C/V_C$ are presented as functions of $y/d_C$ at several successive step edges for the same flow rate where $d_C$ is the critical flow depth and $V_C$ is the critical flow velocity. For a rectangular channel, $d_C$ and $V_C$ equal :

$$d_C = \sqrt[3]{\frac{Q_W^2}{W}} \quad (5\text{-}1)$$

$$V_C = \sqrt{g * d_C} \quad (5\text{-}2)$$

where $Q_W$ is the water discharge, g is the gravity acceleration and W is the channel width. For the data shown in Figure 5-1, the flow aeration was nil at step edge 6, immediately upstream of the inception point. Between step edges 6 and 7, some strong self-aeration took place, and the amount of entrained air and the mean air content were about constant between the step edges 7 and 10. The depth-averaged void fraction was $C_{mean} = 0.36$ at the last step edge (step edge 10).

The void fraction profiles showed consistently a similar shape (Fig. 5-1 and 5-2). The dimensionless distributions presented a S-shape profile that was observed in previous studies : e.g., RUFF and FRIZELL (1994), CHANSON and TOOMBES (1997), BOES (2000a) and CHANSON and TOOMBES (2002a). For all the data, the void fraction distribution measurements compared well with an analytical solution of the advective diffusion equation for air bubbles :

$$C = 1 - \tanh^2\left(K' - \frac{\frac{y}{Y_{90}}}{2 * D_o} + \frac{\left(\frac{y}{Y_{90}} - \frac{1}{3}\right)^3}{3 * D_o}\right) \quad (5\text{-}3)$$

where y is distance measured normal to the pseudo-invert, $Y_{90}$ is the characteristic distance where C = 90%. K' is an integration constant and $D_o$ is a function of the mean air concentration $C_{mean}$ only :

$$K' = K^* + \frac{1}{2 * D_o} - \frac{8}{81 * D_o} \quad (5\text{-}4)$$

$$K^* = \tanh^{-1}(\sqrt{0.1}) = 0.32745015... \quad (5\text{-}5)$$

$$C_{mean} = 0.7622 * (1.0434 - \exp(-3.614 * D_o)) \quad (5\text{-}6)$$

Equation (5-3) was found to fit well skimming flow data (CHANSON and TOOMBES 2002a). Figure 5-2 shows a comparison between Equation (5-3) and some dimensionless void fraction data.

Fig. 5-1 - Dimensionless distributions of void fraction C and bubble count rate $F^*d_c/V_c$ for $d_c/h = 1.15$, single-tip probe ($\varnothing = 0.35$ mm)

(A) Step edge 7

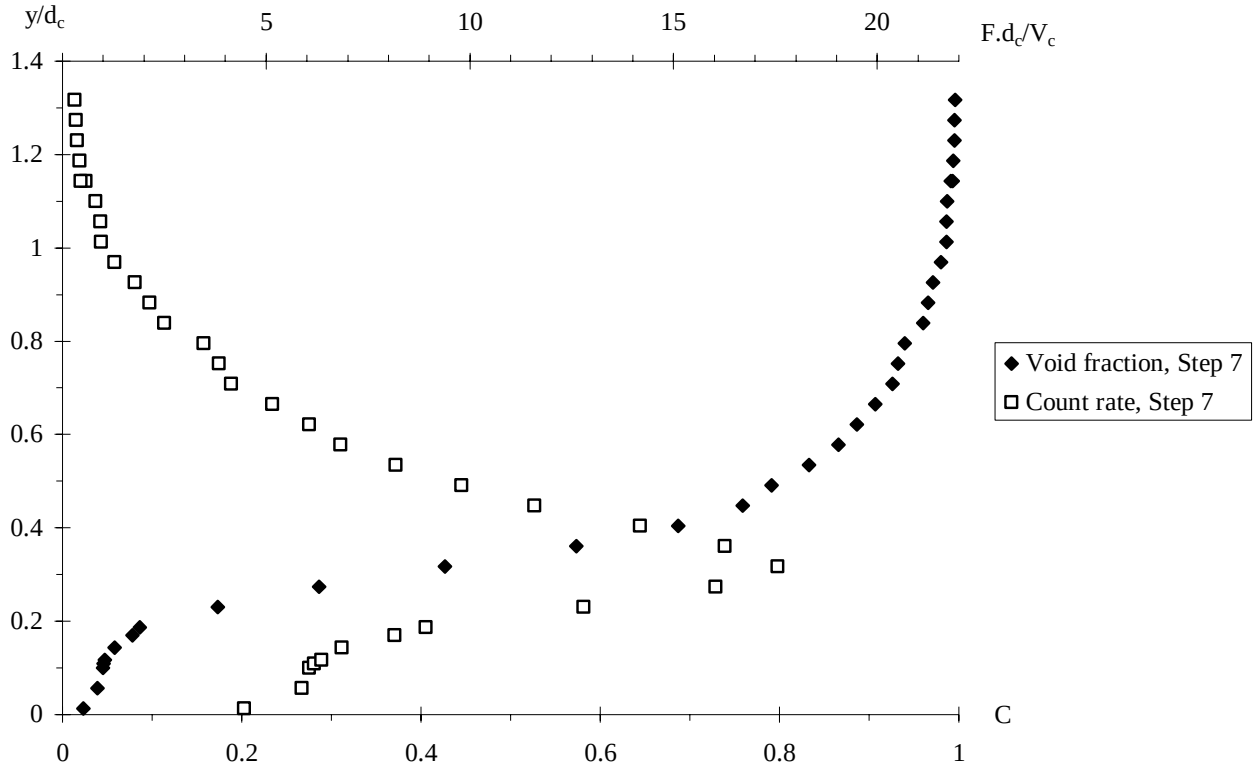


(B) Step edge 8

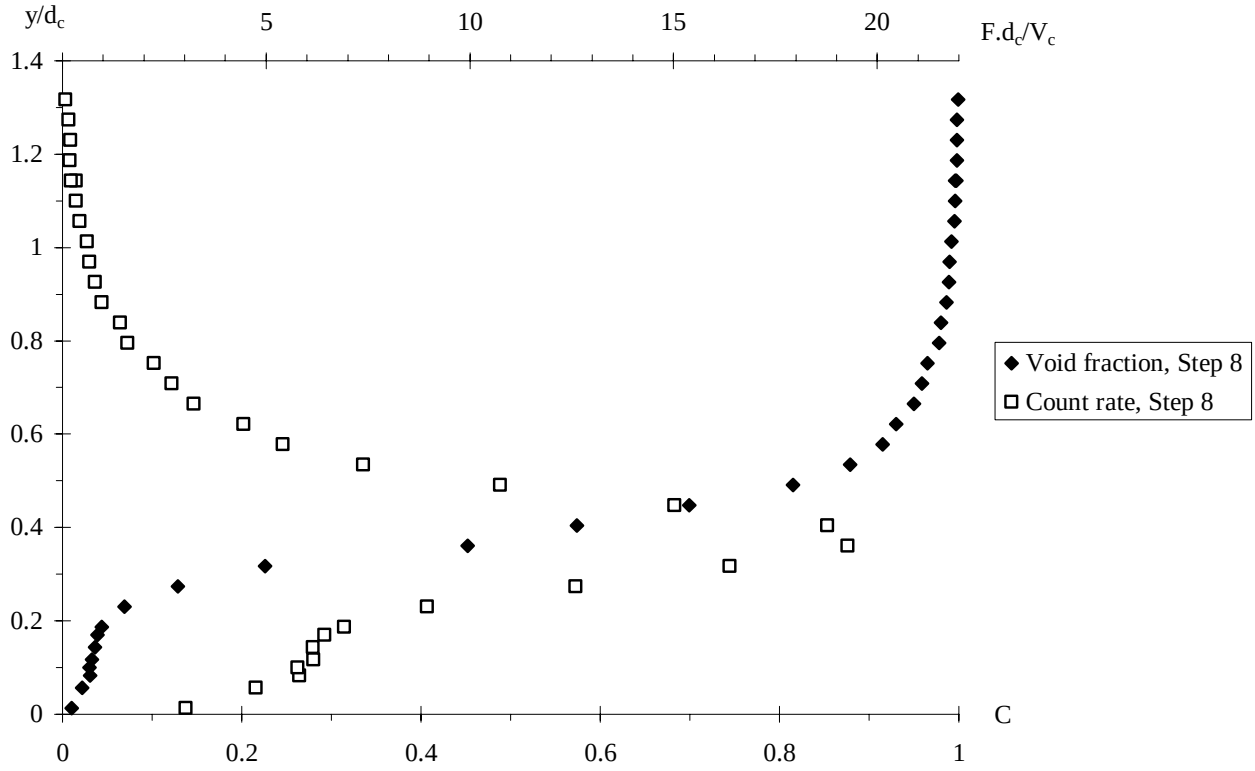

(C) Step edge 9

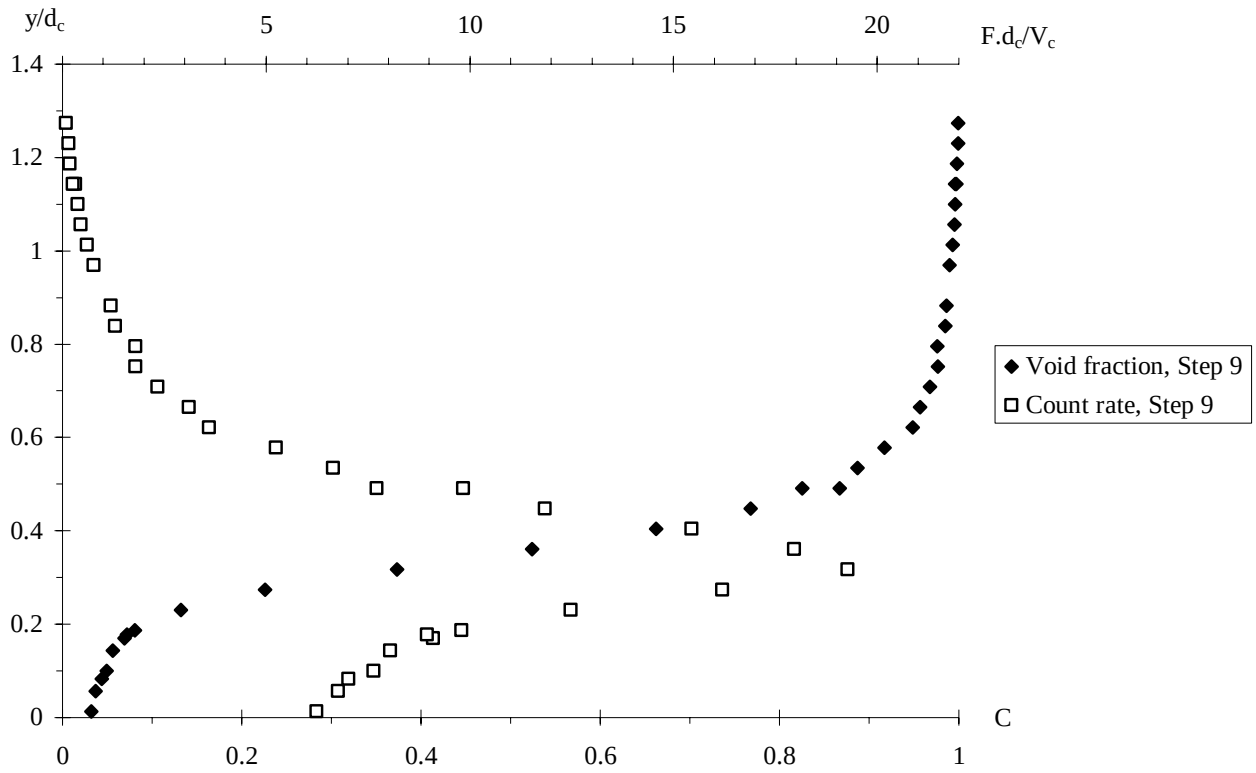


(D) Step edge 10

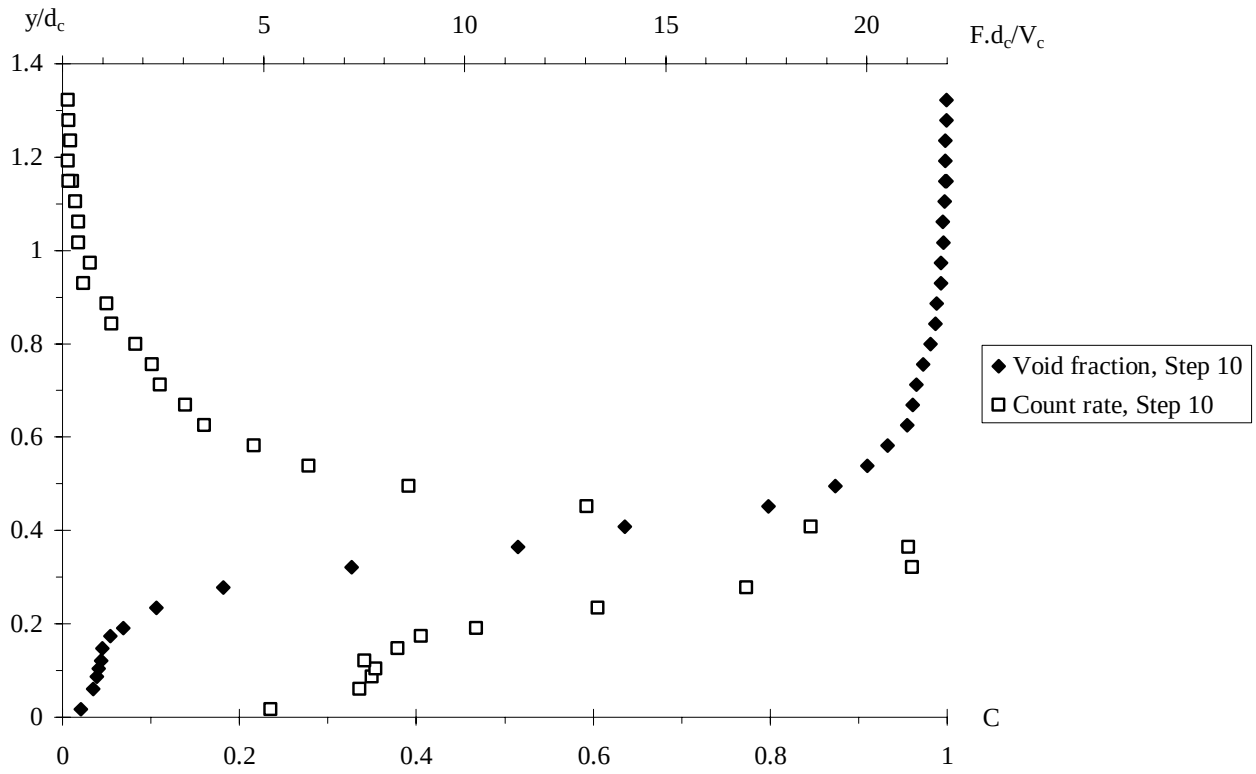

Fig. 5-2 - Dimensionless distributions of void fraction C as functions of $y/Y_{90}$ - Comparison between Equation (5-3) and experimental data

(A) $d_C/h = 1.33$, double-tip probe ($\varnothing = 0.25$ mm)

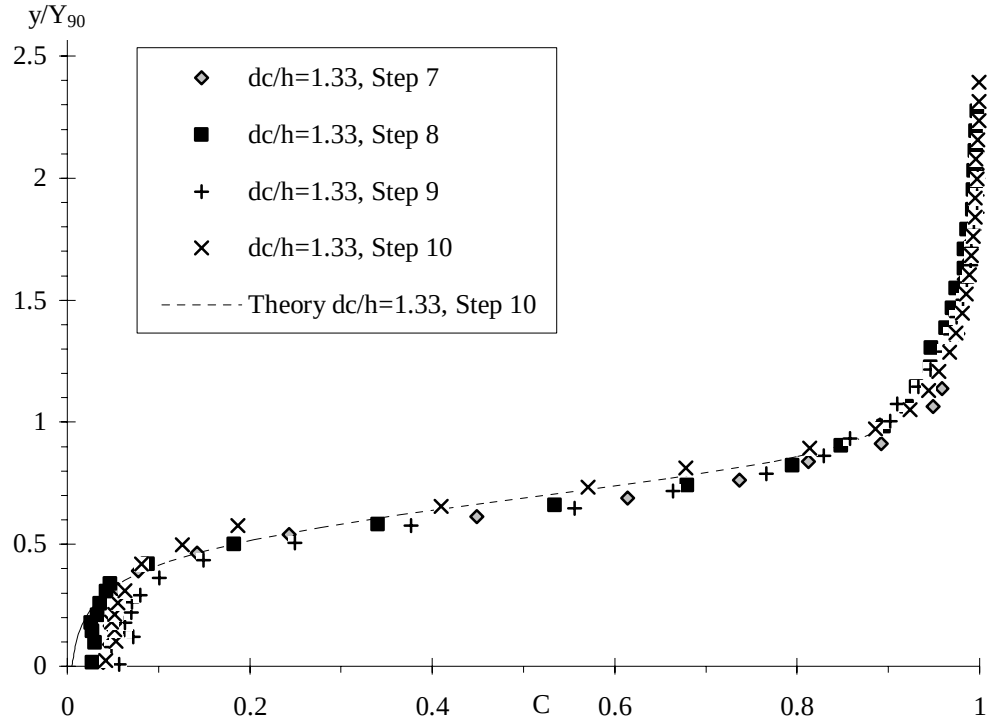


(B) $d_C/h = 1.57$, single-tip probe ($\varnothing = 0.35$ mm)

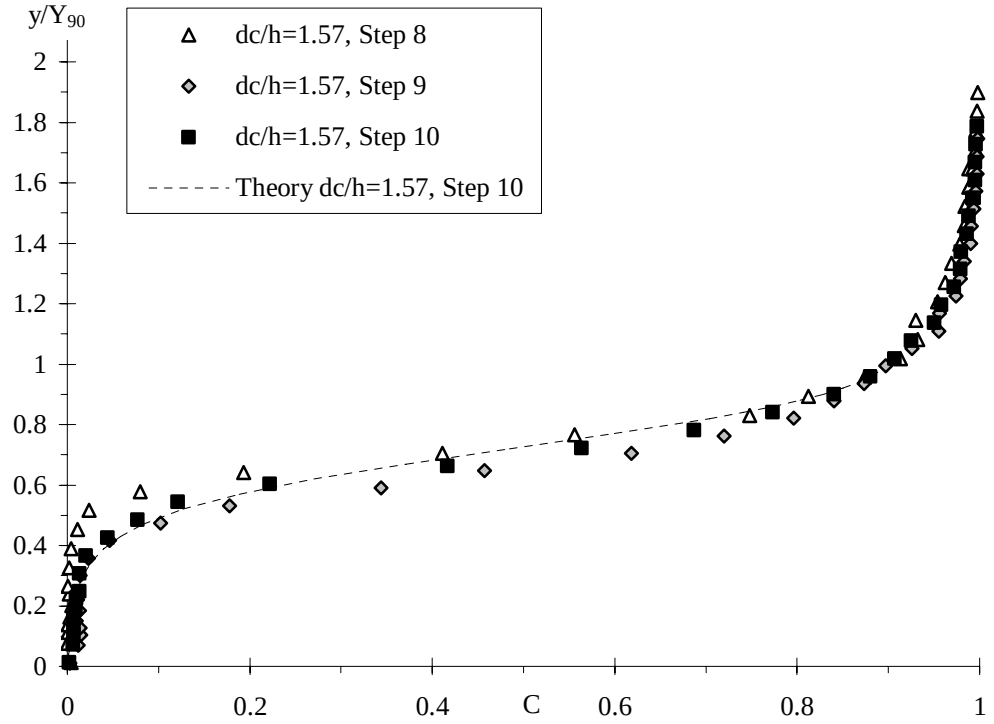

Fig. 5-3 - Air concentration distributions in prototype stepped spillway : comparison with Equation (5-3) - Measurements at Brushes Clough dam spillway (BAKER 1994) with inclined downward steps ($\theta$ = 18.4º, h = 0.19 m, $\delta$ = - 5.6º)

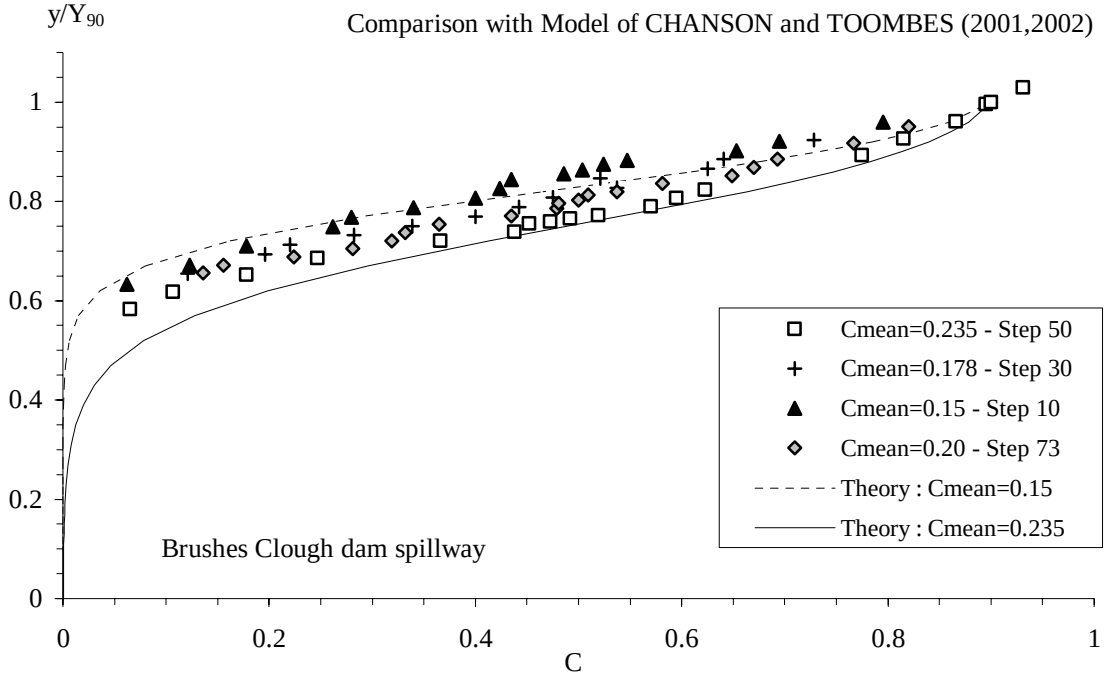


Remarks

Although developed for smooth chute flows at uniform equilibrium (CHANSON and TOOMBES 2001), Equation (5-3) was tested successfully against skimming flow data on prototype stepped chutes and near-full scale facilities as shown in Figure 5-3. A similar comparison between model and prototype data was performed by CHANSON and TOOMBES (1997, Fig. 5-4). This comparative analysis shown in Figure 5-3 is a rare model-prototype comparison suggesting little scale effects in terms of void fraction distributions in skimming flows.

*5.1.2 Bubble count rate distribution*

Typical dimensionless distributions of bubble count rate are presented in Figure 5-1. The data were recorded at several step edges for one flow rate. The data showed consistently a characteristic shape with a maximum value observed for void fractions between 35 and 60%. A similar pattern was observed in smooth chute and stepped spillway flows (e.g. CHANSON 1997b, CHANSON and TOOMBES 2001, TOOMBES 2002, GONZALEZ and CHANSON 2004, KOKPINAR 2005).

The relationship between bubble frequency and void fraction exhibited systematically a characteristic parabolic shape :

$$\frac{F}{F_{max}} = 4 * C * (1 - C) \quad (5\text{-}7)$$

where the maximum bubble frequency $F_{max}$ occurs at about C ~ 0.5. Equation (5-7) is compared with experimental data in Figure 5-4. For the present study, the maximum bubble count rate was observed for $0.35 \leq C \leq 0.6$ although most data sets were within $0.4 \leq C \leq 0.5$. TOOMBES (2002) demonstrated some

theoretical validity of Equation (5-7) and he extended the reasoning to air-water flow situations when the maximum bubble count rate is observed for $C \neq 0.5$ (TOOMBES 2002, pp. 190-195).

Discussion

TOOMBES (2002) proposed a better predictive model based upon the characteristics of the streamwise structure of the air-water flow. He introduced two correction factors $\alpha$ and $\beta$ that are functions of the local void fraction and flow conditions :

$$F = \frac{V}{\alpha * \beta * \lambda} * C * (1 - C) \qquad (5\text{-}8)$$

where V is the interfacial velocity, and $\lambda$ is a constant length scale factor. Basically $\lambda$ is a length scale such that the probability of a discrete element ([2]) of that size being air or water is independent of the surrounding segments. The correction factor $\alpha$ accounts for the average size of discrete air elements having a different value to the average size of water elements at any given point, while the correction factor $\beta$ allows for variations of discrete element length scales with the void fraction. Equation (5-8) was derived on the basis of theoretical considerations and it was successfully compared with experimental data for a wide range of flow situations (TOOMBES 2002).

Fig. 5-4 - Dimensionless relationship between bubble count rate and void fraction C in skimming flows - Comparison between Equation (5-7) and experimental data

(A) $d_c/h = 1.0$, single-tip probe ($\varnothing = 0.35$ mm)

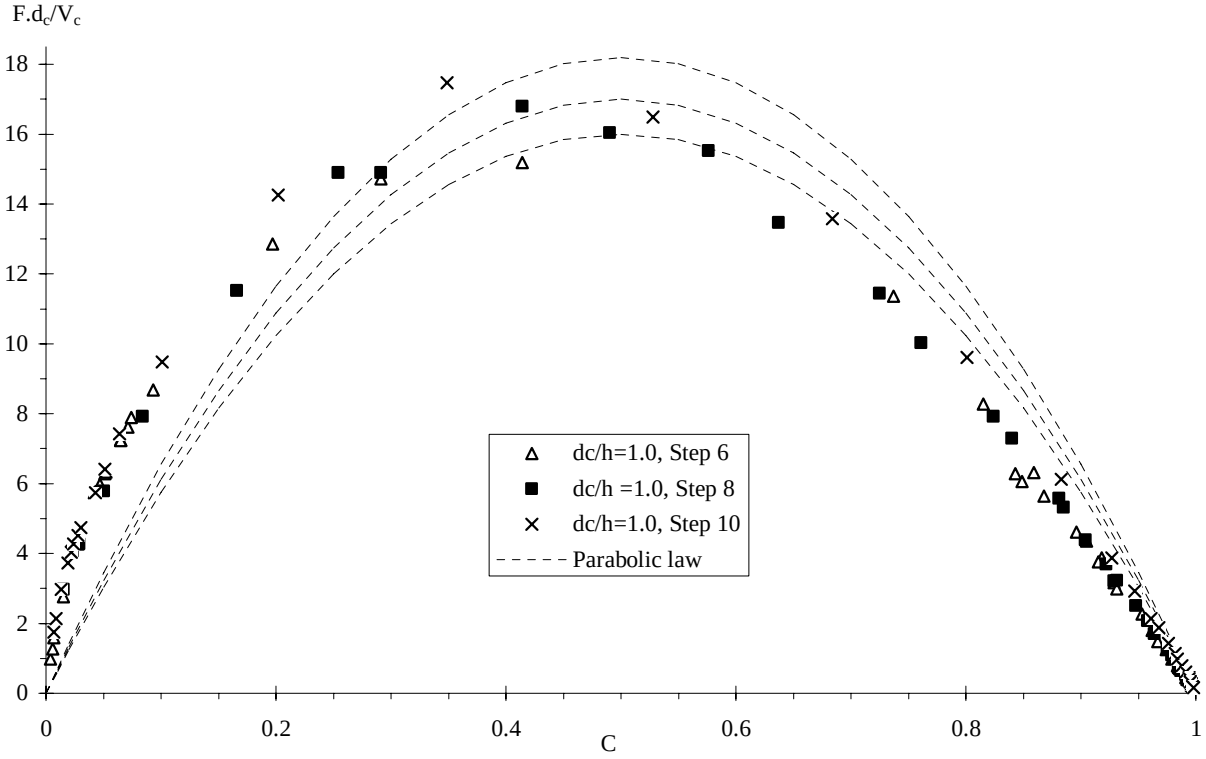


[2]Herein the term "element" denotes chord length or chord time.

(B) $d_C/h = 1.57$, single-tip probe (∅ = 0.35 mm)

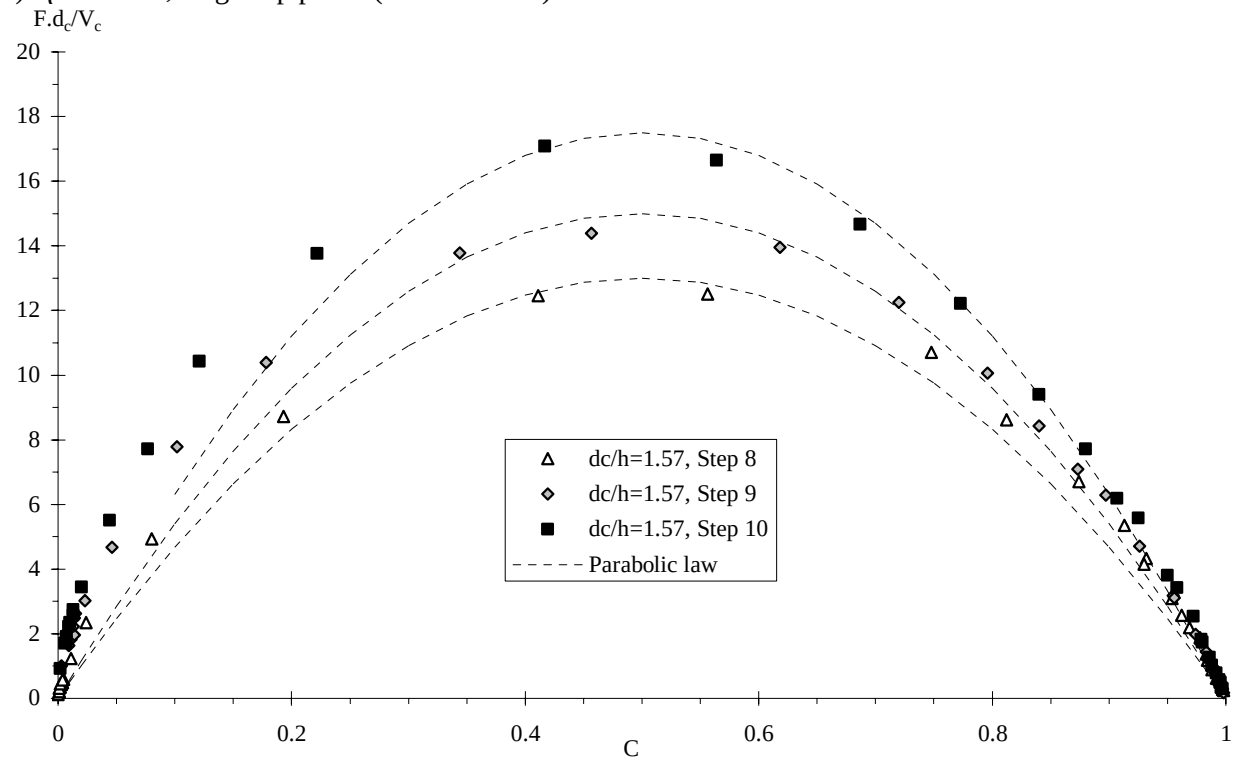


Another reasoning yields a relationship similar to Equations (5-7) and (5-8). The bubble count rate F equals half of the number of air-water interfaces. That is, F must be proportional to the rate of change of the instantaneous void fraction $c$ :

$$F \propto c_{rms}^2 = C * (1 - C) \quad (5\text{-}9)$$

where $c$ equals 0 or 1. The probability distribution function of the instantaneous void fraction $c$ is bi-modal. Simple considerations show that its variance $c_{rms}^2$ equals C*(1 - C) where the void fraction C is the time-averaged local void fraction. In Equation (5-7), the coefficient of proportionality between F and $c_{rms}^2$ is $4*F_{max}$.

Note that the variance of instantaneous void fraction is physically meaningless in itself because it depends only on the time-averaged void fraction : $c_{rms}^2 = C*(1 - C)$. Its relevance is restricted to some understanding of the relationship between bubble count rate and time-averaged void fraction (Eq. (5-9)) and for its correlation to the velocity fluctuations which plays some role in the drag reduction process (MURAI et al. 2006).

## 5.2 Interfacial velocity and turbulence level distributions

At each step edge, the time-averaged velocity and turbulent velocity fluctuation profiles showed some characteristic shapes (Fig. 5-5). The interfacial velocity distributions presented a smooth shape similar to earlier results on stepped chutes (e.g. BOES 2000a, CHANSON and TOOMBES 2002a, YASUDA and CHANSON 2003, GONZALEZ 2005). The turbulent intensity profiles exhibited some maximum turbulence level for $0.3 \leq y/d_C \leq 0.4$ which corresponded to about $C \approx 0.4$ to 0.6 (Fig. 5-5).

The interfacial velocity distributions showed some self-similarity (Fig. 5-5 & 5-6). All the time-averaged velocity distributions followed closely a power-law function for $y/Y_{90} \leq 1$. For $y/Y_{90} > 1$, the velocity profile was quasi-uniform. That is :

$$\frac{V}{V_{90}} = \left(\frac{y}{Y_{90}}\right)^{1/N} \qquad 0 \leq \frac{y}{Y_{90}} \leq 1 \quad (5\text{-}10)$$

$$\frac{V}{V_{90}} = 1 \qquad 1 \leq \frac{y}{Y_{90}} \leq 2.5 \quad (5\text{-}11)$$

where $V_{90}$ is the characteristic air-water velocity at $y = Y_{90}$. Several researchers observed the velocity profile described by Equation (5-10) (e.g. MATOS 2000, BOES 2000a, CHANSON and TOOMBES 2002a). But few studies documented the velocity distribution in the upper spray region (GONZALEZ 2005).

Present data are compared with Equations (5-10) and (5-11) in Figure 5-6. For the present experiments, the exponent N was about 10, although it varied between a step edge and the next consecutive step edge for a given flow rate. The variations are believed to reflect some flow interactions between adjacent shear layers and cavity flows.

In the upper flow region, the flow structure consisted predominantly of individual water droplets and packets surrounded by air. The present results showed a quasi-uniform velocity profile for $y > Y_{90}$ and the finding tended to suggest that most droplets were in a free-fall trajectory. Since the ejected droplets had a response time of nearly two orders of magnitude larger than that of the surrounding air flow, their velocity was dominated by the ejection process.

Fig. 5-5 - Dimensionless distributions of time-averaged interfacial velocity $V/V_C$ and turbulence intensity Tu for $d_C/h$ = 1.15, 1.33 and 1.45 at step edge 10

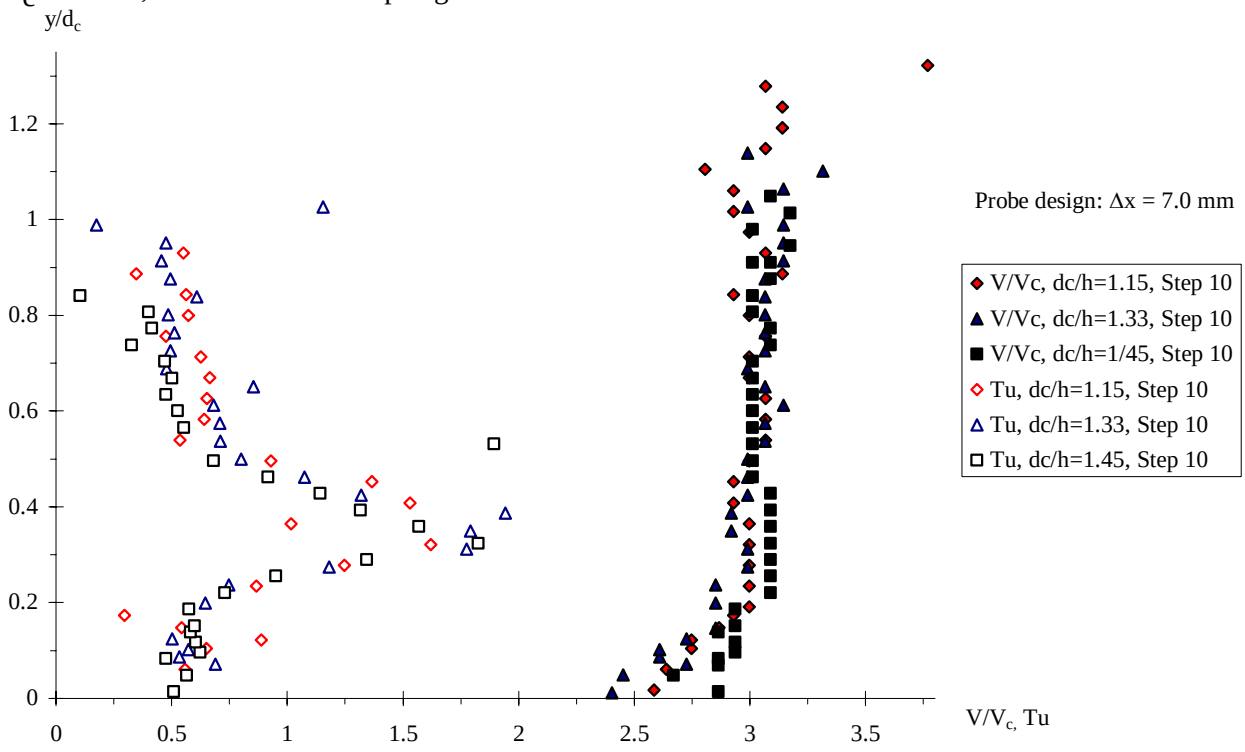

Fig. 5-6 - Dimensionless time-averaged interfacial velocity distributions - Comparison with a 1/10 power law (Eq. (5-10)) and with Equation (5-11)

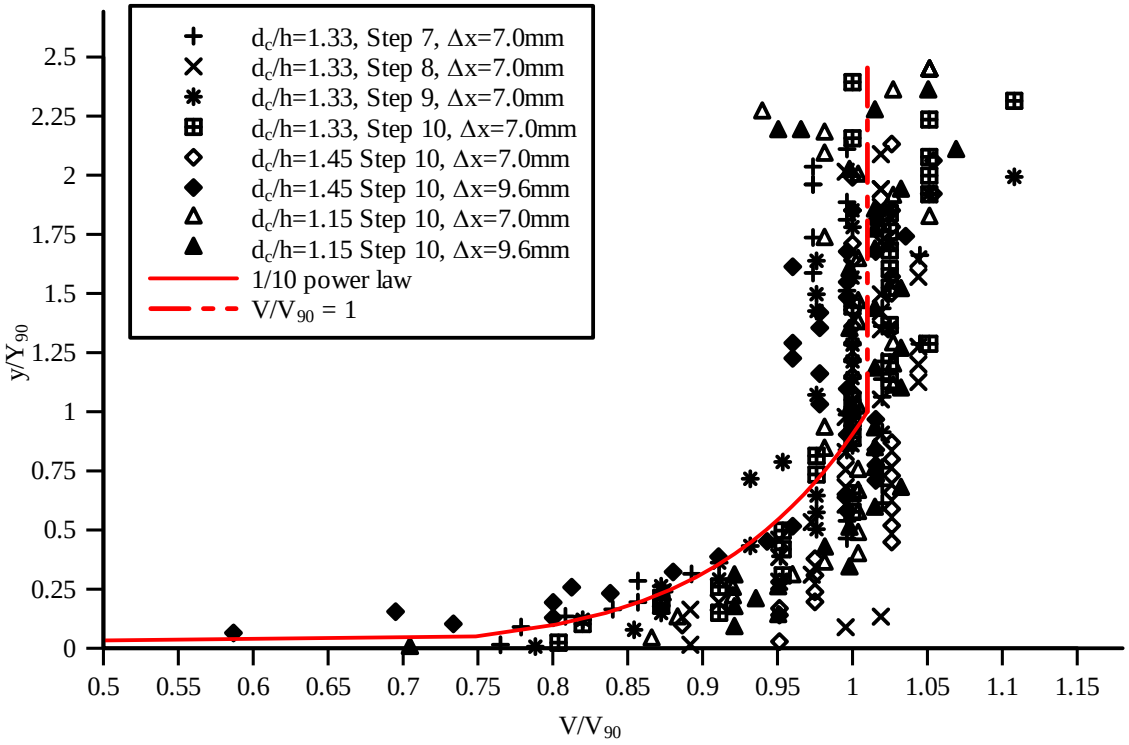


The present data showed some strong correlation between the turbulence intensity Tu and the bubble count rate. This is illustrated in Figure 5-7 presenting the turbulence intensity Tu as a function of the dimensionless bubble count rate $F*d_c/V_c$. The data collapsed relatively well into a single curve :

$$Tu = 0.25 + a * \left(\frac{F * d_c}{V_c}\right)^b \quad (5\text{-}12)$$

with a = 0.035 and b = 1.2 for the present data set. CHANSON and TOOMBES (2002a) proposed first such a relationship that was also observed by YASUDA and CHANSON (2003) and GONZALEZ et al. (2005). Equation (5-12) reflects a monotonic increase in turbulence levels with an increase in bubble count rate. The limit for F = 0 is Tu = 0.25 that is close to monophase flow measurements on a stepped chute upstream of the inception point of free-surface aeration (OHTSU and YASUDA 1997, AMADOR et al. 2004a). It is hypothesised that the large number of air-water interfaces associated with high air-water count rates contributes to some increased turbulence levels compared to clear-water skimming flows. For $0.05 \leq C \leq 0.95$, the air-water flow structure is dominated by collisions between bubbles, droplets and packets, and by interactions between particles and turbulent shear. These dynamic processes yield large fluctuations in air-water interfacial velocity and high turbulence levels. The continuous deformations and modification of the air-water interfacial structure do induce large turbulence levels measured by the intrusive phase-detection probe (in this case the double-tip conductivity probe).

Fig. 5-7 - Dimensionless relationship between turbulence intensity Tu and bubble count rate $F*d_C/V_C$ - Comparison between data and Equation (5-12)

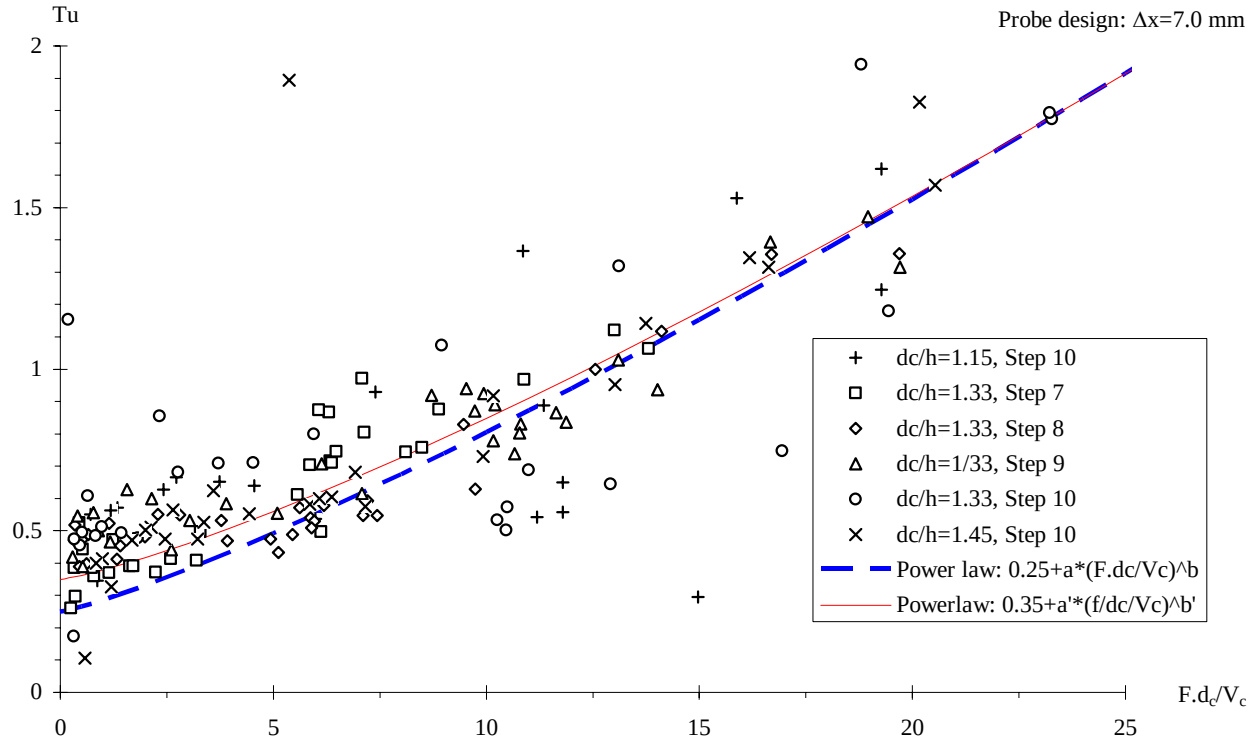


## 5.3 Probability distribution functions of air bubble and water droplet chords

The probability distribution functions of chord sizes were analysed in terms of bubble chords in the bubbly flow (C < 0.3) and in terms of droplet chord lengths in the spray region (C > 0.7). Typical results are presented in Figure 5-8 which shows some examples of normalised chord size distributions. For each graph, the caption and legend provide the local air-water flow properties (C, F) and probe details. The histogram columns represent each the probability of chord size in a 0.5 mm chord interval. For example, the probability of bubble chords between 1 and 1.5 mm is represented by the column labelled 1 mm. Chord sizes larger than 15 mm are regrouped in the last column (> 15).

In the bubbly flow region (C < 0.3), the probability distribution functions showed a broad spectrum of bubble chords at each location. The range of bubble chord extended from less than 0.3 mm to more than 15 mm (Fig. 5-8). The bubble chord size distributions were skewed with a preponderance of small bubbles relative to the mean. In Figure 5-8, the mode of the probability distribution function was observed for chords between 0.5 and 1.5 mm. The probability distribution functions of bubble chord tended to follow a log–normal distribution at all locations and for all discharges. The result is consistent with the earlier data of CHANSON and TOOMBES (2002a) and GONZALEZ et al. (2005) in skimming flows.

In the spray region, the probability distribution functions of drop sizes showed also a wide range of droplet chords at each location. While the droplet chord size distributions were skewed with a preponderance of small droplets, the probability density function was flatter than that of the bubble chords (Fig. 5-8). In the upper spray region (C > 0.95), the probability distribution functions did not follow a log-normal distribution.

Fig. 5-8 - Probability distribution functions of chord sizes in skimming flows

(A) $d_C/h$ = 1.15, Step 10, double-tip probe (∅ = 0.25 mm, Δx = 7.0 mm)

(A1) Bubble chord size data (C < 0.3)

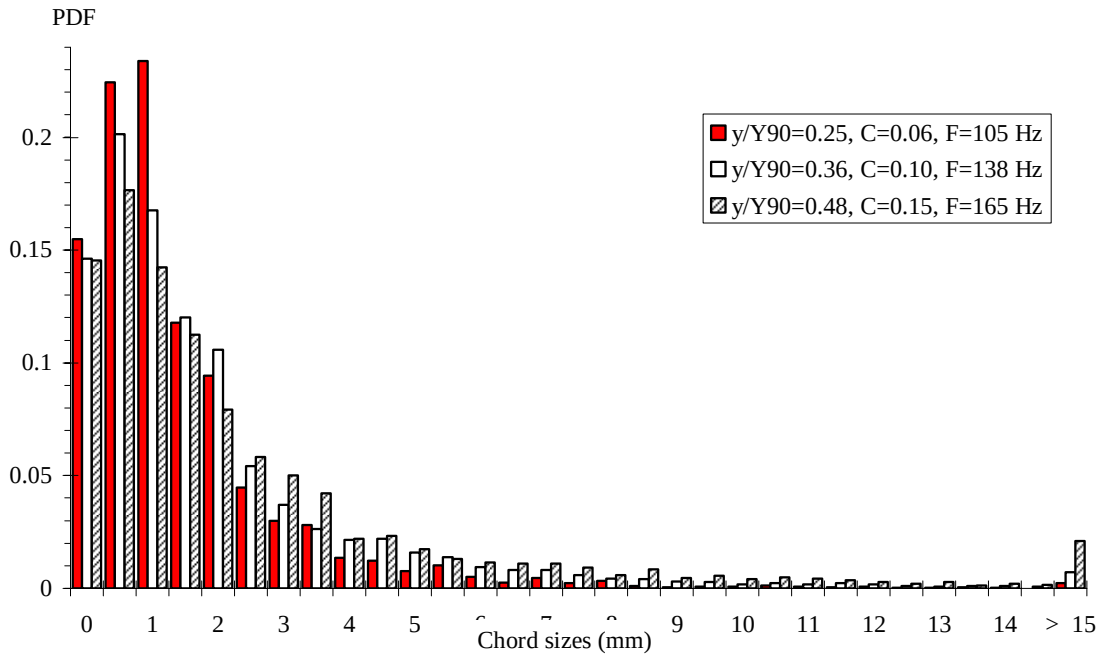


(A2) Droplet chord size data (C > 0.7)

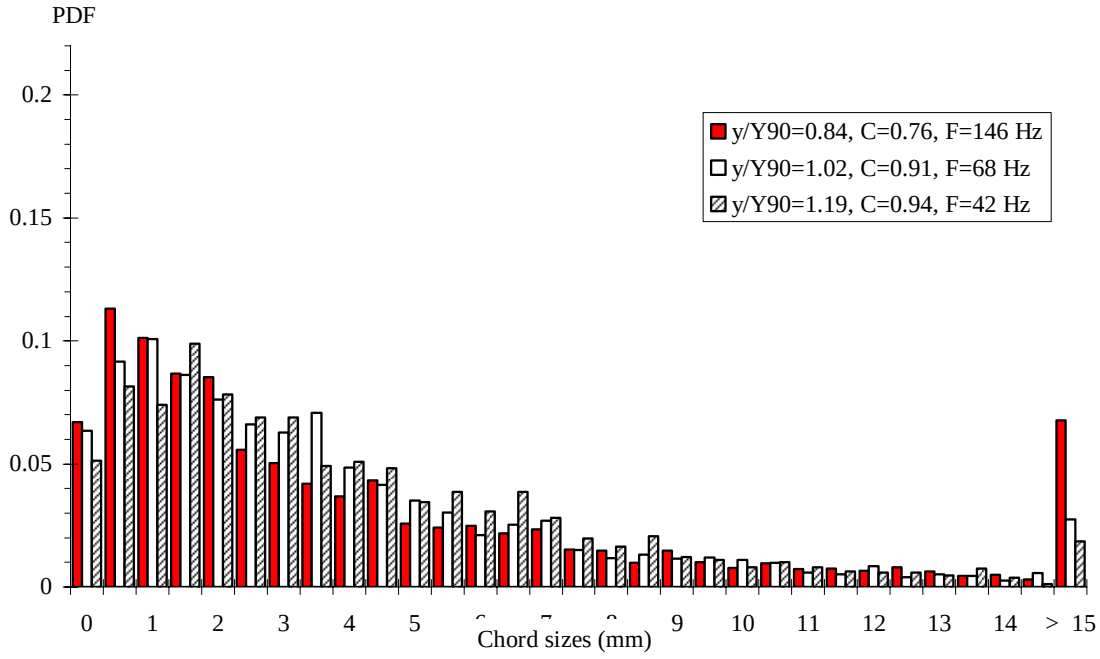

(B) $d_C/h$ = 1.45, Step 10, double-tip probe (∅ = 0.25 mm, Δx = 7.0 mm)

(B1) Bubble chord size data (C < 0.3)

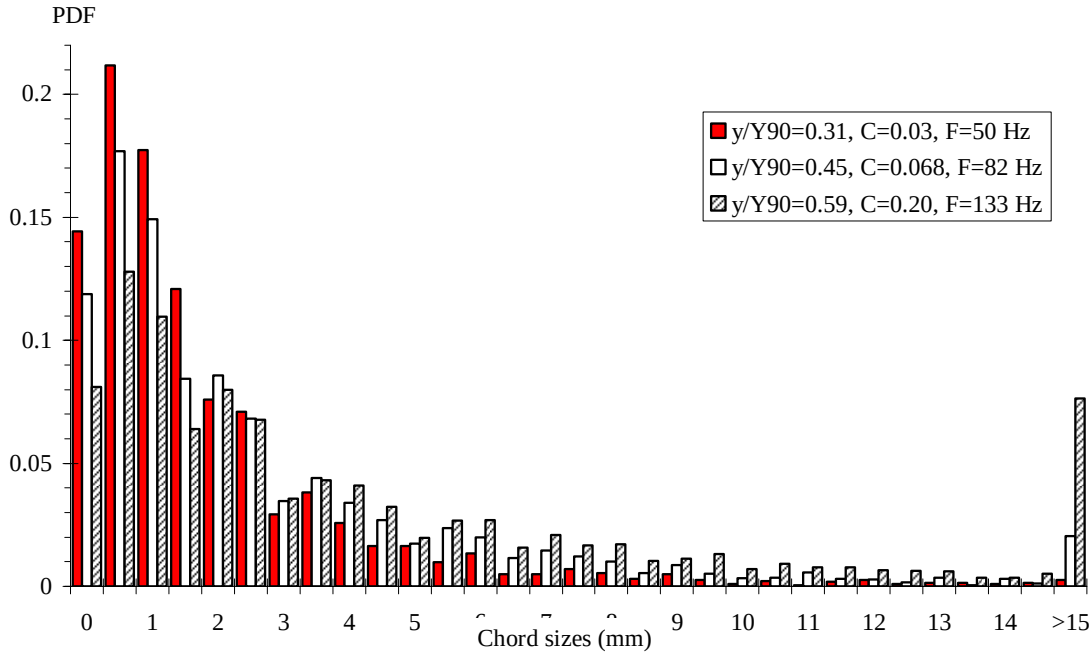


(B2) Droplet chord size data (C > 0.7)

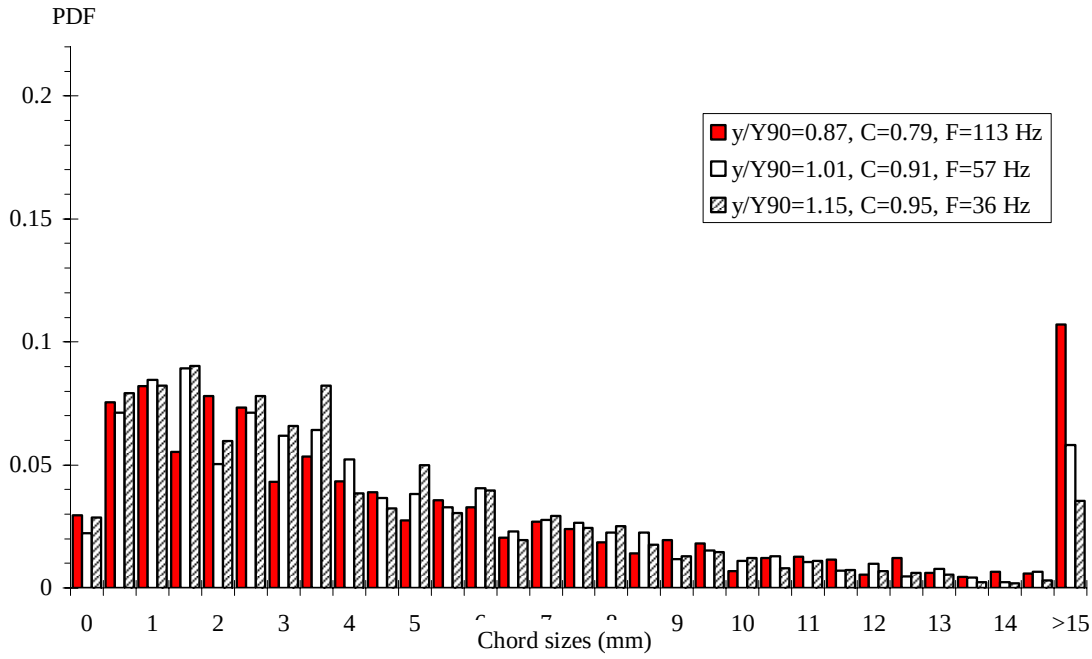

# 6. INTEGRAL TURBULENT TIME AND LENGTH SCALES IN AIR-WATER SKIMMING FLOWS

## 6.1 Presentation

The correlation analyses were applied to some experiments during which two identical sensors separated by a distance Y were recorded simultaneously (Table 6-1). For some experiments, the probe sensors were located at the same vertical and streamwise distances y and x respectively, but they were separated in the transverse direction by a known distance $\Delta z$. For the experiments using the dual-tip probe, both sensors were located at the same vertical distance y, but they were separated in the streamwise direction by a known distance $\Delta x$.

Auto- and cross-correlation analyses were performed on the raw probe output signals (paragraph 3.4). Basic results included the maximum cross-correlation coefficient $(R_{xy})_{max}$, and the correlation time scales $T_{xx}$ and $T_{xy}$ where :

$$T_{xx} = \int_{\tau=0}^{\tau=\tau(R_{xx}=0)} R_{xx}(\tau) * d\tau \quad (6\text{-}1)$$

$$T_{xy} = \int_{\tau=\tau(R_{xy}=(R_{xy})_{max})}^{\tau=\tau(R_{xy}=0)} R_{xy}(\tau) * d\tau \quad (6\text{-}2)$$

where $R_{xx}$ is the normalised auto-correlation function, $\tau$ is the time lag, $R_{xy}$ is the normalised cross-correlation function between probe output signals, and $(R_{xy})_{max}$ the maximum cross-correlation coefficient (paragraph 3.4). Further relevant experimental results included the integral turbulent length scale $L_{xy}$, the integral turbulent time scale $\mathbf{T}$ and the advection length scale $L_{xx}$ that are defined as :

$$L_{xy} = \int_{Y=0}^{Y=Y((R_{xy})_{max}=0)} (R_{xy})_{max} * dY \quad (6\text{-}3)$$

$$\mathbf{T} = \frac{\int_{Y=0}^{Y=Y((R_{xy})_{max}=0)} (R_{xy})_{max} * T_{xy} * dY}{L_{xy}} \quad (6\text{-}4)$$

$$L_{xx} = V * T_{xx} \quad (6\text{-}5)$$

where Y is the separation distance between probe sensors and V is the interfacial velocity.

Present experimental flow conditions are summarised in Table 6-1. All correlation analysis results are reported in Appendices D and E.

Table 6-1 - Experimental measurements in skimming flows with identical probe sensors (Present study)

| $q_W$ | $\frac{d_C}{h}$ | Re | Instrumentation | $\Delta x$ | $\Delta z$ | Step edge | Comments |
|---|---|---|---|---|---|---|---|
| $m^2/s$ | | | | mm | mm | | |
| (1) | (2) | (3) | (4) | (5) | (6) | (7) | (8) |
| 0.116 | 1.15 | 4.6 E+5 | 2 single-tip probes | 0 | 8.45 | 7 | Run 060410a. |
| | | | | 0 | 8.45 | 8 | Run 060410b. |
| | | | | 0 | 8.45 | 9 | Run 060410c. |
| | | | | 0 | 3.6 | 10 | Run 0604508b. |
| | | | | 0 | 6.3 | 10 | Run 060412c. |
| | | | | 0 | 8.45 | 10 | Run 060411a. |
| | | | | 0 | 10.75 | 10 | Run 060411b. |
| | | | | 0 | 13.7 | 10 | Run 060411c. |
| | | | | 0 | 16.7 | 10 | Run 060412a. |
| | | | | 0 | 21.7 | 10 | Run 060412b. |
| | | | | 0 | 29.5 | 10 | Run 060413a. |
| | | | | 0 | 40.3 | 10 | Run 060508a. |
| 0.161 | 1.45 | 6.4 E+5 | 2 single-tip probes | 0 | 8.45 | 8 | Run 060512a. |
| | | | | 0 | 8.45 | 9 | Run 060512b. |
| | | | | 0 | 3.6 | 10 | Run 060509a. |
| | | | | 0 | 8.45 | 10 | Run 060511b. |
| | | | | 0 | 13.7 | 10 | Run 060509b. |
| | | | | 0 | 21.7 | 10 | Run 060510a. |
| | | | | 0 | 40.3 | 10 | Run 060510b. |
| | | | | 0 | 55.7 | 10 | Run 060511a. |
| 0.116 | 1.15 | 4.6 E+5 | 1 dual-tip probe | 7.0 | 1.4 | 10 | Run 060530a. |
| | | | | 9.6 | 1.4 | 10 | Run 060613a. |
| 0.143 | 1.33 | 5.7 E+5 | 1 dual-tip probe | 7.0 | 1.4 | 7 | Run 060614a. |
| | | | | 7.0 | 1.4 | 8 | Run 060614b. |
| | | | | 7.0 | 1.4 | 9 | Run 060615a. |
| | | | | 7.0 | 1.4 | 10 | Run 060615b. |
| 0.161 | 1.45 | 6.4 E+5 | 1 dual-tip probe | 7.0 | 1.4 | 10 | Run 060530b. |
| | | | | 9.6 | 1.4 | 10 | Run 060613b. |

Notes : $d_C$ : critical flow depth; Re : Reynolds number defined in terms of the hydraulic diameter; W : channel width.

*Correlation functions*

The correlation functions exhibited similar patterns for all investigated flow conditions with either a transverse or longitudinal separation (Table 6-1). Typical auto- and cross-correlation functions are presented in Figures 6-1 and 6-2.

The auto-correlation functions did not follow a Gaussian error function. Overall the auto-correlation functions $R_{XX}$ were best fitted by :

$$R_{XX} = \frac{1}{1 + \left(\frac{\tau}{T_{0.5}}\right)^{1.3}} \quad (6\text{-}6)$$

where $\tau$ is the time lag and $T_{0.5}$ is the time lag for which $R_{xx} = 0.5$. Figure 6-1 presents some comparison between Equation (6-6) and experimental data.

The experimental results showed that the cross-correlation functions exhibited clearly a marked maximum $(R_{xy})_{max}$ and followed a symmetrical "Gaussian" shape (Fig. 6-2). The maximum cross-correlation $(R_{xy})_{max}$ was a function of the sensor separation distance Y. Typically $(R_{xy})_{max}$ decreased with increasing sensor separation Y as illustrated in Figure 6-3. Within the range of investigations (Table 6-1), the transverse cross-correlation maxima dropped sharply for $\Delta z > 0.040$ m. The cross-correlation functions $R_{xy}$ followed closely a Gaussian error function :

$$\frac{R_{xy}}{(R_{xy})_{max}} = \exp\left(-\frac{1}{1443} * \frac{(\tau - T)^2}{\tau_{0.5}}\right) \qquad \frac{\tau - T}{\tau_{0.5}} < 2 \quad (6\text{-}7)$$

where $(R_{xy})_{max}$ is the maximum normalised cross-correlation value observed for the time lag $\tau = T$, and $\tau_{0.5}$ is the time lag for which $R_{xy} = 0.5*(R_{xy})_{max}$ (Fig. 3-3). The finding (Eq. (6-7)) was observed systematically for all cross-correlation functions with both transverse and streamwise sensor separations. Figure 6-2 presents a comparison between Equation (6-7) and experimental results. Figure 6-2A shows some data for $0.1 < y/Y_{90} < 1.1$ with one transverse spacing, and Figure 6-2B presents some data obtained with several transverse spacings $\Delta z$. Experimental details are given in the figure captions and legends. The results indicated that the data fitted Equation (6-7) reasonably well for $(\tau\text{-}T)/\tau_{0.5} < 2$.

Some earlier studies reported streamwise cross-correlation function data that followed relatively closely a Gaussian error function (e.g. CHANSON 2002, CHANSON and TOOMBES 2002a). Note that the radius of curvature of the cross-correlation function at $\tau = T$ is $\lambda_r = 0.8493*\tau_{0.5}$.

Fig. 6-1 - Examples of auto-correlation functions - Flow conditions: $d_c/h = 1.15$, Re = 4.6 E+5, single-tip probe ($\varnothing$ = 0.35 mm), Step edge 10 - Comparison with Equation (6-6)

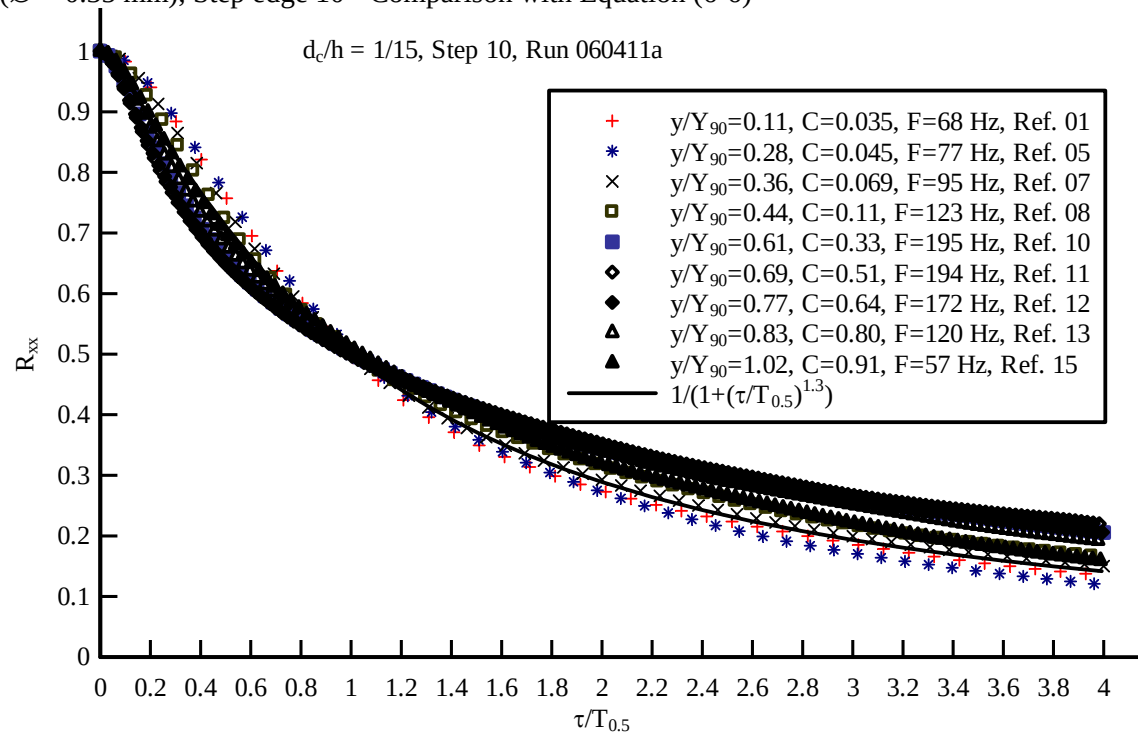

Fig. 6-2 - Examples of cross-correlation functions for two probe sensors separated by a transverse distance $\Delta z$ - Flow conditions: $d_c/h$ = 1.15, Re = 4.6 E+5, single-tip probe (∅ = 0.35 mm) - Comparison with Equation (6-7)

(A) Step edge 10, $\Delta z$ = 8.45 mm

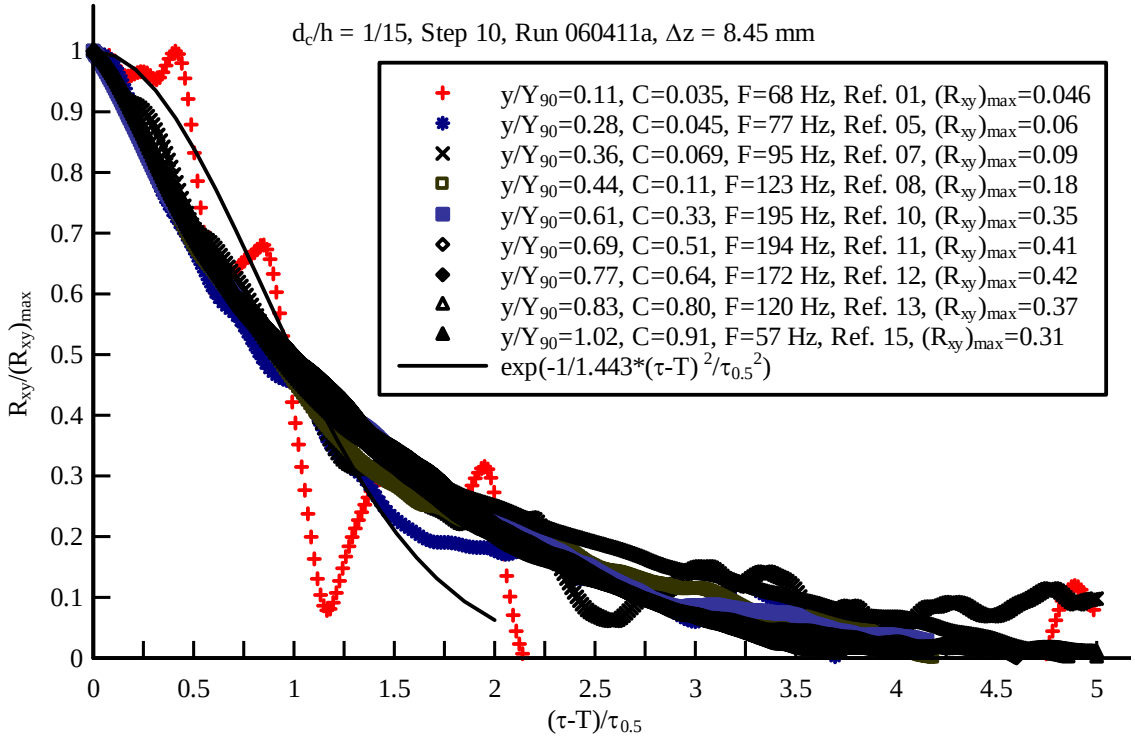


(B) Step edge 10, $y/Y_{90}$ = 0.44, C = 0.11, F = 123 Hz

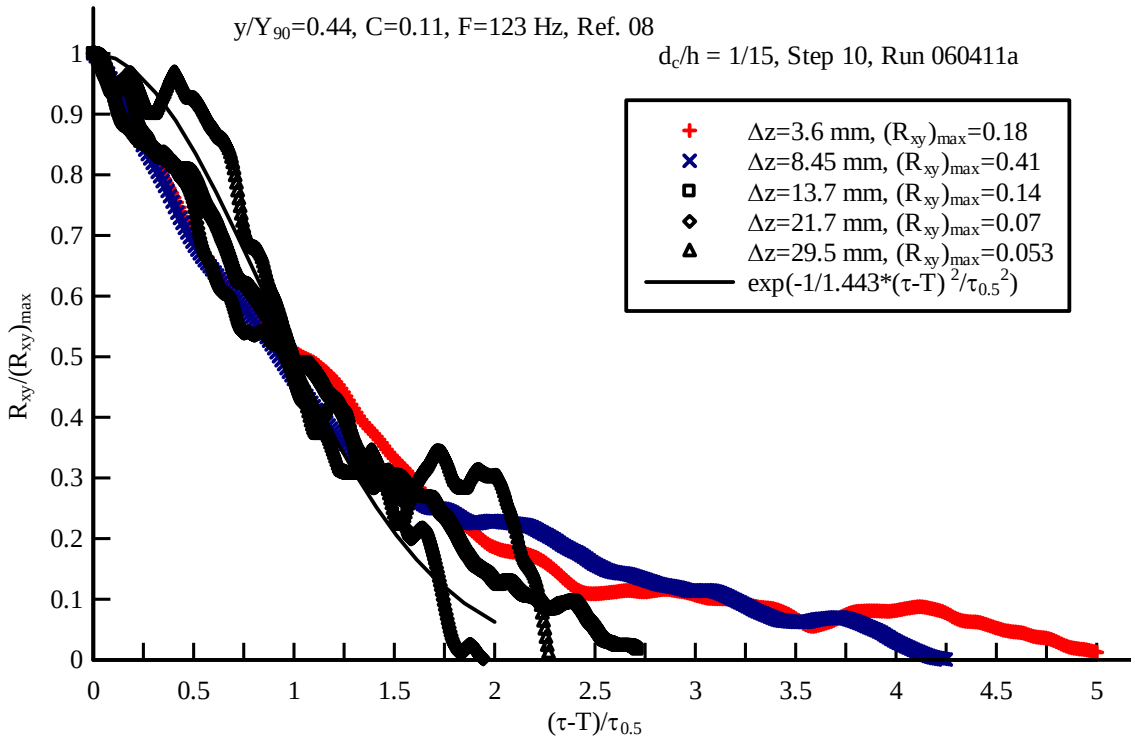

Fig. 6-3 - Dimensionless distributions of maximum cross-correlation coefficients between two probe sensors separated by a transverse distance Δz - Flow conditions: $d_C/h$ = 1.45, Re = 6.4 E+5, single-tip probe (∅ = 0.35 mm), Step edge 10

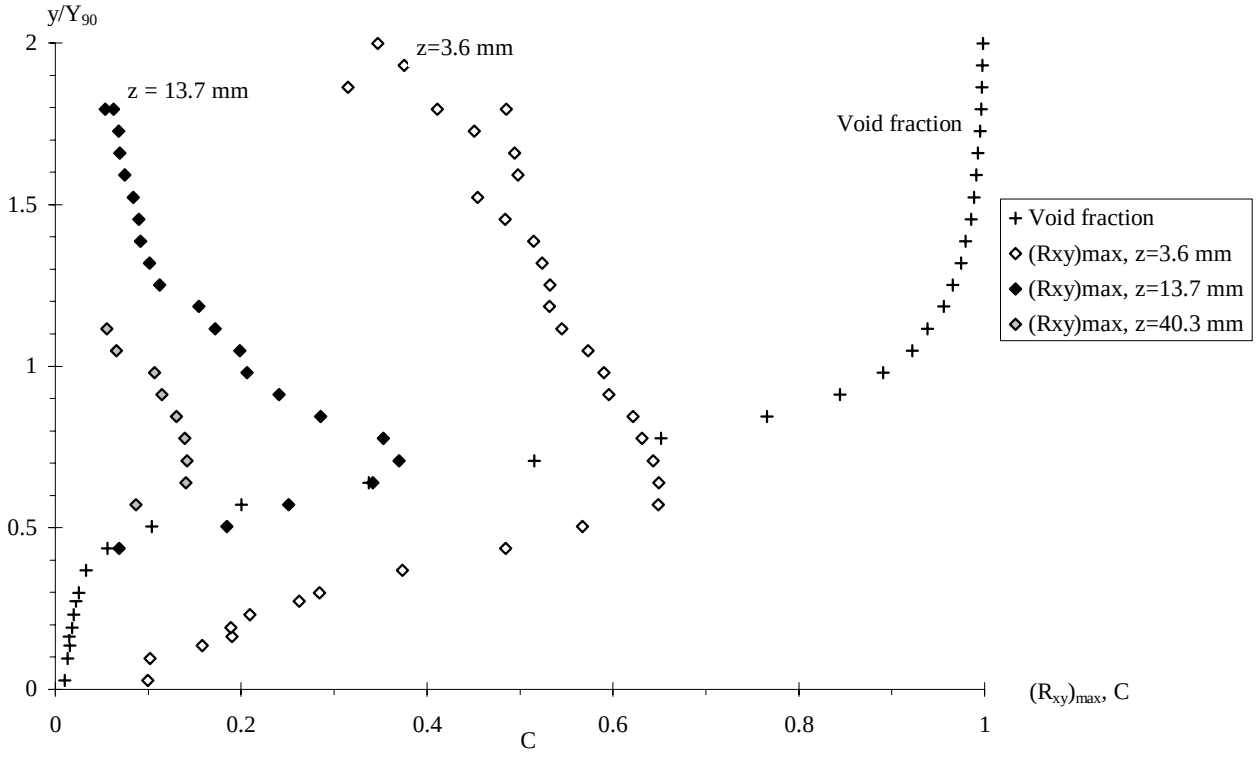


*Cross-correlation function : discussion*

In a developing boundary layer, FAVRE et al. (1957-58) observed that the transverse correlation coefficient of streamwise velocity dropped down to 0.2 at a transverse distance of about 0.1 to 0.15 times the boundary layer thickness δ. Their experiments were conducted in a 0.8 m wide smooth flat plate with hot-wire probes. The free-stream velocity was 12.2 m/s and the boundary layer thickness was about 33 mm.

In the present study, the transverse correlation coefficient between phase-detection probe signals dropped for a dimensionless transverse distance of about $\Delta z/h > 0.4$ and $\Delta z/Y_{90} > 2/3$. The results are of the same order of magnitude as the monophase flow results of FAVRE et al. (1957-58), and the differences may be a combination of differences in flow conditions, measurement and metrology.

## 6.2 Transverse integral time and length scales

Some typical distributions of correlation time scales $T_{XX}$ and $T_{XY}$ are presented in Figure 6-4. A definition sketch of typical skimming flow results is presented in Figure 6-4A. Figure 6-4B shows the vertical distributions of correlation time scales for several transverse spacings for the same flow conditions and at the same cross-section as the data shown in Figure 6-2. Note that the correlation time scales are presented in a dimensional form (units: seconds). Figure 6-4C presents a typical relationship between void fraction and correlation time scales at a given flow cross-section.

The results showed consistently that the auto-correlation time scales $T_{XX}$ were larger than the transverse cross-correlation time scales $T_{XY}$. $T_{XX}$ represents an integral time scale of the longitudinal bubbly flow

structures (Fig. 6-4). It is a characteristic time of the eddies advecting the air-water interfaces in the streamwise direction. $T_{xy}$ is a characteristic time scale of the vortices with a transverse length scale $\Delta z$ advecting the air-water flow structures. The cross-correlation time scale $T_{xy}$ was nearly independent of the transverse separation $\Delta z$ for $3 \leq \Delta z \leq 20$ mm, but it decreased with increasing transverse spacings for larger separation distances. This is illustrated in Figure 6-5. The present result suggested that some transverse length scale of the bubbly shear flow must be smaller than about 0.025 m or 0.25*h where h is the step height.

The relationship between the cross-correlation time scale $T_{xy}$ and the void fraction followed closely a parabolic law :

$$\frac{T_{xy}}{(T_{xy})_{max}} = 4 * C *(1 - C) \qquad (6\text{-}8)$$

where $(T_{xy})_{max}$ is the maximum cross-correlation time scale $T_{xy}$ in the cross-section for a given separation distance $\Delta z$. Equation (6-8) is compared with experimental data in Figure 6-4C. Experimental observations of maximum time scale $(T_{xy})_{max}$ are reported in Table 6-2.

Both the distributions of auto- and cross-correlation time scales $T_{xx}$ and $T_{xy}$ presented a similar parabolic shape for $0 \leq C \leq 0.95$ at all step edges and for all investigated flow rates (Fig. 6-4). However a marked change of shape for the auto-correlation time scale $T_{xx}$ distribution was systematically observed in the upper spray region ($C > 0.95$). This change in profile is sketched in Figure 6-4A and highlighted in Figures 6-4B and 6-4C with an arrow. It is suggested that the pattern may indicate a change in the spray structure with the upper spray region . For $C > 0.95$, the spray consisted primarily of ejected droplets that do not interact with the rest of the flow.

Fig. 6-4 - Distributions of auto- and cross-correlation time scales $T_{xx}$ and $T_{xy}$ in skimming flows for several transverse distances $\Delta z$

(A) Definition sketch

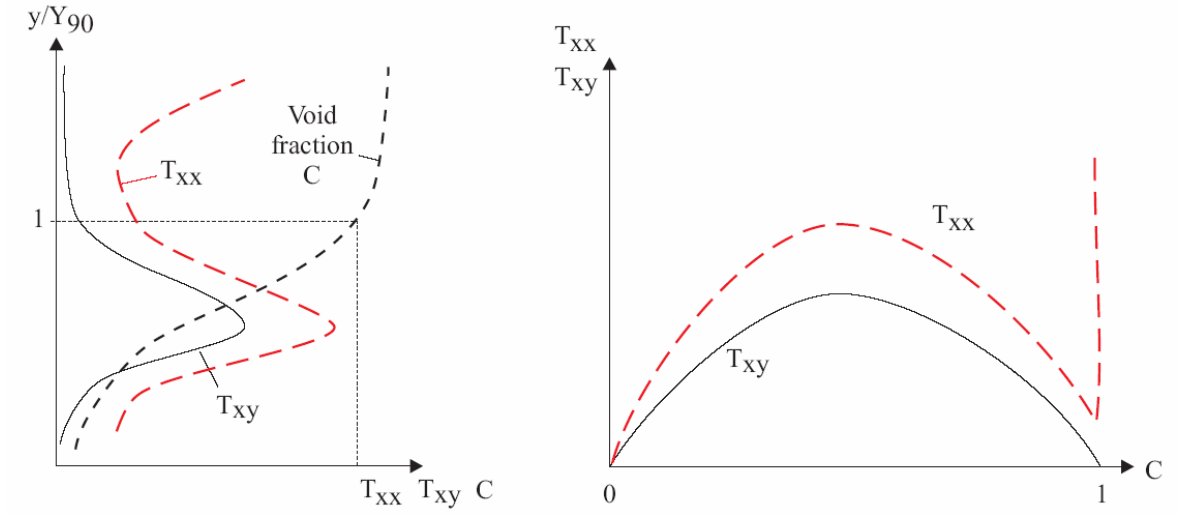

(B) Normal distributions for $d_C/h$ = 1.15, Re = 4.6 E+5, single-tip probe (∅ = 0.35 mm), Step edge 10 - Comparison with the measured void fraction distribution

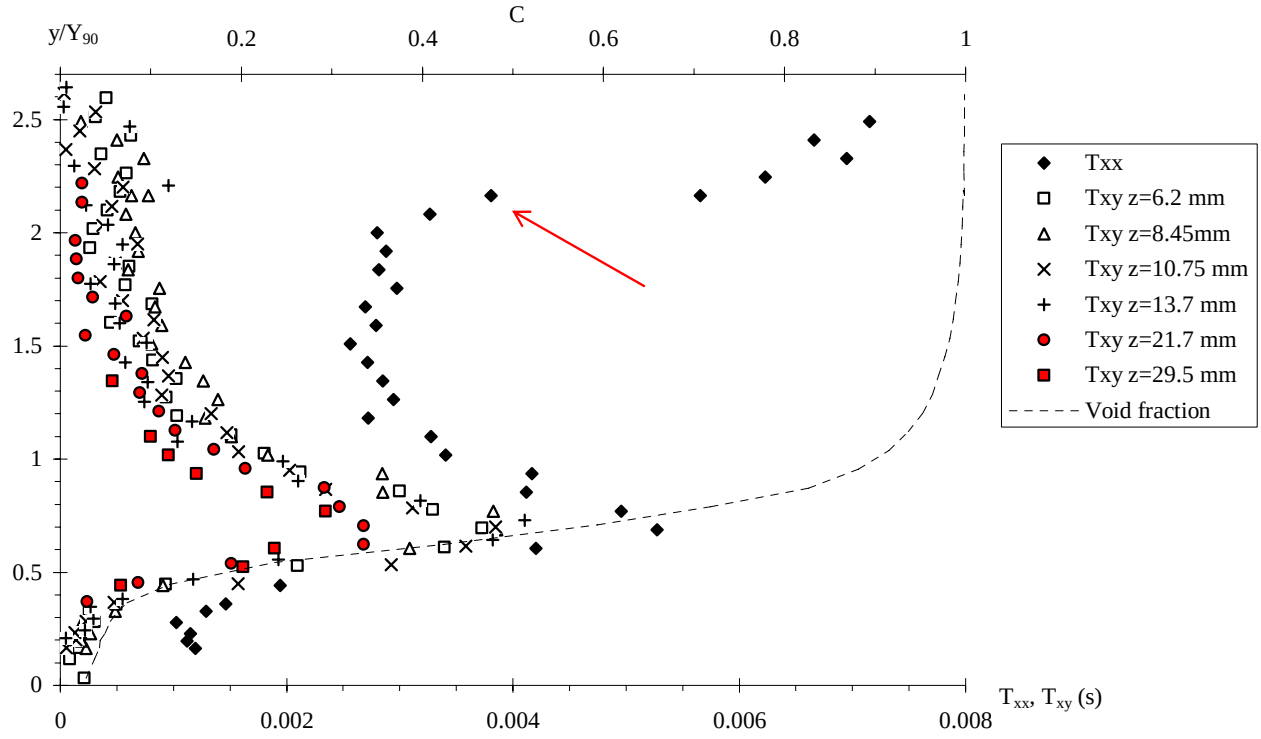


(C) Relationship between auto- and cross-correlation time scales and void fraction in a cross-section - Flow conditions: $d_C/h$ = 1.15, Re = 4.6 E+5, single-tip probe (∅ = 0.35 mm), Step edge 10 - Comparison with Equation (6-8)

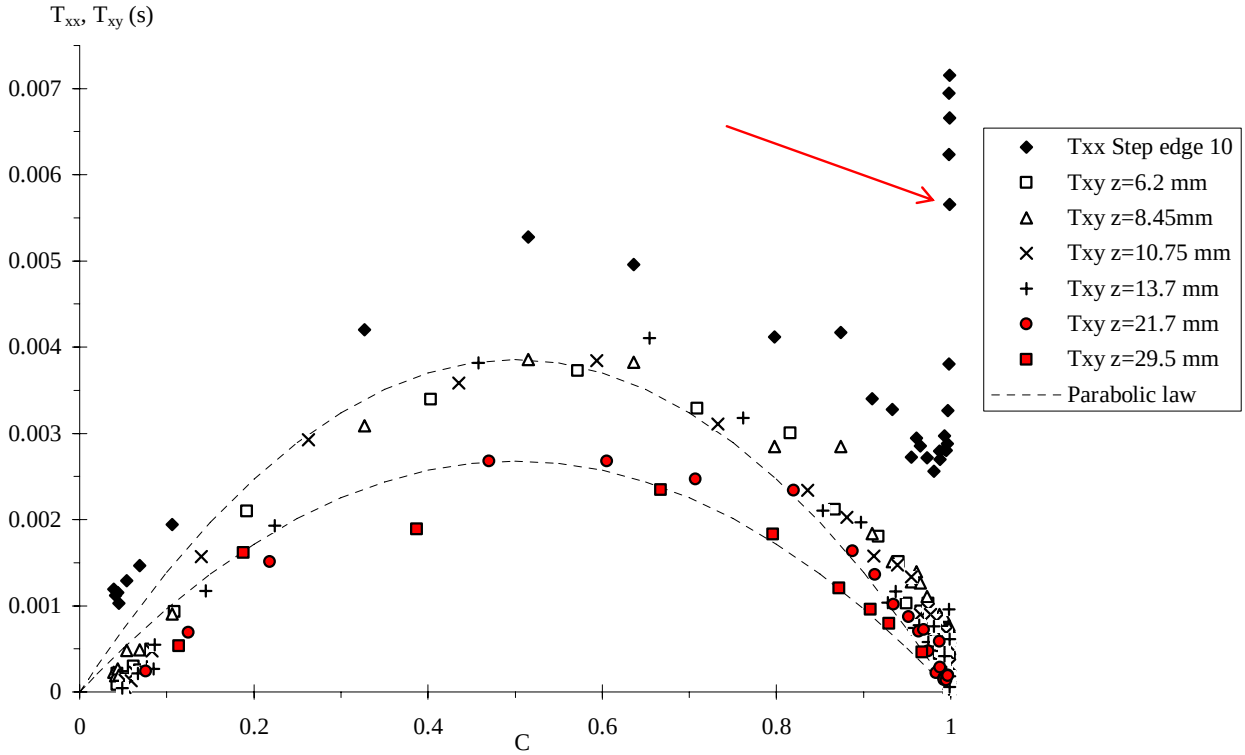

Fig. 6-5 - Effect of the transverse separation Δz on the cross-correlation time scale $T_{xy}$ in skimming flows - Flow conditions: $d_c/h$ = 1.15, Re = 4.6 E+5, single-tip probe (∅ = 0.35 mm), Step edge 10

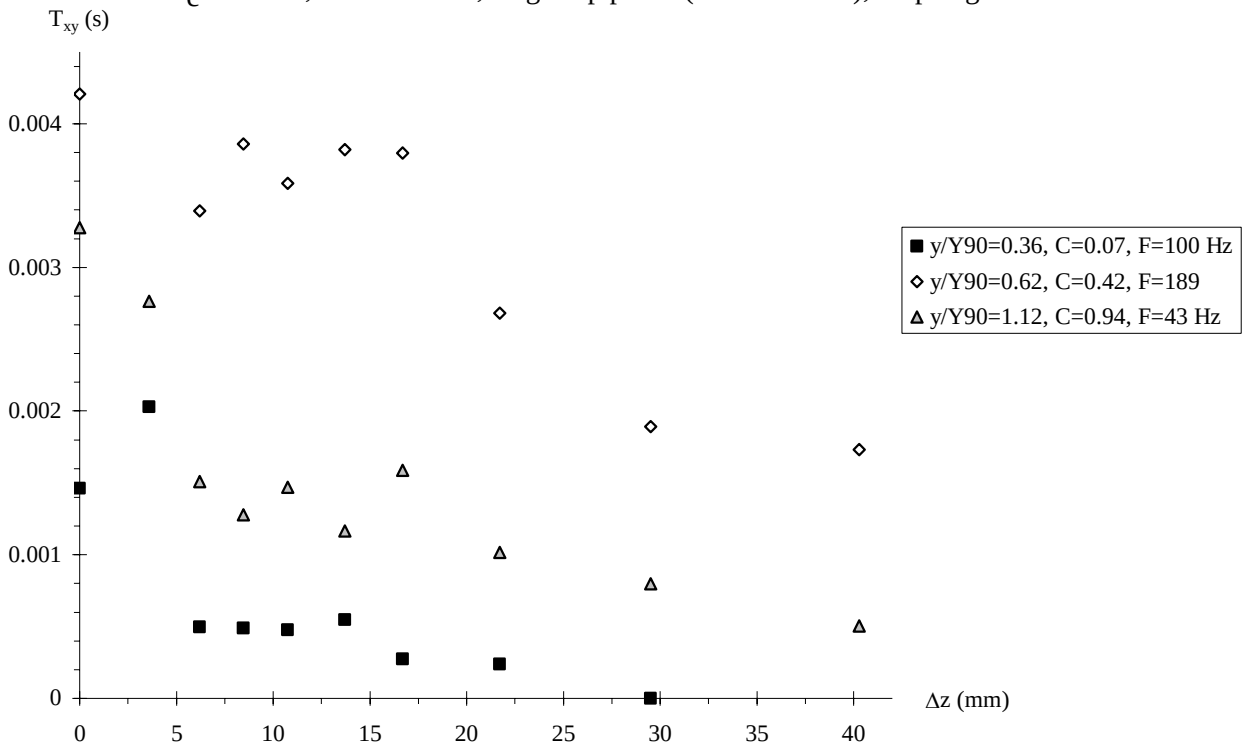


Table 6-2 - Experimental observations of maxima of transverse cross-correlation time scale $T_{xy}$ and of maximum cross-correlation $(R_{xy})_{max}$ in a cross-section as a function of the transverse separation distance (Present study)

| $q_w$ | $\frac{d_c}{h}$ | Re | Instrumentation | Step edge | Δz | Maximum $(R_{xy})_{max}$ | $(T_{xy})_{max}$ | Comments |
|---|---|---|---|---|---|---|---|---|
| $m^2/s$ | | | | | mm | | s | |
| (1) | (2) | (3) | (4) | (5) | (6) | (7) | (8) | (9) |
| 0.116 | 1.15 | 4.6 E+5 | 2 single-tip probes | 10 | 0 | 1 (+) | 0.0053 (+) | |
| | | | | | 3.6 | 0.6339 | 0.005 | Run 060508b. |
| | | | | | 6.3 | 0.4504 | 0.0037 | Run 060412c. |
| | | | | | 8.45 | 0.4293 | 0.0039 | Run 060411a. |
| | | | | | 10.75 | 0.3914 | 0.0038 | Run 060411b. |
| | | | | | 13.7 | 0.3172 | 0.0041 | Run 060411c. |
| | | | | | 16.7 | 0.3215 | 0.0039 | Run 060412a. |
| | | | | | 21.7 | 0.2391 | 0.0027 | Run 060412b. |
| | | | | | 29.5 | 0.182 | 0.0023 | Run 060413a. |
| | | | | | 40.3 | 0.1516 | 0.0023 | Run 060508a. |
| 0.161 | 1.45 | 6.4 E+5 | 2 single-tip probes | 10 | 0 | 1 (+) | 0.0055 (+) | |
| | | | | | 3.6 | 0.6493 | 0.0048 | Run 060509a. |
| | | | | | 8.45 | 0.468 | 0.0041 | Run 060511b. |
| | | | | | 13.7 | 0.37 | 0.0044 | Run 060509b. |
| | | | | | 21.7 | 0.2845 | 0.0040 | Run 060510a. |
| | | | | | 40.3 | 0.1417 | 0.0020 | Run 060510b. |
| | | | | | 55.7 | 0.1166 | 0.0019 | Run 060511a. |

Notes : $d_C$ : critical flow depth; Re : Reynolds number defined in terms of the hydraulic diameter; W : channel width; ($^+$) : auto-correlation results.

*Transverse integral turbulent length and time scales $L_{xy}$ and $\mathbf{T}$*

Some experiments were repeated with several transverse separation distances Y = Δz. The transverse turbulent length and time scales, $L_{xy}$ and $\mathbf{T}$ respectively, were calculated. All the results are given in Appendix E. Typical results in terms of dimensionless turbulent length scale $L_{xy}/Y_{90}$, integral turbulent time scale $\mathbf{T}*\sqrt{g/Y_{90}}$ and advection length scale $L_{xx}/Y_{90}$ are presented in Figure 6-6. The measured void fraction data are also shown in Figure 6-6. The data showed that the turbulent and advection length scales $L_{xy}$ and $L_{xx}$ were of the same order of magnitude although $L_{xy} \leq L_{xx}$.

The turbulent length scale $L_{xy}$ represents a measure of the transverse size of the large vortical structures advecting the air bubbles and air-water packets. The turbulence time scale $\mathbf{T}$ characterises the integral turbulent time scale of these large eddies. The advection length scale $L_{xx}$ is a characteristic longitudinal size of the large advecting eddies. Within Taylor's hypothesis of separate and additive advection and diffusion processes, the advection and turbulent length scales should be equal : $L_{xy} \approx L_{xx}$.

The present results highlighted that the relationships between the integral length scales $L_{xy}$ and $L_{xx}$ and integral time scale $\mathbf{T}$, and the void fraction had a "skewed parabolic shape" with a maxima occurring for void fractions between 0.6 and 0.7 (Fig. 6-7). The dimensionless distributions of transverse turbulent length scale $L_{xy}/Y_{90}$, transverse integral turbulent time scale $\mathbf{T}*\sqrt{g/Y_{90}}$ and advection length scale $L_{xx}/Y_{90}$ were best correlated by :

$$\frac{L_{xy}}{(L_{xy})_{max}} = 1.75 * C^{0.57} * (1 - C)^{0.324} \qquad 0 \leq C \leq 1 \quad (6\text{-}9)$$

$$\frac{\mathbf{T}}{\mathbf{T}_{max}} = 1.97 * C^{0.59} * (1 - C)^{0.5} \qquad 0 \leq C < 0.97 \quad (6\text{-}10)$$

$$\frac{L_{xx}}{(L_{xx})_{max}} = 1.6 * C^{0.55} * (1 - C)^{0.3} \qquad 0 \leq C < 0.97 \quad (6\text{-}11)$$

where $(L_{xy})_{max}$, $\mathbf{T}_{max}$, and $(L_{xx})_{max}$ are the characteristic maxima in the cross-section (Table 6-3). Equation (6-9) to (6-11) are compared with data in Figure 6-7. Note that Equations (6-10) and (6-11) are not valid in the upper spray region (C > 0.95 to 0.97).

The transverse air-water turbulent length scales were closely related to the characteristic air-water depth $Y_{90}$: i.e., $L_{xy}/Y_{90} \approx 0.05$ to 0.2 (Fig. 6-7, Table 6-3). This result was irrespective of the dimensionless flow rate $d_C/h$ and Reynolds numbers within the range of the experiments.

Fig. 6-6 - Dimensionless distributions of air-water transverse turbulent length scales $L_{xy}/Y_{90}$, transverse integral turbulent time scale $T^*\sqrt{g/Y_{90}}$ and advection length scale $L_{xx}/Y_{90}$ - Single-tip probe (∅ = 0.35 mm)

(A) $d_C/h$ = 1.15, Re = 4.6 E+5, Step edge 10

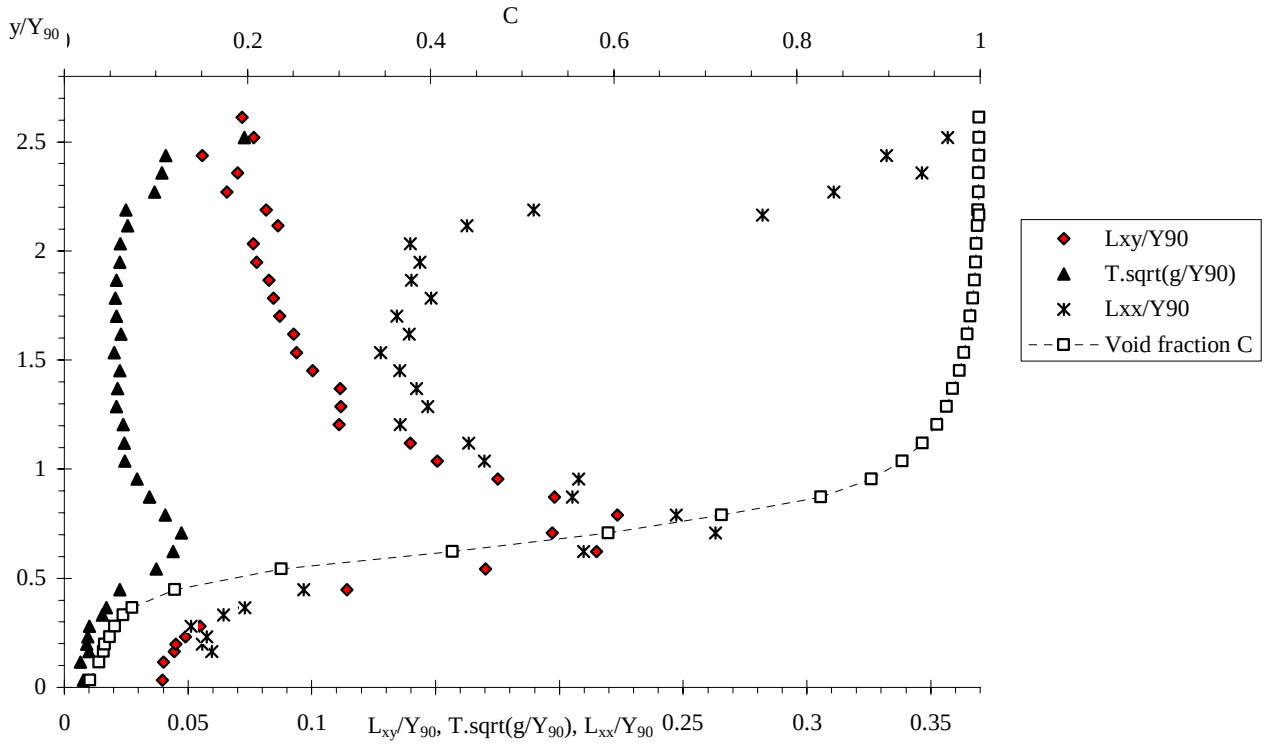


(B) $d_C/h$ = 1.45, Re = 6.4 E+5, Step edge 10

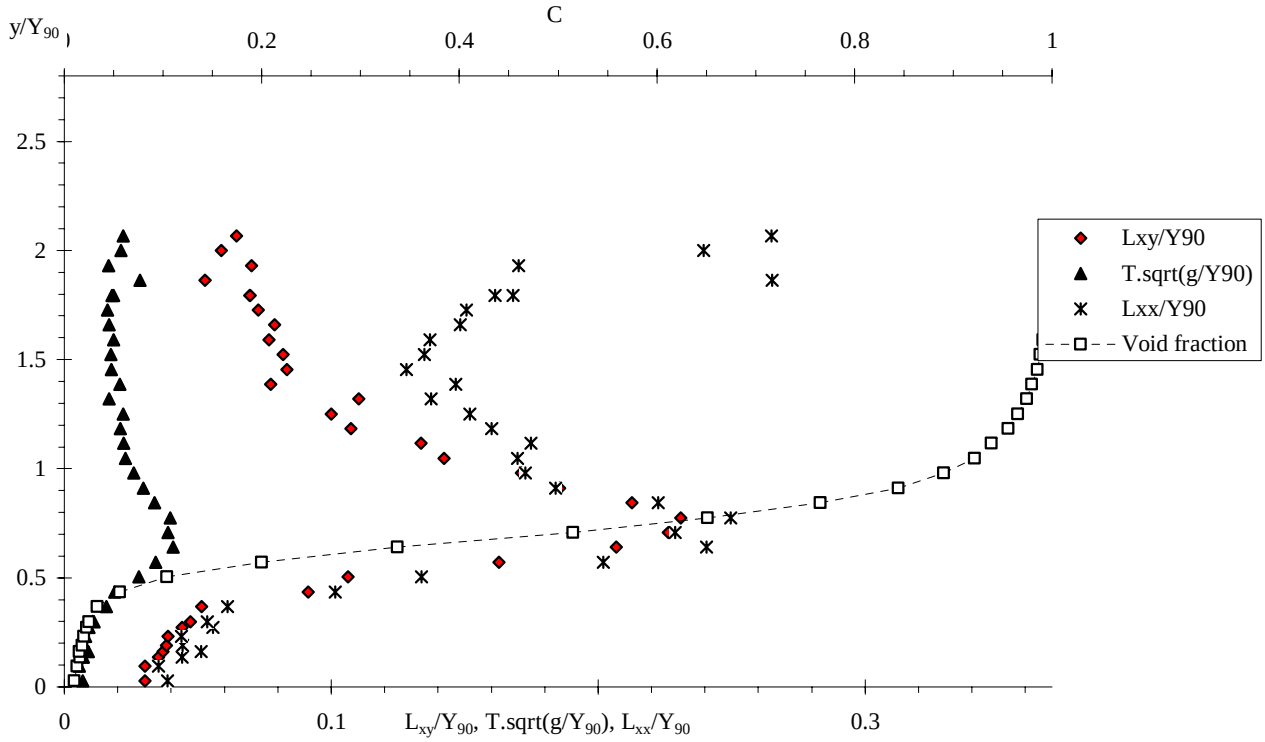

Fig. 6-7 - Dimensionless relationship between transverse turbulent length scale $L_{xy}/Y_{90}$, transverse integral time scale $T^*\sqrt{g/Y_{90}}$ and advection length scale $L_{xx}/Y_{90}$, and void fraction at Step 10- Single-tip probe (∅ = 0.35 mm) - Comparison with Equation (6-9) to (6-11)

(A) $d_c/h$ = 1.15, Re = 4.6 E+5, Step edge 10

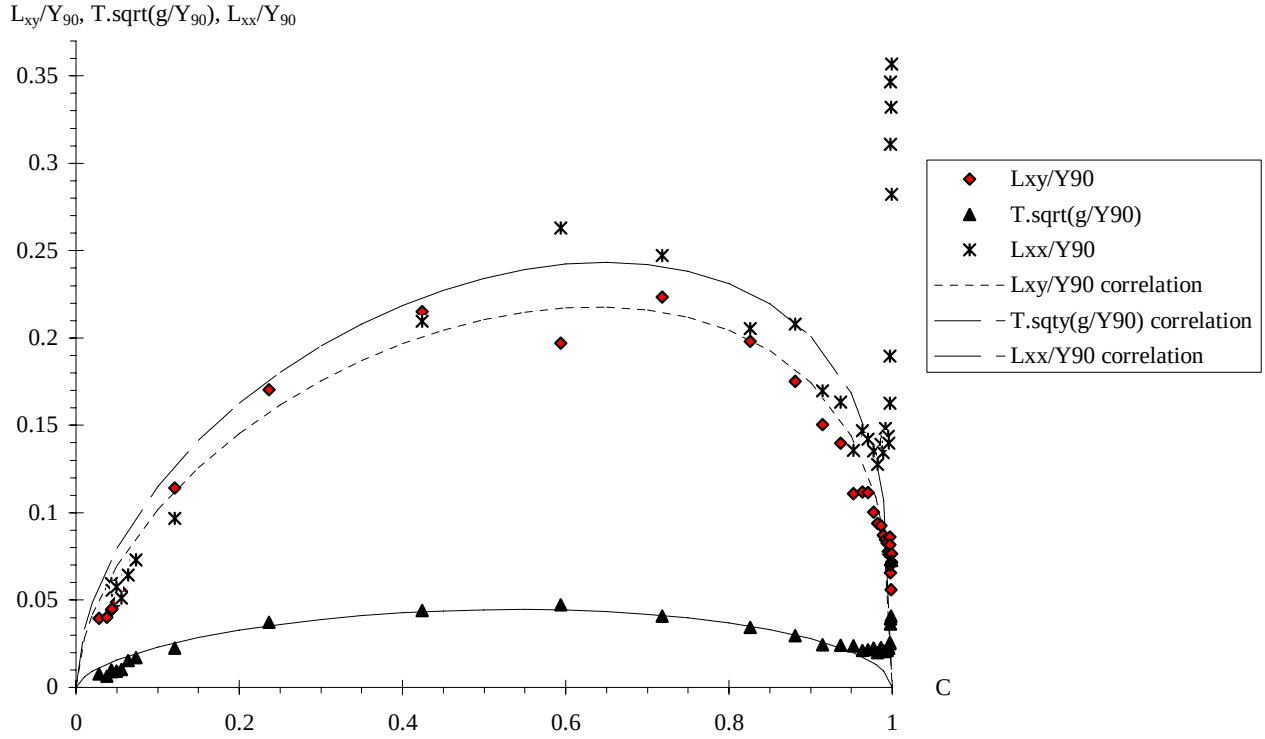


(B) $d_c/h$ = 1.45, Re = 6.4 E+5, Step edge 10

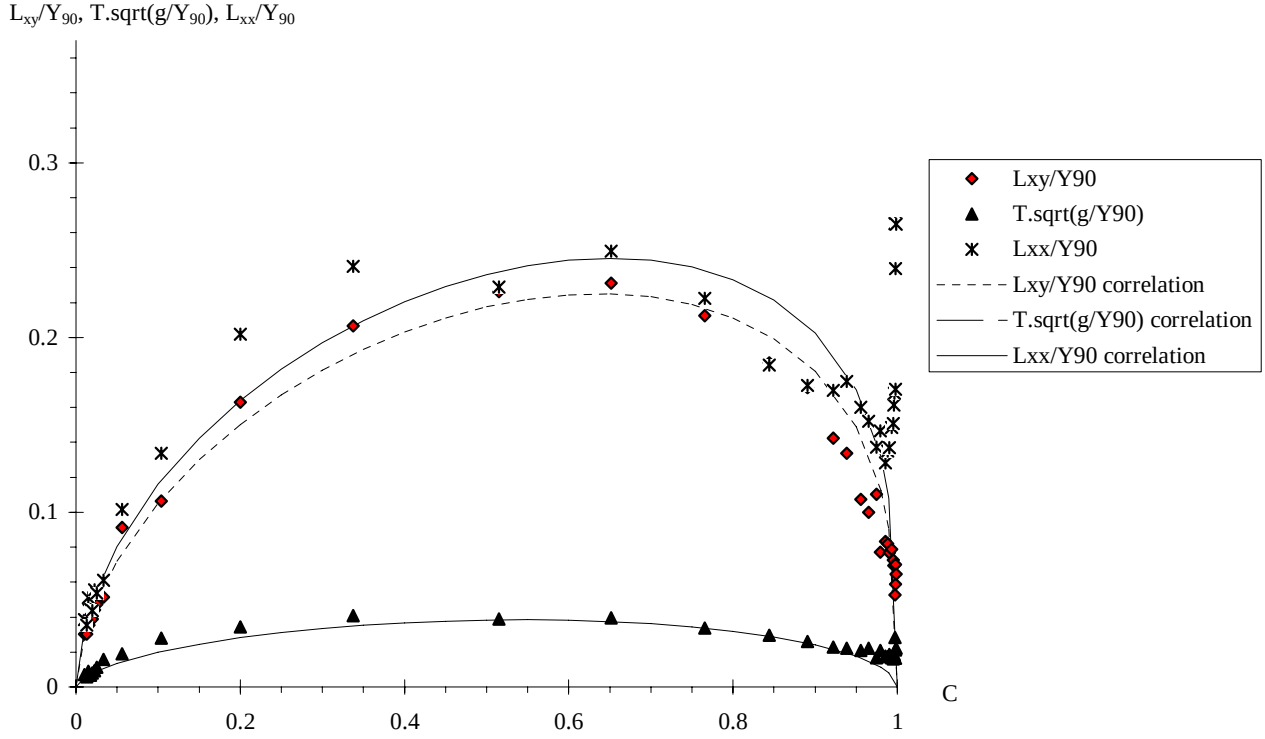

Table 6-3 - Characteristic integral turbulent length and time scales, and advection length scales in skimming flows on a stepped chute (transverse and streamwise integral turbulent scales)

| Parameter | $\frac{d_c}{h} = 1.15$ | $\frac{d_c}{h} = 1.45$ | Remarks |
|---|---|---|---|
| (1) | (2) | (3) | (4) |
| Transverse scales ($Y = \Delta z$) | | | Single-tip probe data ($\varnothing$ = 0.35 mm). |
| $(L_{xy})_{max}/Y_{90}$ | 0.223 | 0.231 | |
| $T_{max}*\sqrt{g/Y_{90}}$ | 0.0473 | 0.0408 | $0 \leq C < 0.97$ |
| $(L_{xx})_{max}/Y_{90}$ | 0.263 | 0.265 | $0 \leq C < 0.97$ |
| Streamwise scales ($Y = \Delta x$) | | | Double-tip probe data ($\varnothing$ = 0.25 mm). |
| $(L_{xy})_{max}/Y_{90}$ | 0.1865 | 0.151 | |
| $T_{max}*\sqrt{g/Y_{90}}$ | 0.0472 | 0.041 | $0 \leq C < 0.97$ |
| $(L_{xx})_{max}/Y_{90}$ | 0.231 | 0.132 | $0 \leq C < 0.97$ |

## 6.3 Streamwise integral time and length scales

Experimental results in terms of longitudinal integral turbulent length and time scales showed some trends similar to those observed with the transverse integral turbulent scales. Figures 6-8 and 6-9 present the streamwise integral scales obtained for the same flow conditions as the transverse integral scale data shown in Figures 6-6 and 6-7.

Herein the integral turbulent length scale $L_{xy}$ represented a measure of the longitudinal scale of large vortices which advected the air bubbles and air-water packets. The present data showed that the streamwise and advection length scales were about the same although $L_{xy} \leq L_{xx}$. Both the transverse and streamwise turbulent length scales were close and the results yielded $L_{xy}/Y_{90} \approx 0.1$ to 0.2. The integral turbulent length scales were maximum for about C = 0.6 to 0.7 (Fig. 6-7 and 6-9, Table 6-3). Table 6-3 summarises the characteristic turbulent length and time scales for the present study.

The integral turbulent time scale $T$ characterises the time scale of the large eddies advecting the air bubbles. The streamwise and transverse integral turbulent time scales were close and the data yielded $0.01 \leq T*\sqrt{g/Y_{90}} \leq 0.06$ (Fig. 6-6 and 6-8, Table 6-3).

Fig. 6-8 - Distributions of auto- and cross-correlation time scales $T_{xx}$ and $T_{xy}$ in skimming flows for several streamwise separation distances Δx - Double-tip conductivity probe (∅ = 0.25 mm) - Comparison with the measured void fraction distribution

(A) $d_C/h$ = 1.15, Re = 4.6 E+5, Step edge 10

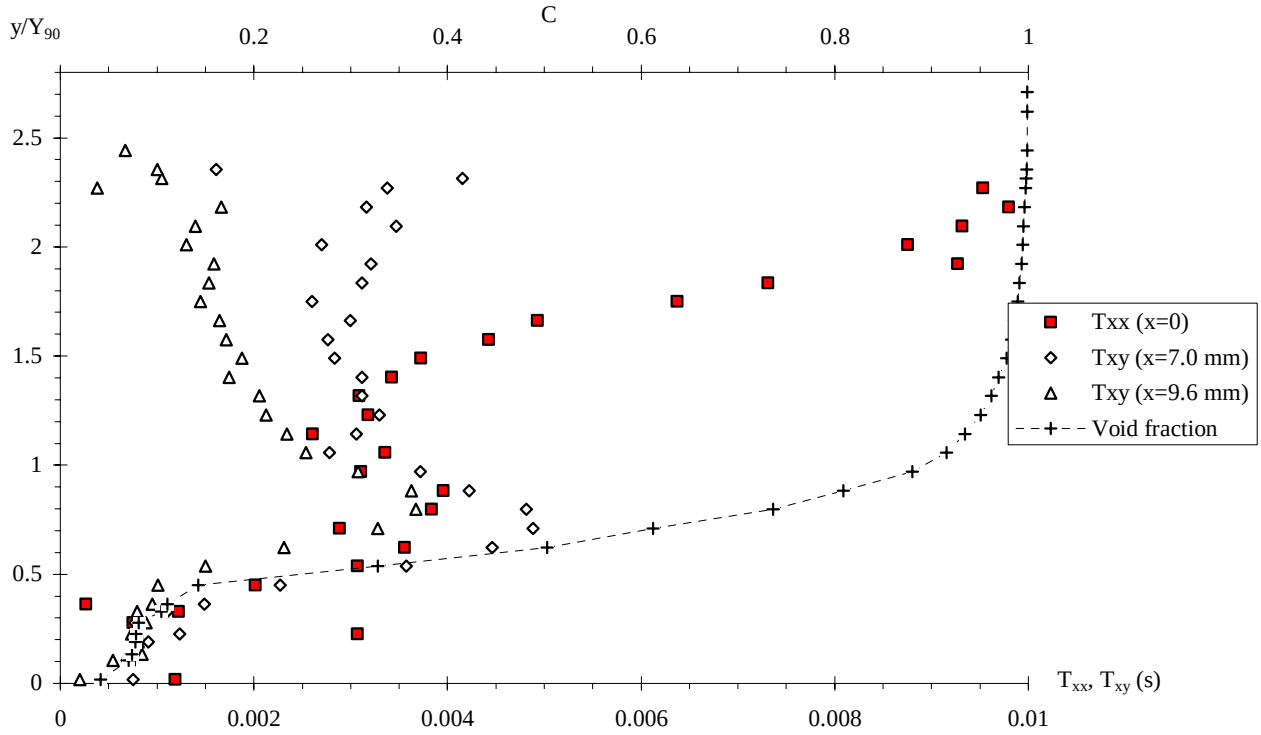


(B) $d_C/h$ = 1.45, Re = 6.4 E+5, Step edge 10

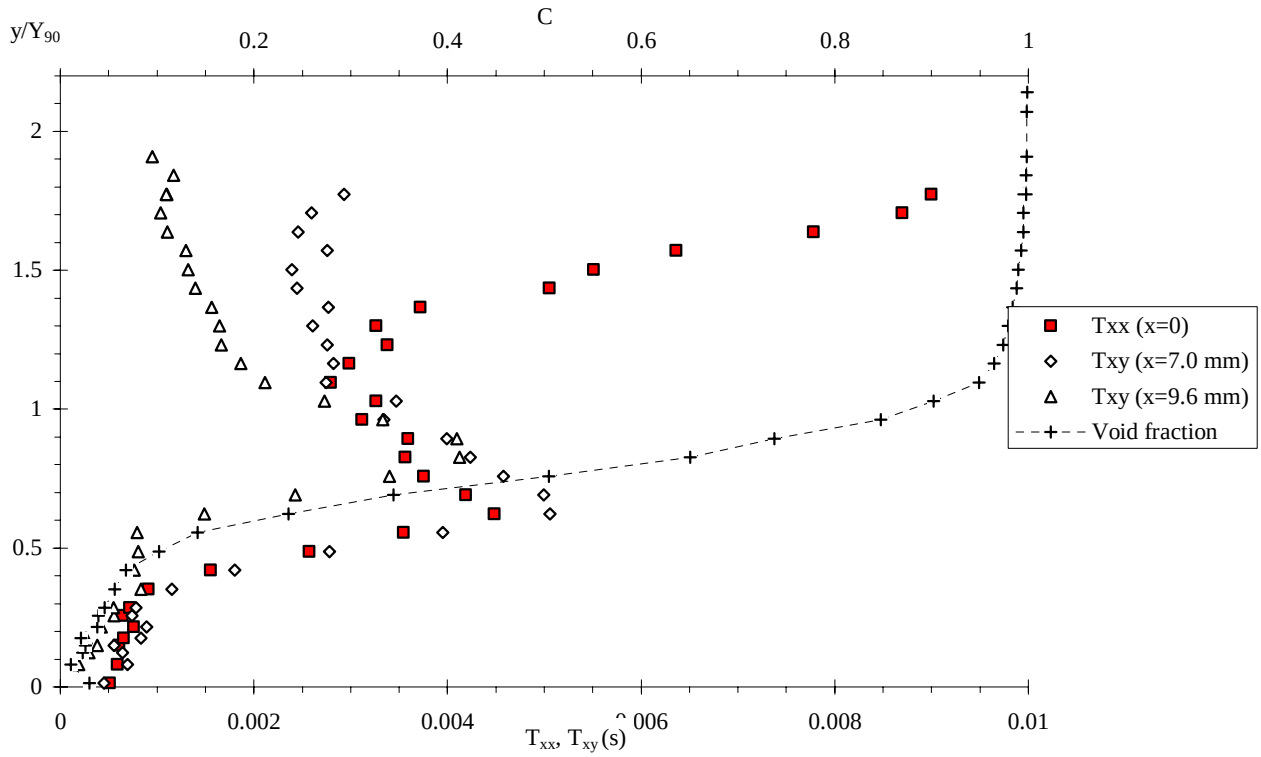

Fig. 6-9 - Dimensionless distributions of streamwise turbulent length scales $L_{xy}/Y_{90}$, streamwise integral time scale $\mathbf{T}^*\sqrt{g/Y_{90}}$ and advection length scale $L_{xx}/Y_{90}$ - Double-tip probe (∅ = 0.25 mm)

(A) $d_C/h$ = 1.15, Re = 4.6 E+5, Step edge 10

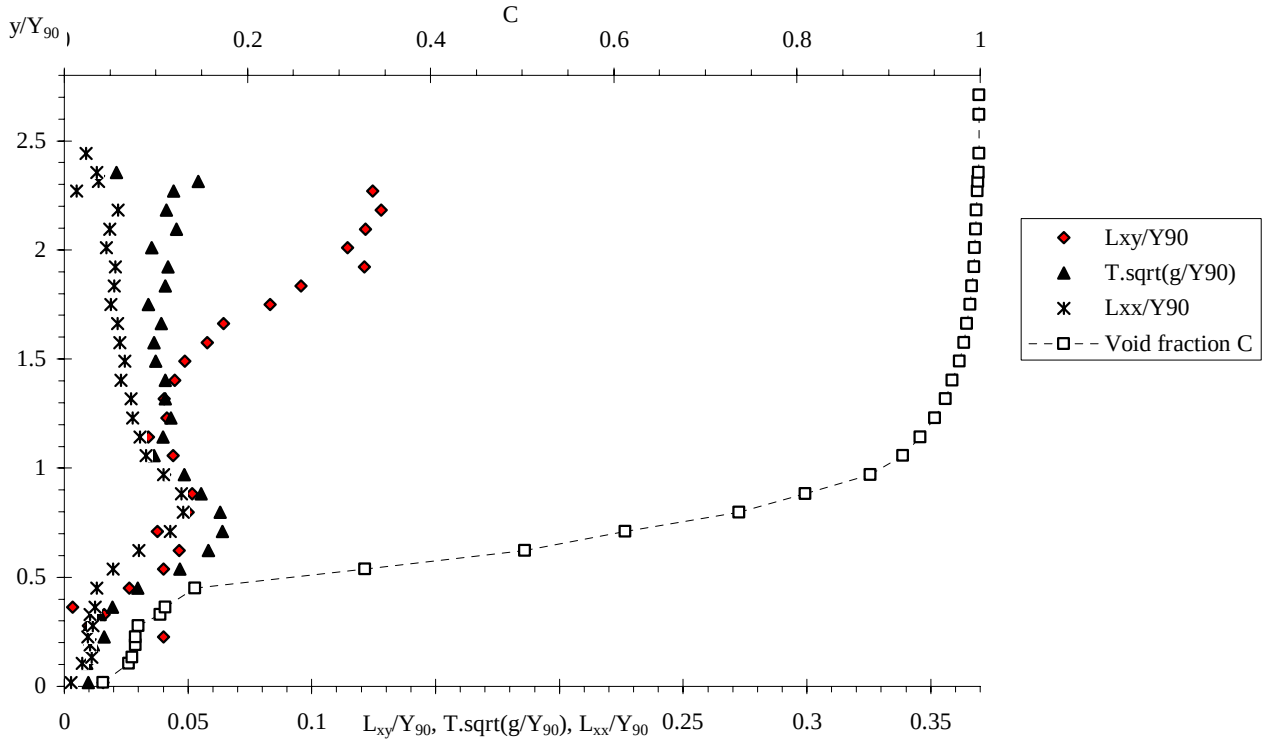


(B) $d_C/h$ = 1.45, Re = 6.4 E+5, Step edge 10

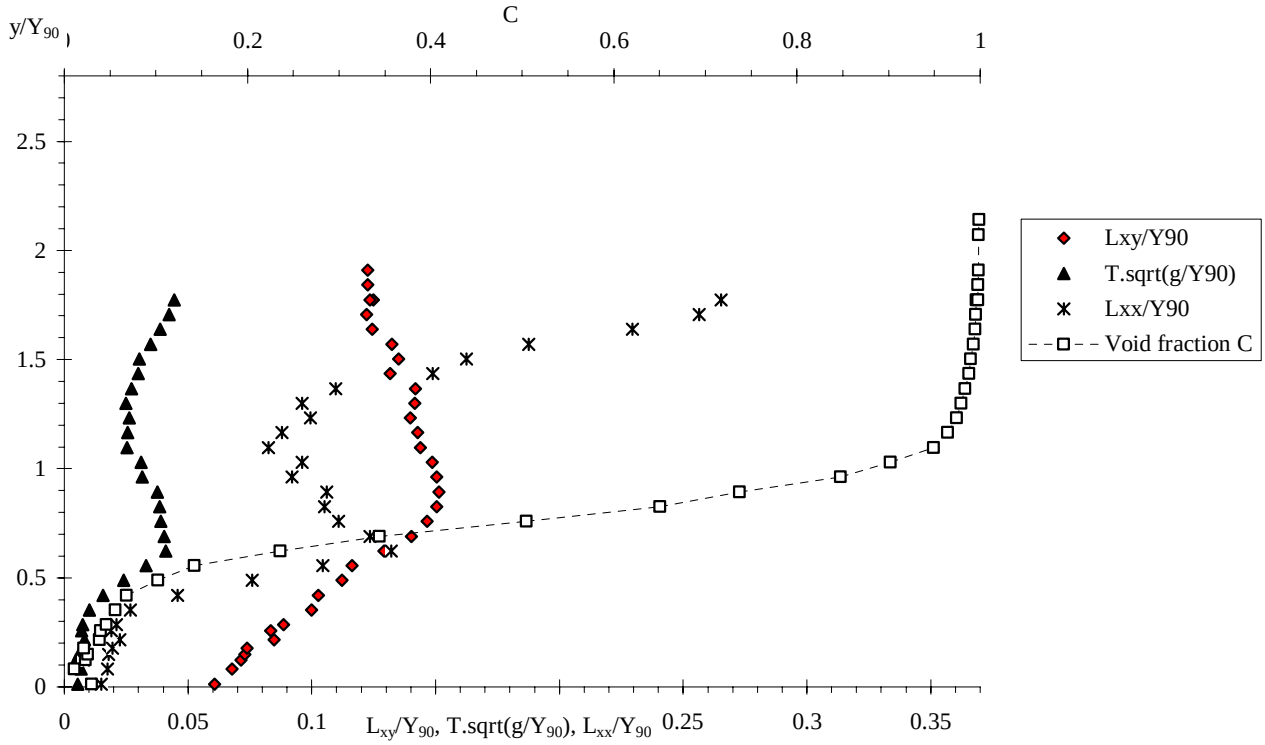

## 6.4 Discussion

Some researchers studied fundamental processes affecting free-surface deformations and air-water free-surfaces: e.g., SARPKAYA (1996), CHANSON (1997a), BROCCHINI and PEREGRINE (2001), MOUAZE et al. (2005). However, few results were reported on turbulent length scales in bubbly shear flows but one study in hydraulic jumps (CHANSON 2006a). It is believed that the present data sets are unique.

What is the physical significance of the air-water integral turbulent length scale $L_{xy}$ ? In bubbly flows, the turbulent length scales are closely linked with the characteristic sizes of the large-size eddies and their interactions with entrained air bubbles. This was evidenced by high-speed photographs demonstrated air bubble trapping in the large eddies of developing mixing layers (e.g. HOYT and SELLIN 1989, CHANSON 1997a). Herein the integral turbulent length scale $L_{xy}$ represents a measure of the size of large vortical structures advecting air bubbles in the skimming flows. Present results emphasise that both streamwise and transverse turbulent length scales were nearly equal and they were closely related to the characteristic air-water depth $Y_{90}$ : i.e., $L_{xy}/Y_{90} \approx 0.1$ to 0.2. The result was irrespective of the Reynolds numbers within the range of the experiments.

The advection length scale equals $L_{xx} = V * T_{xx}$. If the turbulent advection and diffusion of the bubbles are two separate additive processes, the advection length scale is about the integral turbulent length scale $L_{xy}$ defined in terms of a streamwise separation distance Y. Present results showed close results for $0 < C < 0.95$ (Fig. 6-9). Some substantial difference was however observed in the upper spray region (C . 0.95 to 0.97) implying that the assumption of independent advection and diffusion processes and the hypothesis of "frozen turbulence" were not valid in this upper spray region.

## 7. DISCUSSION

### 7.1 Self-similarity in air-water flow properties

In the field of fluid mechanics, many flow types present some self-similarity. A self-similar process is one whose spatial distribution of properties at various times can be obtained from one another by a similarity transformation (BARENBLATT 1994,1996). Self-similarity is a powerful tool in turbulence flow research, and skimming flows on a stepped chute are one type of turbulent flows involving a wide spectrum of spatial and temporal scales. The non-linear interactions among vortices and particles at different scales lead usually to a complex flow structure. Thus relationships among flows at different scales are of crucial significance in understanding and controlling these flows. They play also a major role in comparing analytical, experimental and numerical results as these results are for different scales, and most stepped spillway applications are for prototype flow conditions with flow Reynolds number between 1 E+6 and more than 1 E+9 that cannot be modelled numerically nor physically.

In the present study self-similarity was observed in terms of the distributions of air-water flow properties. Table 7-1 summarises some basic self-similarity equations that were observed during the present work. Self-similarity is illustrated for example in Figures 7-1, 5-6, 5-7, 6-2, and 6-7. These self-similar relationships were observed at both macroscopic and microscopic levels. For example, the distributions of void fraction and interfacial velocity at a macroscopic level, and the cross-correlation function and probability distribution functions of particle chords at a microscopic level (Table 7-1).

Self-similarity is closely linked with dynamic similarity (Section 2). In paragraph 2.2, it was argued that it is nearly impossible to achieve a true dynamic similarity in stepped spillway models because of number of relevant dimensionless parameters. Yet the experimental results showed a number of self-similar relationships (Table 7-1) that remain invariant under changes of scale : i.e., they have scaling symmetry which led in turn to remarkable application at prototype scales. Clearly the present results are most significant because they demonstrate a number of self-similar relationships characterising the air-water flow properties in skimming flow above stepped chutes. They provide a picture general enough to be used, as a first approximation, to characterise the air-water flow field in similar stepped spillway structures irrespective of the physical scale.

### 7.2 Flow resistance and residual energy

On a stepped chute, the skimming flows are characterised by significant form losses. The water skims over the step edges with formation of recirculating vortices between the main stream and the step corners. Form drag is predominant. Downstream of the inception point of free-surface aeration, the flow was gradually-varied flow during the present study. The average shear stress between the skimming flow and the cavity recirculation was deduced from the measured friction slope $S_f$ :

$$f_e = \frac{8 * \tau_o}{\rho_w * U_w^2} = \frac{8 * g * \left( \int_{y=0}^{y=Y_{90}} (1 - C) * dy \right) * S_f}{U_w^2} \qquad \text{Gradually-varied flow (7-1)}$$

where $f_e$ is the equivalent Darcy-Weisbach friction factor, C is the local void fraction, y is measured normal to the pseudo-invert formed by the step edges, $Y_{90}$ is the distance normal to the pseudo-bottom where C =

90%, $U_w$ is the water flow velocity : $U_w = q_w/d$, $q_w$ is the water discharge per unit discharge and d is the equivalent clear-water depth. The friction slope ($S_f = - \partial H/\partial x$) is the slope of the total head line, where H is the mean total head (HENDERSON 1966, CHANSON 1999a,2004a). Free-surface aeration is always substantial in prototype and laboratory skimming flows, and its effects must be accounted for using Equation (7-1).

Table 7-1 - Self-similarity of the air-water flow properties in skimming flow above stepped chutes

| Flow property (1) | Self-similarity (2) | Remarks (3) |
|---|---|---|
| Void fraction distribution | $C = 1 - \tanh^2(\chi)$ | $\chi = K' - \frac{y'}{2*D_o} + \frac{\left(y'-\frac{1}{3}\right)^3}{3*D_o}$<br>$0 \leq y' \leq 1$<br>Equation (5-3). |
| Bubble count rate distribution | $\frac{F}{F_{max}} = 4 * C * (1 - C)$ | $0 \leq C \leq 1$<br>Equation (5-7). |
| Interfacial velocity distribution | $\frac{V}{V_{90}} = y'^{1/N}$ | $0 \leq y' \leq 1$<br>Equation (5-10). |
| | $\frac{V}{V_{90}} = 1$ | $1 \leq y' \leq 2.5$<br>Equation (5-11). |
| Turbulence level distribution | $Tu = 0.25 + a * \left(\frac{F * d_c}{V_c}\right)^b$ | $0 \leq C \leq 1$<br>Equation (5-12). |
| Probability distribution functions of bubble chords | Log-normal distribution | $0 \leq C \leq 0.3$ |
| Probability distribution functions of droplet chords | Log-normal distribution | $0.7 \leq C \leq 0.95$ |
| Cross-correlation function | $R_{xx} = \frac{1}{1 + \left(\frac{\tau}{T_{0.5}}\right)^{1.3}}$ | $0 \leq y' \leq 1$<br>Equation (6-6). |
| Cross-correlation function (between two probe sensors separated by a distance Y) | $\frac{R_{xy}}{(R_{xy})_{max}} = \exp\left(-\frac{1}{1443} * \frac{(\tau - T)^2}{\tau_{0.5}}\right)$ | $0 \leq y' \leq 1$<br>Equation (6-7).<br>Both transverse and streamwise probe sensor separations. |
| Cross-correlation time scale distribution (between two probe sensors separated by a distance Y) | $\frac{T_{xy}}{(T_{xy})_{max}} = 4 * C * (1 - C)$ | $0 \leq C \leq 1$<br>Equation (6-8).<br>Both transverse and streamwise probe sensor separations. |
| Distribution of transverse integral turbulent length scale | $\frac{L_{xy}}{(L_{xy})_{max}} = 1.75 * C^{0.57} * (1-C)^{0.324}$ | $0 \leq C \leq 1$<br>Equation (6-9). |
| Distribution of transverse integral turbulent time scale | $\frac{T}{T_{max}} = 1.97 * C^{0.59} * (1 - C)^{0.5}$ | $0 \leq C \leq 0.97$<br>Equation (6-10). |
| Distribution of advection turbulent length scale | $\frac{L_{xx}}{(L_{xx})_{max}} = 1.6 * C^{0.55} * (1 - C)^{0.3}$ | $0 \leq C \leq 0.97$<br>Equation (6-11). |

Note : $y' = y/Y_{90}$.

Fig. 7-1 - Self-similarity in air-water skimming flows on a stepped chute

(A) Dimensionless void fraction distributions : $C = 1 - \tanh^2(\chi)$ with $\chi = K' - y'/(2*D_o) + (y'-1/3)^3/(3*D_o)$

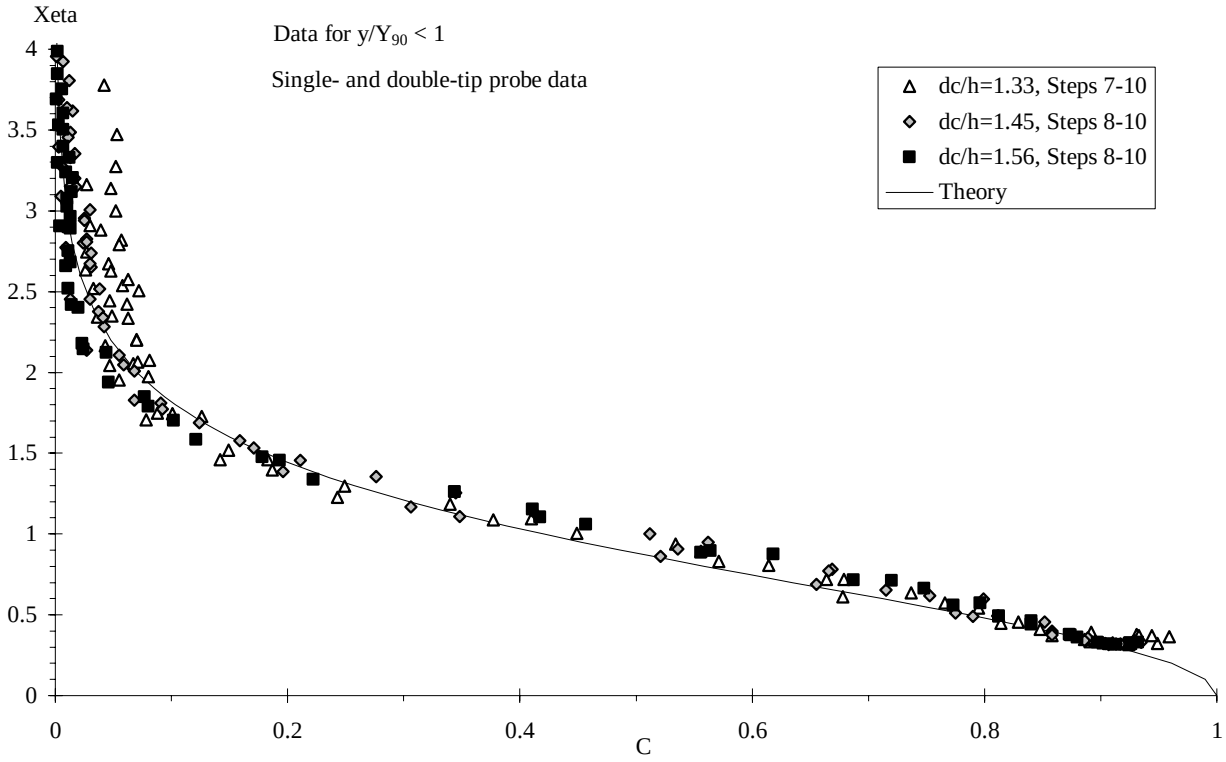


(B) Dimensionless bubble count rate distributions : $F/F_{max} = 4 * C * (1 - C)$

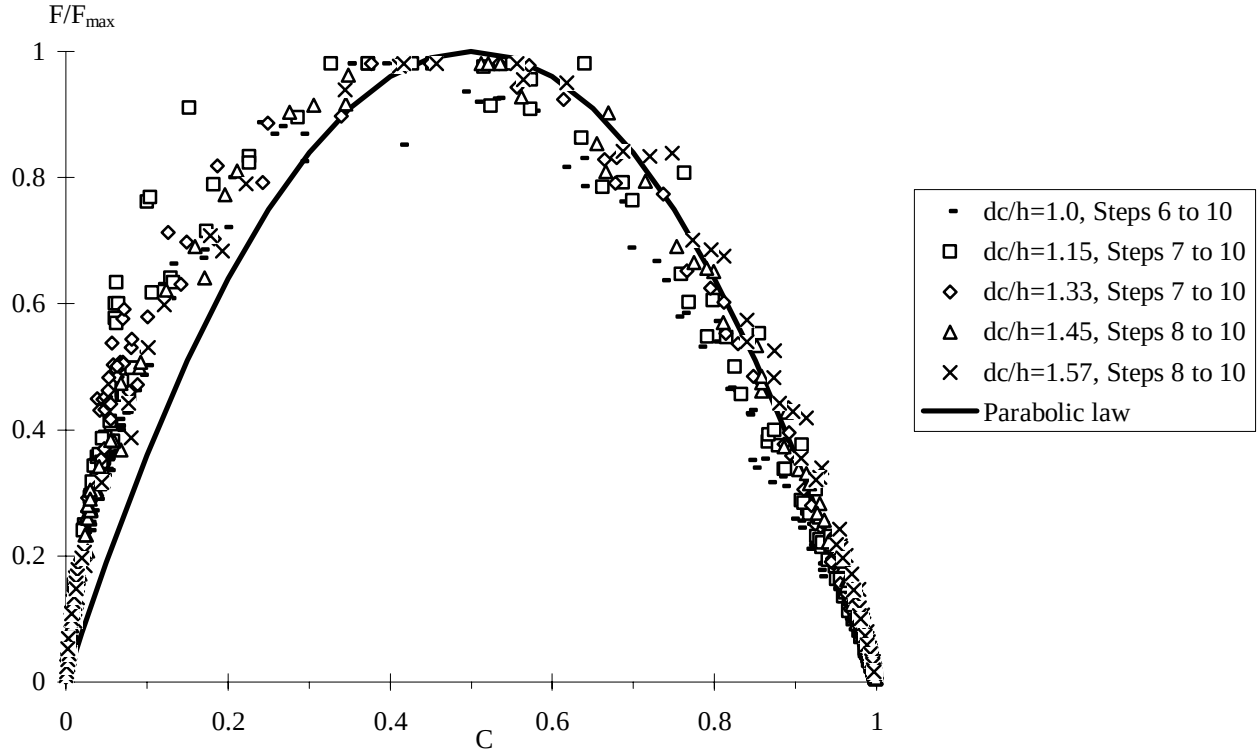

Flow resistance results are presented Figure 7-2 where the friction factor in skimming flows is plotted as a function of the dimensionless step roughness height $h*\cos\theta/D_H$, where h is the step height, θ is the angle between the pseudo-bottom formed by the step edges and the horizontal, and $D_H$ is the hydraulic diameter. All the data are reported in Appendix C. In average, in the present study, the equivalent Darcy friction factor was $f_e \approx 0.14$ downstream of the inception point of free-surface aeration. The results are close to earlier results obtained in the same facility. Note that Equation (7-1) represents the equivalent Darcy friction factor in the aerated flow region only. In the developing boundary layer region, AMADOR et al. (2006) derived the flow resistance by applying an integral momentum method to PIV measurements and their results yielded f = 0.125 for $d_c/h = 2.1$ and Re = 4.4 E+5.

In Figure 7-2, the present flow resistance results are further compared with a comprehensive re-analysis of flow resistance data in skimming flows (CHANSON et al. 2002, CHANSON 2006b). The details of the experimental technique are summarised in the figure caption (Fig. 7-2). Overall, the equivalent Darcy friction factor was typically between 0.1 and 0.35 with no obvious correlation with the relative step roughness height, Reynolds, Froude nor Weber numbers, and the present data were comparable to previous studies. The friction factor data compared favourably with a simplified analytical model of the pseudo-boundary shear stress which may be expressed, in dimensionless form, as :

$$f_d = \frac{2}{\sqrt{\pi}} * \frac{1}{K} \quad (7\text{-}2)$$

where $f_d$ is an equivalent Darcy friction factor estimate of the form drag, and 1/K is the dimensionless expansion rate of the shear layer. Equation (7-2) predicts $f_d \approx 0.2$ for K = 6 that is close to the observed friction factors (Fig. 7-2).

*Residual energy*

For the present investigations, the rate of energy dissipation $\Delta H/H_{max}$ and the dimensional residual energy $H_{res}/d_c$ were estimated at the downstream end of the chute (Step 10), and the results are summarised in Table 7-2. The residual head $H_{res}$ is the total head at the downstream end of the chute, and it equals :

$$H_{res} = d * \cos\theta + \frac{U_w^2}{2 * g} \quad (7\text{-}3)$$

where d is the equivalent clear-water depth and $U_w$ is the flow velocity ($U_w = q_w/d$). The present results showed a decreasing rate of energy dissipation on the stepped chute with increasing discharge. For design engineers, however, it is more relevant to consider the dimensionless residual head $H_{res}/d_c$. Present results implied that the dimensionless residual head was about $2.4 \leq H_{res}/d_c \leq 3.3$, increasing slightly with increasing flow rate.

Note that the present results were obtained with a fully-developed, aerated flow at the chute downstream end. For larger discharges, the flow might not be fully-developed at the downstream end, and that the residual energy could be considerably larger (CHANSON 2001, MEIRELES et al. 2006).

Fig. 7-2 - Equivalent Darcy-Weisbach friction factor in air-water skimming flows - Comparison between present data and earlier studies (ANDRE et al. 2003, BaCara 1991, BOES 2000a, CHAMANI and RAJARATNAM 1999, CHANSON and TOOMBES 2001,2002a, GONZALEZ and CHANSON 2004, MATOS 2000, SHVAJNSHTEIN 1999, YASUDA and OHTSU 1999) for large size model data (Re > 1 E+5 and h > 0.02 m)

| | | |
|---|---|---|
| f | equivalent Darcy friction factor deduced from clear-water flow readings | BaCara (1991), SHVAJNSHTEIN (1999), YASUDA and OHTSU (1999) |
| $f_e$ | equivalent Darcy friction factor in air-water flow deduced from detailed void fraction measurements | ANDRE et al. (2003), BOES (2000a), CHAMANI and RAJARATNAM 1999, CHANSON and TOOMBES (2001,2002a), GONZALEZ and CHANSON (2004), MATOS (2000) |

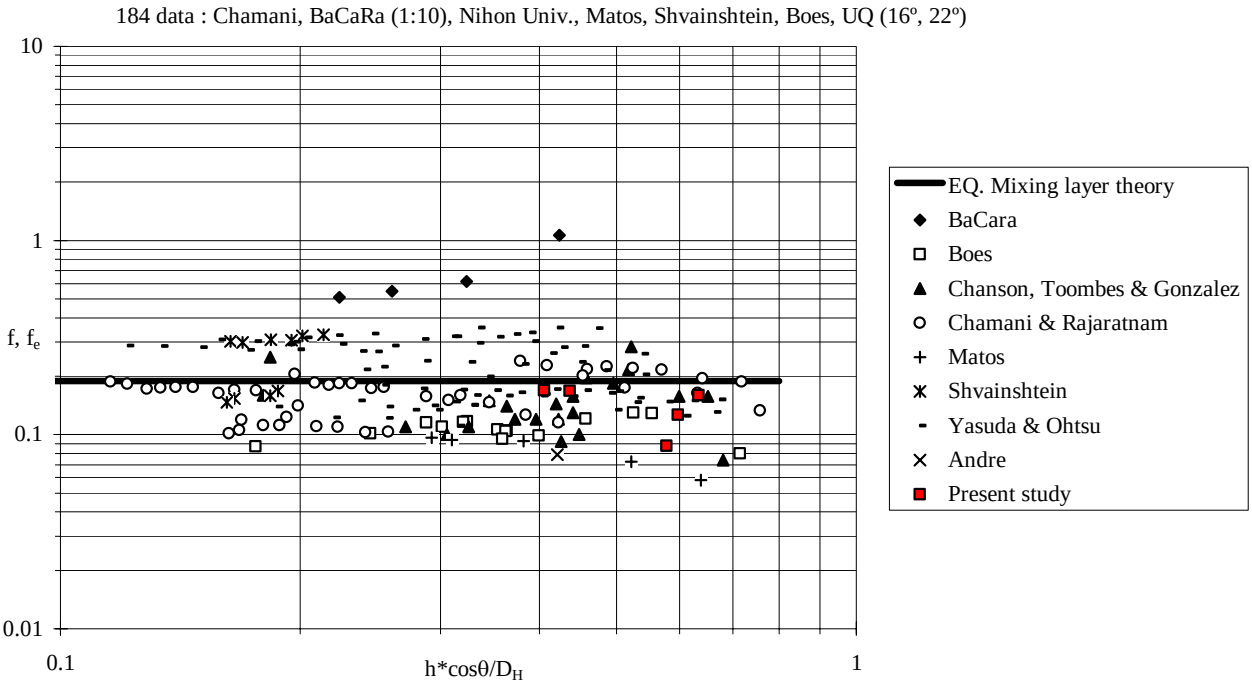


Table 7-2 - Rate of energy dissipation and dimensional residual energy at the downstream end of the stepped chute (Step 10)

| $\frac{d_c}{h}$ | $\frac{\Delta H}{H_{max}}$ | $\frac{H_{res}}{d_c}$ | Remarks |
|---|---|---|---|
| (1) | (2) | (3) | (4) |
| 1.0 | 0.58 | 2.96 | Measured at Step edge 10. |
| 1.15 | 0.54 | 2.85 | |
| 1.33 | 0.52 | 2.48 | |
| 1.45 | 0.51 | 2.35 | |
| 1.57 | 0.40 | 3.32 | |

## 7.3 Spray structure : the upper spray region

In the present study, detailed air-water flow measurements were conducted in the spray region. That region of the flow is characterised by water droplets surrounded by air and it is defined herein as C > 0.7. Herein, the air-water properties were recorded for void fractions C up to 0.999 corresponding to $y/Y_{90}$ up to 2.5. The

experimental data showed some distinctive features in the upper spray region defined as C > 0.95 to 0.97, especially in terms of droplet chord size distributions and advection integral length scale distributions.

In the lower spray region (0.7 < C < 0.9 to 0.95), the probability distribution functions of water chord were skewed with a preponderance of small droplets relative to the mean and they followed closely a log-normal distribution (paragraph 5.3). The distributions of advection length scale $L_{XX}$ showed a decrease in dimensionless length scales $L_{XX}/Y_{90}$ with increasing distance y/Y90 and decreasing liquid fraction (1-C).

Some different results were observed in the upper spray region (C > 0.95 to 0.97). The probability distribution functions of droplet chords were relatively flat and did not follow a log-normal distribution. The PDF maxima were about 0.1 to 0.15 and most droplet chords were between 0.5 and 8 mm. For C > 0.95 to 0.97, the distributions of advection integral length scale showed increasing length scale with decreasing liquid fraction (1-C) (paragraphs 6.2 & 6.3). The result might suggest the existence of longitudinal "streaks" of water drops.

It is believed that the contrasting features of the upper spray region reflected a change in the microscopic flow structure. That is, the upper spray region consisted primarily of ejected water droplets that did not interact with the main flow nor with the surrounding air. These droplets tended to follow some ballistic trajectory (Fig. 7-3) and their "history" was dominated by the initial ejection process and possibly by droplet collisions.

Fig. 7-3 - High-speed photographs of water droplets in ballistic trajectory, viewed from upstream - Skimming flows, h = 0.1 m, $\theta = 21.8^{o}$

(A) $d_C/h = 1.45$, Re = 6.9 E+5 (shutter speed 1/125 s) - Note probe support in background

(B) $d_C/h$ = 1.35, Re = 6.2 E+5 (shutter speed 1/200 s)- Note the double-tip probe in background

## 8. CONCLUSION

New air-water flow measurements were performed in skimming flows on a large stepped spillway model (Fig. 8-1). The channel slope was 21.8º, the step height was 0.1 m and the flow Reynolds numbers ranged from 3.8 E+5 to 7.1 E+5. Two types of phase-detection intrusive probes were used : single-tip conductivity probes (∅ = 0.35 mm) and double-tip conductivity probes (∅ = 0.25 mm). Measurements were conducted in the air-water flow region downstream of the inception point of free-surface aeration. For some experiments, two probe sensors were separated by a known transverse or longitudinal distance and sampled simultaneously at 20 kHz for 45 seconds. An advanced signal processing technique with new signal correlation analyses was developed. It was applied systematically to the present data sets.

The air water flow properties presented some basic characteristics that were qualitatively and quantitatively similar to previous studies in skimming flows. These included the distributions of void fraction, bubble count rate and interfacial velocity, the distributions of air and water chord sizes, and the flow resistance estimates. Further some self-similar relationships were observed systematically at both macroscopic and microscopic levels (Table 7-1). These included the distributions of void fraction, bubble count rate, interfacial velocity and turbulence level at a macroscopic scale, and the bubble chord distributions and auto- and cross-correlation functions at the microscopic level. Self-similarity is closely linked with dynamic similarity (Section 2). Although it is nearly impossible to achieve a true dynamic similarity in stepped spillway models because of the number of relevant dimensionless parameters, the experimental results showed a number of self-similar relationships that remained invariant under changes of scale. This result leads in turn to remarkable applications at prototype scales. The present findings are significant because they provides a picture general enough to be used to characterise the air-water flow field in prototype stepped spillways.

Correlation analyses yielded a characterisation of the large eddies advecting the bubbles. Basic results included the transverse and streamwise integral turbulent length scales, the transverse and longitudinal integral time scales, and the advection length scale. In air-water shear flows, the turbulent length scales were closely linked with the characteristics of the large-size eddies and their interactions with entrained air bubbles. Herein the turbulent length scales characterised a measure of the size of large vortical structures advecting air bubbles in the skimming flows. Both streamwise and transverse integral turbulent length scales were closely related to the characteristic air-water depth $Y_{90}$ : i.e., $L_{xy}/Y_{90} \approx 0.05$ to 0.2. The integral turbulent time scales were within $0.01 \leq \mathbf{T}^*\sqrt{g/Y_{90}} \leq 0.06$. The results were irrespective of the Reynolds numbers within the range of the experiments.

Experimental measurements were conducted thoroughly in the spray region for $y/Y_{90}$ up to 2.5 and C up to 0.999. The results highlighted the existence of an upper spray region for C > 0.95 to 0.97 (Fig. 8-1B). In the upper spray region, the distributions of droplet chord sizes and the distributions of integral advection scales ($T_{XX}$, $L_{XX}$) presented some marked difference with the rest of the flow. It is suggested that these patterns highlighted a change in spray structure, whereby the upper spray region consisted primarily of ejected droplets. The ejected droplets followed some ballistic trajectory, and they interacted little with the surrounding air nor with the rest of the flow until they re-attached.

Fig. 8-1 - Photographs of the experimental test section

(A) Side view, $d_C/h = 1.0$, Re = 3.8 E+5, Shutter speed: 1/80 s

(B) Looking downstream at some ejected droplets in the upper spray region for $d_C/h = 1.33$, Re = 5.7 E+5, Shutter speed: 1/320 s - The distance y between the pseudo-bottom formed by the step edges and the lower trolley support is shown

## 9. ACKNOWLEDGMENTS

The writers thank Dr Carlos GONZALEZ (Cardno Brisbane, Australia), Dr Stefano PAGLIARA (University of Pisa, Italy), and Dr Fréderic MURZYN (ESTACA Laval, France) for their expert review of the report and valuable comments.

The writers thank also Graham ILLIDGE and Clive BOOTH (The University of Queensland) for their technical assistance.

Lastly the first writer acknowledges the helpful support of her family.

# APPENDIX A - AIR/WATER CHORD MEASUREMENTS WITH A SINGLE-TIP CONDUCTIVITY PROBE

## A.1 Presentation

New experiments were performed in the Gordon McKAY Hydraulics Laboratory at the University of Queensland in the experimental channel which was previously used by CHANSON and TOOMBES (2001,2002a,2003) and GONZALEZ (2005) with smooth step faces, and by GONZALEZ et al. (2005) (Table A-1). The test section consisted of a broad-crested weir followed by ten identical steps (h = 0.1 m, l = 0.25 m). Air-water flow properties were measured with phase-detection intrusive probes : namely single-tip conductivity probes and double-tip conductivity probes (Table A-1).

Herein, we focus on some basic air-water chord measurements performed with the single-tip conductivity probes (needle probe design). The probe consisted of a sharpened rod (platinum wire ∅ = 0.35 mm) coated with non-conductive epoxy and set into a stainless steel surgical needle (∅ = 1.42 mm) acting as the second electrode as sketched in Figure A-1. The probe was excited by an electronic system (Ref. UQ82.518) designed with a response time less than 10 μs and the probe signal output was scanned at 20 kHz for 45 s.

Table A-1 - Experimental investigations of stepped chute flows on flat slopes ($\theta < 30^o$)

| Reference | $\theta$ deg. | Step geometry | Flow conditions | Instrumentation | Remarks |
|---|---|---|---|---|---|
| (1) | (2) | (3) | (4) | (5) | (6) |
| GONZALEZ et al. (2005)<br>Configuration S (smooth steps) | 21.8 | h = 0.1 m<br>l = 0.25 m<br>Smooth horizontal steps | $q_W$ = 0.01 to 0.219 $m^2/s$,<br>Re = 4 E+4 to 9 E+5. | Double-tip conductivity probe (Ø = 0.025 mm).<br>scanned at: 20 kHz for 20 s | Experiments CMH_05.<br>W = 1 m. |
| Present study | 21.8 | h = 0.1 m<br>l = 0.25 m | | | Experiments GH_06.<br>W = 1 m. |
| Series 1 | | | $q_W$ = 0.095 to 0.18 $m^2/s$,<br>Re = 3.8 E+5 to 7.1 E+5 | Single-tip conductivity probe (Ø = 0.35 mm)<br>scanned at: 20 kHz for 45 s | |
| Series 2 | | | $q_W$ = 0.12 to 0.16 $m^2/s$,<br>Re = 4.6 E+5 to 6.4 E+5 | Double-tip conductivity probe (Ø = 0.25 mm)<br>scanned at: 20 kHz for 45 s | |

Notes : h : step height; l : step length; $q_W$ : discharge per unit width; Re : flow Reynolds number defined in terms of hydraulic diameter.

Fig. A-1 - Sketch of a single-tip conductivity probe

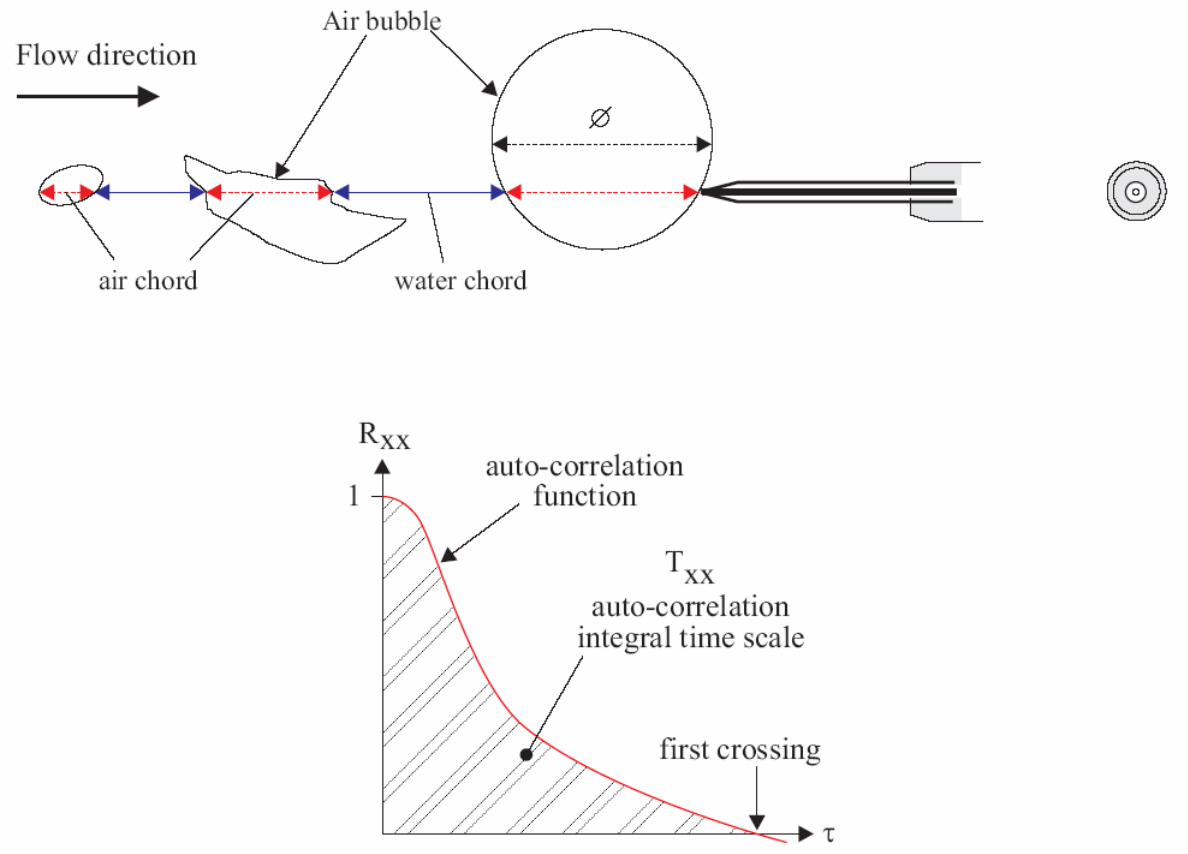


*Signal processing*

The measurement principle of a conductivity probe is based upon the difference in electrical resistivity between air and water. The resistance of water is one thousand times lower than the resistance of air bubbles. When the probe tip is in contact with water, current will flow between the tip and the supporting metal; when it is in contact with air no current will flow. A sketch of the single-tip conductivity probe is presented in Figure A-1.

In the present study, the air-water flow properties were calculated using a single threshold technique and the threshold was set at about 45 to 55% of the air-water voltage range. The basic outputs are the void fraction, bubble count rate and air/water chord times. The void fraction C is the proportion of time that the probe tip is in the air. The bubble count rate F is the number of bubbles impacting the probe tip per second. The air/water chord time is defined as the time spent by the air/water phase on the probe sensor. Bubble chord times were calculated from the raw probe signal. Statistical analyses of chord time distributions yield the median chord time, standard deviation, skewness and kurtosis of both air and water chord times, as well as the probability distribution functions of air and water chord times at each sampling location.

## A.2 Pseudo-chord sizes

Herein the chord time results are presented in terms of pseudo-bubble/droplet chord size ch defined as :

$$ch = U_w * t_{ch} \quad \text{(A-1)}$$

where $t_{ch}$ is the air/water chord time, $U_w$ is the mean flow velocity defined as : $U_w = q_w/d$, $q_w$ is the flow rate per unit width and d is the equivalent clear-water depth. The pseudo chord size ch is not equal to the air/water chord length because the mean flow velocity $U_w$ may differ from the interfacial velocity.

The writers re-analysed some chord size data by GONZALEZ et al. (2005) obtained in the same chute with an identical step geometry. Their data were recorded with a 0.025 mm sensor scanned at 20 kHz for 20 s (Table A-1). With the double-tip probe, the signal processing yielded the true air/water chord sizes. Note that the chord size measurement is not a bubble/droplet diameter, but a characteristic streamwise size of the air/water particle as sketched in Figure A-1.

Measurements of true chord sizes and pseudo-chord sizes (Eq. A-1) were compared in terms of their probability distribution functions. Figure A-2 shows some typical normalised chord length probability distribution functions where each data point represents the probability of a bubble/droplet chord in 0.5 mm intervals : e.g., the probability of a chord length from 1.0 to 1.5 mm is represented by the data point labelled 1.25. The probability of bubble chord lengths greater than 15 mm is not shown for clarity. In Figure A-2, the measured bubble chord length distribution is the thick solid line and the thin dashed line is the pseudo-chord size distribution calculated using Equation (A-1). For the same flow conditions, Table A-2 presents some relative errors between true chord size and pseudo-chord size estimates for one cross-section. The data showed that the probability distribution functions were skewed with a preponderance of small particles relative the mean size. The distributions functions tended to follow closely a log-normal distributions for void fractions less than 0.93. For larger void fractions, the data did not follow a log-normal shape, but the number of particles might be insufficient for the results to be statistically meaningful.

The comparative analysis showed that Equation (A-1) overestimated the air/water chord sizes by 2% in average for $0 \leq C \leq 0.97$. This was indeed a very small difference. For $C > 0.97$, the error was larger but the droplet populations were small and not statistically representative. In this report, air/water chord time data will be presented in terms of pseudo-chord sizes because the results are easier to comprehend and to compare with dual-tip probe data, visual observations, high-speed photographs and movies. The approximation is supported by the very small differences between true and pseudo-chord sizes.

## A.3 Effect of probe sensor size on chord data

The effects of the probe sensor size on chord size data were tested for one flow rate. For $d_C/h = 1.15$, the present pseudo-chord data (0.35 mm probe sensor) were compared with pseudo-chord size data obtained by GONZALEZ et al. (2005) for $d_C/h = 1.18$ with a 0.025 mm probe sensor. CHANSON and TOOMBES (2002c) tested the performances of two probe sensors sizes (0.025 and 0.35 mm) in skimming flows. Their data indicated consistently larger measured count rates with the 0.025 mm sensor probe.

Fig. A-2 - Chord size distributions in skimming flows : comparison between measured chord lengths and Equation (A-1) - Experimental data by GONZALEZ et al. (2005), $d_c/h$ = 1.18, Re = 5 E+5, Step 10, Sensor size : 0.025 mm

(A) $y/Y_{90}$ = 0.29, C = 0.107, F = 177.5 Hz, V = 3.1 m/s, 3550 bubbles

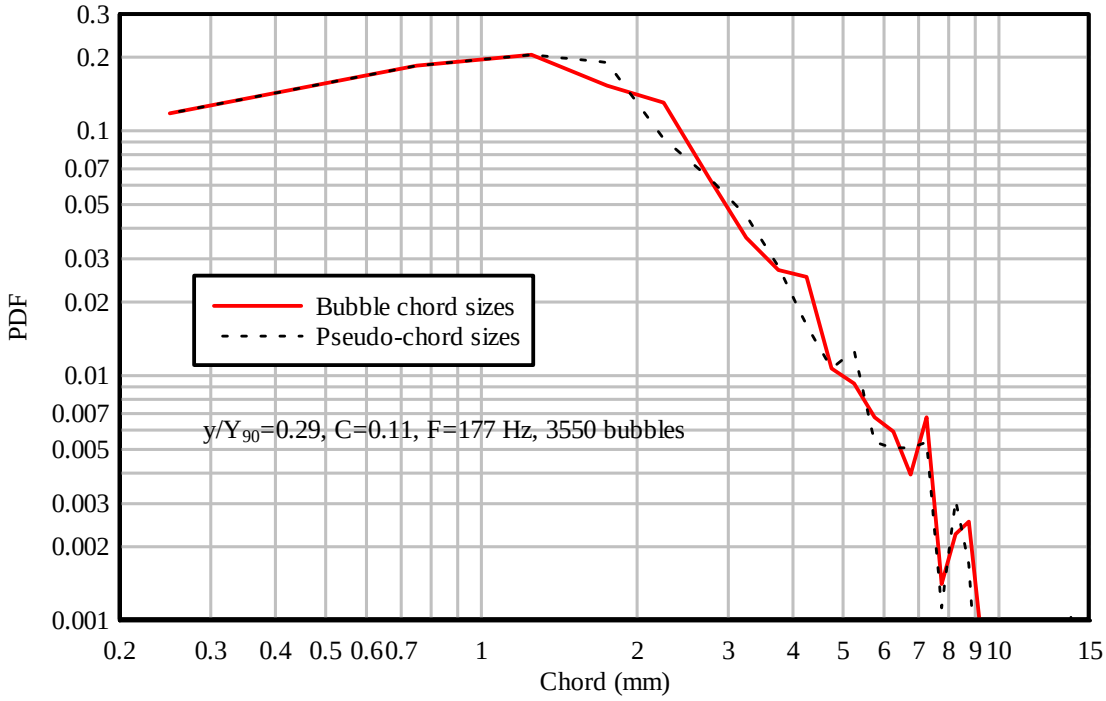


(B) $y/Y_{90}$ = 0.87, C = 0.82, F = 170 Hz, V = 3.52 m/s, 3397 droplets

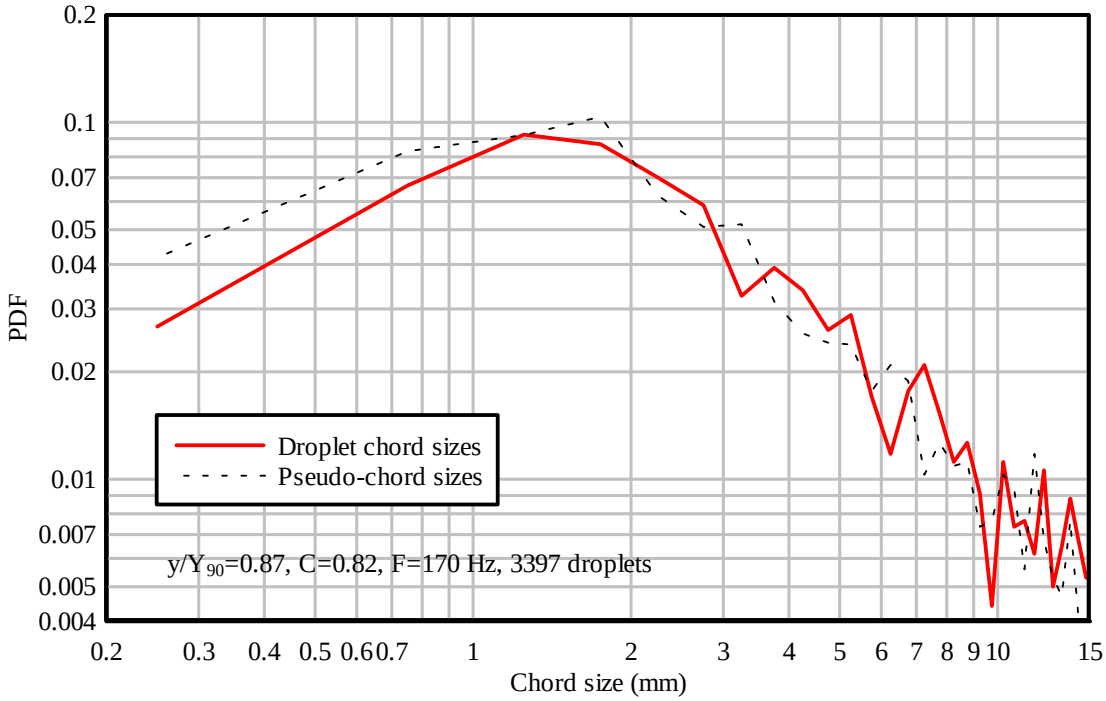

Table A-2 - Relative error between chord sizes and pseudo-chord size for $d_C/h = 1.18$, step 10

| Ref. | Void Fraction | Nb of bubbles/droplets | Relative error (%) |
|---|---|---|---|
| (1) | (2) | (3) | (4) |
| 05 | 0.107 | 3550 | 2.0 |
| 10 | 0.218 | 4980 | -3.7 |
| 12 | 0.327 | 5601 | -3.5 |
| 17 | 0.817 | 3397 | 0.82 |
| 19 | 0.893 | 2059 | 1.4 |
| 20 | 0.922 | 1476 | -4.4 |
| 21 | 0.943 | 1119 | 8.7 |
| 22 | 0.961 | 785 | 4.9 |
| 24 | 0.973 | 518 | 11.6 |
| 25 | 0.98 | 409 | 14.6 |
| 27 | 0.987 | 274 | 9.9 |
| 28 | 0.99 | 198 | -28.6 |
| 30 | 0.996 | 82 | -15.4 |

Notes : Data : GONZALEZ et al. (2005); Errors calculated for bubble chord for C < 0.3 and droplet chords for C > 0.7.

A typical comparison is shown in Figure A-3. The figure caption and legend list the air-water flow conditions including local void fraction, count rates and the total number of bubbles/particles. Note that, for both experiments, the probes were scanned at 20 kHz per sensor, but the scan duration was 20 s for the data set of GONZALEZ et al. (2005) (0.025 mm sensor probe) versus 45 s for the present data set (0.35 mm sensor probe). Figure A-3 shows some pseudo-chord size probability distribution functions where each data point represents the probability of a chord length in 0.5 mm intervals. In Figure A-3, the pseudo-chord data with the 0.025 mm probe sensor are drawn with the thick solid line while the thin dashed line shows the data obtained with the 0.35 mm probe sensor. For the same flow conditions, Table A-3 presents some relative errors between the 0.025 mm and 0.35 mm sensors in terms of pseudo-chord sizes for one cross-section. The relative error was calculated for bubble chords (C < 0.3) and droplet chords (C > 0.7).

The present comparison tested systematically the effects of the probe sensor size in terms of the pseudo-chord size probability distribution functions. The comparative results showed consistently larger measured count rates and a broader range of bubble/droplet sizes with the 0.025 mm probe sensor (Table A-3, columns 3 and 6). The pseudo chord sizes measured with 0.35 mm sensor were typically 18 to 50% larger (average 28%) than the pseudo-chord lengths measured with the 0.025 mm probe sensor. This suggested the existence of a significant proportion of small bubbles/droplets with sizes ranging from 0.025 to 0.35 mm. In the upper spray/splashing region (i.e. C > 0.97) however, the pseudo-droplet chord data were close implying that most water droplets were larger than 0.35 mm.

## A.3 Discussion

The notion of pseudo-chord size was used in earlier studies. For example, CHANSON et al. (2002,2006) in plunging jet flows. Generally the concept of pseudo-chord sizes is easier to comprehend and to compare with visual observations, high-speed photographs and movies than the bubble/droplet chord time data. However it is essential to validate Equation (A-1) in any complex air-water flows before using it.

The effects of probe sensor size on the air-water flow properties were seldom tested but in a few studies (CHANSON and TOOMBES 2002c). It is acknowledged that the probe sensor size may affect the results when the sensor size is large than the smallest bubbles. The true accuracy of the data is however a combination of both probe sensor size and scan rate, while the scan duration must be long enough to ensure a statistically meaningful sample.

Fig. A-3 - Normalised probability distribution functions of bubble/droplet chord sizes : comparison between 0.025 mm and 0.35 mm sensor probe sensor sizes

(A) Bubbly flow region

| Probe sensor size (mm) | $d_C/h$ | Step number | C | F (Hz) | Reference | Run |
|---|---|---|---|---|---|---|
| 0.025 | 1.18 | 10 | 0.107 | 177.5 | GONZALEZ et al. (2005) | Sm13S10_05 |
| 0.35 | 1.15 | 10 | 0.106 | 118.1 | Present study | 060411S10_04 |

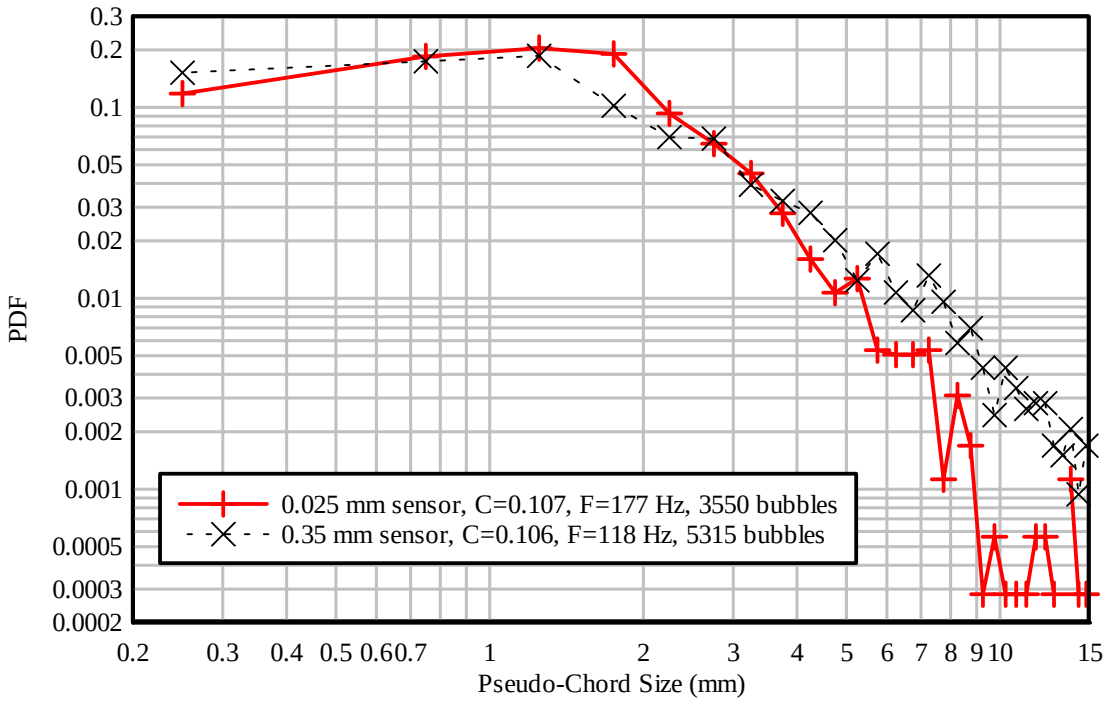

(B) Spray region

| Probe sensor size (mm) | $d_C/h$ | Step number | C | F (Hz) | Reference | Run |
|---|---|---|---|---|---|---|
| 0.025 | 1.18 | 10 | 0.893 | 102.9 | GONZALEZ et al. (2005) | Sm13S10_19 |
| 0.35 | 1.15 | 10 | 0.874 | 82.3 | Present study | 060411S10_14 |

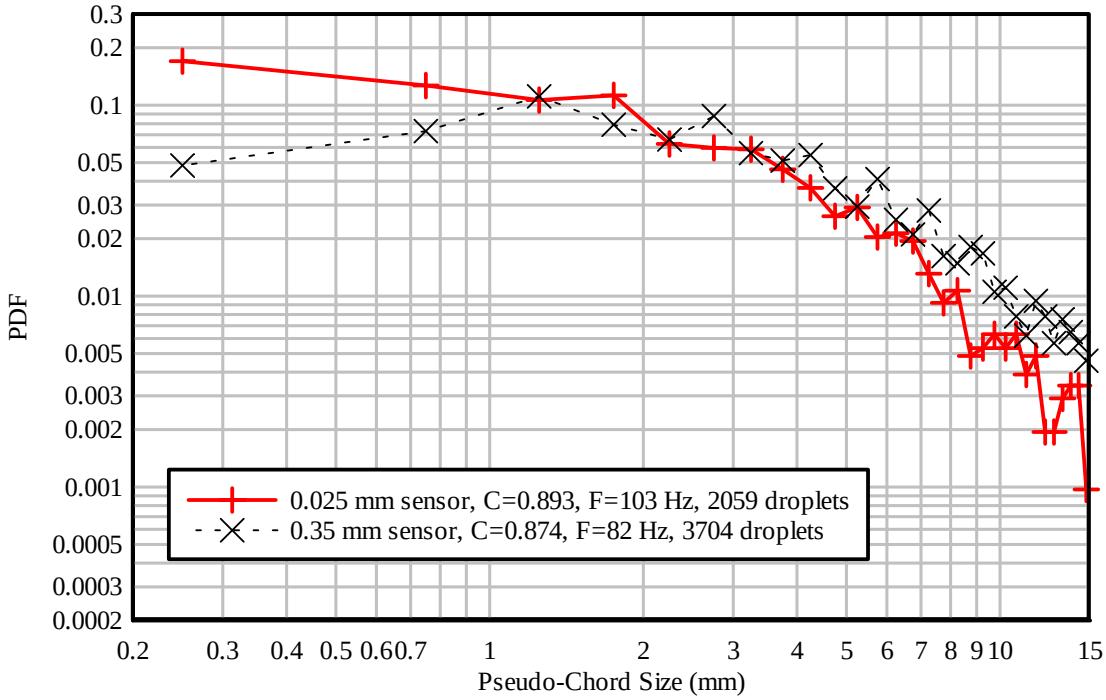


Table A-3 - Effect of the probe sensor size on the relative error in terms of pseudo-chords for $d_C/h$ = 1.15, step 10

| GONZALEZ et al.(2005) | | | Present Study | | | Relative error (%) |
|---|---|---|---|---|---|---|
| Ref. (1) | C (2) | F (Hz) (3) | Ref. (4) | C (5) | F (Hz) (6) | (7) |
| 05 | 0.107 | 177.5 | 08 | 0.106 | 118.0 | 46.8 |
| 10 | 0.218 | 249.1 | 09 | 0.182 | 159.0 | 18.7 |
| 12 | 0.327 | 183.6 | 10 | 0.327 | 177.0 | 20.1 |
| 17 | 0.817 | 169 | 13 | 0.798 | 120.0 | 44.2 |
| 19 | 0.893 | 102.0 | 14 | 0.974 | 82.0 | 49.7 |
| 20 | 0.922 | 73.0 | 15 | 0.91 | 57.0 | 38.7 |
| 21 | 0.943 | 55.9 | 16 | 0.933 | 43.6 | 13.5 |
| 22 | 0.961 | 39.2 | 18 | 0.961 | 27.8 | 15.5 |
| 24 | 0.973 | 25.8 | 20 | 0.973 | 19.4 | 5.5 |
| 25 | 0.98 | 20.4 | 21 | 0.981 | 15.5 | 8.2 |
| 27 | 0.987 | 13.6 | 22 | 0.987 | 10.5 | -4.1 |
| 28 | 0.99 | 9.8 | 24 | 0.993 | 7.1 | -- |
| 29 | 0.994 | 7.05 | 27 | 0.995 | 4.0 | -- |
| 30 | 0.996 | 4.05 | 28 | 0.996 | 4.4 | -12.9 |

Notes : Errors calculated for bubble chord for C < 0.3 and droplet chords for C > 0.7.

## APPENDIX B - SUMMARY OF AIR-WATER FLOW PROPERTIES

*Notation*

| | |
|---|---|
| C | void fraction defined as the volume of air per unit volume of air and water; |
| $C_{mean}$ | depth-average vid fraction defined in terms of $Y_{90}$ : $C_{mean} = 1 - d/Y_{90}$; |
| d | equivalent clear water flow depth defined as: $d = \int_{C=0}^{C=0.90} (1 - C) * dy$ ; |
| $d_c$ | critical flow depth (m); |
| $F_{max}$ | maximum bubble count rate (Hz) at a given cross-section; |
| f | equivalent Darcy-Weisbach friction factor in air-water skimming flows; |
| g | gravity constant: g = 9.80 $m/s^2$ in Brisbane, Australia; |
| $Q_w$ | water discharge ($m^3/s$); |
| W | channel width (m); |
| x | distance along the channel bottom (m); |
| $Y_{90}$ | characteristic depth (m) where the void fraction is 90%. |

*Results*

| Run | $Q_w$ | Probe | Step edge | d | $Y_{90}$ | $F_{max}$ | $V_{90}$ | $C_{mean}$ |
|---|---|---|---|---|---|---|---|---|
| | $m^3/s$ | | | m | m | Hz | m/s | |
| (1) | (2) | (3) | (4) | (5) | (6) | (7) | (8) | (9) |
| 060323a | 0.0948 | 1-tip probe | 6 | 0.0331 | 0.0790 | 150.4 | -- | 0.580 |
| | | | 7 | 0.0388 | 0.0645 | 148.8 | -- | 0.399 |
| | | | 8 | 0.0401 | 0.0645 | 166.4 | -- | 0.379 |
| | | | 9 | 0.0380 | 0.0805 | 144.9 | -- | 0.528 |
| | | | 10 | 0.0333 | 0.0585 | 173.1 | -- | 0.431 |
| 060410a | 0.1164 | 1-tip probe | 7 | 0.0390 | 0.0748 | 161.9 | -- | 0.479 |
| | | | 8 | 0.0458 | 0.0645 | 177.8 | -- | 0.290 |
| | | | 9 | 0.0335 | 0.0635 | 177.8 | -- | 0.472 |
| | | | 10 | 0.0389 | 0.0610 | 194.9 | -- | 0.363 |
| 060614a | 0.1431 | 2-tip probe | 7 | 0.0428 | 0.0668 | 118.4 | 3.27 | 0.393 |
| | | | 8 | 0.0407 | 0.0620 | 168.9 | 3.27 | 0.343 |
| | | | 9 | 0.0440 | 0.0703 | 169.1 | 3.42 | 0.410 |
| | | | 10 | 0.0409 | 0.0633 | 199.7 | 3.42 | 0.390 |
| 060512a | 0.1612 | 1-tip probe | 8 | 0.0497 | 0.0745 | 129.4 | -- | 0.333 |
| | | | 9 | 0.0476 | 0.0783 | 142.7 | -- | 0.392 |
| | | | 10 | 0.0520 | 0.0735 | 154.1 | -- | 0.293 |
| 060404a | 0.1798 | 1-tip probe | 8 | 0.0574 | 0.0795 | 99.0 | -- | 0.278 |
| | | | 9 | 0.0562 | 0.0865 | 113.9 | -- | 0.350 |
| | | | 10 | 0.0575 | 0.0845 | 135.2 | -- | 0.319 |

## APPENDIX C - FLOW RESISTANCE IN SKIMMING FLOWS

### C.1 Presentation

On smooth chutes, the flow resistance is primarily skin friction. Skimming flows over a stepped spillway are characterised by significant form losses. The water skims over the step edges with formation of recirculating vortices between the main stream and the step corners. Form drag is predominant and, as KAZEMIPOUR and APELT (1983) stressed out, the form losses cannot be modelled satisfactorily by a Gauckler-Manning or Darcy-Weisbach formula. Nevertheless this study presents the flow resistance data in terms of an equivalent Darcy friction factor f because it is a dimensionless shear stress that derives from the momentum equation. ([1]).

In *uniform equilibrium flows*, the momentum principle states that the boundary friction force equals exactly the gravity force component in the flow direction (HENDERSON 1966, CHANSON 2001a,2004a). That is, the weight of water component acting parallel to the pseudo-bottom formed by the step edges. It yields:

$$\tau_o * P_w = \rho_w * g * A_w * \sin\theta \qquad \text{Uniform equilibrium (C-1)}$$

where $\tau_o$ is the average shear stress between the skimming flow and recirculating fluid underneath, $P_w$ is the wetted perimeter, $\rho_w$ is the water density, g is the gravity constant, $A_w$ is the water flow cross-section area and $\theta$ is the mean bed inclination angle. In dimensionless terms, and for a wide channel, Equation (C-1) becomes :

$$f_e = \frac{8 * \tau_o}{\rho_w * U_w^2} = \frac{8 * g * \left( \int_{y=0}^{y=Y_{90}} (1 - C) * dy \right) * \sin\theta}{U_w^2} \qquad \text{Uniform equilibrium (C-2)}$$

where $f_e$ is the Darcy friction factor for air-water flow, C is the local void fraction, y is measured normal to the pseudo-invert formed by the step edges, $Y_{90}$ is the distance normal to the pseudo-bottom where C = 90% and $U_w$ is the water flow velocity : $U_w = q_w/d$, $q_w$ is the water discharge per unit discharge and d is the equivalent clear-water depth. The dimensionless shear stress is analogous to the Darcy friction factor ([2]) but it characterises the form drag loss.

In gradually-varied flows, the average shear stress between the skimming flow and the cavity recirculation are deduced from the friction slope $S_f$ ([3]). For a wide channel the energy equation yields :

$$f_e = \frac{8 * \tau_o}{\rho_w * U_w^2} = \frac{8 * g * \left( \int_{y=0}^{y=Y_{90}} (1 - C) * dy \right) * S_f}{U_w^2} \qquad \text{Gradually-varied flow (C-3)}$$

where the friction slope equals $S_f = - \partial H/\partial x$, H is the mean total head and x is the curvilinear coordinate along the flow direction. Free-surface aeration is always substantial in prototype and laboratory skimming flows, and its effects must be accounted for using Equations (C-2) to (C-3).

---

[1]This approach facilitates further a comparison between smooth and stepped chute data.

[2]For a smooth invert chute, the boundary shear stress is defined as : $\tau_o = f_e * \rho_w * U_w^2/8$ (e.g. CHANSON 1999a, p. 74).

[3]The friction slope is the slope of the total head line (HENDERSON 1966, CHANSON 1999a,2004a).

In the present study, the air-water flow measurements were performed systematically at step edges downstream of the inception point of free-surface aeration. Uniform equilibrium flow conditions were not achieved at the downstream end of the chute and the flow resistance was calculated using Equation (C-3). Importantly Equation (C-3) gives the equivalent Darcy friction factor in the aerated flow region only. It does not characterise the flow resistance in the clear-water flow region upstream of the inception point ([4]).

## C.2 Experimental results

Flow resistance results are given in Table C-1 and Figure C-1. In Figure C-1, the present data are compared with a comprehensive re-analysis of flow resistance in skimming flows for large-size model data (h > 0.020 m, Re > 1E + 5), where Re is the flow Reynolds number defined in terms of the hydraulic diameter $D_H$ (CHANSON et al. 2002, CHANSON 2006b). The flow resistance data are presented in Figure C-1 in terms of the equivalent Darcy friction factor as a function of the dimensionless step roughness height $h*\cos\theta/D_H$. Details of experimental technique are given in the caption.

Present flow resistance data are close to past study results in the same facility. In average for five flow rates, the equivalent Darcy friction factor in the present study was $f_e \approx 0.14$ downstream of the inception point of free-surface aeration. Overall, the equivalent Darcy friction factor in skimming flows ranged typically between 0.1 and 0.35 with no obvious correlation with the relative step roughness height, Reynolds, Froude nor Weber numbers (CHANSON et al. 2002, CHANSON 2004c). Experimental data with pressurised intakes tended to exhibit lower flow resistance (CHANSON 2006b).

The friction factor data compared however favourably with a simplified analytical model of the pseudo-boundary shear stress which may be expressed in dimensionless form as :

$$f_d = \frac{2}{\sqrt{\pi}} * \frac{1}{K} \quad \text{(C-4)}$$

where $f_d$ is an equivalent Darcy friction factor estimate of the form drag, and 1/K is the dimensionless expansion rate of the shear layer. The coefficient 1/K is assumed to be constant in a Prandtl mixing length model (RAJARATNAM 1976, SCHLICHTING 1979). Equation (C-4) predicts $f_d \approx 0.2$ for K = 6 that is close to observed friction factors (Fig. C-1).

[4]AMADOR et al. (2006) derived the flow resistance in the developing boundary layer flow over a stepped chute based upon an integral momentum method. Using PIV measurements, their results yielded f = 0.125 in average for $\theta = 51.3^o$, h = 0.05 m, $d_C/h = 2.1$ and Re = 4.4 E+5.

Table C-1 - Flow resistance in skimming flow (Present study)

| Ref. | $Q_w$ $m^3/s$ | $d_c/h$ | Re | $f_e$ | Remarks |
|---|---|---|---|---|---|
| (1) | (2) | (3) | (4) | (5) | (6) |
| 060323a | 0.0948 | 1 | 3.8E+05 | 0.159 | Step edges 6 to 10. |
| 060410a | 0.1164 | 1.15 | 4.6E+05 | 0.126 | Step edges 7 to 10. |
| 060614a | 0.1431 | 1.33 | 5.7E+05 | 0.087 | Step edges 7 to 10. |
| 060512a | 0.1612 | 1.45 | 6.4E+05 | 0.168 | Step edges 8 to 10. |
| 060404a | 0.1798 | 1.57 | 7.1E+05 | 0.169 | Step edges 8 to 10. |

Fig. C-1 - Equivalent Darcy-Weisbach friction factor in air-water skimming flow - Comparison between present data, earlier studies (ANDRE et al. 2003, BaCara 1991, BOES 2000a, CHAMANI and RAJARATNAM 1999, CHANSON and TOOMBES 2001,2002a, GONZALEZ and CHANSON 2004, MATOS 2000, SHVAJNSHTEIN 1999, YASUDA and OHTSU 1999) for large size model data (Re > 1 E+5 and h > 0.02 m), and Equation (C-4)

| | | |
|---|---|---|
| f | equivalent Darcy friction factor deduced from clear-water flow readings | BaCara (1991), SHVAJNSHTEIN (1999), YASUDA and OHTSU (1999) |
| $f_e$ | equivalent Darcy friction factor in air-water flow deduced from detailed void fraction measurements | ANDRE et al. (2003), BOES (2000a), CHAMANI and RAJARATNAM 1999, CHANSON and TOOMBES (2001,2002a), GONZALEZ and CHANSON (2004), MATOS (2000) |

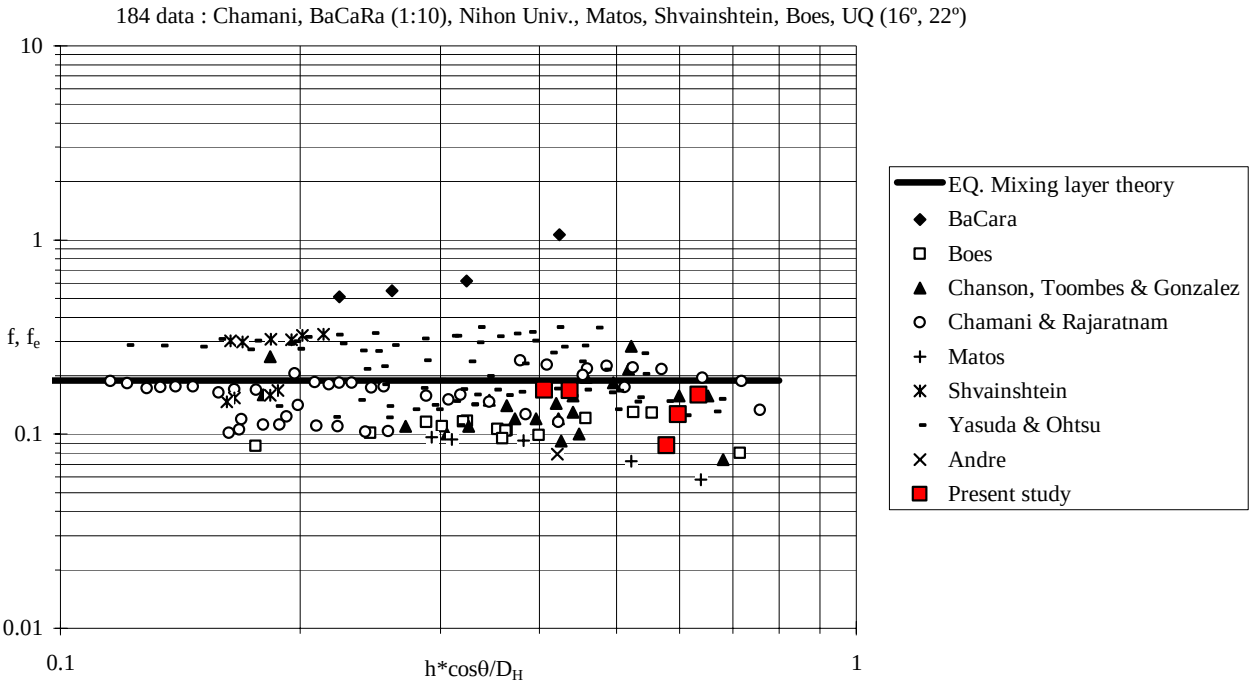

## APPENDIX D - AIR-WATER FLOW TIME SCALES IN SKIMMING FLOWS ON A STEPPED CHUTE

### D.1 Presentation

Air-water flow measurements were performed for a range of experiments. For some runs, two identical phase-detection sensors were recorded simultaneously. In some experiments, the probe sensors were located at the same vertical and streamwise distances y and x respectively, but they were separated in the transverse direction by a known distance $\Delta z$. Each single-tip conductivity probe consisted of a sharpened rod (platinum wire $\varnothing$ = 0.35 mm) which was insulated except for its tip and set into a metal supporting tube (stainless steel surgical needle $\varnothing$ = 1.42 mm) acting as the second electrode. The reference probe was located on the channel centreline. The second probe sensor was separated in the transverse direction by a known spacing $\Delta z$.

For other series of experiments, the two sensors were located at the same vertical distance y, but they were separated in the longitudinal direction by a known distance $\Delta x$. These experiments were conducted with some dual-tip probe. Each sensor consisted of a sharpened rod (platinum wire $\varnothing$ = 0.25 mm) which was insulated except for its tip and set into a metal supporting tube (stainless steel surgical needle $\varnothing$ = 0.5 mm (internal) and 0.8 mm (external)). The stainless steel tube acted as the second electrode and it was separated from the inner wire by some insulating epoxy. The longitudinal spacing between probe sensors $\Delta x$ was measured with a microscope.

The probes were excited by an electronics (UQ82.518) designed with a response time less than 10 ms and calibrated with a square wave generator. Each sensor was scanned at 20 kHz for 45 seconds. Table D-1 summarises the range of investigations. Section D.2 presents the correlation analysis technique. All data sets are regrouped in Sections D3 and D4.

*Notation*

| | |
|---|---|
| C | void fraction defined as the volume of air per unit volume of air and water; |
| F | air bubble count rate (Hz) defined as the number of detected air bubbles per unit time; |
| g | gravity acceleration ($m/s^2$) : g = 9.80 $m/s^2$ in Brisbane (Australia); |
| $q_w$ | water discharge per unit width ($m^2/s$); |
| Re | Reynolds number defined in terms of the hydraulic diameter; |
| $R_{xx}$ | normalised auto-correlation function (reference probe); |
| $R_{xy}$ | normalised cross-correlation function between two probe output signals; |
| $(R_{xy})max$ | maximum cross-correlation between two probe output signals; |
| $T_{xx}$ | auto-correlation integral time scale : $T_{xx} = \int_{\tau=0}^{\tau=\tau(R_{xx}=0)} R_{xx}(\tau) * d\tau$ |
| $T_{xy}$ | cross-correlation integral time scale : $T_{xy} = \int_{\tau=\tau(R_{xy}=(R_{xy})_{max})}^{\tau=\tau(R_{xy}=0)} R_{xy}(\tau) * d\tau$ |
| $T_{0.5}$ | characteristic time lag $\tau$ for which $R_{xx}$ = 0.5; |

| | |
|---|---|
| V | interfacial velocity (m/s); |
| W | channel width (m); |
| y | distance (m) measured normal to the flow direction; |
| $\Delta x$ | streamwise separation distance (m) between probe sensors; |
| $\Delta z$ | transverse separation distance (m) between probe sensors; |
| $\mu$ | dynamic viscosity (Pa.s); |
| $\rho$ | density (kg/m$^3$); |
| $\tau$ | time lag (s); |
| $\tau_{0.5}$ | characteristic time lag $\tau$ for which $R_{xy} = 0.5 * (R_{xy})_{max}$; |
| $\varnothing$ | diameter (m); |

*Subscript*

| | |
|---|---|
| xx | auto-correlation of reference probe signal; |
| xy | cross-correlation; |

Table D-1 - Experimental measurements in skimming flows with identical probe sensors (Present study)

| $q_w$ | $\frac{d_c}{h}$ | Re | Instrumentation | $\Delta x$ | $\Delta z$ | Step edge | Comments |
|---|---|---|---|---|---|---|---|
| $m^2/s$ | | | | mm | mm | | |
| (1) | (2) | (3) | (4) | (5) | (6) | (7) | (8) |
| 0.116 | 1.15 | 4.6 E+5 | Two single-tip probes | | | | W = 1.0 m, h = 0.10 m, l = 0.25 m. |
| | | | | 0 | 8.45 | 7 | Run 060410a. |
| | | | | 0 | 8.45 | 8 | Run 060410b. |
| | | | | 0 | 8.45 | 9 | Run 060410c. |
| | | | | 0 | 3.6 | 10 | Run 060508b. |
| | | | | 0 | 6.3 | 10 | Run 060412c. |
| | | | | 0 | 8.45 | 10 | Run 060411a. |
| | | | | 0 | 10.75 | 10 | Run 060411b. |
| | | | | 0 | 13.7 | 10 | Run 060411c. |
| | | | | 0 | 16.7 | 10 | Run 060412a. |
| | | | | 0 | 21.7 | 10 | Run 060412b. |
| | | | | 0 | 29.5 | 10 | Run 060413a. |
| | | | | 0 | 40.3 | 10 | Run 060508a. |
| 0.161 | 1.45 | 6.4 E+5 | Two single-tip probes | | | | W = 1.0 m, h = 0.10 m, l = 0.25 m. |
| | | | | 0 | 8.45 | 8 | Run 060512a. |
| | | | | 0 | 8.45 | 9 | Run 060512b. |
| | | | | 0 | 3.6 | 10 | Run 060509a. |
| | | | | 0 | 8.45 | 10 | Run 060511b. |
| | | | | 0 | 13.7 | 10 | Run 060509b. |
| | | | | 0 | 21.7 | 10 | Run 060510a. |
| | | | | 0 | 40.3 | 10 | Run 060510b. |
| | | | | 0 | 55.7 | 10 | Run 060511a. |
| 0.116 | 1.15 | 4.6 E+5 | One dual-tip probe | | | | W = 1.0 m, h = 0.10 m, l = 0.25 m. |
| | | | | 7.0 | 1.4 | 10 | Run 060530a. |

| | | | | | | | |
|---|---|---|---|---|---|---|---|
| | | | | 9.6 | 1.4 | 10 | Run 060613a. |
| 0.143 | 1.33 | 5.7 E+5 | One dual-tip probe | | | | |
| | | | | 7.0 | 1.4 | 7 | Run 060614a. |
| | | | | 7.0 | 1.4 | 8 | Run 060614b. |
| | | | | 7.0 | 1.4 | 9 | Run 060615a. |
| | | | | 7.0 | 1.4 | 10 | Run 060615b. |
| 0.161 | 1.45 | 6.4 E+5 | One dual-tip probe | | | | W = 1.0 m, h = 0.10 m, l = 0.25 m. |
| | | | | 7.0 | 1.4 | 10 | Run 060530b. |
| | | | | 9.6 | 1.4 | 10 | Run 060613b. |

Notes : $d_C$ : critical flow depth; h : step height; l : step length; Re : Reynolds number defined in terms of the hydraulic diameter; W = channel width.

## D.2 Correlation analyses

The probe signals were analysed in terms of the auto-correlation and cross-correlation functions calculated from the raw probe output signals. (Any analysis based upon the thresholded signals, or square-wave signals, tends to ignore the contributions of the smallest air-water particles.) The original signal data of 900,000 samples per sensor were segmented because the periodogram resolution is inversely proportional to the number of samples and it could be biased with large data sets (HAYES 1996, GONZALEZ 2005). All data signals were sub-divided into fifteen non-overlapping segments of 60,000 samples.

Basic results included the maximum cross-correlation coefficient $(R_{xy})_{max}$, and the correlation time scales $T_{xx}$ and $T_{xy}$ where :

$$T_{xx} = \int_{\tau=0}^{\tau=\tau(R_{xx}=0)} R_{xx}(\tau) * d\tau \qquad \text{(D-1)}$$

$$T_{xy} = \int_{\tau=\tau(R_{xy}=(R_{xy})_{max})}^{\tau=\tau(R_{xy}=0)} R_{xy}(\tau) * d\tau \qquad \text{(D-2)}$$

where $R_{xx}$ is the normalised auto-correlation function, $\tau$ is the time lag, and $R_{xy}$ is the normalised cross-correlation function between the two probe output signals (Fig. D-1). All auto-correlation results are presented for the reference probe sensor : that is, the reference probe on the channel centreline (z = 0) or the leading tip.

*Discussion*

Auto- and cross-correlation calculations were most successful for $0.05 \leq C \leq 0.95$. In the upper spray region ($C \geq 0.90$ to 0.95) and at some other locations, the calculations were unsuccessful for a number of reasons. These included flat cross-correlation functions without a distinctive peak, non-crossing of the correlation function(s) with the zero line, correlation functions with several peaks, meaningless correlation trends ... Such data points are indicated with (--) in the following tables of results.

While most correlation calculations can be automated, it must be stressed that human intervention are essential to validate each calculation step. Herein all calculations were performed by hand and all meaningless results were rejected.

Fig. D-1 - Auto- and cross-correlation functions for two identical phase-detection probes separated by a known distance Y - Definition sketches

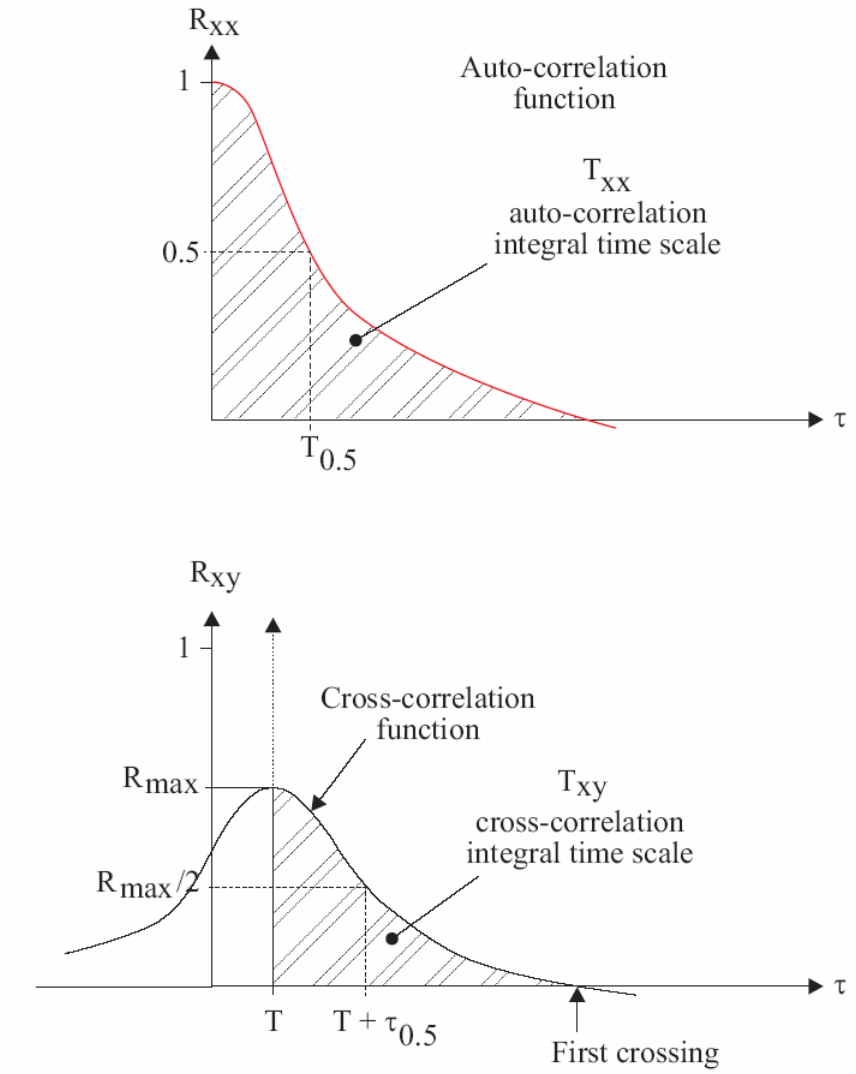


## D.3 Experimental results in terms of transverse separation Δz

*D.3.1 Experimental results for $d_C/h$ = 1.15*

| | |
|---|---|
| Location : | The University of Queensland (Australia) |
| Date : | April-June 2006 |
| Experiments by : | G. CAROSI |
| Data processing by: | G. CAROSI and H. CHANSON |
| Data analysis by : | H. CHANSON and G. CAROSI |
| Experiment characteristics : | Channel: width: 1.0 m, slope: 21.8º, h = 0.10 m, l = 0.25 m, 10 identical steps. Open channel with perspex sidewalls and smooth marine plywood staircase invert.<br>$Q_W$ = 0.1164 $m^3/s$, $d_C$ = 0.115 m, Re = 4.6 E+5 |
| Instrumentation : | Two single-tip conductivity probe (∅ = 0.35 mm). Transverse separation distance Δz.<br>Scan rate: 20 kHz per probe sensor, Sampling duration: 45 sec. |

| Comments : | Inflow conditions : broad-crested weir.<br>Inception of free-surface aeration: between step edges 6 and 7.<br>Correlation analyses performed on fifteen segments of 60,000 samples. |
|---|---|

D.3.1.1 Step edge 7

| Δz<br>mm | y<br>mm | C | F<br>Hz | $T_{xx}$<br>sec. | $(R_{xy})_{max}$ | $T_{xy}$<br>sec. |
|---|---|---|---|---|---|---|
| 8.45 | 1.5 | 0.023 | 41.2 | 0.001138 | 0.039598 | **0.000253** |
| | 6.5 | 0.039 | 54.2 | 0.001846 | 0.029276 | **0.000241** |
| | 11.5 | 0.045 | 55.9 | 0.001549 | 0.069302 | 0.000342 |
| | 12.5 | 0.046 | 57 | 0.001642 | 0.056696 | 0.000204 |
| | 13.5 | 0.047 | 58.7 | 0.001415 | 0.054021 | 0.000244 |
| | 16.5 | 0.058 | 63.2 | 0.001674 | 0.095058 | 0.000435 |
| | 19.5 | 0.078 | 75.2 | 0.001915 | 0.117507 | 0.000176 |
| | 21.5 | 0.086 | 82.3 | 0.001985 | 0.153981 | 0.000974 |
| | 26.5 | 0.173 | 118 | 0.003083 | 0.237158 | 0.001573 |
| | 31.5 | 0.286 | 147.9 | 0.003673 | 0.30839 | 0.002397 |
| | 36.5 | 0.427 | 161.9 | 0.004054 | 0.329295 | 0.002663 |
| | 41.5 | 0.573 | 150 | 0.003812 | 0.336687 | 0.002424 |
| | 46.5 | 0.687 | 130.8 | 0.003557 | 0.323703 | 0.002274 |
| | 51.5 | 0.759 | 106.8 | 0.003311 | 0.299907 | 0.001678 |
| | 56.5 | 0.791 | 90.4 | 0.003068 | 0.286926 | 0.00165 |
| | 61.5 | 0.833 | 75.4 | 0.003052 | 0.277592 | 0.001372 |
| | 66.5 | 0.866 | 62.9 | 0.003162 | 0.253003 | 0.001436 |
| | 71.5 | 0.886 | 55.8 | 0.00305 | 0.262698 | 0.001448 |
| | 76.5 | 0.907 | 47.5 | 0.002923 | 0.235481 | 0.001212 |
| | 81.5 | 0.926 | 38.2 | 0.003063 | 0.250306 | 0.001333 |
| | 86.5 | 0.932 | 35.4 | 0.00292 | 0.24193 | 0.001135 |
| | 91.5 | 0.94 | 32 | 0.003033 | 0.219811 | 0.001172 |
| | 96.5 | 0.96 | 23.1 | 0.002899 | 0.213702 | 0.000897 |
| | 101.5 | 0.966 | 19.7 | 0.002779 | 0.206452 | 0.001104 |
| | 106.5 | 0.971 | 16.4 | 0.003116 | 0.210604 | 0.00102 |
| | 111.5 | 0.98 | 11.8 | 0.002879 | 0.175065 | 0.000594 |
| | 116.5 | 0.986 | 8.7 | 0.003167 | 0.18069 | 0.001245 |
| | 121.5 | 0.986 | 8.6 | 0.003087 | 0.195403 | 0.001037 |
| | 126.5 | 0.987 | 7.5 | 0.003379 | 0.197714 | 0.001102 |
| | 131.5 | 0.991 | 5.3 | 0.003628 | 0.166628 | 0.001249 |
| | 131.5 | 0.993 | 4.2 | 0.004918 | 0.144221 | 0.000868 |
| | 136.5 | 0.994 | 3.9 | 0.005275 | 0.177924 | 0.000784 |
| | 141.5 | 0.995 | 3.3 | 0.00705 | 0.180191 | 0.001755 |
| | 146.5 | 0.995 | 3.1 | 0.007349 | 0.13411 | 0.000849 |

Notes : *Blue italic* : suspicious data; **Red Bold** : possibly incorrect data; (--) : meaningless data.

D.3.1.2 Step edge 8

| Δz<br>mm | y<br>mm | C | F<br>Hz | $T_{xx}$<br>sec. | $(R_{xy})_{max}$ | $T_{xy}$<br>sec. |
|---|---|---|---|---|---|---|
| 8.45 | 1.5 | 0.01 | 28 | -- | -- | -- |
| | 6.5 | 0.022 | 43.8 | -- | -- | -- |
| | 9.5 | 0.031 | 53.7 | 0.000208 | 0.034112 | 0.000231 |

| | | | | | |
|---|---|---|---|---|---|
| 11.5 | 0.03 | 53.2 | 0.000649 | 0.023608 | 0.000157 |
| 13.5 | 0.033 | 56.8 | 0.000782 | 0.040429 | 0.000209 |
| 16.5 | 0.036 | 56.7 | 0.000659 | 0.043847 | 0.000201 |
| 19.5 | 0.039 | 59.3 | 0.000613 | 0.040833 | 0.000167 |
| 21.5 | 0.044 | 63.8 | 0.000701 | 0.070214 | 0.000354 |
| 26.5 | 0.069 | 82.5 | 0.001139 | 0.120278 | 0.000667 |
| 31.5 | 0.129 | 116.2 | 0.00222 | 0.208081 | 0.001601 |
| 36.5 | 0.226 | 151.1 | 0.002786 | 0.310492 | 0.002545 |
| 41.5 | 0.452 | 177.8 | 0.003388 | 0.368183 | 0.003352 |
| 46.5 | 0.574 | 173.2 | 0.003074 | 0.379823 | 0.003282 |
| 51.5 | 0.699 | 138.5 | *0.003456* | 0.386382 | *0.003325* |
| 56.5 | 0.815 | 99.1 | 0.002638 | 0.334799 | *0.002593* |
| 61.5 | 0.879 | 68.1 | 0.002269 | 0.301261 | 0.002009 |
| 66.5 | 0.915 | 49.9 | 0.001174 | 0.269959 | 0.001773 |
| 71.5 | 0.93 | 41 | 0.001883 | 0.242849 | 0.001522 |
| 76.5 | 0.95 | 29.7 | *0.00209* | 0.234915 | *0.001435* |
| 81.5 | 0.959 | 24.7 | 0.001704 | 0.218581 | 0.00113 |
| 86.5 | 0.965 | 20.7 | *0.001757* | 0.186307 | *0.001077* |
| 91.5 | 0.978 | 14.7 | *0.001775* | 0.199186 | *0.001085* |
| 96.5 | 0.98 | 13 | *0.000269* | 0.192624 | 0.000906 |
| 101.5 | 0.986 | 8.9 | *0.000403* | 0.190426 | 0.0007 |
| 106.5 | 0.989 | 7.3 | *0.001585* | 0.128367 | 0.000632 |
| 111.5 | 0.99 | 6.1 | *0.001759* | 0.146703 | 0.000656 |
| 116.5 | 0.992 | 5.6 | *0.001715* | 0.165646 | *0.000638* |
| 121.5 | 0.995 | 3.9 | *0.001724* | 0.118605 | 0.000283 |
| 126.5 | 0.996 | 3.1 | *0.001697* | 0.11617 | *0.000433* |
| 131.5 | 0.996 | 3.1 | *0.001986* | 0.179758 | 0.000566 |
| 131.5 | 0.997 | 2 | *0.002152* | 0.136295 | *0.000478* |
| 136.5 | 0.998 | 1.7 | *0.001923* | 0.117221 | *0.000476* |
| 141.5 | 0.998 | 1.8 | *0.002144* | 0.147577 | *0.000871* |
| 146.5 | 0.998 | 1.4 | *0.003138* | 0.073672 | *0.000159* |
| 151.5 | 0.999 | 0.7 | -- | -- | -- |

Notes : *Blue italic* : suspicious data; **Red Bold** : possibly incorrect data; (--) : meaningless data.

D.3.1.3 Step edge 9

| $\Delta z$ mm | y mm | C | F Hz | $T_{xx}$ sec. | $(R_{xy})_{max}$ | $T_{xy}$ sec. |
|---|---|---|---|---|---|---|
| 8.45 | 1.5 | 0.032 | 57.6 | 0.00119 | 0.032832 | 0.000238 |
| | 6.5 | 0.037 | 62.4 | 0.001199 | 0.035902 | 0.00026 |
| | 9.5 | 0.044 | 64.8 | 0.001195 | 0.051598 | 0.000324 |
| | 11.5 | 0.049 | 70.5 | 0.001038 | 0.062925 | 0.000441 |
| | 16.5 | 0.056 | 74.2 | 0.000286 | 0.095865 | 0.00047 |
| | 19.5 | 0.069 | 83.9 | 0.001248 | 0.123403 | 0.000611 |
| | 20.5 | 0.072 | 82.5 | 0.001213 | 0.136883 | 0.000639 |
| | 21.5 | 0.081 | 90.4 | 0.001336 | 0.154601 | 0.001 |
| | 26.5 | 0.132 | 115 | 0.002067 | 0.233391 | 0.001449 |
| | 31.5 | 0.226 | 149.4 | 0.002878 | 0.330521 | 0.002659 |
| | 36.5 | 0.373 | 177.8 | 0.003327 | 0.381587 | 0.003342 |
| | 41.5 | 0.524 | 165.7 | 0.003248 | 0.416467 | 0.003498 |
| | 46.5 | 0.662 | 142.4 | 0.00266 | 0.363789 | 0.002655 |
| | 51.5 | 0.768 | 109.2 | 0.002191 | 0.331338 | 0.002129 |
| | 56.5 | 0.825 | 90.7 | 0.002037 | 0.330177 | 0.001862 |

| | | | | | |
|---|---|---|---|---|---|
| 56.5 | 0.867 | 71.2 | 0.002086 | 0.314084 | 0.001793 |
| 61.5 | 0.887 | 61.3 | 0.001857 | 0.29519 | 0.001563 |
| 66.5 | 0.917 | 48.3 | 0.001823 | 0.274568 | 0.001479 |
| 71.5 | 0.9487 | 33.2 | 0.002001 | 0.263716 | 0.001391 |
| 76.5 | 0.957 | 28.6 | *0.001852* | 0.273583 | *0.001529* |
| 81.5 | 0.968 | 21.5 | *0.002099* | 0.239386 | *0.001461* |
| 86.5 | 0.977 | 16.6 | *0.003849* | 0.237739 | *0.00106* |
| 91.5 | 0.976 | 16.6 | *0.001787* | 0.220008 | 0.001217 |
| 96.5 | 0.985 | 12 | *0.001936* | 0.21219 | *0.001134* |
| 101.5 | 0.986 | 11 | *0.001738* | 0.165755 | 0.000668 |
| 111.5 | 0.99 | 7.1 | *0.001826* | 0.17029 | *0.001009* |
| 116.5 | 0.993 | 5.6 | *0.001817* | 0.15927 | 0.000758 |
| 121.5 | 0.995 | 4.1 | *0.002268* | 0.196018 | *0.00052* |
| 126.5 | 0.996 | 3.5 | *0.00227* | 0.158337 | *0.000524* |
| 131.5 | 0.996 | 2.9 | *0.00245* | 0.140632 | *0.000692* |
| 131.5 | 0.997 | 2.4 | *0.002111* | 0.142107 | 0.000674 |
| 136.5 | 0.998 | 1.6 | *0.004578* | 0.149602 | *0.000383* |
| 141.5 | 0.999 | 1.4 | *0.003469* | 0.132007 | *0.000504* |
| 146.5 | 0.999 | 0.8 | *0.006519* | 0.154553 | *0.000953* |

Notes : *Blue italic* : suspicious data; **Red Bold** : possibly incorrect data; (--) : meaningless data.

D.3.1.4 Step edge 10

| $\Delta z$ mm | y mm | C | F Hz | $(R_{xy})_{max}$ | $T_{xy}$ sec. |
|---|---|---|---|---|---|
| 3.6 | 2 | 0.03 | 57.5 | 0.158185 | 0.000623 |
| | 7 | 0.031 | 55.7 | 0.169267 | 0.000544 |
| | 10 | 0.04 | 65.2 | 0.195803 | 0.000575 |
| | 12 | 0.035 | 56.8 | 0.192472 | 0.000535 |
| | 14 | 0.043 | 66.7 | 0.221972 | 0.000619 |
| | 17 | 0.057 | 77.8 | 0.28246 | 0.0009 |
| | 20 | 0.095 | 105.5 | 0.389683 | *0.001726* |
| | 22 | 0.114 | 117.2 | 0.41402 | 0.00203 |
| | 27 | 0.169 | 135.8 | 0.506588 | 0.003035 |
| | 32 | 0.34 | 184.1 | 0.592643 | 0.004291 |
| | 37 | 0.514 | 185.1 | 0.627345 | *0.005006* |
| | 42 | 0.68 | 152.9 | 0.633925 | 0.004395 |
| | 47 | 0.785 | 108.6 | 0.628892 | 0.003962 |
| | 52 | 0.847 | 84.3 | 0.611512 | 0.003464 |
| | 57 | 0.896 | 60.4 | 0.594158 | 0.003121 |
| | 62 | 0.927 | 47.3 | 0.577221 | 0.002622 |
| | 67 | 0.935 | 37.8 | 0.570193 | 0.002765 |
| | 72 | 0.953 | 30.4 | 0.554563 | 0.002443 |
| | 77 | 0.967 | 23.9 | 0.524584 | *0.002076* |
| | 82 | 0.973 | 18.8 | 0.534248 | *0.00209* |
| | 87 | 0.981 | 14.8 | 0.512693 | *0.002453* |
| | 92 | 0.984 | 12.4 | 0.520675 | *0.001963* |
| | 97 | 0.988 | 9.1 | 0.53526 | *0.002453* |
| | 102 | 0.993 | 4.6 | 0.469976 | *0.002065* |
| | 107 | 0.993 | 6.6 | 0.483538 | *0.001812* |
| | 112 | 0.995 | 5 | 0.470599 | *0.001946* |
| | 117 | 0.995 | 4.3 | 0.461753 | *0.00213* |
| | 122 | 0.997 | 2.5 | 0.470253 | *0.002171* |
| | 127 | 0.998 | 1.8 | 0.586978 | *0.002436* |
| | 132 | 0.999 | 1.3 | 0.448505 | *0.002174* |

| | | | | | |
|---|---|---|---|---|---|
| | 132 | 0.999 | 0.7 | 0.292012 | *0.002121* |
| | 137 | 0.999 | 0.9 | 0.318358 | *0.00211* |
| | 142 | 0.999 | 0.9 | 0.41464 | *0.00213* |
| | 147 | 0.999 | 1 | 0.28518 | *0.001851* |
| | 152 | 1 | 0.5 | -- | -- |

Notes : *Blue italic* : suspicious data; **Red Bold** : possibly incorrect data; (--) : meaningless data.

| $\Delta z$ | y | C | F | $(R_{xy})_{max}$ | $T_{xy}$ |
|---|---|---|---|---|---|
| mm | mm | | Hz | | sec. |
| 6.2 | 2 | 0.043 | 79.8 | 0.033749 | 0.000212 |
| | 7 | 0.043 | 78.9 | 0.028173 | 8.18E-05 |
| | 10 | 0.051 | 86 | 0.039177 | 0.000162 |
| | 12 | 0.051 | 87.3 | 0.050949 | **0.000175** |
| | 14 | 0.051 | 85.5 | 0.048991 | 0.000149 |
| | 17 | 0.062 | 95.2 | 0.070501 | 0.0003 |
| | 20 | 0.069 | 102 | 0.085866 | 0.000257 |
| | 22 | 0.082 | 110.1 | 0.105475 | 0.000498 |
| | 27 | 0.109 | 130.7 | 0.186996 | 0.000932 |
| | 32 | 0.192 | 168 | 0.308611 | 0.002095 |
| | 37 | 0.403 | 177.8 | 0.412795 | 0.003394 |
| | 42 | 0.572 | 177.8 | 0.448469 | 0.003728 |
| | 47 | 0.709 | 159.9 | 0.450443 | 0.003289 |
| | 52 | 0.816 | 114.1 | 0.432183 | 0.003001 |
| | 57 | 0.867 | 86.9 | 0.351419 | 0.00212 |
| | 62 | 0.917 | 57.1 | 0.334977 | 0.001803 |
| | 67 | 0.94 | 43.5 | 0.299723 | 0.001511 |
| | 72 | 0.949 | 35.2 | 0.261851 | 0.001031 |
| | 77 | 0.966 | 26.3 | 0.267562 | 0.000938 |
| | 82 | 0.974 | 21 | 0.261579 | 0.001028 |
| | 87 | 0.976 | 17.7 | 0.270546 | 0.000816 |
| | 92 | 0.983 | 14 | 0.241304 | 0.0007 |
| | 97 | 0.987 | 11.1 | 0.222471 | 0.000446 |
| | 102 | 0.989 | 8.6 | 0.205582 | *0.000814* |
| | 107 | 0.992 | 6.6 | 0.221689 | *0.000576* |
| | 112 | 0.994 | 5.1 | 0.208606 | *0.000609* |
| | 117 | 0.996 | 3.4 | 0.16207 | *0.000261* |
| | 122 | 0.996 | 3.8 | 0.179831 | 0.000295 |
| | 127 | 0.997 | 2.4 | 0.216852 | *0.000415* |
| | 132 | 0.997 | 2.8 | 0.19021 | *0.000531* |
| | 137 | 0.998 | 1.6 | 0.184822 | *0.000587* |
| | 142 | 0.998 | 1.8 | 0.157231 | 0.000363 |
| | 147 | 0.999 | 1.4 | 0.111714 | *0.000624* |
| | 152 | 0.999 | 1.2 | 0.134326 | *0.000314* |
| | 157 | 0.999 | 0.9 | 0.086934 | 0.000406 |

Notes : *Blue italic* : suspicious data; **Red Bold** : possibly incorrect data; (--) : meaningless data.

| $\Delta z$ | y | C | F | $T_{xx}$ | $(R_{xy})_{max}$ | $T_{xy}$ |
|---|---|---|---|---|---|---|
| mm | mm | | Hz | sec. | | sec. |
| 8.45 | 2 | 0.021 | 47.8 | -- | -- | -- |
| | 7 | 0.035 | 68.2 | -- | -- | -- |
| | 10 | 0.039 | 71 | 0.001195 | 0.039862 | 0.000229 |
| | 12 | 0.041 | 71.8 | 0.001118 | 0.030559 | **0.000187** |
| | 14 | 0.044 | 69.3 | 0.001152 | 0.058069 | *0.00027* |
| | 17 | 0.045 | 76.9 | 0.001026 | 0.059802 | *0.000193* |
| | 20 | 0.054 | 82.3 | 0.001288 | 0.082879 | *0.000485* |

| | | | | | |
|---|---|---|---|---|---|
| 22 | 0.069 | 94.9 | 0.001464 | 0.089351 | **0.000489** |
| 27 | 0.106 | 122.8 | 0.001941 | 0.181247 | 0.000905 |
| 37 | 0.327 | 194.9 | 0.004205 | 0.412343 | 0.003858 |
| 42 | 0.515 | 194 | 0.005275 | 0.429348 | 0.003828 |
| 47 | 0.636 | 171.6 | 0.004955 | 0.378996 | 0.002849 |
| 52 | 0.798 | 120.3 | 0.004118 | 0.38045 | 0.002845 |
| 57 | 0.874 | 79.4 | 0.004168 | 0.319106 | 0.001836 |
| 62 | 0.91 | 56.5 | 0.003405 | 0.289437 | 0.00151 |
| 67 | 0.933 | 44 | 0.003277 | 0.260788 | 0.001279 |
| 72 | 0.955 | 32.5 | 0.002721 | 0.255749 | *0.001394* |
| 77 | 0.961 | 28.2 | *0.002943* | 0.247855 | 0.001266 |
| 82 | 0.965 | 22.4 | 0.002852 | 0.227229 | *0.001105* |
| 87 | 0.973 | 20.5 | *0.002716* | 0.186716 | 0.000806 |
| 92 | 0.981 | 16.7 | *0.002562* | 0.171111 | 0.000898 |
| 97 | 0.987 | 11.2 | *0.002792* | 0.169898 | 0.000836 |
| 102 | 0.988 | 10.1 | *0.002695* | 0.145445 | 0.000876 |
| 107 | 0.993 | 4.8 | *0.002972* | 0.120924 | 0.000601 |
| 112 | 0.993 | 6.4 | *0.002814* | 0.159079 | *0.000688* |
| 117 | 0.996 | 3.7 | *0.002881* | 0.131298 | 0.000663 |
| 122 | 0.995 | 3.6 | *0.002801* | 0.147952 | *0.000579* |
| 127 | 0.997 | 2.9 | *0.003264* | 0.13718 | *0.000777* |
| 132 | 0.998 | 2.3 | *0.003805* | 0.116257 | *0.00063* |
| 132 | 0.999 | 1.4 | *0.005658* | -- | -- |
| 137 | 0.998 | 1.2 | *0.006233* | 0.122243 | *0.00051* |
| 142 | 0.998 | 1.9 | 0.006948 | 0.15187 | *0.000741* |
| 147 | 0.999 | 1.4 | *0.006659* | 0.081157 | *0.000503* |
| 152 | 0.999 | 1.2 | *0.007154* | 0.099427 | 0.000182 |

Notes : *Blue italic* : suspicious data; **Red Bold** : possibly incorrect data; (--) : meaningless data.

| $\Delta z$ | y | C | F | $(R_{xy})_{max}$ | $T_{xy}$ |
|---|---|---|---|---|---|
| mm | mm | | Hz | | sec. |
| 10.75 | 2 | 0.033 | 65.6 | -- | -- |
| | 7 | 0.041 | 77.9 | -- | -- |
| | 10 | 0.052 | 84.1 | 0.021898 | **5.35E-05** |
| | 12 | 0.052 | 85.3 | 0.025106 | **0.000138** |
| | 14 | 0.059 | 94.3 | 0.033983 | 0.000129 |
| | 17 | 0.064 | 95.6 | 0.057365 | 0.000226 |
| | 22 | 0.083 | 111.3 | 0.088022 | 0.000476 |
| | 27 | 0.14 | 142.4 | 0.211847 | 0.00157 |
| | 32 | 0.263 | 185.3 | 0.282966 | 0.002924 |
| | 37 | 0.435 | 209.1 | 0.360338 | 0.003583 |
| | 42 | 0.594 | 185.5 | 0.391415 | 0.003846 |
| | 47 | 0.733 | 152.8 | 0.346699 | 0.003111 |
| | 52 | 0.836 | 100.3 | 0.313994 | 0.002342 |
| | 57 | 0.881 | 74.6 | 0.277629 | 0.002027 |
| | 62 | 0.912 | 60.1 | 0.249525 | 0.001576 |
| | 67 | 0.939 | 44.9 | 0.221428 | 0.00147 |
| | 72 | 0.955 | 33.7 | 0.185232 | *0.001335* |
| | 77 | 0.965 | 26.2 | 0.146827 | 0.000896 |
| | 82 | 0.974 | 21.8 | 0.190872 | *0.000958* |
| | 87 | 0.977 | 17.5 | 0.163553 | *0.0009* |
| | 92 | 0.981 | 15.1 | 0.151483 | 0.000735 |
| | 97 | 0.984 | 12.7 | 0.133015 | 0.000828 |
| | 102 | 0.988 | 9.9 | 0.12937 | 0.000551 |
| | 107 | 0.991 | 7.3 | 0.115336 | 0.000354 |
| | 112 | 0.994 | 5.1 | 0.101391 | 0.000484 |
| | 117 | 0.995 | 4.3 | 0.11032 | *0.000685* |
| | 122 | 0.996 | 3.5 | 0.093171 | 0.000377 |

| | | | | | |
|---|---|---|---|---|---|
| | 127 | 0.996 | 3.5 | 0.093375 | *0.000457* |
| | 132 | 0.997 | 2.5 | 0.131413 | *0.000556* |
| | 137 | 0.998 | 1.7 | 0.083488 | *0.000301* |
| | 142 | 0.998 | 1.8 | 0.092421 | 5.2E-05 |
| | 147 | 0.998 | 1.4 | 0.041026 | *0.000172* |
| | 152 | 0.999 | 1.3 | 0.056421 | *0.000313* |
| | 157 | 0.999 | 1.1 | 0.028816 | 3.37E-05 |

Notes : *Blue italic* : suspicious data; **Red Bold** : possibly incorrect data; (--) : meaningless data.

| $\Delta z$ | y | C | F | $(R_{xy})_{max}$ | $T_{xy}$ |
|---|---|---|---|---|---|
| mm | mm | | Hz | | sec. |
| 13.7 | 2 | 0.033 | 68.7 | -- | -- |
| | 7 | 0.049 | 86.3 | -- | -- |
| | 10 | 0.05 | 85.3 | -- | -- |
| | 12 | 0.049 | 82.2 | 0.014551 | 4.74E-05 |
| | 14 | 0.067 | 102.3 | 0.033448 | 0.000217 |
| | 17 | 0.077 | 104.4 | 0.048978 | 0.000291 |
| | 20 | 0.085 | 112.6 | 0.040326 | 0.000268 |
| | 22 | 0.086 | 111.9 | 0.060137 | 0.000549 |
| | 27 | 0.145 | 146.1 | 0.135366 | 0.001174 |
| | 32 | 0.224 | 184 | 0.207485 | 0.001928 |
| | 37 | 0.458 | 210.4 | 0.317194 | *0.003819* |
| | 42 | 0.654 | 175.1 | 0.30809 | 0.004105 |
| | 47 | 0.762 | 134.7 | 0.293931 | 0.003181 |
| | 52 | 0.853 | 93.8 | 0.238829 | 0.002102 |
| | 57 | 0.897 | 67.8 | 0.215513 | 0.001966 |
| | 62 | 0.928 | 51 | 0.161563 | 0.001037 |
| | 67 | 0.937 | 42.7 | 0.151676 | 0.001166 |
| | 72 | 0.958 | 32.2 | 0.103897 | 0.000741 |
| | 77 | 0.964 | 28.1 | 0.109676 | *0.000772* |
| | 82 | 0.974 | 21.7 | 0.10755 | 0.000577 |
| | 87 | 0.981 | 15.2 | 0.095628 | *0.000766* |
| | 92 | 0.983 | 13.1 | 0.093721 | 0.000526 |
| | 97 | 0.988 | 9.6 | 0.057554 | *0.000485* |
| | 102 | 0.992 | 7.8 | 0.074179 | 0.000268 |
| | 107 | 0.99 | 7.3 | 0.058817 | *0.000477* |
| | 112 | 0.993 | 5.8 | 0.054683 | *0.000551* |
| | 117 | 0.993 | 5.3 | 0.073196 | 0.000419 |
| | 122 | 0.995 | 4.6 | 0.034342 | 0.000228 |
| | 127 | 0.998 | 2 | 0.077217 | *0.000956* |
| | 132 | 0.997 | 2.2 | 0.052943 | *0.000123* |
| | 137 | 0.998 | 1.9 | -- | -- |
| | 142 | 0.999 | 1.3 | 0.045236 | *0.000613* |
| | 147 | 0.998 | 1.6 | 0.029252 | 3.14E-05 |
| | 152 | 0.999 | 1.2 | 0.034407 | 5.69E-05 |
| | 157 | 0.999 | 0.8 | 0.053532 | *0.000184* |

Notes : *Blue italic* : suspicious data; **Red Bold** : possibly incorrect data; (--) : meaningless data.

| $\Delta z$ | y | C | F | $(R_{xy})_{max}$ | $T_{xy}$ |
|---|---|---|---|---|---|
| mm | mm | | Hz | | sec. |
| 16.7 | 2 | 0.02 | 38.5 | -- | -- |
| | 7 | 0.023 | 43.1 | -- | -- |
| | 10 | 0.025 | 42.7 | -- | -- |
| | 12 | 0.028 | 46.6 | -- | -- |
| | 14 | 0.033 | 52 | -- | -- |

| | | | | | |
|---|---|---|---|---|---|
| | 17 | 0.038 | 58.2 | -- | -- |
| | 20 | 0.053 | 69.6 | 0.041741 | 0.000291 |
| | 22 | 0.059 | 72.7 | 0.046857 | *0.000272* |
| | 27 | 0.12 | 112.8 | 0.138677 | *0.001544* |
| | 32 | 0.245 | 154.7 | 0.256048 | 0.003016 |
| | 37 | 0.396 | 172.7 | 0.316665 | 0.003796 |
| | 42 | 0.58 | 163.4 | 0.321489 | 0.00377 |
| | 47 | 0.732 | 123.4 | 0.304742 | 0.00391 |
| | 52 | 0.817 | 92.4 | 0.262547 | 0.002709 |
| | 57 | 0.863 | 71.6 | 0.218607 | 0.00235 |
| | 62 | 0.898 | 56.1 | 0.179784 | 0.001455 |
| | 67 | 0.928 | 42.1 | 0.16047 | *0.001586* |
| | 72 | 0.942 | 34.3 | 0.15877 | *0.001728* |
| | 77 | 0.959 | 27.7 | 0.120136 | *0.001317* |
| | 82 | 0.966 | 22.4 | 0.112714 | *0.001541* |
| | 87 | 0.977 | 15.4 | 0.10188 | *0.00136* |
| | 92 | 0.979 | 14.7 | 0.078795 | *0.00097* |
| | 97 | 0.982 | 12.5 | 0.078795 | *0.00097* |
| | 102 | 0.986 | 10 | 0.086232 | *0.00087* |
| | 107 | 0.991 | 7 | 0.072424 | 0.000554 |
| | 112 | 0.993 | 5.6 | 0.046026 | *0.000509* |
| | 117 | 0.994 | 4.4 | -- | -- |
| | 122 | 0.995 | 3.8 | 0.046218 | *0.000513* |
| | 127 | 0.997 | 2.7 | -- | -- |
| | 132 | 0.997 | 2.9 | 0.062121 | 0.000424 |
| | 137 | 0.998 | 1.5 | 0.048318 | *0.000533* |
| | 142 | 0.998 | 1.8 | -- | *8.6E-05* |
| | 147 | 0.999 | 1.4 | -- | -- |
| | 152 | 0.999 | 0.9 | -- | -- |
| | 157 | 0.999 | 0.8 | -- | -- |

Notes : *Blue italic* : suspicious data; **Red Bold** : possibly incorrect data; (--) : meaningless data.

| $\Delta z$ mm | y mm | C | F Hz | $(R_{xy})_{max}$ | $T_{xy}$ sec. |
|---|---|---|---|---|---|
| 21.7 | 2 | 0.032 | 71 | -- | -- |
| | 7 | 0.043 | 78 | -- | -- |
| | 10 | 0.046 | 81.5 | -- | -- |
| | 12 | 0.052 | 88.8 | -- | -- |
| | 14 | 0.054 | 87.6 | -- | -- |
| | 17 | 0.06 | 93.6 | -- | -- |
| | 20 | 0.074 | 104.9 | -- | -- |
| | 22 | 0.076 | 107.4 | 0.03327 | 0.000239 |
| | 27 | 0.125 | 140.9 | 0.069534 | 0.000691 |
| | 32 | 0.218 | 177.8 | 0.136396 | *0.001511* |
| | 37 | 0.47 | 177.8 | 0.212364 | 0.00268 |
| | 42 | 0.605 | 177.8 | 0.239136 | 0.00268 |
| | 47 | 0.707 | 159.5 | 0.217778 | 0.002469 |
| | 52 | 0.82 | 116.2 | 0.199857 | 0.002336 |
| | 57 | 0.887 | 79.1 | 0.151437 | 0.001636 |
| | 62 | 0.913 | 60.5 | 0.126211 | 0.00136 |
| | 67 | 0.934 | 47.5 | 0.085117 | *0.001017* |
| | 72 | 0.952 | 35.3 | 0.073861 | 0.000872 |
| | 77 | 0.963 | 28.6 | 0.083064 | *0.000703* |
| | 82 | 0.969 | 24.9 | 0.076541 | *0.000725* |
| | 87 | 0.974 | 20 | 0.064038 | *0.000474* |
| | 92 | 0.983 | 14 | 0.036482 | *0.000222* |
| | 97 | 0.987 | 11.2 | 0.049278 | *0.000587* |
| | 102 | 0.988 | 9.7 | 0.032742 | *0.00029* |

| | | | | | |
|---|---|---|---|---|---|
| | 107 | 0.992 | 6.8 | 0.02762 | *0.000161* |
| | 112 | 0.992 | 6.6 | 0.031273 | *0.000142* |
| | 117 | 0.995 | 4.4 | 0.034354 | 0.000135 |
| | 122 | 0.997 | 2.8 | -- | -- |
| | 127 | 0.997 | 2.5 | 0.03471 | *0.000193* |
| | 132 | 0.997 | 2.4 | 0.033649 | 0.000191 |
| | 137 | 0.998 | 2 | -- | -- |
| | 142 | 0.998 | 1.4 | -- | -- |
| | 147 | 0.999 | 1.1 | -- | -- |
| | 152 | 0.999 | 1.1 | -- | -- |
| | 157 | 0.999 | 0.7 | -- | -- |

Notes : *Blue italic* : suspicious data; **Red Bold** : possibly incorrect data; (--) : meaningless data.

| $\Delta z$ mm | y mm | C | F Hz | $(R_{xy})_{max}$ | $T_{xy}$ sec. |
|---|---|---|---|---|---|
| 29.5 | 2 | 0.023 | 0.2 | -- | -- |
| | 7 | 0.034 | 66.2 | -- | -- |
| | 10 | 0.043 | 76.2 | -- | -- |
| | 12 | 0.039 | 72 | -- | -- |
| | 14 | 0.045 | 75.4 | -- | -- |
| | 17 | 0.052 | 83 | -- | -- |
| | 20 | 0.06 | 89 | -- | -- |
| | 22 | 0.067 | 96.5 | -- | -- |
| | 27 | 0.114 | 127.9 | 0.053267 | 0.000534 |
| | 32 | 0.188 | 161.2 | 0.124866 | 0.001614 |
| | 37 | 0.387 | 177.8 | 0.154782 | 0.001892 |
| | 47 | 0.667 | 167.6 | 0.181993 | *0.002346* |
| | 52 | 0.796 | 118.3 | 0.156013 | 0.00183 |
| | 57 | 0.872 | 78.8 | 0.117262 | 0.001203 |
| | 62 | 0.908 | 59.5 | 0.075743 | 0.000959 |
| | 67 | 0.929 | 46.1 | 0.073171 | 0.000797 |
| | 72 | 0.949 | 35.8 | -- | -- |
| | 77 | 0.963 | 26.3 | -- | -- |
| | 82 | 0.967 | 24.6 | 0.043878 | 0.000461 |
| | 87 | 0.979 | 16.2 | -- | -- |
| | 92 | 0.982 | 14.4 | -- | -- |
| | 97 | 0.986 | 11.4 | -- | -- |
| | 102 | 0.988 | 9.7 | -- | -- |
| | 107 | 0.992 | 7.4 | -- | -- |
| | 112 | 0.994 | 5.2 | -- | -- |
| | 117 | 0.995 | 4.6 | -- | -- |
| | 122 | 0.997 | 2.9 | -- | -- |
| | 127 | 0.996 | 3.6 | -- | -- |
| | 132 | 0.997 | 2.4 | -- | -- |
| | 137 | -- | 1.8 | -- | -- |
| | 147 | 0.999 | 1.1 | -- | -- |
| | 152 | 0.999 | 0.8 | -- | -- |
| | 157 | 0.999 | 0.8 | -- | -- |

Notes : *Blue italic* : suspicious data; **Red Bold** : possibly incorrect data; (--) : meaningless data.

| $\Delta z$ mm | y mm | C | F Hz | $(R_{xy})_{max}$ | $T_{xy}$ sec. |
|---|---|---|---|---|---|
| 40.3 | 22 | 0.071 | 91.6 | -- | -- |
| | 27 | 0.127 | 121 | 0.051034 | 0.000391 |
| | 32 | 0.229 | 164.9 | 0.095555 | 0.00132 |

| | | | | |
|---|---|---|---|---|
| 37 | 0.351 | 177.8 | 0.142367 | 0.001731 |
| 42 | 0.515 | 177.8 | 0.122922 | 0.001418 |
| 47 | 0.664 | 154.3 | 0.151645 | 0.002296 |
| 52 | 0.8 | 104.2 | 0.081088 | 0.001323 |
| 57 | 0.861 | 79.4 | 0.076761 | 0.00112 |
| 62 | 0.897 | 60.5 | 0.048962 | 0.000267 |
| 67 | 0.926 | 44 | 0.048503 | *0.000506* |
| 72 | 0.949 | 33.6 | -- | -- |
| 77 | 0.954 | 30.2 | 0.022588 | 0.000148 |
| 82 | 0.967 | 23.2 | -- | -- |

Notes : *Blue italic* : suspicious data; **Red Bold** : possibly incorrect data; (--) : meaningless data.

*D.3.2 Experimental results for $d_C/h = 1.45$*

| | |
|---|---|
| Location : | The University of Queensland (Australia) |
| Date : | April-June 2006 |
| Experiments by : | G. CAROSI |
| Data processing by: | G. CAROSI and H. CHANSON |
| Data analysis by : | H. CHANSON and G. CAROSI |
| Experiment characteristics : | Channel: width: 1.0 m, slope: 21.8º, h = 0.10 m, l = 0.25 m, 10 identical steps. Open channel with perspex sidewalls and smooth marine plywood staircase invert.<br>$Q_W$ = 0.1612 $m^3/s$, $d_C$ = 0.145 m, Re = 6.4 E+5 |
| Instrumentation : | Two single-tip conductivity probe (∅ = 0.35 mm). Transverse separation distance Δz.<br>Scan rate: 20 kHz per probe sensor, Sampling duration: 45 sec. |
| Comments : | Inflow conditions : broad-crested weir.<br>Inception of free-surface aeration: between step edges 7 and 8.<br>Correlation analyses performed on fifteen segments of 60,000 samples. |

D.3.2.1 Step edge 8

| Δz mm | y mm | C | F Hz | $T_{xx}$ sec. | $(R_{xy})_{max}$ | $T_{xy}$ sec. |
|---|---|---|---|---|---|---|
| 8.45 | 1.5 | 0.001 | 3.2 | 0.000355 | -- | -- |
| | 6.5 | 0.003 | 6.1 | 0.000449 | -- | -- |
| | 9.5 | 0.004 | 7.5 | 0.000719 | -- | -- |
| | 11.5 | 0.003 | 6.5 | 0.000394 | -- | -- |
| | 13.5 | 0.006 | 10 | 0.001692 | -- | -- |
| | 16.5 | 0.005 | 9 | 0.00053 | -- | -- |
| | 19.5 | 0.007 | 11.8 | 0.00052 | 0.049273 | 0.000152 |
| | 21.5 | 0.009 | 13 | 0.000564 | 0.062959 | 0.000252 |
| | 26.5 | 0.013 | 16.7 | 0.000826 | 0.065619 | 0.000384 |
| | 31.5 | 0.027 | 27.4 | 0.001493 | 0.15587 | 0.000976 |
| | 36.5 | 0.068 | 48.6 | *0.002414* | 0.274678 | *0.002043* |
| | 41.5 | 0.171 | 84.6 | *0.003218* | 0.376068 | *0.003083* |
| | 46.5 | 0.345 | 121 | *0.003697* | 0.435922 | *0.003958* |
| | 51.5 | 0.512 | 129.4 | *0.003804* | 0.448027 | *0.004165* |
| | 56.5 | 0.669 | 119.1 | *0.003628* | 0.413605 | *0.003561* |
| | 61.5 | 0.799 | 86 | *0.00294* | 0.35245 | *0.002494* |
| | 66.5 | 0.852 | 70.4 | *0.002696* | 0.317522 | *0.002255* |
| | 71.5 | 0.889 | 56.5 | *0.002519* | 0.300835 | *0.002014* |
| | 76.5 | 0.907 | 46.9 | *0.002458* | 0.287712 | *0.00175* |

| | | | | | | |
|---|---|---|---|---|---|---|
| | 81.5 | 0.93 | 37.4 | *0.002679* | 0.263545 | *0.00178* |
| | 86.5 | 0.949 | 28.1 | *0.002778* | 0.273884 | *0.001706* |
| | 91.5 | 0.959 | 24.3 | *0.002606* | 0.233332 | *0.001625* |
| | 96.5 | 0.956 | 25.3 | *0.00232* | 0.236056 | *0.001544* |
| | 101.5 | 0.972 | 17.3 | *0.002129* | 0.201313 | *0.001205* |
| | 106.5 | 0.976 | 14.3 | *0.002026* | 0.245969 | *0.00126* |
| | 111.5 | 0.983 | 10.7 | *0.002387* | 0.216309 | *0.001179* |
| | 116.5 | 0.985 | 10.2 | *0.001975* | 0.181623 | *0.000726* |
| | 121.5 | 0.99 | 6.8 | *0.002135* | 0.148415 | *0.000785* |
| | 126.5 | 0.992 | 6.4 | *0.002206* | 0.136806 | *0.001137* |
| | 131.5 | 0.991 | 6.5 | *0.00209* | 0.169506 | *0.000807* |
| | 131.5 | 0.994 | 4 | *0.002507* | 0.145739 | *0.000791* |
| | 136.5 | 0.995 | 3.3 | *0.002394* | 0.128645 | *0.000581* |
| | 141.5 | 0.997 | 2.7 | *0.002336* | 0.116997 | *0.000625* |
| | 146.5 | 0.997 | 2.1 | *0.002589* | 0.093473 | *0.000716* |

Notes : *Blue italic* : suspicious data; **Red Bold** : possibly incorrect data; (--) : meaningless data.

D.3.2.2 Step edge 9

| $\Delta z$ | y | C | F | $T_{xx}$ | $(R_{xy})_{max}$ | $T_{xy}$ |
|---|---|---|---|---|---|---|
| mm | mm | | Hz | sec. | | sec. |
| 8.45 | 1.5 | 0.013 | 26.3 | 0.000739 | -- | -- |
| | 6.5 | 0.025 | 38.4 | 0.001162 | 0.058648 | 0.000243 |
| | 9.5 | 0.027 | 37.8 | 0.00164 | 0.050659 | 0.000332 |
| | 11.5 | 0.031 | 39.9 | 0.00141 | 0.088398 | *0.000734* |
| | 13.5 | 0.031 | 39.5 | 0.00143 | 0.082299 | *0.000636* |
| | 16.5 | 0.038 | 44.5 | *0.001561* | 0.085998 | 0.000542 |
| | 19.5 | 0.037 | 43.8 | 0.001423 | 0.105406 | 0.000737 |
| | 21.5 | 0.042 | 45.8 | 0.001348 | 0.16899 | 0.001022 |
| | 26.5 | 0.059 | 55.6 | 0.001273 | 0.099872 | 0.000665 |
| | 31.5 | 0.091 | 72.7 | 0.001827 | 0.241151 | 0.00153 |
| | 36.5 | 0.159 | 100.5 | 0.00261 | 0.33251 | 0.002629 |
| | 41.5 | 0.276 | 131.6 | 0.003136 | 0.388097 | 0.003264 |
| | 46.5 | 0.411 | 142.7 | *0.003658* | 0.433142 | 0.003926 |
| | 51.5 | 0.562 | 135 | *0.00345* | 0.429691 | *0.003558* |
| | 56.5 | 0.666 | 117.8 | 0.002735 | 0.424157 | *0.003068* |
| | 61.5 | 0.753 | 100.5 | *0.002858* | 0.375266 | 0.002748 |
| | 66.5 | 0.811 | 82.9 | *0.00271* | 0.358838 | *0.002332* |
| | 71.5 | 0.858 | 67.2 | 0.002139 | 0.341548 | 0.001995 |
| | 76.5 | 0.886 | 54.3 | 0.002244 | 0.324843 | 0.001907 |
| | 81.5 | 0.917 | 45.8 | *0.002118* | 0.279371 | 0.001516 |
| | 86.5 | 0.929 | 38.1 | *0.002274* | 0.304788 | *0.001785* |
| | 91.5 | 0.943 | 31.7 | *0.002381* | 0.270212 | *0.001672* |
| | 96.5 | 0.963 | 23.6 | *0.002049* | 0.224755 | *0.00117* |
| | 101.5 | 0.97 | 19.4 | *0.002296* | 0.229541 | *0.001248* |
| | 106.5 | 0.98 | 14 | *0.002138* | 0.213727 | *0.001179* |
| | 111.5 | 0.98 | 13.6 | *0.002381* | 0.223751 | 0.001224 |
| | 116.5 | 0.983 | 11.8 | *0.001986* | 0.174763 | 0.000823 |
| | 121.5 | 0.988 | 8.3 | *0.002402* | 0.198373 | *0.001089* |
| | 126.5 | 0.99 | 7 | *0.002303* | 0.209296 | *0.001029* |
| | 131.5 | 0.991 | 6.2 | *0.002277* | 0.167164 | *0.000316* |
| | 131.5 | 0.994 | 4.2 | *0.002173* | 0.158214 | *0.000749* |
| | 136.5 | 0.996 | 2.6 | *0.002487* | 0.126307 | *0.000498* |
| | 141.5 | 0.997 | 3 | *0.002634* | 0.121011 | *0.000322* |
| | 146.5 | 0.997 | 2.2 | *0.002734* | 0.103776 | *0.000414* |

Notes : *Blue italic* : suspicious data; **Red Bold** : possibly incorrect data; (--) : meaningless data.

D.3.2.3 Step edge 10

| Δz mm | y mm | C | F Hz | $(R_{xy})_{max}$ | $T_{xy}$ sec. |
|---|---|---|---|---|---|
| 3.6 | 2 | 0.022 | 39.9 | 0.099504 | 0.000453 |
| | 7 | 0.018 | 33.7 | 0.101896 | 0.000283 |
| | 10 | 0.022 | 35.6 | 0.15787 | 0.000452 |
| | 12 | 0.025 | 40.9 | 0.190176 | 0.00069 |
| | 14 | 0.027 | 41.5 | 0.188603 | 0.00039 |
| | 17 | 0.029 | 44 | 0.209376 | 0.000605 |
| | 20 | 0.03 | 43.7 | 0.262669 | 0.000692 |
| | 22 | 0.038 | 49.3 | 0.284375 | 0.001091 |
| | 27 | 0.061 | 63.3 | 0.373629 | 0.001835 |
| | 32 | 0.106 | 87.9 | 0.484859 | 0.002877 |
| | 37 | 0.192 | 120.2 | 0.567565 | 0.003831 |
| | 42 | 0.356 | 145.9 | 0.649016 | *0.004683* |
| | 47 | 0.521 | 154.8 | 0.649348 | *0.004816* |
| | 52 | 0.66 | 137.8 | 0.643395 | 0.004075 |
| | 57 | 0.748 | 114.4 | 0.6313 | 0.003712 |
| | 62 | 0.808 | 97.6 | 0.621748 | 0.003143 |
| | 67 | 0.859 | 75 | 0.595864 | 0.003134 |
| | 72 | 0.905 | 56.4 | 0.590193 | *0.002729* |
| | 77 | 0.932 | 42.4 | 0.573615 | *0.002295* |
| | 82 | 0.941 | 38.8 | 0.545173 | *0.00222* |
| | 87 | 0.958 | 28.5 | 0.531459 | 0.001821 |
| | 92 | 0.964 | 24.5 | 0.532311 | *0.002492* |
| | 97 | 0.976 | 17.7 | 0.523779 | *0.001686* |
| | 102 | 0.98 | 15.1 | 0.514571 | *0.00176* |
| | 107 | 0.986 | 11.3 | 0.483799 | *0.001588* |
| | 112 | 0.988 | 8.9 | 0.454517 | *0.001527* |
| | 117 | 0.991 | 6.7 | 0.498068 | *0.001631* |
| | 122 | 0.992 | 5.8 | 0.494381 | *0.001397* |
| | 127 | 0.996 | 3.2 | 0.450932 | *0.001078* |
| | 132 | 0.996 | 3 | 0.485283 | *0.001188* |
| | 132 | 0.997 | 2.8 | 0.411066 | *0.001293* |
| | 137 | 0.998 | 2.3 | 0.315081 | *0.000917* |
| | 142 | 0.998 | 1.7 | 0.375474 | *0.000967* |
| | 147 | 0.999 | 1.6 | 0.347041 | *0.000727* |
| | 152 | 0.999 | 1.2 | 0.372967 | *0.000773* |

Notes : *Blue italic* : suspicious data; **Red Bold** : possibly incorrect data; (--) : meaningless data.

| Δz mm | y mm | C | F Hz | $T_{xx}$ sec. | $(R_{xy})_{max}$ | $T_{xy}$ sec. |
|---|---|---|---|---|---|---|
| 8.45 | 2 | 0.008 | 20.8 | 0.000853 | -- | -- |
| | 7 | 0.012 | 27.9 | 0.00078 | -- | -- |
| | 10 | 0.015 | 30.2 | 0.000973 | 0.025536 | 4.93E-05 |
| | 12 | 0.013 | 25.6 | 0.001131 | 0.023117 | 6.72E-05 |
| | 14 | 0.017 | 31.2 | 0.000982 | 0.043561 | 0.000248 |
| | 17 | 0.018 | 32.8 | 0.000969 | 0.032841 | 0.000206 |
| | 20 | 0.025 | 37.5 | 0.001233 | 0.065581 | 0.000239 |
| | 22 | 0.024 | 37.5 | 0.001184 | 0.093218 | 0.000368 |
| | 27 | 0.03 | 43.7 | 0.001351 | 0.081444 | 0.000332 |
| | 32 | 0.055 | 61.7 | *0.002243* | 0.183291 | 0.001153 |

| | | | | | |
|---|---|---|---|---|---|
| 37 | 0.092 | 81.6 | *0.002956* | 0.255018 | 0.001668 |
| 42 | 0.211 | 130.5 | 0.004463 | 0.390404 | *0.003162* |
| 47 | 0.306 | 147.4 | 0.005319 | 0.448788 | *0.004126* |
| 52 | 0.536 | 157.9 | 0.005057 | 0.455203 | 0.003983 |
| 57 | 0.655 | 137.6 | 0.005516 | 0.468004 | 0.004079 |
| 62 | 0.775 | 107.2 | *0.004919* | 0.436758 | *0.003763* |
| 67 | 0.858 | 76.4 | 0.004069 | 0.361126 | 0.002426 |
| 72 | 0.904 | 54.3 | *0.003816* | 0.345901 | *0.002217* |
| 77 | 0.927 | 43.1 | *0.00375* | 0.296393 | 0.001831 |
| 82 | 0.94 | 35.8 | *0.003863* | 0.292538 | *0.001744* |
| 87 | 0.962 | 24.7 | *0.003537* | 0.270508 | *0.001566* |
| 92 | 0.969 | 19.8 | *0.003358* | 0.25594 | *0.001295* |
| 97 | 0.977 | 16 | *0.003036* | 0.232306 | *0.001247* |
| 102 | 0.981 | 13.2 | *0.003242* | 0.217154 | *0.001137* |
| 107 | 0.987 | 9.8 | *0.002833* | 0.170989 | *0.0011* |
| 112 | 0.99 | 7.8 | *0.002983* | 0.210569 | *0.00094* |
| 117 | 0.992 | 6.2 | *0.003028* | 0.186865 | 0.000693 |
| 122 | 0.994 | 4.8 | *0.00328* | 0.18043 | *0.000513* |
| 127 | 0.996 | 3.4 | *0.00333* | 0.115671 | *0.00069* |
| 132 | 0.997 | 2.7 | *0.003568* | 0.106955 | *0.000575* |
| 132 | 0.997 | 2.2 | *0.003715* | 0.136502 | *0.000928* |
| 137 | 0.997 | 2.1 | *0.005863* | 0.147605 | *0.001263* |
| 142 | 0.998 | 1.8 | *0.003762* | 0.126155 | *0.000693* |
| 147 | 0.998 | 1.6 | *0.005294* | 0.099393 | *0.000331* |
| 152 | 0.999 | 1.1 | *0.005855* | 0.075653 | *0.000445* |

Notes : *Blue italic* : suspicious data; **Red Bold** : possibly incorrect data; (--) : meaningless data.

| $\Delta z$ | y | C | F | $(R_{xy})_{max}$ | $T_{xy}$ |
|---|---|---|---|---|---|
| mm | mm | | Hz | | sec. |
| 13.7 | 2 | 0.009 | 21.2 | -- | -- |
| | 7 | 0.014 | 28.1 | -- | -- |
| | 10 | 0.018 | 34.7 | -- | -- |
| | 12 | 0.017 | 33.8 | -- | -- |
| | 14 | 0.02 | 36.6 | -- | -- |
| | 17 | 0.023 | 38.4 | -- | -- |
| | 20 | 0.023 | 38.8 | -- | -- |
| | 22 | 0.03 | 44.4 | -- | -- |
| | 27 | 0.037 | 49.6 | -- | -- |
| | 32 | 0.046 | 56.5 | 0.068875 | 0.000515 |
| | 37 | 0.119 | 98.2 | 0.184595 | *0.001805* |
| | 42 | 0.186 | 119.7 | 0.251277 | *0.002627* |
| | 47 | 0.358 | 159.3 | 0.341293 | *0.00427* |
| | 52 | 0.519 | 156.8 | 0.37 | *0.004411* |
| | 57 | 0.666 | 136.2 | 0.352815 | 0.003769 |
| | 62 | 0.774 | 107.9 | 0.285568 | 0.002928 |
| | 67 | 0.85 | 82.7 | 0.240592 | *0.002551* |
| | 72 | 0.876 | 67.5 | 0.206681 | 0.001853 |
| | 77 | 0.908 | 53.3 | 0.19846 | *0.001881* |
| | 82 | 0.935 | 39.4 | 0.171901 | *0.001548* |
| | 87 | 0.95 | 31 | 0.154642 | *0.001509* |
| | 92 | 0.961 | 26.3 | 0.112389 | *0.001005* |
| | 97 | 0.972 | 19.6 | 0.101666 | *0.000805* |
| | 102 | 0.978 | 15.7 | 0.091734 | *0.000554* |
| | 107 | 0.983 | 12.5 | 0.089973 | *0.000952* |
| | 112 | 0.985 | 10.8 | 0.083816 | *0.000816* |
| | 117 | 0.988 | 9.1 | 0.074718 | *0.000659* |
| | 122 | 0.992 | 6.3 | 0.069384 | *0.00049* |
| | 127 | 0.994 | 4.7 | 0.068335 | 0.000322 |

| | | | | | |
|---|---|---|---|---|---|
| | 132 | 0.996 | 3.1 | 0.062823 | *0.00033* |
| | 132 | 0.996 | 3.6 | 0.053583 | *0.000217* |
| | 137 | 0.998 | 2 | -- | -- |
| | 142 | 0.997 | 2.1 | -- | -- |
| | 147 | 0.998 | 1.9 | 0.042303 | *4.25E-05* |
| | 152 | 0.998 | 1.4 | -- | -- |

Notes : *Blue italic* : suspicious data; **Red Bold** : possibly incorrect data; (--) : meaningless data.

| $\Delta z$ | y | C | F | $(R_{xy})_{max}$ | $T_{xy}$ |
|---|---|---|---|---|---|
| mm | mm | | Hz | | sec. |
| 21.7 | 2 | 0.004 | 11 | -- | -- |
| | 7 | 0.01 | 22.3 | -- | -- |
| | 10 | 0.013 | 25.8 | -- | -- |
| | 12 | 0.012 | 24 | -- | -- |
| | 14 | 0.012 | 24 | -- | -- |
| | 17 | 0.014 | 28.1 | -- | -- |
| | 20 | 0.015 | 27.8 | -- | -- |
| | 22 | 0.016 | 29.7 | -- | -- |
| | 27 | 0.023 | 35.1 | -- | -- |
| | 32 | 0.033 | 42.1 | -- | -- |
| | 37 | 0.06 | 62.2 | 0.083233 | 0.000908 |
| | 42 | 0.108 | 85.2 | 0.130063 | *0.001258* |
| | 47 | 0.222 | 127 | 0.208383 | *0.002712* |
| | 52 | 0.396 | 155.5 | 0.255555 | *0.003356* |
| | 57 | 0.532 | 147.2 | 0.284473 | *0.003956* |
| | 62 | 0.704 | 124.3 | 0.246368 | *0.003282* |
| | 67 | 0.795 | 95.2 | 0.245163 | *0.003001* |
| | 72 | 0.866 | 66.9 | 0.199363 | *0.002385* |
| | 77 | 0.916 | 47.6 | 0.143855 | *0.001732* |
| | 82 | 0.926 | 43.4 | 0.13481 | 0.001324 |
| | 87 | 0.947 | 31.7 | 0.109588 | *0.001149* |
| | 92 | 0.965 | 22.7 | 0.095288 | 0.001036 |
| | 97 | 0.969 | 20.3 | 0.077942 | 0.000743 |
| | 102 | 0.978 | 15.3 | -- | -- |
| | 107 | 0.984 | 11.9 | 0.062037 | *0.000633* |
| | 112 | 0.989 | 8.2 | 0.051796 | *0.000525* |
| | 117 | 0.989 | 8.3 | -- | -- |
| | 122 | 0.992 | 5.8 | 0.040173 | *0.000233* |
| | 127 | 0.993 | 5 | 0.045095 | *0.000442* |
| | 132 | 0.996 | 3.5 | 0.022657 | *0.000107* |
| | 132 | 0.996 | 3 | 0.040402 | 5.24E-05 |
| | 137 | 0.996 | 2.7 | -- | -- |
| | 142 | 0.998 | 1.8 | 0.046693 | *0.000113* |
| | 147 | 0.998 | 1.6 | 0.020593 | *2.43E-05* |
| | 152 | 0.999 | 1.4 | 0.045742 | *8.29E-05* |

Notes : *Blue italic* : suspicious data; **Red Bold** : possibly incorrect data; (--) : meaningless data.

| $\Delta z$ | y | C | F | $(R_{xy})_{max}$ | $T_{xy}$ |
|---|---|---|---|---|---|
| mm | mm | | Hz | | sec. |
| 40.3 | 22 | 0.022 | 34 | -- | -- |
| | 27 | 0.025 | 37.1 | -- | -- |
| | 32 | 0.048 | 55.7 | 0.030402 | 0.000104 |
| | 37 | 0.096 | 79.9 | -- | -- |
| | 42 | 0.156 | 104.5 | 0.087065 | *0.001302* |
| | 47 | 0.312 | 143.2 | 0.140587 | *0.001975* |

| | | | | |
|---|---|---|---|---|
| 52 | 0.502 | 156.2 | 0.141711 | 0.001733 |
| 57 | 0.667 | 137.7 | 0.139181 | *0.001957* |
| 62 | 0.759 | 109.3 | 0.130445 | *0.001652* |
| 67 | 0.836 | 80.8 | 0.114481 | *0.001558* |
| 72 | 0.886 | 59.3 | 0.106652 | *0.001208* |
| 77 | 0.916 | 47.9 | 0.066078 | *0.000793* |
| 82 | 0.939 | 36.6 | 0.055418 | 0.000896 |
| 87 | 0.95 | 32.4 | -- | -- |
| 92 | 0.964 | 23.1 | -- | -- |
| 97 | 0.976 | 15.8 | 0.050844 | 0.000498 |
| 102 | 0.98 | 12.5 | -- | -- |

Notes : *Blue italic* : suspicious data; **Red Bold** : possibly incorrect data; (--) : meaningless data.

| $\Delta z$ mm | y mm | C | F Hz | $(R_{xy})_{max}$ | $T_{xy}$ sec. |
|---|---|---|---|---|---|
| 54.7 | 22 | 0.022 | 36.2 | -- | -- |
| | 27 | 0.027 | 35.8 | -- | -- |
| | 32 | 0.049 | 53.3 | -- | -- |
| | 37 | 0.077 | 72.6 | -- | -- |
| | 42 | 0.173 | 113.2 | -- | -- |
| | 47 | 0.336 | 151.5 | 0.069687 | 0.001218 |
| | 52 | 0.457 | 156.7 | 0.109424 | *0.001543* |
| | 57 | 0.638 | 137.4 | 0.116555 | *0.001896* |
| | 62 | 0.764 | 107 | 0.112778 | *0.00164* |
| | 67 | 0.856 | 76.4 | 0.050864 | 0.000513 |
| | 72 | 0.893 | 58.6 | -- | -- |
| | 77 | 0.927 | 44.3 | 0.034142 | *0.000379* |
| | 82 | 0.949 | 31 | -- | -- |
| | 87 | 0.961 | 24.6 | -- | -- |

Notes : *Blue italic* : suspicious data; **Red Bold** : possibly incorrect data; (--) : meaningless data.

## D.4 Experimental results in terms of streamwise separation $\Delta x$

### *D.4.1 Experimental results for $d_C/h = 1.15$*

| | |
|---|---|
| Location : | The University of Queensland (Australia) |
| Date : | April-June 2006 |
| Experiments by : | G. CAROSI |
| Data processing by: | G. CAROSI and H. CHANSON |
| Data analysis by : | H. CHANSON and G. CAROSI |
| Experiment characteristics : | Channel: width: 1.0 m, slope: 21.8°, h = 0.10 m, l = 0.25 m, 10 identical steps. Open channel with perspex sidewalls and smooth marine plywood staircase invert.<br>$Q_W$ = 0.1164 $m^3/s$, $d_C$ = 0.115 m, Re = 4.6 E+5 |
| Instrumentation : | Double-tip conductivity probe (∅ = 0.35 mm, $\Delta x$). Streamwise/longitudinal separation distance $\Delta x$.<br>Scan rate: 20 kHz per probe sensor, Sampling duration: 45 sec. |
| Comments : | Inflow conditions : broad-crested weir.<br>Inception of free-surface aeration: between step edges 6 and 7.<br>Correlation analyses performed on fifteen segments of 60,000 samples. |

D.4.1.1 Step edge 10, Δx = 7.0 mm

| Δx | y | C | F | $T_{xx}$ | $(R_{xy})_{max}$ | $T_{xy}$ | Tu |
|---|---|---|---|---|---|---|---|
| mm | mm | | Hz | sec. | | sec. | |
| 7.0 | 2 | 0.062 | 114.9 | 0.00119 | 0.264389 | 0.000754 | -- |
| | 7 | 0.061 | 108.8 | 0.00072 | 0.255737 | 0.000691 | 0.55763 |
| | 12 | 0.065 | 108.8 | 0.000793 | 0.31752 | 0.000907 | 0.649896 |
| | 14 | 0.061 | 104.7 | 0.00307 | 0.304801 | 0.001234 | 0.888 |
| | 17 | 0.062 | 103.2 | 0.000751 | 0.323598 | 0.000769 | 0.542867 |
| | 20 | 0.1 | 138.1 | 0.001225 | 0.42137 | 0.001108 | 0.295671 |
| | 22 | 0.104 | 139.4 | 0.000265 | 0.457885 | 0.001492 | -- |
| | 27 | 0.152 | 165.1 | 0.002016 | 0.536603 | 0.002271 | 0.864995 |
| | 32 | 0.373 | 207.1 | 0.00307 | 0.62678 | 0.003575 | 1.245963 |
| | 37 | 0.551 | 228.5 | 0.003559 | 0.681533 | 0.004459 | 1.619106 |
| | 42 | 0.64 | 208.5 | 0.002885 | 0.707943 | 0.004886 | 1.016596 |
| | 47 | 0.763 | 146.4 | *0.003835* | 0.71271 | *0.004813* | 1.529532 |
| | 52 | 0.855 | 100.2 | *0.003957* | 0.716521 | *0.004226* | 1.365287 |
| | 57 | 0.908 | 68.2 | *0.003107* | 0.714641 | *0.003718* | 0.92975 |
| | 62 | 0.925 | 55.3 | *0.003356* | 0.682112 | *0.002779* | 0.536476 |
| | 67 | 0.943 | 42 | *0.00261* | 0.715595 | *0.00306* | 0.639129 |
| | 72 | 0.954 | 34.5 | *0.003179* | 0.719335 | *0.003297* | 0.65151 |
| | 77 | 0.966 | 25.1 | *0.003087* | 0.703615 | *0.003114* | 0.665568 |
| | 82 | 0.973 | 22.4 | *0.003422* | 0.68642 | *0.003114* | 0.626625 |
| | 87 | 0.981 | 15.8 | *0.003724* | 0.669381 | *0.002835* | 0.476352 |
| | 92 | 0.985 | 12.4 | *0.004424* | 0.622795 | *0.002766* | 0.572504 |
| | 97 | 0.987 | 10.9 | *0.004932* | 0.643073 | *0.002994* | 0.562814 |
| | 102 | 0.991 | 8 | *0.006372* | 0.567063 | *0.002601* | 0.345584 |
| | 107 | 0.992 | 6.6 | *0.007313* | 0.60096 | *0.003118* | 0.550167 |
| | 112 | 0.994 | 5.7 | *0.00927* | 0.539257 | *0.003212* | -- |
| | 117 | 0.995 | 4.7 | *0.008757* | 0.545707 | 0.002699 | -- |
| | 122 | 0.996 | 3.6 | *0.009318* | 0.55074 | 0.00347 | -- |
| | 127 | 0.997 | 2.9 | *0.009796* | 0.520841 | *0.003164* | -- |
| | 132 | 0.997 | 2.6 | *0.00953* | 0.534634 | *0.003377* | -- |
| | 137 | 0.998 | 1.7 | -- | 0.488095 | *0.004152* | -- |
| | 137 | 0.998 | 1.5 | -- | 0.332272 | *0.001608* | -- |
| | 142 | 0.999 | 1.3 | -- | 0.477699 | -- | -- |
| | 147 | 0.999 | 1 | -- | -- | -- | -- |
| | 152 | 0.999 | 1 | -- | 0.434798 | -- | -- |

Notes : *Blue italic* : suspicious data; **Red Bold** : possibly incorrect data; (--) : meaningless data.

D.4.1.2 Step edge 10, Δx = 9.6 mm

| Δx | y | C | F | $(R_{xy})_{max}$ | $T_{xy}$ | Tu |
|---|---|---|---|---|---|---|
| mm | mm | | Hz | | sec. | |
| 9.6 | 0 | 0.022 | 52.6 | 0.038459 | 0.000204 | 0.687788 |
| | 5 | 0.08 | 137.8 | 0.16166 | 0.000547 | 0.660602 |
| | 8 | 0.091 | 146 | 0.204673 | 0.000845 | 0.654595 |
| | 10 | 0.09 | 145.6 | 0.218867 | 0.000803 | 0.5319 |
| | 12 | 0.095 | 148.8 | 0.223153 | 0.000737 | 0.536114 |
| | 15 | 0.1 | 150.5 | 0.242839 | 0.000886 | 0.638843 |
| | 18 | 0.109 | 157.2 | 0.246755 | 0.000792 | -- |
| | 20 | 0.117 | 162 | 0.272943 | 0.000948 | 0.579795 |
| | 25 | 0.133 | 175.9 | 0.302928 | 0.001006 | 0.561041 |
| | 30 | 0.283 | 201.4 | 0.382121 | 0.001503 | 0.661304 |
| | 35 | 0.455 | 237.2 | 0.456723 | 0.002311 | 0.895614 |

| | | | | | |
|---|---|---|---|---|---|
| 40 | 0.585 | 257.5 | 0.529283 | 0.00328 | 1.13515 |
| 45 | 0.71 | 240 | 0.576331 | *0.003674* | 1.174311 |
| 50 | 0.763 | 166.9 | 0.577746 | *0.003626* | 1.106536 |
| 55 | 0.852 | 118.6 | 0.581312 | *0.003075* | 0.835481 |
| 60 | 0.906 | 77.7 | 0.584708 | 0.002538 | 0.658357 |
| 65 | 0.926 | 61.7 | 0.569659 | *0.002338* | 0.612871 |
| 70 | 0.947 | 46 | 0.571163 | *0.002124* | 0.548644 |
| 75 | 0.958 | 36.4 | 0.566752 | *0.002056* | 0.498758 |
| 80 | 0.966 | 30.9 | 0.556409 | *0.001745* | 0.461192 |
| 85 | 0.974 | 23.2 | 0.53619 | *0.001879* | 0.512495 |
| 90 | 0.98 | 19.1 | 0.537882 | *0.001717* | 0.481148 |
| 95 | 0.984 | 14.3 | 0.540713 | *0.001646* | 0.415056 |
| 100 | 0.987 | 12.6 | 0.50333 | *0.001447* | 0.456337 |
| 105 | 0.99 | 10.1 | 0.527014 | *0.001536* | 0.419261 |
| 110 | 0.992 | 7.4 | 0.52155 | *0.001587* | -- |
| 115 | 0.993 | 6.6 | 0.486483 | *0.001301* | 0.460031 |
| 120 | 0.994 | 5.9 | 0.509765 | *0.001398* | 0.399447 |
| 125 | 0.995 | 4.3 | 0.461084 | *0.001664* | 0.492853 |
| 130 | 0.997 | 2.9 | 0.363794 | *0.000382* | 0.366637 |
| 130 | 0.997 | 2.8 | 0.448422 | *0.00105* | 0.392292 |
| 135 | 0.998 | 2.1 | 0.432515 | 0.001003 | 0.395014 |
| 140 | 0.999 | 1.4 | 0.297799 | 0.000673 | 0.361881 |

Notes : *Blue italic* : suspicious data; **Red Bold** : possibly incorrect data; (--) : meaningless data.

*D.4.2 Experimental results for $d_C/h = 1.33$*

| | |
|---|---|
| Location : | The University of Queensland (Australia) |
| Date : | April-June 2006 |
| Experiments by : | G. CAROSI |
| Data processing by: | G. CAROSI and H. CHANSON |
| Data analysis by : | H. CHANSON and G. CAROSI |
| Experiment characteristics : | Channel: width: 1.0 m, slope: 21.8º, h = 0.10 m, l = 0.25 m, 10 identical steps. Open channel with perspex sidewalls and smooth marine plywood staircase invert.<br>$Q_W$ = 0.1431 $m^3/s$, $d_C$ = 0.133 m, Re = 5.7 E+5 |
| Instrumentation : | Double-tip conductivity probe (∅ = 0.35 mm, Δx = 7.0 mm). Streamwise/longitudinal separation distance Δx.<br>Scan rate: 20 kHz per probe sensor, Sampling duration: 45 sec. |
| Comments : | Inflow conditions : broad-crested weir.<br>Inception of free-surface aeration: between step edges 6 and 7.<br>Correlation analyses performed on fifteen segments of 60,000 samples. |

D.4.2.1 Step edge 7, Δx = 7.0 mm

| Δx | y | C | F | $T_{xx}$ | $(R_{xy})_{max}$ | $T_{xy}$ | Tu |
|---|---|---|---|---|---|---|---|
| mm | mm | | Hz | sec. | | sec. | |
| 7.0 | 1 | 0.039 | 54.3 | *0.001579* | 0.376365 | *0.001414* | 0.71526 |
| | 6 | 0.046 | 54.1 | *0.002087* | 0.444767 | 0.002119 | 0.866731 |
| | 9 | 0.058 | 60.7 | *0.002069* | 0.438511 | *0.002264* | 0.971498 |
| | 11 | 0.047 | 52.1 | *0.002085* | 0.476891 | *0.002241* | 0.87424 |
| | 13 | 0.049 | 54.6 | *0.001523* | 0.450022 | *0.001809* | 0.711428 |
| | 16 | 0.07 | 69.6 | 0.001444 | 0.509917 | 0.001918 | 0.744325 |
| | 19 | 0.067 | 61.2 | 0.000604 | 0.529508 | *0.002213* | 0.803926 |

| | | | | | | |
|---|---|---|---|---|---|---|
| 21 | 0.055 | 50.3 | *0.001671* | 0.522856 | 0.002032 | 0.704383 |
| 26 | 0.078 | 55.6 | 0.002022 | 0.652343 | 0.00262 | 0.745315 |
| 31 | 0.142 | 76.2 | *0.002714* | 0.695446 | *0.003246* | 0.875342 |
| 36 | 0.243 | 95.7 | *0.003391* | 0.742968 | *0.004308* | -- |
| 41 | 0.449 | 118.4 | *0.003594* | 0.769282 | *0.004529* | 1.063733 |
| 46 | 0.614 | 111.6 | *0.003959* | 0.777725 | *0.004721* | 1.121155 |
| 51 | 0.737 | 93.4 | *0.003732* | 0.780794 | *0.004535* | 0.967145 |
| 56 | 0.812 | 72.8 | *0.003124* | 0.784843 | *0.003874* | 0.757351 |
| 61 | 0.892 | 47.8 | *0.003071* | 0.783501 | *0.003576* | 0.610889 |
| 66 | 0.891 | 52.5 | *0.002616* | 0.772142 | *0.003041* | 0.497231 |
| 71 | 0.949 | 28.2 | *0.002593* | 0.759315 | *0.002801* | 0.497107 |
| 76 | 0.959 | 22.3 | *0.002507* | 0.773983 | *0.002833* | 0.412965 |
| 81 | 0.948 | 27.4 | *0.002792* | 0.776286 | *0.002889* | 0.409203 |
| 86 | 0.965 | 19.2 | *0.002483* | 0.774714 | *0.002692* | 0.371937 |
| 91 | 0.976 | 14 | *0.002227* | 0.758431 | *0.002398* | 0.391721 |
| 96 | 0.974 | 14.7 | *0.002742* | 0.776436 | *0.002941* | 0.390394 |
| 101 | 0.983 | 10.6 | *0.002289* | 0.717564 | *0.002378* | 0.472662 |
| 106 | 0.983 | 9.8 | *0.002891* | 0.734801 | *0.002748* | 0.370619 |
| 111 | 0.989 | 6.8 | *0.00289* | 0.683911 | *0.002262* | 0.360383 |
| 116 | 0.99 | 6.3 | *0.002983* | 0.706695 | *0.002603* | 0.38552 |
| 121 | 0.993 | 4.5 | *0.003635* | 0.715755 | *0.003096* | 0.443416 |
| 126 | 0.994 | 3.8 | *0.004314* | 0.698192 | *0.003104* | 0.524868 |
| 131 | 0.995 | 3 | *0.003249* | 0.652472 | *0.002713* | 0.297568 |
| 131 | 0.995 | 2.8 | *0.003885* | 0.684631 | *0.003288* | 0.38562 |
| 136 | 0.997 | 2.1 | *0.005665* | 0.540334 | *0.002005* | 0.260521 |
| 141 | 0.997 | 1.8 | -- | -- | -- | -- |

Notes : *Blue italic* : suspicious data; **Red Bold** : possibly incorrect data; (--) : meaningless data.

D.4.2.2 Step edge 8, Δx = 7.0 mm

| Δx mm | y mm | C | F Hz | $T_{xx}$ sec. | $(R_{xy})_{max}$ | $T_{xy}$ sec. | Tu |
|---|---|---|---|---|---|---|---|
| 7.0 | 1 | 0.03 | 51.1 | *0.00068* | 0.160346 | *0.00051* | 0.541202 |
| | 6 | 0.795 | 107.7 | 0.000669 | 0.208917 | 0.00052 | 0.530253 |
| | 9 | 0.997 | 1.9 | 0.000658 | 0.237024 | 0.000588 | 0.487536 |
| | 11 | 0.027 | 50.4 | 0.000647 | 0.29398 | 0.000666 | 0.432534 |
| | 13 | 0.027 | 46.7 | 0.000674 | 0.322964 | 0.000699 | 0.509432 |
| | 16 | 0.026 | 43.9 | 0.000852 | 0.357039 | 0.000913 | 0.578212 |
| | 19 | 0.033 | 50.6 | 0.000756 | 0.365766 | 0.000853 | 0.547116 |
| | 21 | 0.036 | 53.1 | 0.001054 | 0.404832 | 0.001097 | 0.546528 |
| | 26 | 0.043 | 61 | 0.002156 | 0.537376 | 0.002235 | 0.829086 |
| | 31 | 0.047 | 63.8 | *0.003037* | 0.609727 | *0.003366* | 1.117458 |
| | 36 | 0.088 | 81.2 | *0.003918* | 0.679499 | *0.004421* | - |
| | 41 | 0.183 | 121.1 | *0.003962* | 0.710943 | *0.004544* | 1.35632 |
| | 46 | 0.34 | 154.6 | *0.003796* | 0.721029 | *0.004633* | 1.354659 |
| | 51 | 0.534 | 168.9 | *0.003666* | 0.733043 | *0.004155* | 0.999272 |
| | 56 | 0.679 | 143.2 | *0.002692* | 0.756494 | *0.003244* | 0.628629 |
| | 61 | 0.848 | 83.6 | *0.002772* | 0.748431 | *0.003144* | 0.592929 |
| | 66 | 0.895 | 61.9 | *0.00319* | 0.74609 | *0.003382* | 0.571256 |
| | 71 | 0.92 | 48.2 | *0.003151* | 0.766854 | *0.003265* | 0.473505 |
| | 76 | 0.931 | 42.4 | *0.002884* | 0.742764 | *0.003018* | 0.468396 |
| | 81 | 0.946 | 33.7 | *0.002984* | 0.764227 | *0.003143* | 0.531875 |
| | 86 | 0.947 | 32.4 | *0.003008* | 0.743085 | *0.00301* | 0.549557 |
| | 91 | 0.963 | 24.1 | *0.002716* | 0.724061 | *0.002812* | 0.550885 |
| | 96 | 0.97 | 19.6 | *0.002613* | 0.682411 | *0.002639* | 0.481112 |
| | 101 | 0.974 | 17.1 | *0.002877* | 0.74803 | *0.002941* | 0.454156 |
| | 106 | 0.983 | 12.1 | *0.003213* | 0.720062 | *0.002884* | 0.411771 |

| | | | | | | | |
|---|---|---|---|---|---|---|---|
| | 111 | 0.983 | 11.4 | *0.002938* | 0.714971 | *0.002649* | 0.523605 |
| | 116 | 0.986 | 9.8 | *0.003572* | 0.657664 | *0.002683* | 0.487904 |
| | 121 | 0.992 | 5.7 | *0.00397* | 0.630698 | *0.00235* | 0.398042 |
| | 126 | 0.993 | 5.3 | *0.003567* | 0.642847 | *0.002556* | 0.4718 |
| | 131 | 0.994 | 4.4 | *0.005182* | 0.56598 | *0.002346* | 0.389208 |
| | 131 | 0.995 | 3.8 | *0.00481* | 0.648881 | *0.00314* | 0.471728 |
| | 136 | 0.996 | 2.8 | *0.004692* | 0.613263 | *0.003198* | 0.517306 |
| | 141 | 0.996 | 2.9 | -- | -- | -- | -- |

Notes : *Blue italic* : suspicious data; **Red Bold** : possibly incorrect data; (--) : meaningless data.

D.4.2.3 Step edge 9, Δx = 7.0 mm

| Δx mm | y mm | C | F Hz | $T_{xx}$ sec. | $(R_{xy})_{max}$ | $T_{xy}$ sec. | Tu |
|---|---|---|---|---|---|---|---|
| 7.0 | 0.5 | 0.057 | 92.7 | 0.001603 | 0.347479 | *0.001487* | 0.830665 |
| | 5.5 | 0.048 | 74.8 | 0.001697 | 0.411164 | 0.001811 | 0.918665 |
| | 8.5 | 0.072 | 101.9 | 0.001347 | 0.408226 | 0.001599 | 0.835701 |
| | 10.5 | 0.062 | 85.3 | 0.001659 | 0.444109 | 0.001891 | 0.924776 |
| | 12.5 | 0.063 | 83.4 | 0.001925 | 0.441414 | 0.002107 | 0.870024 |
| | 15.5 | 0.07 | 87.5 | 0.001506 | 0.487285 | 0.001992 | 0.889707 |
| | 18.5 | 0.071 | 87.2 | 0.001568 | 0.444809 | 0.001776 | 0.778827 |
| | 20.5 | 0.08 | 91.5 | 0.001442 | 0.500249 | 0.00173 | 0.738502 |
| | 25.5 | 0.101 | 99.8 | 0.001847 | 0.564681 | 0.002309 | 0.864571 |
| | 30.5 | 0.149 | 120.3 | *0.002105* | 0.617373 | *0.002704* | 0.937386 |
| | 35.5 | 0.249 | 152.9 | *0.003083* | 0.681669 | *0.003834* | -- |
| | 40.5 | 0.377 | 169.1 | *0.003276* | 0.723366 | *0.004345* | 1.314698 |
| | 45.5 | 0.556 | 162.6 | *0.003856* | 0.75829 | *0.004994* | 1.472303 |
| | 50.5 | 0.664 | 143 | *0.003686* | 0.757416 | *0.004848* | 1.392821 |
| | 55.5 | 0.766 | 112.4 | *0.002983* | 0.764981 | *0.004133* | 1.028179 |
| | 60.5 | 0.829 | 92.5 | *0.002818* | 0.758787 | *0.003589* | 0.803548 |
| | 65.5 | 0.858 | 81.8 | *0.002789* | 0.759834 | *0.003418* | 0.940336 |
| | 70.5 | 0.902 | 60.8 | *0.002572* | 0.749763 | *0.003129* | 0.614661 |
| | 75.5 | 0.91 | 52.6 | *0.003296* | 0.768848 | *0.003668* | 0.706371 |
| | 80.5 | 0.933 | 43.7 | *0.002821* | 0.754711 | *0.003075* | 0.553842 |
| | 85.5 | 0.946 | 33.4 | *0.003197* | 0.754295 | *0.003268* | 0.583318 |
| | 90.5 | 0.961 | 26.1 | *0.002768* | 0.728013 | *0.00287* | 0.531449 |
| | 95.5 | 0.968 | 22.4 | *0.002807* | 0.709856 | *0.00264* | 0.440988 |
| | 100.5 | 0.975 | 18.4 | *0.003248* | 0.720647 | *0.003102* | 0.599684 |
| | 105.5 | 0.982 | 13.4 | *0.003573* | 0.717162 | *0.003215* | 0.627315 |
| | 110.5 | 0.986 | 10.1 | *0.003227* | 0.705085 | *0.002821* | 0.465233 |
| | 115.5 | 0.99 | 7.7 | *0.003582* | 0.700909 | *0.002943* | 0.500669 |
| | 120.5 | 0.991 | 6.7 | *0.004023* | 0.669627 | *0.002724* | 0.556434 |
| | 125.5 | 0.994 | 4.5 | *0.004305* | 0.615726 | *0.002683* | 0.388839 |
| | 130.5 | 0.996 | 3.5 | *0.005349* | 0.629856 | *0.003205* | 0.545155 |
| | 130.5 | 0.997 | 2.5 | *0.006603* | 0.515989 | *0.002566* | 0.418759 |
| | 135.5 | 0.997 | 1.9 | -- | -- | -- | -- |
| | 140.5 | 0.998 | 1.6 | -- | -- | -- | -- |

Notes : *Blue italic* : suspicious data; **Red Bold** : possibly incorrect data; (--) : meaningless data.

D.4.2.4 Step edge 10, Δx = 7.0 mm

| Δx mm | y mm | C | F Hz | $T_{xx}$ sec. | $(R_{xy})_{max}$ | $T_{xy}$ sec. | Tu |
|---|---|---|---|---|---|---|---|

| | | | | | | | |
|---|---|---|---|---|---|---|---|
| 7.0 | 1.5 | 0.042 | 87.7 | 0.000629 | 0.209806 | 0.000541 | -- |
| | 6.5 | 0.053 | 98.4 | 0.000834 | 0.292804 | 0.000845 | -- |
| | 9.5 | 0.052 | 94.3 | 0.000872 | 0.300971 | 0.000916 | 0.687693 |
| | 11.5 | 0.048 | 88 | 0.000607 | 0.283516 | 0.000723 | 0.533877 |
| | 13.5 | 0.052 | 90 | 0.000683 | 0.311088 | 0.000817 | 0.572963 |
| | 16.5 | 0.055 | 89.8 | 0.000729 | 0.327854 | 0.00074 | 0.502104 |
| | 19.5 | 0.063 | 102 | 0.000694 | 0.358372 | 0.000862 | -- |
| | 26.5 | 0.081 | 110.8 | 0.001078 | 0.450549 | 0.001156 | 0.644338 |
| | 31.5 | 0.126 | 145.3 | 0.001966 | 0.53345 | 0.002136 | 0.747365 |
| | 36.5 | 0.187 | 166.8 | *0.002841* | 0.601759 | *0.003168* | 1.180327 |
| | 41.5 | 0.41 | 199.7 | *0.004049* | 0.683871 | *0.004688* | 1.774786 |
| | 46.5 | 0.571 | 199.2 | *0.004139* | 0.724431 | *0.005108* | 1.792577 |
| | 51.5 | 0.678 | 161.2 | *0.004345* | 0.746485 | *0.005525* | 1.943015 |
| | 56.5 | 0.814 | 112.5 | *0.003821* | 0.759131 | *0.004834* | 1.318069 |
| | 61.5 | 0.886 | 76.8 | *0.003912* | 0.748266 | *0.004497* | 1.073947 |
| | 66.5 | 0.924 | 51 | *0.003507* | 0.741208 | *0.003736* | 0.800066 |
| | 71.5 | 0.944 | 38.8 | *0.003359* | 0.750629 | *0.003534* | 0.710763 |
| | 76.5 | 0.955 | 31.8 | *0.003314* | 0.726486 | *0.003441* | 0.709057 |
| | 81.5 | 0.967 | 23.7 | *0.003387* | 0.726729 | *0.003429* | 0.680787 |
| | 86.5 | 0.974 | 20 | *0.00346* | 0.724215 | *0.003279* | 0.854175 |
| | 91.5 | 0.981 | 15.6 | *0.003112* | 0.686873 | *0.002754* | 0.478292 |
| | 96.5 | 0.985 | 12.3 | *0.003635* | 0.698636 | *0.003055* | 0.494324 |
| | 101.5 | 0.989 | 8.3 | *0.004056* | 0.671801 | *0.002936* | 0.512453 |
| | 106.5 | 0.991 | 7.1 | *0.004026* | 0.646803 | *0.002735* | 0.485592 |
| | 111.5 | 0.993 | 5.5 | *0.004081* | 0.647725 | *0.002824* | 0.608745 |
| | 116.5 | 0.995 | 4.4 | *0.004553* | 0.608084 | *0.00255* | 0.495045 |
| | 121.5 | 0.995 | 4 | *0.005173* | 0.600479 | *0.003014* | 0.454956 |
| | 126.5 | 0.997 | 2.8 | *0.007249* | 0.536074 | *0.002802* | 0.474336 |
| | 131.5 | 0.996 | 2.7 | *0.007113* | 0.629105 | *0.003668* | 0.173744 |
| | 136.5 | 0.998 | 1.6 | *0.009353* | 0.566952 | *0.004487* | 1.154547 |
| | 141.5 | 0.999 | 1.2 | *0.010264* | 0.427093 | *0.002625* | -- |
| | 146.5 | 0.999 | 1.4 | -- | -- | -- | -- |
| | 151.5 | 0.999 | 1 | -- | -- | -- | -- |

Notes : *Blue italic* : suspicious data; **Red Bold** : possibly incorrect data; (--) : meaningless data.

*D.4.3 Experimental results for $d_c/h = 1.45$*

| | |
|---|---|
| Location : | The University of Queensland (Australia) |
| Date : | April-June 2006 |
| Experiments by : | G. CAROSI |
| Data processing by: | G. CAROSI and H. CHANSON |
| Data analysis by : | H. CHANSON and G. CAROSI |
| Experiment characteristics : | Channel: width: 1.0 m, slope: 21.8º, h = 0.10 m, l = 0.25 m, 10 identical steps. Open channel with perspex sidewalls and smooth marine plywood staircase invert.<br>$Q_W$ = 0.1612 $m^3/s$, $d_c$ = 0.145 m, Re = 6.4 E+5 |
| Instrumentation : | Double-tip conductivity probe (∅ = 0.35 mm, Δx). Streamwise/longitudinal separation distance Δx.<br>Scan rate: 20 kHz per probe sensor, Sampling duration: 45 sec. |
| Comments : | Inflow conditions : broad-crested weir.<br>Inception of free-surface aeration: between step edges 7 and 8.<br>Correlation analyses performed on fifteen segments of 60,000 samples. |

D.4.3.1 Step edge 10, Δx = 7.0 mm

| Δx | y | C | F | $T_{xx}$ | $(R_{xy})_{max}$ | $T_{xy}$ | Tu |
|---|---|---|---|---|---|---|---|
| mm | mm | | Hz | sec. | | sec. | |
| 7.0 | 2 | 0.007 | 17.5 | 0.000509 | 0.181468 | 0.000453 | 0.510077 |
| | 7 | 0.01 | 21.8 | 0.000594 | 0.273554 | 0.000698 | 0.56445 |
| | 10 | 0.011 | 23.5 | 0.000263 | 0.248417 | 0.000644 | -- |
| | 12 | 0.013 | 26.5 | 0.000609 | 0.259366 | 0.000555 | 0.4743 |
| | 14 | 0.017 | 29.6 | 0.000657 | 0.306884 | 0.000835 | 0.624014 |
| | 17 | 0.03 | 52.4 | 0.00076 | 0.366902 | 0.000893 | 0.60415 |
| | 20 | 0.027 | 48.2 | 0.000646 | 0.337786 | 0.000744 | 0.581754 |
| | 22 | 0.03 | 50 | 0.000718 | 0.369965 | 0.000784 | 0.599563 |
| | 27 | 0.041 | 58.9 | 0.00091 | 0.454099 | 0.001152 | 0.57449 |
| | 32 | 0.068 | 81.6 | 0.001553 | 0.500399 | *0.001802* | 0.729119 |
| | 37 | 0.124 | 107.1 | *0.002571* | 0.610495 | *0.002779* | 0.951531 |
| | 42 | 0.196 | 133.1 | *0.003545* | 0.673669 | *0.003951* | 1.344192 |
| | 47 | 0.348 | 165.9 | *0.004483* | 0.719679 | *0.005057* | 1.825543 |
| | 52 | 0.521 | 168.9 | *0.004187* | 0.748688 | *0.004992* | 1.5687 |
| | 57 | 0.715 | 136.8 | *0.003756* | 0.755693 | *0.00458* | 1.31569 |
| | 62 | 0.79 | 113.1 | *0.003565* | 0.751256 | *0.004235* | 1.142123 |
| | 67 | 0.858 | 83.6 | *0.003593* | 0.745092 | *0.003994* | 0.9175 |
| | 72 | 0.913 | 57 | *0.003117* | 0.748285 | *0.003344* | 0.680576 |
| | 77 | 0.935 | 44.2 | *0.00326* | 0.747248 | *0.003472* | 1.894483 |
| | 82 | 0.951 | 36.5 | *0.002795* | 0.733112 | *0.002746* | 0.55314 |
| | 87 | 0.965 | 27.7 | *0.002983* | 0.729626 | *0.002819* | 0.526467 |
| | 92 | 0.976 | 20.2 | *0.003376* | 0.707357 | *0.00276* | 0.474946 |
| | 97 | 0.98 | 16.5 | *0.003261* | 0.694297 | *0.002607* | 0.50282 |
| | 102 | 0.982 | 13.9 | *0.00372* | 0.723157 | *0.002771* | 0.470028 |
| | 107 | 0.989 | 9.9 | *0.00505* | 0.637117 | *0.002442* | 0.32658 |
| | 112 | 0.99 | 8.1 | *0.005512* | 0.619228 | *0.002393* | 0.414015 |
| | 117 | 0.992 | 6.9 | *0.00636* | 0.624409 | *0.002756* | 0.399977 |
| | 122 | 0.995 | 4.8 | *0.00778* | 0.583857 | *0.002458* | 0.105463 |
| | 127 | 0.995 | 4 | *0.008697* | 0.555392 | *0.002598* | -- |
| | 132 | 0.995 | 4.3 | 0.008995 | 0.567112 | *0.002934* | -- |
| | 132 | 0.997 | 2.9 | -- | 0.544159 | -- | -- |
| | 137 | 0.997 | 2.6 | -- | 0.541278 | -- | -- |
| | 142 | 0.998 | 1.8 | -- | -- | -- | -- |
| | 147 | 0.998 | 1.7 | -- | -- | -- | -- |
| | 152 | 0.999 | 1 | -- | -- | -- | -- |

Notes : *Blue italic* : suspicious data; **Red Bold** : possibly incorrect data; (--) : meaningless data.

D.4.3.2 Step edge 10, Δx = 9.6 mm

| Δx | y | C | F | $T_{xx}$ | $(R_{xy})_{max}$ | $T_{xy}$ | Tu |
|---|---|---|---|---|---|---|---|
| mm | mm | | Hz | sec. | | sec. | |
| 9.6 | 0 | 0.053 | 5.8 | -- | -- | -- | -- |
| | 5 | 0.012 | 29.5 | 0.049417 | 0.00019 | 0.403972 | -- |
| | 8 | 0.035 | 81.7 | 0.1093 | 0.000296 | 0.381092 | -- |
| | 10 | 0.039 | 84.8 | 0.121427 | 0.000382 | 0.366015 | -- |
| | 12 | 0.026 | 59.9 | 0.096115 | 0.000267 | 0.373153 | -- |
| | 15 | 0.047 | 94.3 | 0.180257 | 0.000421 | 0.388148 | -- |
| | 18 | 0.052 | 99 | 0.184676 | 0.000559 | -- | -- |
| | 20 | 0.062 | 112.7 | 0.222364 | 0.000551 | 0.463487 | -- |
| | 25 | 0.071 | 117.9 | 0.292837 | 0.000835 | 0.499244 | -- |
| | 30 | 0.068 | 113.3 | 0.28901 | 0.000764 | 0.460181 | -- |

| | | | | | | |
|---|---|---|---|---|---|---|
| 35 | 0.08 | 123 | 0.319277 | 0.000808 | 0.438083 | -- |
| 40 | 0.088 | 125 | 0.320664 | 0.000792 | 0.4053 | -- |
| 45 | 0.124 | 149.5 | 0.437437 | 0.001489 | 0.536502 | -- |
| 50 | 0.167 | 153.4 | 0.545563 | *0.002427* | 0.700627 | -- |
| 55 | 0.294 | 185.8 | 0.614334 | *0.003401* | 0.988448 | -- |
| 60 | 0.511 | 192.7 | 0.662247 | *0.004125* | 1.189168 | -- |
| 65 | 0.617 | 179.2 | 0.677186 | 0.004096 | 1.113039 | -- |
| 70 | 0.782 | 128.3 | 0.662946 | 0.003333 | 0.823126 | -- |
| 75 | 0.869 | 88.8 | 0.643304 | 0.002727 | 0.632891 | -- |
| 80 | 0.947 | 43.3 | 0.598996 | 0.002115 | 0.499834 | -- |
| 85 | 0.964 | 31.3 | 0.587268 | *0.001865* | 0.421467 | -- |
| 90 | 0.972 | 25 | 0.569822 | *0.001663* | 0.416834 | -- |
| 95 | 0.978 | 19 | 0.599323 | *0.001644* | 0.367183 | -- |
| 100 | 0.985 | 13.5 | 0.582659 | 0.001566 | 1.202521 | -- |
| 105 | 0.987 | 11.1 | 0.525884 | *0.001398* | 0.409692 | -- |
| 110 | 0.989 | 10 | 0.578211 | *0.001322* | 0.342654 | -- |
| 115 | 0.993 | 6.7 | 0.543289 | *0.001297* | 0.377245 | -- |
| 120 | 0.994 | 5.8 | 0.482436 | *0.001104* | 0.305683 | -- |
| 125 | 0.995 | 4.3 | 0.475139 | *0.001039* | 0.297412 | -- |
| 130 | 0.996 | 3.8 | 0.498344 | *0.001101* | 0.320875 | -- |
| 130 | 0.998 | 2.5 | 0.500669 | *0.001093* | 0.308174 | -- |
| 135 | 0.998 | 2.1 | 0.492897 | *0.001172* | 0.419171 | -- |
| 140 | 0.998 | 1.7 | 0.448952 | *0.000948* | 0.384834 | -- |

Notes : *Blue italic* : suspicious data; **Red Bold** : possibly incorrect data; (--) : meaningless data.

## APPENDIX E - INTEGRAL AIR-WATER LENGTH AND TIME SCALES IN SKIMMING FLOWS ON A STEPPED CHUTE

### E.1 Presentation

When two probe sensors are separated by a transverse or streamwise distance Y, their signals may be analysed in terms of the auto-correlation and cross-correlation functions $R_{XX}$ and $R_{XY}$ respectively (App. D). In the present study, the probe sensors were scanned at 20 kHz for 45 s. The data sets of 900,000 samples per sensor were segmented because the periodogram resolution is inversely proportional to the number of samples and it could be biased with large data sets (HAYES 1996, GONZALEZ 2005). The signals were sub-divided into fifteen non-overlapping segments of 60,000 samples. In addition, the correlation analyses were conducted on the raw probe output signals. With a single-threshold technique, any analysis based upon thresholded signals (or square-wave signals) tends to ignore the contributions of the smallest air-water particles.

Identical experiments were repeated with different separation distances Y (Y = $\Delta z$ or $\Delta x$) and an integral turbulent length scale was calculated as :

$$L_{xy} = \int_{Y=0}^{Y=Y((R_{xy})_{max}=0)} (R_{xy})_{max} * dY \quad (E\text{-}1)$$

where $R_{xy}$ is the normalised cross-correlation function between the two probe output signals, $(R_{xy})_{max}$ the maximum cross-correlation coefficient, and Y is the separation distance. The integral turbulent length scale $L_{xy}$ is a function of the inflow conditions, streamwise position $x/d_C$ and normal distance $y/d_C$. In the present study, the length scale $L_{xy}$ represents a measure of the transverse/streamwise length scale of the large vortical structures advecting air bubbles and air-water packets.

An integral turbulent time scale is :

$$\mathbf{T} = \frac{\int_{Y=0} (R_{xy})_{max} * T_{xy} * dY}{L_{xy}} \quad (E\text{-}2)$$

$\mathbf{T}$ represents the transverse/streamwise integral time scale of the large eddies advecting air bubbles.

*Discussion*

Auto- and cross-correlation calculations were most successful for $0.05 \leq C \leq 0.95$. In the upper spray region ($C \geq 0.90$ to 0.95) and at a few other locations, the calculations were unsuccessful for a number of reasons. These included flat cross-correlation functions without a distinctive peak, non-crossing of the correlation function(s) with the zero line, correlation functions with several peaks, meaningless correlation trends ... Such data points are indicated with (--) in the following tables of results. While most correlation calculations can be automated, it must be stressed that human intervention are essential to validate each calculation step. Herein all calculations were performed by hand and all meaningless results were rejected.

Note that another streamwise length scale is the advection length scale defined as :

$$L_{xx} = V * T_{xx} \quad (E\text{-}3)$$

where V is the advective velocity magnitude and $T_{XX}$ is an auto-correlation time scale of the longitudinal bubbly flow structures :

$$T_{XX} = \int_{\tau=0}^{\tau=\tau(R_{XX}=0)} R_{XX}(\tau) * d\tau \quad \text{(E-4)}$$

$L_{XX}$ is a characteristic longitudinal size of the large eddies advecting air bubbles.

## E.2 Experimental results. (1) Transverse integral length and time scales

*E.2.1 Experimental results for $d_C/h = 1.15$*

| | |
|---|---|
| Location : | The University of Queensland (Australia) |
| Date : | April-June 2006 |
| Experiments by : | G. CAROSI |
| Data processing by: | G. CAROSI and H. CHANSON |
| Data analysis by : | H. CHANSON and G. CAROSI |
| Experiment characteristics : | Channel: width: 1.0 m, slope: 21.8º, h = 0.10 m, l = 0.25 m, 10 identical steps. Open channel with perspex sidewalls and smooth marine plywood staircase invert.<br>$Q_W$ = 0.1164 $m^3/s$, $d_C$ = 0.115 m, Re = 4.6 E+5 |
| Instrumentation : | Two single-tip conductivity probe (∅ = 0.35 mm). Transverse separation distance Δz.<br>Scan rate: 20 kHz per probe sensor, Sampling duration: 45 sec. |
| Comments : | Inflow conditions : broad-crested weir.<br>Inception of free-surface aeration: between step edges 6 and 7.<br>Correlation analyses performed on fifteen segments of 60,000 samples. |

D.2.1.1 Step edge 10

Characteristic air water flow properties

| $Y_{90}$ (+) | d (+) | $C_{mean}$ (+) | $U_W$ (+) | $F_{max}$ (+) |
|---|---|---|---|---|
| m | m | | m/s | Hz |
| 0.0598 | 0.041 | 0.4518 | 3.98 | 189.3 |

| y | C | F | $L_{xy}$ | T | $L_{xx}$ | Remarks |
|---|---|---|---|---|---|---|
| | (+) | (+) | Eq. (E-1) | Eq. (E-2) | Eq. (E-3) | |
| mm | | Hz | mm | millisec. | mm | |
| (1) | (2) | (3) | (4) | (5) | (6) | (4) |
| 2 | 0.028 | 52.4 | 2.37 | 0.593 | -- | Transverse integration. |
| 7 | 0.038 | 70.9 | 2.39 | 0.513 | -- | |
| 10 | 0.043 | 74.7 | 2.65 | 0.772 | 3.563 | |
| 12 | 0.044 | 75.7 | 2.70 | 0.711 | 3.332 | |
| 14 | 0.050 | 79.5 | 2.93 | 0.735 | 3.435 | |
| 17 | 0.055 | 85.5 | 3.28 | 0.797 | 3.060 | |
| 20 | 0.064 | 91.8 | 3.85 | 1.203 | 3.840 | |
| 22 | 0.074 | 100.0 | 4.35 | 1.321 | 4.364 | |
| 27 | 0.121 | 130.8 | 6.82 | 1.748 | 5.786 | |
| 32 | 0.237 | 175.1 | 10.18 | 2.904 | -- | |
| 37 | 0.424 | 189.3 | 12.85 | 3.440 | 12.537 | |
| 42 | 0.594 | 177.9 | 11.78 | 3.691 | 15.725 | |
| 47 | 0.718 | 148.7 | 13.36 | 3.189 | 14.773 | |
| 52 | 0.826 | 104.4 | 11.83 | 2.690 | 12.276 | |
| 57 | 0.881 | 74.3 | 10.47 | 2.303 | 12.426 | |

| | | | | | |
|---|---|---|---|---|---|
| 62 | 0.915 | 55.6 | 9.00 | 1.907 | 10.149 |
| 67 | 0.937 | 42.9 | 8.35 | 1.893 | 9.769 |
| 72 | 0.953 | 33.4 | 6.64 | 1.849 | 8.111 |
| 77 | 0.963 | 26.7 | 6.68 | 1.649 | *8.775* |
| 82 | 0.970 | 22.4 | 6.66 | 1.687 | 8.503 |
| 87 | 0.977 | 17.4 | 6.00 | 1.755 | *8.098* |
| 92 | 0.982 | 14.2 | 5.61 | 1.567 | *7.637* |
| 97 | 0.986 | 11.2 | 5.54 | 1.786 | *8.324* |
| 102 | 0.989 | 8.8 | 5.20 | 1.648 | *8.033* |
| 107 | 0.992 | 6.7 | 5.06 | 1.611 | *8.860* |
| 112 | 0.994 | 5.4 | 4.94 | 1.648 | *8.390* |
| 117 | 0.995 | 4.2 | 4.65 | 1.746 | *8.588* |
| 122 | 0.996 | 3.5 | 4.56 | 1.764 | *8.351* |
| 127 | 0.997 | 2.7 | 5.15 | 2.008 | *9.731* |
| 132 | 0.997 | 2.4 | 4.88 | 1.948 | *11.343* |
| 137 | 0.998 | 1.6 | 3.93 | 2.846 | *18.580* |
| 142 | 0.998 | 1.7 | 4.19 | 3.074 | 20.713 |
| 147 | 0.999 | 1.4 | 3.33 | 3.198 | *19.852* |
| 152 | 0.999 | 1.1 | 4.58 | 5.680 | *21.326* |
| 157 | 0.999 | 0.9 | 4.29 | -- | -- |

Notes :

($^{+}$) : data collected for 360 s at 20 kHz;

$L_{xy}$, **T** : transverse integral scales;

*Blue italic* : suspicious data;

**Red Bold** : possibly incorrect data;

(--) : meaningless data.

Fig. E-1 - Normal distributions of transverse integral length scale $L_{xy}$, (transverse) integral times scale **T**, and streamwise Taylor length scale $L_{xx}$ for $d_c/h$ = 1.15, Step 10 - Comparison with the measured void fraction distribution

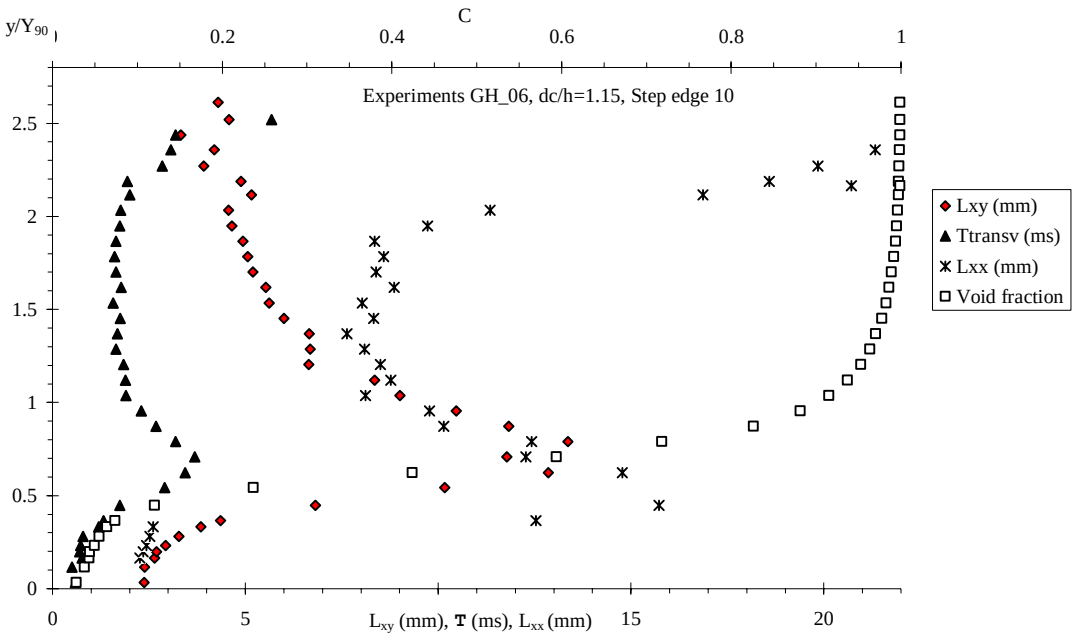

*E.2.2 Experimental results for $d_C/h$ = 1.45*

| | |
|---|---|
| Location : | The University of Queensland (Australia) |
| Date : | April-June 2006 |
| Experiments by : | G. CAROSI |
| Data processing by: | G. CAROSI and H. CHANSON |
| Data analysis by : | H. CHANSON and G. CAROSI |
| Experiment characteristics : | Channel: width: 1.0 m, slope: 21.8°, h = 0.10 m, l = 0.25 m, 10 identical steps. Open channel with perspex sidewalls and smooth marine plywood staircase invert.<br>$Q_W$ = 0.1612 $m^3/s$, $d_C$ = 0.145 m, Re = 6.4 E+5 |
| Instrumentation : | Two single-tip conductivity probe (∅ = 0.35 mm). Transverse separation distance Δz.<br>Scan rate: 20 kHz per probe sensor, Sampling duration: 45 sec. |
| Comments : | Inflow conditions : broad-crested weir.<br>Inception of free-surface aeration: between step edges 7 and 8.<br>Correlation analyses performed on fifteen segments of 60,000 samples. |

D.2.2.1 Step edge 10

Characteristic air water flow properties

| $Y_{90}$ (+) | d (+) | $C_{mean}$ (+) | $U_W$ (+) | $F_{max}$ (+) |
|---|---|---|---|---|
| m | m | | m/s | Hz |
| 0.0735 | 0.052 | 0.2929 | 3.33 | 154.1 |

| y | C | F | $L_{xy}$ | T | $L_{xx}$ | Remarks |
|---|---|---|---|---|---|---|
| | | | Eq. (E-1) | Eq. (E-2) | Eq. (E-3) | |
| mm | | Hz | m | s | m | |
| (1) | (2) | (3) | (4) | (5) | (6) | (4) |
| 2 | 0.010 | 23.0 | 2.220 | 0.607 | 2.837 | Transverse integration. |
| 7 | 0.013 | 27.3 | 2.231 | 0.488 | 2.594 | |
| 10 | 0.016 | 30.3 | 2.596 | 0.616 | 3.236 | |
| 12 | 0.015 | 28.7 | 2.720 | 0.790 | 3.763 | |
| 14 | 0.018 | 32.0 | 2.817 | 0.590 | 3.264 | |
| 17 | 0.020 | 34.1 | 2.850 | 0.688 | 3.222 | |
| 20 | 0.023 | 35.9 | 3.241 | 0.795 | 4.099 | |
| 22 | 0.025 | 38.4 | 3.472 | 0.963 | 3.937 | |
| 27 | 0.033 | 44.0 | 3.790 | 1.364 | 4.492 | |
| 32 | 0.056 | 59.8 | 6.713 | 1.646 | *7.460* | |
| 37 | 0.104 | 85.2 | 7.816 | 2.414 | *9.831* | |
| 42 | 0.200 | 118.5 | 11.972 | 2.967 | *14.843* | |
| 47 | 0.337 | 147.2 | 15.197 | 3.532 | 17.689 | |
| 52 | 0.515 | 154.1 | 16.630 | 3.371 | 16.815 | |
| 57 | 0.652 | 135.4 | 16.979 | 3.432 | 18.345 | |
| 62 | 0.766 | 108.6 | 15.628 | 2.932 | *16.357* | |
| 67 | 0.845 | 80.4 | 13.640 | 2.572 | 13.530 | |
| 72 | 0.891 | 59.6 | 12.589 | 2.252 | *12.691* | |
| 77 | 0.922 | 46.0 | 10.460 | 1.983 | *12.472* | |
| 82 | 0.939 | 37.3 | 9.826 | 1.927 | *12.847* | |
| 87 | 0.956 | 28.2 | 7.894 | 1.823 | *11.764* | |
| 92 | 0.965 | 22.7 | 7.353 | 1.918 | *11.167* | |
| 97 | 0.975 | 17.6 | 8.101 | 1.448 | *10.097* | |
| 102 | 0.980 | 14.2 | 5.678 | 1.810 | *10.782* | |
| 107 | 0.986 | 10.8 | 6.129 | 1.535 | *9.423* | |
| 112 | 0.988 | 8.8 | 6.028 | 1.503 | *9.920* | |
| 117 | 0.991 | 7.1 | 5.642 | 1.608 | *10.070* | |

| | | | | | |
|---|---|---|---|---|---|
| 122 | 0.993 | 5.4 | 5.794 | 1.447 | *10.908* |
| 127 | 0.995 | 4.0 | 5.342 | 1.400 | *11.073* |
| 132 | 0.996 | 3.1 | 5.108 | 1.549 | *11.864* |
| 132 | 0.997 | 2.8 | 5.118 | 1.598 | *12.353* |
| 137 | 0.997 | 2.3 | 3.877 | 2.448 | *19.498* |
| 142 | 0.998 | 1.8 | 5.162 | 1.432 | *12.512* |
| 147 | 0.998 | 1.7 | 4.322 | 1.840 | *17.604* |
| 152 | 0.999 | 1.3 | 4.748 | 1.912 | *19.471* |

Notes :

($^+$) : data collected for 315 s at 20 kHz;

$L_{xy}$, **T** : transverse integral scales;

*Blue italic* : suspicious data;

**Red Bold** : possibly incorrect data;

(--) : meaningless data.

Fig. E-2 - Normal distributions of transverse integral length scale $L_{xy}$, (transverse) integral times scale **T**, and streamwise Taylor length scale $L_{xx}$ for $d_c/h$ = 1.45, Step 10 - Comparison with the measured void fraction distribution

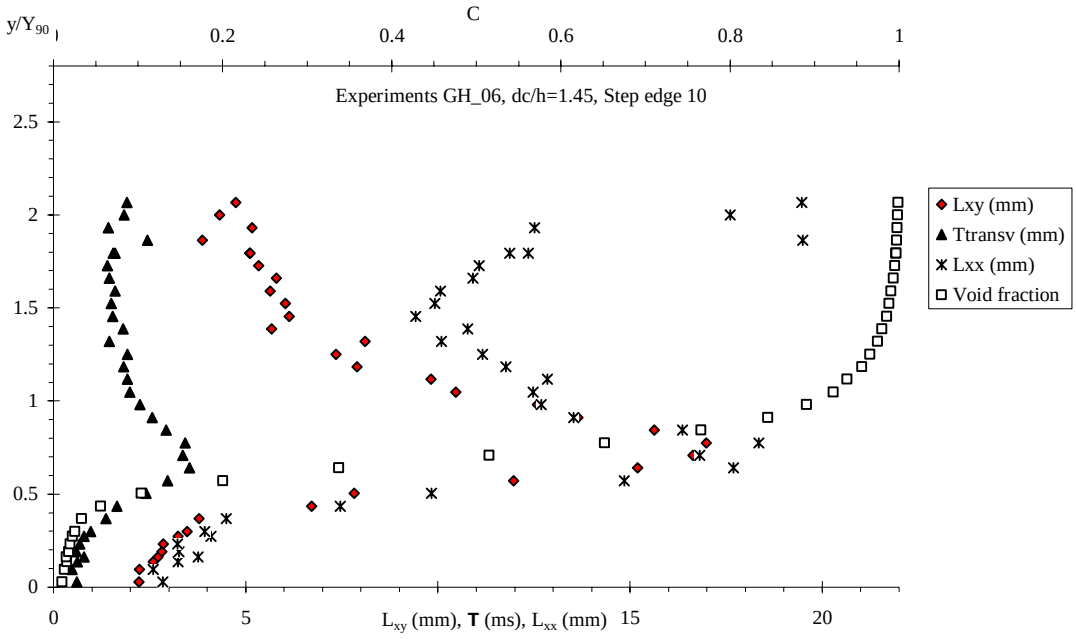


## E.3 Experimental results. (2) Longitudinal/streamwise integral length and time scales

The longitudinal integral scales were calculated based upon the auto- and cross-correlation function for some double-tip probes. Note that only two streamwise probe separation distances were used : $\Delta x$ = 7.0 and 9.6 mm.

### *E.3.1 Experimental results for $d_c/h$ = 1.15*

| | |
|---|---|
| Location : | The University of Queensland (Australia) |
| Date : | April-June 2006 |

| | |
|---|---|
| Experiments by : | G. CAROSI |
| Data processing by: | G. CAROSI and H. CHANSON |
| Data analysis by : | H. CHANSON and G. CAROSI |
| Experiment characteristics : | Channel: width: 1.0 m, slope: 21.8º, h = 0.10 m, l = 0.25 m, 10 identical steps. Open channel with perspex sidewalls and smooth marine plywood staircase invert.<br>$Q_w$ = 0.1164 $m^3$/s, $d_c$ = 0.115 m, Re = 4.6 E+5 |
| Instrumentation : | Double-tip conductivity probes (∅ = 0.25 mm). Transverse separation distance Δx.<br>Scan rate: 20 kHz per probe sensor, Sampling duration: 45 sec. |
| Comments : | Inflow conditions : broad-crested weir.<br>Inception of free-surface aeration: between step edges 6 and 7.<br>Correlation analyses performed on fifteen segments of 60,000 samples. |

D.3.1.1 Step edge 10

Characteristic air water flow properties

| $Y_{90}$ (+) | d (+) | $C_{mean}$ (+) | $U_w$ (+) | $F_{max}$ (+) |
|---|---|---|---|---|
| m | m | | m/s | Hz |
| 0.0574 | 0.0364 | 0.365 | 3.35 | 233 |

| y | C | F | $L_{xy}$ | T | $L_{xx}$ | Remarks |
|---|---|---|---|---|---|---|
| | (+) | (+) | Eq. (E-1) | Eq. (E-2) | Eq. (E-3) | |
| mm | | Hz | mm | millisec. | mm | |
| (1) | (2) | (3) | (4) | (5) | (6) | (4) |
| 1 | 0.042 | 83.8 | 5.02 | 0.90 | 3.99 | Streamwise integration. |
| 6 | 0.071 | 123.3 | 5.78 | 0.63 | 2.41 | |
| 8 | *0.074* | 146.0 | *6.85* | -- | -- | |
| 11 | 0.078 | 127.2 | 6.45 | 0.77 | 2.66 | |
| 13 | 0.078 | 126.8 | 6.41 | 1.70 | 10.28 | |
| 16 | 0.081 | 126.9 | 6.63 | 0.71 | 2.52 | |
| 19 | 0.105 | 147.7 | 7.13 | 1.00 | 4.11 | |
| 21 | 0.111 | 150.7 | 7.47 | 0.84 | 0.89 | |
| 26 | 0.143 | 170.5 | 8.04 | 1.75 | 6.75 | |
| 31 | 0.328 | 204.3 | 8.99 | 2.64 | 10.28 | |
| 36 | 0.503 | 232.9 | 9.74 | 3.22 | 11.93 | |
| 41 | 0.613 | 233.0 | 10.34 | 3.32 | 9.67 | |
| 46 | 0.737 | 193.2 | 10.67 | *3.61* | 12.85 | |
| 51 | 0.809 | 133.6 | 10.69 | *3.43* | 13.26 | |
| 56 | 0.880 | 93.4 | 10.71 | *2.88* | 10.41 | |
| 61 | 0.916 | 66.5 | 10.57 | *2.49* | 11.24 | |
| 66 | 0.935 | 51.9 | 10.64 | *2.35* | 8.74 | |
| 71 | 0.951 | 40.3 | 10.67 | *2.55* | 10.65 | |
| 76 | 0.962 | 30.8 | 10.56 | *2.44* | 10.34 | |
| 81 | 0.970 | 26.7 | 10.41 | *2.47* | 11.46 | |
| 86 | 0.978 | 19.5 | 10.20 | *2.50* | 12.48 | |
| 91 | 0.983 | 15.8 | 9.99 | *2.62* | 14.82 | |
| 96 | 0.986 | 12.6 | 10.10 | *2.84* | 16.52 | |
| 101 | 0.989 | 10.3 | 9.49 | *3.09* | 21.35 | |
| 106 | 0.991 | 8.4 | 9.81 | *3.54* | 24.50 | |
| 111 | 0.993 | 6.6 | 9.48 | *4.12* | 31.06 | |
| 116 | 0.994 | 5.7 | 9.28 | *3.81* | 29.34 | |
| 121 | 0.995 | 4.8 | 9.46 | *4.22* | 31.22 | |
| 126 | 0.996 | 3.6 | 9.00 | *4.40* | 32.82 | |
| 131 | 0.997 | 2.8 | 8.43 | *4.41* | 31.93 | |

| | | | | | |
|---|---|---|---|---|---|
| 133.5 | 0.998 | 2.3 | 8.76 | -- | -- |
| 136 | 0.998 | 1.8 | 7.91 | -- | -- |
| 141 | 0.999 | 1.4 | 7.73 | -- | -- |
| 147 | 0.999 | 1.0 | -- | -- | -- |
| 152 | 0.999 | 1.0 | **6.15** | -- | -- |

Notes :

(+) : data collected for 90 s at 20 kHz;

$L_{xy}$, **T** : transverse integral scales;

*Blue italic* : suspicious data;

**Red Bold** : possibly incorrect data;

(--) : meaningless data.

Fig. E-3 - Normal distributions of streamwise integral length scale $L_{xy}$, (streamwise) integral times scale **T**, and streamwise Taylor length scale $L_{xx}$ for $d_c/h$ = 1.15, Step 10 - Comparison with the measured void fraction distribution

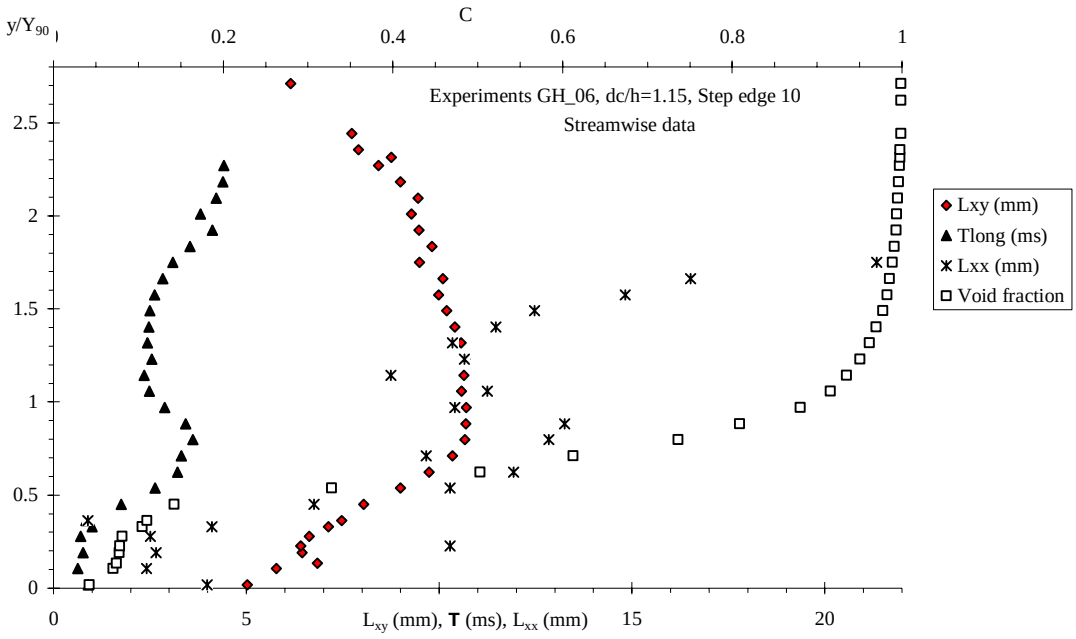


*E.3.2 Experimental results for $d_c/h$ = 1.45*

| | |
|---|---|
| Location : | The University of Queensland (Australia) |
| Date : | April-June 2006 |
| Experiments by : | G. CAROSI |
| Data processing by: | G. CAROSI and H. CHANSON |
| Data analysis by : | H. CHANSON and G. CAROSI |
| Experiment characteristics : | Channel: width: 1.0 m, slope: 21.8°, h = 0.10 m, l = 0.25 m, 10 identical steps. Open channel with perspex sidewalls and smooth marine plywood staircase invert.<br>$Q_w$ = 0.1612 $m^3/s$, $d_c$ = 0.145 m, Re = 6.4 E+5 |

| | |
|---|---|
| Instrumentation : | Double-tip conductivity probes (∅ = 0.25 mm). Transverse separation distance Δx.<br>Scan rate: 20 kHz per probe sensor, Sampling duration: 45 sec. |
| Comments : | Inflow conditions : broad-crested weir.<br>Inception of free-surface aeration: between step edges 6 and 7.<br>Correlation analyses performed on fifteen segments of 60,000 samples. |

D.3.3.2 Step edge 10

Characteristic air water flow properties

| $Y_{90}$ (+) | d (+) | $C_{mean}$ (+) | $U_w$ (+) | $F_{max}$ (+) |
|---|---|---|---|---|
| m | m | | m/s | Hz |
| 0.0758 | 0.0546 | 0.280 | 2.24 | 161.3 |

| y | C | F | $L_{xy}$ | T | $L_{xx}$ | Remarks |
|---|---|---|---|---|---|---|
| | (+) | (+) | Eq. (E-1) | Eq. (E-2) | Eq. (E-3) | |
| mm | | Hz | mm | millisec. | mm | |
| (1) | (2) | (3) | (4) | (5) | (6) | (4) |
| 1 | 0.030 | 11.7 | 4.61 | 0.48 | 1.14 | Streamwise integration. |
| 6 | 0.011 | 25.7 | 5.13 | 0.60 | 1.33 | |
| 9 | 0.023 | 52.6 | 5.40 | 0.42 | 0.59 | |
| 11 | 0.026 | 55.7 | 5.53 | 0.53 | 1.36 | |
| 13 | 0.022 | 44.8 | 5.60 | 0.67 | 1.47 | |
| 16 | 0.039 | 73.4 | 6.43 | 0.72 | 1.70 | |
| 19 | 0.040 | 73.6 | 6.32 | 0.63 | 1.44 | |
| 21 | 0.046 | 81.4 | 6.72 | 0.66 | 1.60 | |
| 26 | 0.056 | 88.4 | 7.58 | 0.90 | 2.03 | |
| 31 | 0.068 | 97.5 | 7.78 | 1.38 | 3.47 | |
| 36 | 0.102 | 115.1 | 8.51 | *2.11* | 5.75 | |
| 41 | 0.142 | 129.1 | 8.82 | *2.91* | 7.93 | |
| 46 | 0.236 | 157.7 | 9.80 | *3.61* | 10.02 | |
| 51 | 0.344 | 161.2 | 10.64 | *3.55* | 9.36 | |
| 56 | 0.505 | 161.3 | 11.12 | *3.43* | 8.40 | |
| 61 | 0.651 | 152.9 | 11.41 | *3.39* | 7.97 | |
| 66 | 0.738 | 131.4 | 11.48 | *3.30* | 8.03 | |
| 71 | 0.848 | 92.7 | 11.40 | *2.77* | 6.97 | |
| 76 | 0.902 | 66.5 | 11.27 | *2.73* | 7.29 | |
| 81 | 0.949 | 39.9 | 10.91 | *2.23* | 6.25 | |
| 86 | 0.965 | 29.5 | 10.82 | *2.26* | 6.67 | |
| 91 | 0.974 | 22.6 | 10.60 | *2.31* | 7.55 | |
| 96 | 0.979 | 17.8 | 10.73 | *2.19* | 7.29 | |
| 101 | 0.984 | 13.7 | 10.76 | *2.38* | 8.32 | |
| 106 | 0.988 | 10.5 | 9.98 | *2.63* | 11.29 | |
| 111 | 0.990 | 9.1 | 10.23 | *2.67* | 12.32 | |
| 116 | 0.993 | 6.8 | 10.03 | *3.07* | 14.22 | |
| 121 | 0.995 | 5.3 | 9.44 | *3.41* | 17.40 | |
| 126 | 0.995 | 4.2 | 9.25 | *3.72* | 19.45 | |
| 131 | 0.996 | 4.1 | 9.46 | *3.90* | 20.11 | |
| 131 | 0.998 | 2.7 | 9.37 | -- | -- | |
| 136 | 0.998 | 2.4 | 9.30 | -- | -- | |
| 141 | 0.998 | 1.8 | *9.29* | -- | -- | |
| 147 | 0.998 | 1.7 | -- | -- | -- | |
| 152 | 0.999 | 1.0 | -- | -- | -- | |

Notes :

(+) : data collected for 90 s at 20 kHz;

$L_{xy}$, **T** : transverse integral scales;

*Blue italic* : suspicious data;

**Red Bold** : possibly incorrect data;

(--) : meaningless data.

Fig. E-4 - Normal distributions of streamwise integral length scale $L_{xy}$, (streamwise) integral times scale **T**, and streamwise Taylor length scale $L_{xx}$ for $d_c/h$ = 1.45, Step 10 - Comparison with the measured void fraction distribution

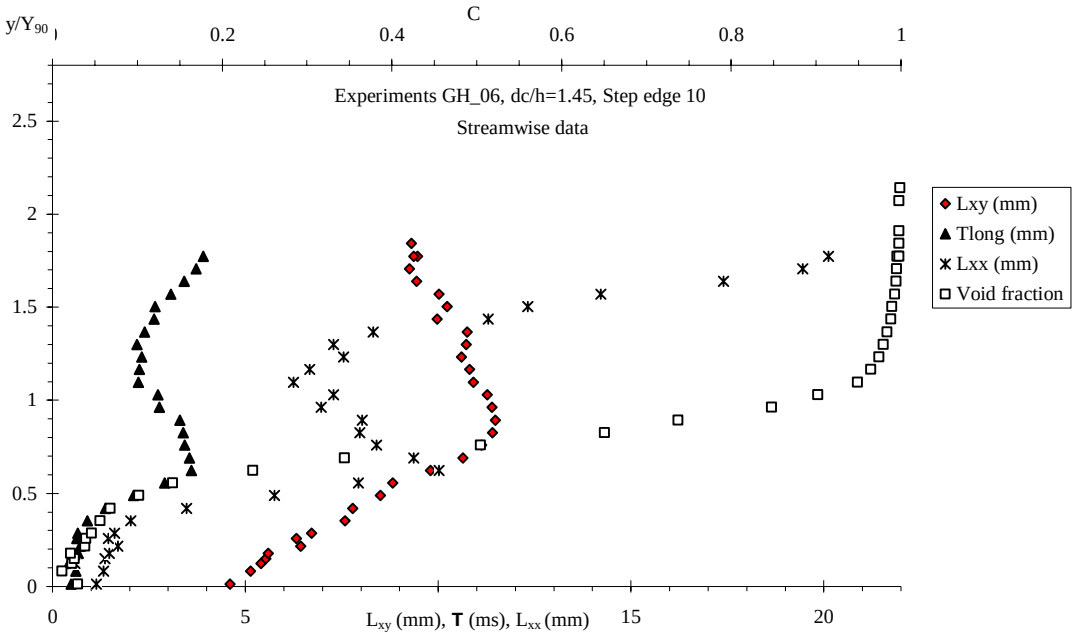

## APPENDIX F - EXPERIMENTAL MEASUREMENTS OF VOID FRACTION, BUBBLE COUNT RATE, INTERFACIAL VELOCITY AND TURBULENCE INTENSITY IN SKIMMING FLOWS ON A STEPPED CHUTE

*Notation*

C void fraction defined as the volume of air per unit volume of air and water;

F bubble count rate (Hz) defined as the number of bubbles pierced by the probe sensor per second;

h step height (m);

l step length (m);

Tu turbulence intensity u'/V calculated by correlation analyses;

u' root mean square of longitudinal component of turbulent velocity (m/s);

V time-averaged interfacial velocity (m/s);

### F.1 Experimental data for $d_C/h = 1.0$

| | |
|---|---|
| Location : | The University of Queensland (Australia) |
| Date : | April-June 2006 |
| Experiments by : | G. CAROSI |
| Data processing by: | G. CAROSI and H. CHANSON |
| Data analysis by : | H. CHANSON and G. CAROSI |
| Experiment characteristics : | Channel: width: 1.0 m, slope: 21.8º, h = 0.10 m, l = 0.25 m, 10 identical steps. Open channel with perspex sidewalls and smooth marine plywood staircase invert.<br>$Q_w$ = 0.0948 $m^3/s$, $d_c$ = 0.10 m, Re = 3.85 E+5 |
| Instrumentation : | Single-tip conductivity probe (∅ = 0.35 mm).<br>Scan rate: 20 kHz per probe sensor, Sampling duration: 45 sec. |
| Comments : | Inflow conditions : broad-crested weir.<br>Inception of free-surface aeration: step edge 5. |

| Run | Step edge | y mm | C | F Hz | Run | Step edge | y mm | C | F Hz |
|---|---|---|---|---|---|---|---|---|---|
| 060322a | 6 | 1.0 | 0.004 | 9.7 | 060327a | 7 | 13.0 | 0.047 | 49.7 |
| | | 1.5 | 0.006 | 12.5 | | | 16.0 | 0.052 | 50.9 |
| | | 2.0 | 0.007 | 15.8 | | | 19.0 | 0.060 | 55.5 |
| | | 3.0 | 0.015 | 27.4 | | | 21.0 | 0.074 | 65.0 |
| | | 5.0 | 0.028 | 42.4 | | | 23.0 | 0.065 | 60.7 |
| | | 6.0 | 0.043 | 57.2 | | | 26.0 | 0.099 | 76.2 |
| | | 7.0 | 0.042 | 56.8 | | | 28.0 | 0.127 | 92.4 |
| | | 8.0 | 0.047 | 59.3 | | | 31.0 | 0.168 | 104.1 |
| | | 9.0 | 0.051 | 62.3 | | | 34.0 | 0.264 | 133.8 |
| | | 10.0 | 0.052 | 62.7 | | | 36.0 | 0.349 | 148.8 |
| | | 11.0 | 0.065 | 71.8 | | | 41.0 | 0.533 | 140.6 |
| | | 11.5 | 0.071 | 75.4 | | | 46.0 | 0.636 | 126.1 |
| | | 12.0 | 0.074 | 78.1 | | | 51.0 | 0.801 | 86.8 |
| | | 13.0 | 0.065 | 71.7 | | | 56.0 | 0.844 | 65.4 |

| | | | | | | | | | |
|---|---|---|---|---|---|---|---|---|---|
| | | 16.0 | 0.093 | 86.0 | | | 61.0 | 0.883 | 51.0 |
| | | 21.0 | 0.197 | 127.3 | | | 66.0 | 0.909 | 40.1 |
| | | 26.0 | 0.291 | 145.8 | | | 71.0 | 0.926 | 31.7 |
| | | 31.0 | 0.414 | 150.4 | | | 76.0 | 0.948 | 22.6 |
| | | 41.0 | 0.737 | 112.5 | | | 81.0 | 0.971 | 13.5 |
| | | 46.0 | 0.815 | 82.0 | | | 86.0 | 0.968 | 15.2 |
| | | 51.0 | 0.859 | 62.5 | | | 91.0 | 0.979 | 10.0 |
| | | 56.0 | 0.905 | 43.1 | | | 96.0 | 0.985 | 7.6 |
| | | 61.0 | 0.843 | 62.2 | | | 101.0 | 0.981 | 9.2 |
| | | 66.0 | 0.849 | 60.0 | | | 106.0 | 0.997 | 1.6 |
| | | 71.0 | 0.868 | 55.8 | | | 111.0 | 0.998 | 1.4 |
| | | 76.0 | 0.896 | 45.7 | | | 116.0 | 0.998 | 1.3 |
| | | 81.0 | 0.918 | 38.3 | | | 121.0 | 0.994 | 3.2 |
| | | 86.0 | 0.915 | 37.2 | | | 126.0 | 0.994 | 2.9 |
| | | 91.0 | 0.929 | 31.4 | | | 131.0 | 0.996 | 2.4 |
| | | 96.0 | 0.931 | 29.6 | | | 141.0 | 0.998 | 1.4 |
| | | 106.0 | 0.953 | 22.5 | | | 146.0 | 0.998 | 1.3 |
| | | 111.0 | 0.962 | 17.8 | | | 1.0 | 0.000 | 0.9 |
| | | 116.0 | 0.967 | 14.7 | | | 136.0 | 0.997 | 1.6 |
| | | 121.0 | 0.974 | 12.4 | | | | | |
| | | 126.0 | 0.979 | 9.7 | | | | | |
| | | 131.0 | 0.984 | 7.8 | | | | | |
| | | 136.0 | 0.987 | 6.5 | | | | | |
| | | 141.0 | 0.991 | 4.4 | | | | | |
| | | 146.0 | 0.992 | 4.0 | | | | | |
| | | 156.0 | 0.996 | 2.2 | | | | | |

| Run | Step edge | y | C | F | Run | Step edge | y | C | F |
|---|---|---|---|---|---|---|---|---|---|
| | | mm | | Hz | | | mm | | Hz |
| 060327b | 8 | 6.0 | 0.015 | 29.5 | 060328a | 9 | 1.0 | 0.018 | 25.9 |
| | | 11.0 | 0.023 | 40.2 | | | 1.5 | 0.021 | 28.6 |
| | | 16.0 | 0.029 | 42.3 | | | 4.0 | 0.032 | 40.1 |
| | | 21.0 | 0.050 | 57.3 | | | 8.0 | 0.041 | 46.4 |
| | | 26.0 | 0.084 | 78.5 | | | 9.0 | 0.046 | 51.0 |
| | | 31.0 | 0.166 | 114.2 | | | 6.0 | 0.039 | 42.8 |
| | | 36.0 | 0.291 | 147.6 | | | 11.0 | 0.056 | 57.1 |
| | | 41.0 | 0.490 | 158.8 | | | 13.0 | 0.056 | 54.0 |
| | | 46.0 | 0.637 | 133.4 | | | 18.0 | 0.084 | 74.0 |
| | | 51.0 | 0.761 | 99.4 | | | 19.0 | 0.092 | 77.4 |
| | | 56.0 | 0.840 | 72.3 | | | 21.0 | 0.129 | 98.0 |
| | | 61.0 | 0.885 | 52.7 | | | 23.0 | 0.115 | 93.3 |
| | | 66.0 | 0.922 | 36.6 | | | 26.0 | 0.237 | 131.2 |
| | | 71.0 | 0.929 | 31.8 | | | 31.0 | 0.392 | 144.9 |
| | | 76.0 | 0.948 | 24.9 | | | 36.0 | 0.506 | 135.9 |
| | | 81.0 | 0.958 | 20.6 | | | 41.0 | 0.614 | 120.7 |
| | | 86.0 | 0.964 | 16.8 | | | 46.0 | 0.694 | 101.8 |
| | | 91.0 | 0.975 | 12.5 | | | 51.0 | 0.753 | 85.6 |
| | | 96.0 | 0.979 | 10.9 | | | 56.0 | 0.782 | 78.5 |
| | | 101.0 | 0.981 | 9.7 | | | 61.0 | 0.818 | 68.9 |
| | | 106.0 | 0.985 | 7.2 | | | 66.0 | 0.841 | 62.6 |
| | | 111.0 | 0.986 | 6.9 | | | 71.0 | 0.865 | 55.5 |
| | | 116.0 | 0.991 | 5.2 | | | 76.0 | 0.881 | 49.8 |
| | | 121.0 | 0.993 | 3.7 | | | 81.0 | 0.907 | 42.2 |
| | | 126.0 | 0.994 | 3.6 | | | 86.0 | 0.916 | 37.0 |
| | | 131.0 | 0.995 | 3.3 | | | 91.0 | 0.928 | 33.6 |

| | | | | | |
|---|---|---|---|---|---|
| 136.0 | 0.997 | 1.9 | 96.0 | 0.942 | 28.3 |
| 49.0 | 0.725 | 113.3 | 101.0 | 0.956 | 22.6 |
| 54.0 | 0.824 | 78.5 | 106.0 | 0.962 | 20.4 |
| 59.0 | 0.881 | 55.2 | 111.0 | 0.972 | 14.8 |
| 64.0 | 0.904 | 43.4 | 116.0 | 0.979 | 11.8 |
| 69.0 | 0.931 | 32.0 | 121.0 | 0.984 | 9.0 |
| 34.0 | 0.254 | 147.6 | 126.0 | 0.985 | 8.5 |
| 39.0 | 0.414 | 166.4 | 131.0 | 0.990 | 6.1 |
| 44.0 | 0.576 | 153.8 | 136.0 | 0.991 | 5.6 |
| | | | 141.0 | 0.993 | 4.5 |

| Run | Step edge | y | C | F |
|---|---|---|---|---|
| | | mm | | Hz |
| 060328b | 10 | 1.0 | 0.007 | 17.4 |
| | | 2.0 | 0.009 | 21.2 |
| | | 4.0 | 0.013 | 29.4 |
| | | 6.0 | 0.019 | 36.9 |
| | | 9.0 | 0.022 | 39.9 |
| | | 11.0 | 0.024 | 42.4 |
| | | 13.0 | 0.028 | 44.8 |
| | | 16.0 | 0.030 | 46.9 |
| | | 19.0 | 0.043 | 56.8 |
| | | 21.0 | 0.051 | 63.5 |
| | | 23.0 | 0.064 | 73.6 |
| | | 26.0 | 0.101 | 94.0 |
| | | 31.0 | 0.202 | 141.2 |
| | | 36.0 | 0.349 | 173.1 |
| | | 41.0 | 0.528 | 163.3 |
| | | 46.0 | 0.684 | 134.5 |
| | | 51.0 | 0.801 | 95.2 |
| | | 56.0 | 0.883 | 60.6 |
| | | 61.0 | 0.927 | 38.4 |
| | | 66.0 | 0.947 | 29.0 |
| | | 71.0 | 0.961 | 21.1 |
| | | 76.0 | 0.968 | 18.6 |
| | | 81.0 | 0.976 | 14.1 |
| | | 86.0 | 0.982 | 11.3 |
| | | 91.0 | 0.984 | 9.7 |
| | | 96.0 | 0.988 | 7.6 |
| | | 101.0 | 0.988 | 7.8 |
| | | 106.0 | 0.991 | 6.0 |
| | | 111.0 | 0.994 | 4.5 |
| | | 116.0 | 0.994 | 4.2 |
| | | 121.0 | 0.995 | 3.3 |
| | | 131.0 | 0.996 | 2.7 |
| | | 126.0 | 0.995 | 3.2 |
| | | 136.0 | 0.997 | 1.9 |
| | | 141.0 | 0.998 | 1.6 |

## F.2 Experimental data for $d_C/h = 1.15$

| | |
|---|---|
| Location : | The University of Queensland (Australia) |
| Date : | April-June 2006 |

| | |
|---|---|
| Experiments by : | G. CAROSI |
| Data processing by: | G. CAROSI and H. CHANSON |
| Data analysis by : | H. CHANSON and G. CAROSI |
| Experiment characteristics : | Channel: width: 1.0 m, slope: 21.8º, h = 0.10 m, l = 0.25 m, 10 identical steps. Open channel with perspex sidewalls and smooth marine plywood staircase invert.<br>$Q_w$ = 0.1164 $m^3$/s, $d_c$ = 0.115 m, Re = 4.6 E+5 |
| Instrumentation : | Single-tip conductivity probe (∅ = 0.35 mm).<br>Scan rate: 20 kHz per probe sensor, Sampling duration: 45 sec. |
| Comments : | Inflow conditions : broad-crested weir.<br>Inception of free-surface aeration: between step edges 6 to 7. |

| Run | Step edge | y | C | F | Run | Step edge | y | C | F |
|---|---|---|---|---|---|---|---|---|---|
| | | mm | | Hz | | | mm | | Hz |
| 060410a | 7 | 1.5 | 0.023 | 41.2 | 060410b | 8 | 1.5 | 0.010 | 28.0 |
| | | 6.5 | 0.039 | 54.2 | | | 6.5 | 0.022 | 43.8 |
| | | 11.5 | 0.045 | 55.9 | | | 9.5 | 0.031 | 53.7 |
| | | 12.5 | 0.046 | 57.0 | | | 11.5 | 0.030 | 53.2 |
| | | 13.5 | 0.047 | 58.7 | | | 13.5 | 0.033 | 56.8 |
| | | 16.5 | 0.058 | 63.2 | | | 16.5 | 0.036 | 56.7 |
| | | 19.5 | 0.078 | 75.2 | | | 19.5 | 0.039 | 59.3 |
| | | 21.5 | 0.086 | 82.3 | | | 21.5 | 0.044 | 63.8 |
| | | 26.5 | 0.173 | 118.0 | | | 26.5 | 0.069 | 82.5 |
| | | 31.5 | 0.286 | 147.9 | | | 31.5 | 0.129 | 116.2 |
| | | 36.5 | 0.427 | 161.9 | | | 36.5 | 0.226 | 151.1 |
| | | 41.5 | 0.573 | 150.0 | | | 41.5 | 0.452 | 177.8 |
| | | 46.5 | 0.687 | 130.8 | | | 46.5 | 0.574 | 173.2 |
| | | 51.5 | 0.759 | 106.8 | | | 51.5 | 0.699 | 138.5 |
| | | 56.5 | 0.791 | 90.4 | | | 56.5 | 0.815 | 99.1 |
| | | 61.5 | 0.833 | 75.4 | | | 61.5 | 0.879 | 68.1 |
| | | 66.5 | 0.866 | 62.9 | | | 66.5 | 0.915 | 49.9 |
| | | 71.5 | 0.886 | 55.8 | | | 71.5 | 0.930 | 41.0 |
| | | 76.5 | 0.907 | 47.5 | | | 76.5 | 0.950 | 29.7 |
| | | 81.5 | 0.926 | 38.2 | | | 81.5 | 0.959 | 24.7 |
| | | 86.5 | 0.932 | 35.4 | | | 86.5 | 0.965 | 20.7 |
| | | 91.5 | 0.940 | 32.0 | | | 91.5 | 0.978 | 14.7 |
| | | 96.5 | 0.960 | 23.1 | | | 96.5 | 0.980 | 13.0 |
| | | 101.5 | 0.966 | 19.7 | | | 101.5 | 0.986 | 8.9 |
| | | 106.5 | 0.971 | 16.4 | | | 106.5 | 0.989 | 7.3 |
| | | 111.5 | 0.980 | 11.8 | | | 111.5 | 0.990 | 6.1 |
| | | 116.5 | 0.986 | 8.7 | | | 116.5 | 0.992 | 5.6 |
| | | 121.5 | 0.986 | 8.6 | | | 121.5 | 0.995 | 3.9 |
| | | 126.5 | 0.987 | 7.5 | | | 126.5 | 0.996 | 3.1 |
| | | 131.5 | 0.991 | 5.3 | | | 131.5 | 0.996 | 3.1 |
| | | 131.5 | 0.993 | 4.2 | | | 131.5 | 0.997 | 2.0 |
| | | 136.5 | 0.994 | 3.9 | | | 136.5 | 0.998 | 1.7 |
| | | 141.5 | 0.995 | 3.3 | | | 141.5 | 0.998 | 1.8 |
| | | 146.5 | 0.995 | 3.1 | | | 146.5 | 0.998 | 1.4 |
| | | 151.5 | 0.996 | 2.8 | | | 151.5 | 0.999 | 0.7 |

| Run | Step edge | y | C | F | Run | Step edge | y | C | F |
|---|---|---|---|---|---|---|---|---|---|
| | | mm | | Hz | | | mm | | Hz |

| | | | | | | | | | |
|---|---|---|---|---|---|---|---|---|---|
| 060410c | 9 | 1.5 | 0.032 | 57.6 | 060411a | 10 | 2.0 | 0.021 | 47.8 |
| | | 6.5 | 0.037 | 62.4 | | | 7.0 | 0.035 | 68.2 |
| | | 9.5 | 0.044 | 64.8 | | | 10.0 | 0.039 | 71.0 |
| | | 11.5 | 0.049 | 70.5 | | | 12.0 | 0.041 | 71.8 |
| | | 16.5 | 0.056 | 74.2 | | | 14.0 | 0.044 | 69.3 |
| | | 19.5 | 0.069 | 83.9 | | | 17.0 | 0.045 | 76.9 |
| | | 20.5 | 0.072 | 82.5 | | | 20.0 | 0.054 | 82.3 |
| | | 21.5 | 0.081 | 90.4 | | | 22.0 | 0.069 | 94.9 |
| | | 26.5 | 0.132 | 115.0 | | | 27.0 | 0.106 | 122.8 |
| | | 31.5 | 0.226 | 149.4 | | | 32.0 | 0.182 | 156.9 |
| | | 36.5 | 0.373 | 177.8 | | | 37.0 | 0.327 | 194.9 |
| | | 41.5 | 0.524 | 165.7 | | | 42.0 | 0.515 | 194.0 |
| | | 46.5 | 0.662 | 142.4 | | | 47.0 | 0.636 | 171.6 |
| | | 51.5 | 0.768 | 109.2 | | | 52.0 | 0.798 | 120.3 |
| | | 56.5 | 0.825 | 90.7 | | | 57.0 | 0.874 | 79.4 |
| | | 56.5 | 0.867 | 71.2 | | | 62.0 | 0.910 | 56.5 |
| | | 61.5 | 0.887 | 61.3 | | | 67.0 | 0.933 | 44.0 |
| | | 66.5 | 0.917 | 48.3 | | | 72.0 | 0.955 | 32.5 |
| | | 71.5 | 0.949 | 33.2 | | | 77.0 | 0.961 | 28.2 |
| | | 76.5 | 0.957 | 28.6 | | | 82.0 | 0.965 | 22.4 |
| | | 81.5 | 0.968 | 21.5 | | | 87.0 | 0.973 | 20.5 |
| | | 86.5 | 0.977 | 16.6 | | | 92.0 | 0.981 | 16.7 |
| | | 91.5 | 0.976 | 16.6 | | | 97.0 | 0.987 | 11.2 |
| | | 96.5 | 0.985 | 12.0 | | | 102.0 | 0.988 | 10.1 |
| | | 101.5 | 0.986 | 11.0 | | | 107.0 | 0.993 | 4.8 |
| | | 111.5 | 0.990 | 7.1 | | | 112.0 | 0.993 | 6.4 |
| | | 116.5 | 0.993 | 5.6 | | | 117.0 | 0.996 | 3.7 |
| | | 121.5 | 0.995 | 4.1 | | | 122.0 | 0.995 | 3.6 |
| | | 126.5 | 0.996 | 3.5 | | | 127.0 | 0.997 | 2.9 |
| | | 131.5 | 0.996 | 2.9 | | | 132.0 | 0.998 | 2.3 |
| | | 131.5 | 0.997 | 2.4 | | | 132.0 | 0.999 | 1.4 |
| | | 136.5 | 0.998 | 1.6 | | | 137.0 | 0.998 | 1.2 |
| | | 141.5 | 0.999 | 1.4 | | | 142.0 | 0.998 | 1.9 |
| | | 146.5 | 0.999 | 0.8 | | | 147.0 | 0.999 | 1.4 |
| | | | | | | | 152.0 | 0.999 | 1.2 |

| | |
|---|---|
| Location : | The University of Queensland (Australia) |
| Date : | April-June 2006 |
| Experiments by : | G. CAROSI |
| Data processing by: | G. CAROSI and H. CHANSON |
| Data analysis by : | H. CHANSON and G. CAROSI |
| Experiment characteristics : | Channel: width: 1.0 m, slope: 21.8º, h = 0.10 m, l = 0.25 m, 10 identical steps. Open channel with perspex sidewalls and smooth marine plywood staircase invert.<br>$Q_W$ = 0.1164 $m^3$/s, $d_C$ = 0.115 m, Re = 4.6 E+5 |
| Instrumentation : | Double-tip conductivity probe (∅ = 0.25 mm, Δx = 7.0 mm).<br>Scan rate: 20 kHz per probe sensor, Sampling duration: 45 sec. |
| Comments : | Inflow conditions : broad-crested weir.<br>Inception of free-surface aeration: between step edges 6 to 7. |

| Run | Step edge | y | V | C | F | Tu u'/V |
|---|---|---|---|---|---|---|
| | | mm | m/s | | Hz | |
| 060530a | 10 | 2.0 | 2.75 | 0.062 | 114.9 | -- |

| | | | | |
|---|---|---|---|---|
| 7.0 | 2.80 | 0.061 | 108.8 | 0.56 |
| 12.0 | 2.92 | 0.065 | 108.8 | 0.65 |
| 14.0 | 2.92 | 0.061 | 104.7 | 0.89 |
| 17.0 | 3.04 | 0.062 | 103.2 | 0.54 |
| 20.0 | 3.11 | 0.100 | 138.1 | 0.30 |
| 22.0 | 3.18 | 0.104 | 139.4 | -- |
| 27.0 | 3.18 | 0.152 | 165.1 | 0.86 |
| 32.0 | 3.18 | 0.373 | 177.8 | 1.25 |
| 37.0 | 3.18 | 0.551 | 177.8 | 1.62 |
| 42.0 | 3.18 | 0.640 | 177.8 | 1.02 |
| 47.0 | 3.11 | 0.763 | 146.4 | 1.53 |
| 52.0 | 3.11 | 0.855 | 100.2 | 1.37 |
| 57.0 | 3.18 | 0.908 | 68.2 | 0.93 |
| 62.0 | 3.26 | 0.925 | 55.3 | 0.54 |
| 67.0 | 3.26 | 0.943 | 42.0 | 0.64 |
| 72.0 | 3.26 | 0.954 | 34.5 | 0.65 |
| 77.0 | 3.18 | 0.966 | 25.1 | 0.67 |
| 82.0 | 3.18 | 0.973 | 22.4 | 0.63 |
| 87.0 | 3.26 | 0.981 | 15.8 | 0.48 |
| 92.0 | 3.18 | 0.985 | 12.4 | 0.57 |
| 97.0 | 3.11 | 0.987 | 10.9 | 0.56 |
| 102.0 | 3.33 | 0.991 | 8.0 | 0.35 |
| 107.0 | 3.26 | 0.992 | 6.6 | 0.55 |
| 112.0 | 3.18 | 0.994 | 5.7 | -- |
| 117.0 | 3.11 | 0.995 | 4.7 | -- |
| 122.0 | 3.11 | 0.996 | 3.6 | -- |
| 127.0 | 2.98 | 0.997 | 2.9 | -- |
| 132.0 | 3.26 | 0.997 | 2.6 | -- |
| 137.0 | 3.33 | 0.998 | 1.7 | -- |
| 137.0 | 3.33 | 0.998 | 1.5 | -- |
| 142.0 | 3.33 | 0.999 | 1.3 | -- |
| 147.0 | 3.26 | 0.999 | 1.0 | -- |
| 152.0 | 4.00 | 0.999 | 1.0 | -- |

## F.3 Experimental data for $d_C/h = 1.33$

| | |
|---|---|
| Location : | The University of Queensland (Australia) |
| Date : | April-June 2006 |
| Experiments by : | G. CAROSI |
| Data processing by: | G. CAROSI and H. CHANSON |
| Data analysis by : | H. CHANSON and G. CAROSI |
| Experiment characteristics : | Channel: width: 1.0 m, slope: 21.8º, h = 0.10 m, l = 0.25 m, 10 identical steps. Open channel with perspex sidewalls and smooth marine plywood staircase invert.<br>$Q_W$ = 0.1431 $m^3/s$, $d_C$ = 0.133 m, Re = 5.7 E+5 |
| Instrumentation : | Double-tip conductivity probe (∅ = 0.25 mm, Δx = 7.0 mm).<br>Scan rate: 20 kHz per probe sensor, Sampling duration: 45 sec. |
| Comments : | Inflow conditions : broad-crested weir.<br>Inception of free-surface aeration: between step edges 6 to 7. |

| Run | Step edge | y | V | C | F | Tu u'/V |
|---|---|---|---|---|---|---|
| | | mm | m/s | | Hz | |
| 060614a | 7 | 1.0 | 2.50 | 0.039 | 54.3 | 0.72 |

| | | | | | | |
|---|---|---|---|---|---|---|
| | | 6.0 | 2.55 | 0.046 | 54.1 | 0.87 |
| | | 9.0 | 2.64 | 0.058 | 60.7 | 0.97 |
| | | 11.0 | 2.75 | 0.047 | 52.1 | 0.87 |
| | | 13.0 | 2.80 | 0.049 | 54.6 | 0.71 |
| | | 16.0 | 2.86 | 0.070 | 69.6 | 0.74 |
| | | 19.0 | 2.80 | 0.067 | 61.2 | 0.80 |
| | | 21.0 | 2.92 | 0.055 | 50.3 | 0.70 |
| | | 26.0 | 3.11 | 0.078 | 55.6 | 0.75 |
| | | 31.0 | 3.26 | 0.142 | 76.2 | 0.88 |
| | | 36.0 | 3.26 | 0.243 | 95.7 | -- |
| | | 41.0 | 3.33 | 0.449 | 118.4 | 1.06 |
| | | 46.0 | 3.33 | 0.614 | 111.6 | 1.12 |
| | | 51.0 | 3.33 | 0.737 | 93.4 | 0.97 |
| | | 56.0 | 3.26 | 0.812 | 72.8 | 0.76 |
| | | 61.0 | 3.33 | 0.892 | 47.8 | 0.61 |
| | | 66.0 | 3.26 | 0.891 | 52.5 | 0.50 |
| | | 71.0 | 3.33 | 0.949 | 28.2 | 0.50 |
| | | 76.0 | 3.33 | 0.959 | 22.3 | 0.41 |
| | | 81.0 | 3.33 | 0.948 | 27.4 | 0.41 |
| | | 86.0 | 3.42 | 0.965 | 19.2 | 0.37 |
| | | 91.0 | 3.33 | 0.976 | 14.0 | 0.39 |
| | | 96.0 | 3.33 | 0.974 | 14.7 | 0.39 |
| | | 101.0 | 3.26 | 0.983 | 10.6 | 0.47 |
| | | 106.0 | 3.18 | 0.983 | 9.8 | 0.37 |
| | | 111.0 | 3.42 | 0.989 | 6.8 | 0.36 |
| | | 116.0 | 3.18 | 0.990 | 6.3 | 0.39 |
| | | 121.0 | 3.26 | 0.993 | 4.5 | 0.44 |
| | | 126.0 | 3.26 | 0.994 | 3.8 | 0.52 |
| | | 131.0 | 3.18 | 0.995 | 3.0 | 0.30 |
| | | 131.0 | 3.18 | 0.995 | 2.8 | 0.39 |
| | | 136.0 | 3.18 | 0.997 | 2.1 | 0.26 |
| | | 141.0 | 3.26 | 0.997 | 1.8 | -- |
| 060614b | 8 | 1.0 | 2.92 | 0.027 | 50.4 | 0.54 |
| | | 6.0 | 2.92 | 0.030 | 51.1 | 0.53 |
| | | 9.0 | 2.98 | 0.027 | 46.7 | 0.49 |
| | | 11.0 | 2.86 | 0.026 | 43.9 | 0.43 |
| | | 13.0 | 3.11 | 0.033 | 50.6 | 0.51 |
| | | 16.0 | 3.18 | 0.036 | 53.1 | 0.58 |
| | | 19.0 | 3.11 | 0.043 | 61.0 | 0.55 |
| | | 21.0 | 3.11 | 0.047 | 63.8 | 0.55 |
| | | 26.0 | 3.18 | 0.088 | 81.2 | 0.83 |
| | | 31.0 | 3.26 | 0.183 | 121.1 | 1.12 |
| | | 36.0 | 3.26 | 0.340 | 154.6 | -- |
| | | 41.0 | 3.26 | 0.534 | 168.9 | 1.36 |
| | | 46.0 | 3.26 | 0.679 | 143.2 | 1.35 |
| | | 51.0 | 3.26 | 0.795 | 107.7 | 1.00 |
| | | 56.0 | 3.33 | 0.848 | 83.6 | 0.63 |
| | | 61.0 | 3.26 | 0.895 | 61.9 | 0.59 |
| | | 66.0 | 3.33 | 0.920 | 48.2 | 0.57 |
| | | 71.0 | 3.42 | 0.931 | 42.4 | 0.47 |
| | | 76.0 | 3.42 | 0.946 | 33.7 | 0.47 |
| | | 81.0 | 3.42 | 0.947 | 32.4 | 0.53 |
| | | 86.0 | 3.33 | 0.963 | 24.1 | 0.55 |
| | | 91.0 | 3.33 | 0.970 | 19.6 | 0.55 |
| | | 96.0 | 3.33 | 0.974 | 17.1 | 0.48 |
| | | 101.0 | 3.42 | 0.983 | 12.1 | 0.45 |

| | | | | | | |
|---|---|---|---|---|---|---|
| | | 106.0 | 3.42 | 0.983 | 11.4 | 0.41 |
| | | 111.0 | 3.33 | 0.986 | 9.8 | 0.52 |
| | | 116.0 | 3.33 | 0.992 | 5.7 | 0.49 |
| | | 121.0 | 3.33 | 0.993 | 5.3 | 0.40 |
| | | 126.0 | 3.33 | 0.994 | 4.4 | 0.47 |
| | | 131.0 | 3.33 | 0.995 | 3.8 | 0.39 |
| | | 131.0 | 3.26 | 0.996 | 2.8 | 0.47 |
| | | 136.0 | 3.33 | 0.996 | 2.9 | 0.52 |
| | | 141.0 | 3.33 | 0.997 | 1.9 | -- |
| 060615a | 9 | 0.5 | 2.69 | 0.057 | 92.7 | 0.83 |
| | | 5.5 | 2.92 | 0.048 | 74.8 | 0.92 |
| | | 8.5 | 2.80 | 0.072 | 101.9 | 0.84 |
| | | 10.5 | 2.98 | 0.062 | 85.3 | 0.92 |
| | | 12.5 | 2.98 | 0.063 | 83.4 | 0.87 |
| | | 15.5 | 2.98 | 0.070 | 87.5 | 0.89 |
| | | 18.5 | 2.98 | 0.071 | 87.2 | 0.78 |
| | | 20.5 | 3.11 | 0.080 | 91.5 | 0.74 |
| | | 25.5 | 3.11 | 0.101 | 99.8 | 0.86 |
| | | 30.5 | 3.18 | 0.149 | 120.3 | 0.94 |
| | | 35.5 | 3.33 | 0.249 | 152.9 | -- |
| | | 40.5 | 3.33 | 0.377 | 169.1 | 1.31 |
| | | 45.5 | 3.33 | 0.556 | 162.6 | 1.47 |
| | | 50.5 | 3.18 | 0.664 | 143.0 | 1.39 |
| | | 55.5 | 3.26 | 0.766 | 112.4 | 1.03 |
| | | 60.5 | 3.42 | 0.829 | 92.5 | 0.80 |
| | | 65.5 | 3.42 | 0.858 | 81.8 | 0.94 |
| | | 70.5 | 3.42 | 0.902 | 60.8 | 0.61 |
| | | 75.5 | 3.33 | 0.910 | 52.6 | 0.71 |
| | | 80.5 | 3.42 | 0.933 | 43.7 | 0.55 |
| | | 85.5 | 3.42 | 0.946 | 33.4 | 0.58 |
| | | 90.5 | 3.42 | 0.961 | 26.1 | 0.53 |
| | | 95.5 | 3.50 | 0.968 | 22.4 | 0.44 |
| | | 100.5 | 3.33 | 0.975 | 18.4 | 0.60 |
| | | 105.5 | 3.33 | 0.982 | 13.4 | 0.63 |
| | | 110.5 | 3.42 | 0.986 | 10.1 | 0.47 |
| | | 115.5 | 3.33 | 0.990 | 7.7 | 0.50 |
| | | 120.5 | 3.50 | 0.991 | 6.7 | 0.56 |
| | | 125.5 | 3.42 | 0.994 | 4.5 | 0.39 |
| | | 130.5 | 3.42 | 0.996 | 3.5 | 0.55 |
| | | 130.5 | 3.50 | 0.997 | 2.5 | 0.42 |
| | | 135.5 | 3.59 | 0.997 | 1.9 | -- |
| | | 140.5 | 3.78 | 0.998 | 1.6 | -- |
| 060615b | 10 | 1.5 | 2.75 | 0.042 | 87.7 | -- |
| | | 6.5 | 2.80 | 0.053 | 98.4 | -- |
| | | 9.5 | 3.11 | 0.052 | 94.3 | 0.69 |
| | | 11.5 | 2.98 | 0.048 | 88.0 | 0.53 |
| | | 13.5 | 2.98 | 0.052 | 90.0 | 0.57 |
| | | 16.5 | 3.11 | 0.055 | 89.8 | 0.50 |
| | | 19.5 | 3.26 | 0.063 | 102.0 | -- |
| | | 26.5 | 3.26 | 0.081 | 110.8 | 0.64 |
| | | 31.5 | 3.26 | 0.126 | 145.3 | 0.75 |
| | | 36.5 | 3.42 | 0.187 | 166.8 | 1.18 |
| | | 41.5 | 3.42 | 0.410 | 199.7 | 1.77 |
| | | 46.5 | 3.33 | 0.571 | 199.2 | 1.79 |
| | | 51.5 | 3.33 | 0.678 | 161.2 | 1.94 |
| | | 56.5 | 3.42 | 0.814 | 112.5 | 1.32 |

| | | | | |
|---|---|---|---|---|
| 61.5 | 3.42 | 0.886 | 76.8 | 1.07 |
| 66.5 | 3.42 | 0.924 | 51.0 | 0.80 |
| 71.5 | 3.50 | 0.944 | 38.8 | 0.71 |
| 76.5 | 3.50 | 0.955 | 31.8 | 0.71 |
| 81.5 | 3.59 | 0.967 | 23.7 | 0.68 |
| 86.5 | 3.50 | 0.974 | 20.0 | 0.85 |
| 91.5 | 3.42 | 0.981 | 15.6 | 0.48 |
| 96.5 | 3.50 | 0.985 | 12.3 | 0.49 |
| 101.5 | 3.50 | 0.989 | 8.3 | 0.51 |
| 106.5 | 3.50 | 0.991 | 7.1 | 0.49 |
| 111.5 | 3.50 | 0.993 | 5.5 | 0.61 |
| 116.5 | 3.50 | 0.995 | 4.4 | 0.50 |
| 121.5 | 3.59 | 0.995 | 4.0 | 0.45 |
| 126.5 | 3.59 | 0.997 | 2.8 | 0.47 |
| 131.5 | 3.59 | 0.996 | 2.7 | 0.17 |
| 136.5 | 3.42 | 0.998 | 1.6 | 1.15 |
| 141.5 | 3.59 | 0.999 | 1.2 | -- |
| 146.5 | 3.78 | 0.999 | 1.4 | -- |
| 151.5 | 3.42 | 0.999 | 1.0 | -- |

## F.4 Experimental data for $d_C/h = 1.45$

| | |
|---|---|
| Location : | The University of Queensland (Australia) |
| Date : | April-June 2006 |
| Experiments by : | G. CAROSI |
| Data processing by: | G. CAROSI and H. CHANSON |
| Data analysis by : | H. CHANSON and G. CAROSI |
| Experiment characteristics : | Channel: width: 1.0 m, slope: 21.8º, h = 0.10 m, l = 0.25 m, 10 identical steps. Open channel with perspex sidewalls and smooth marine plywood staircase invert.<br>$Q_W$ = 0.1612 $m^3/s$, $d_C$ = 0.145 m, Re = 6.4 E+5 |
| Instrumentation : | Single-tip conductivity probe (∅ = 0.35 mm).<br>Scan rate: 20 kHz per probe sensor, Sampling duration: 45 sec. |
| Comments : | Inflow conditions : broad-crested weir.<br>Inception of free-surface aeration: between step edges 7 to 8. |

| Run | Step edge | y | C | F | Run | Step edge | y | C | F |
|---|---|---|---|---|---|---|---|---|---|
| | | mm | | Hz | | | mm | | Hz |
| 060512a | 8 | 1.5 | 0.001 | 3.2 | 060512b | 9 | 1.5 | 0.013 | 26.3 |
| | | 6.5 | 0.003 | 6.1 | | | 6.5 | 0.025 | 38.4 |
| | | 9.5 | 0.004 | 7.5 | | | 9.5 | 0.027 | 37.8 |
| | | 11.5 | 0.003 | 6.5 | | | 11.5 | 0.031 | 39.9 |
| | | 13.5 | 0.006 | 10.0 | | | 13.5 | 0.031 | 39.5 |
| | | 16.5 | 0.005 | 9.0 | | | 16.5 | 0.038 | 44.5 |
| | | 19.5 | 0.007 | 11.8 | | | 19.5 | 0.037 | 43.8 |
| | | 21.5 | 0.009 | 13.0 | | | 21.5 | 0.042 | 45.8 |
| | | 26.5 | 0.013 | 16.7 | | | 26.5 | 0.059 | 55.6 |
| | | 31.5 | 0.027 | 27.4 | | | 31.5 | 0.091 | 72.7 |
| | | 36.5 | 0.068 | 48.6 | | | 36.5 | 0.159 | 100.5 |
| | | 41.5 | 0.171 | 84.6 | | | 41.5 | 0.276 | 131.6 |
| | | 46.5 | 0.345 | 121.0 | | | 46.5 | 0.411 | 142.7 |
| | | 51.5 | 0.512 | 129.4 | | | 51.5 | 0.562 | 135.0 |
| | | 56.5 | 0.669 | 119.1 | | | 56.5 | 0.666 | 117.8 |

| | | | | | |
|---|---|---|---|---|---|
| 61.5 | 0.799 | 86.0 | 61.5 | 0.753 | 100.5 |
| 66.5 | 0.852 | 70.4 | 66.5 | 0.811 | 82.9 |
| 71.5 | 0.889 | 56.5 | 71.5 | 0.858 | 67.2 |
| 76.5 | 0.907 | 46.9 | 76.5 | 0.886 | 54.3 |
| 81.5 | 0.930 | 37.4 | 81.5 | 0.917 | 45.8 |
| 86.5 | 0.949 | 28.1 | 86.5 | 0.929 | 38.1 |
| 91.5 | 0.959 | 24.3 | 91.5 | 0.943 | 31.7 |
| 96.5 | 0.956 | 25.3 | 96.5 | 0.963 | 23.6 |
| 101.5 | 0.972 | 17.3 | 101.5 | 0.970 | 19.4 |
| 106.5 | 0.976 | 14.3 | 106.5 | 0.980 | 14.0 |
| 111.5 | 0.983 | 10.7 | 111.5 | 0.980 | 13.6 |
| 116.5 | 0.985 | 10.2 | 116.5 | 0.983 | 11.8 |
| 121.5 | 0.990 | 6.8 | 121.5 | 0.988 | 8.3 |
| 126.5 | 0.992 | 6.4 | 126.5 | 0.990 | 7.0 |
| 131.5 | 0.991 | 6.5 | 131.5 | 0.991 | 6.2 |
| 131.5 | 0.994 | 4.0 | 131.5 | 0.994 | 4.2 |
| 136.5 | 0.995 | 3.3 | 136.5 | 0.996 | 2.6 |
| 141.5 | 0.997 | 2.7 | 141.5 | 0.997 | 3.0 |
| 146.5 | 0.997 | 2.1 | 146.5 | 0.997 | 2.2 |
| | | | 151.5 | 0.998 | 1.8 |

| Run | Step edge | y | C | F |
|---|---|---|---|---|
| | | mm | | Hz |
| 060511b | 10 | 2.0 | 0.008 | 20.8 |
| | | 7.0 | 0.012 | 27.9 |
| | | 10.0 | 0.015 | 30.2 |
| | | 12.0 | 0.013 | 25.6 |
| | | 14.0 | 0.017 | 31.2 |
| | | 17.0 | 0.018 | 32.8 |
| | | 20.0 | 0.025 | 37.5 |
| | | 22.0 | 0.024 | 37.5 |
| | | 27.0 | 0.030 | 43.7 |
| | | 32.0 | 0.055 | 61.7 |
| | | 37.0 | 0.092 | 81.6 |
| | | 42.0 | 0.211 | 130.5 |
| | | 47.0 | 0.306 | 147.4 |
| | | 52.0 | 0.536 | 157.9 |
| | | 57.0 | 0.655 | 137.6 |
| | | 62.0 | 0.775 | 107.2 |
| | | 67.0 | 0.858 | 76.4 |
| | | 72.0 | 0.904 | 54.3 |
| | | 77.0 | 0.927 | 43.1 |
| | | 82.0 | 0.940 | 35.8 |
| | | 87.0 | 0.962 | 24.7 |
| | | 92.0 | 0.969 | 19.8 |
| | | 97.0 | 0.977 | 16.0 |
| | | 102.0 | 0.981 | 13.2 |
| | | 107.0 | 0.987 | 9.8 |
| | | 112.0 | 0.990 | 7.8 |
| | | 117.0 | 0.992 | 6.2 |
| | | 122.0 | 0.994 | 4.8 |
| | | 127.0 | 0.996 | 3.4 |
| | | 132.0 | 0.997 | 2.7 |
| | | 132.0 | 0.997 | 2.2 |
| | | 137.0 | 0.997 | 2.1 |

| | | |
|---|---|---|
| 142.0 | 0.998 | 1.8 |
| 147.0 | 0.998 | 1.6 |
| 152.0 | 0.999 | 1.1 |

| | |
|---|---|
| Location : | The University of Queensland (Australia) |
| Date : | April-June 2006 |
| Experiments by : | G. CAROSI |
| Data processing by: | G. CAROSI and H. CHANSON |
| Data analysis by : | H. CHANSON and G. CAROSI |
| Experiment characteristics : | Channel: width: 1.0 m, slope: 21.8º, h = 0.10 m, l = 0.25 m, 10 identical steps. Open channel with perspex sidewalls and smooth marine plywood staircase invert.<br>$Q_W$ = 0.1612 $m^3$/s, $d_C$ = 0.145 m, Re = 6.4 E+5 |
| Instrumentation : | Double-tip conductivity probe (∅ = 0.25 mm, Δx = 7.0 mm).<br>Scan rate: 20 kHz per probe sensor, Sampling duration: 45 sec. |
| Comments : | Inflow conditions : broad-crested weir.<br>Inception of free-surface aeration: between step edges 7 to 8. |

| Run | Step edge | y | V | C | F | Tu u'/V |
|---|---|---|---|---|---|---|
| | | mm | m/s | | Hz | |
| 060530b | 10 | 2.0 | 3.42 | 0.007 | 17.5 | 0.51 |
| | | 7.0 | 3.18 | 0.010 | 21.8 | 0.56 |
| | | 10.0 | 3.42 | 0.011 | 23.5 | -- |
| | | 12.0 | 3.42 | 0.013 | 26.5 | 0.47 |
| | | 14.0 | 3.50 | 0.017 | 29.6 | 0.62 |
| | | 17.0 | 3.50 | 0.030 | 52.4 | 0.60 |
| | | 20.0 | 3.42 | 0.027 | 48.2 | 0.58 |
| | | 22.0 | 3.50 | 0.030 | 50.0 | 0.60 |
| | | 27.0 | 3.50 | 0.041 | 58.9 | 0.57 |
| | | 32.0 | 3.68 | 0.068 | 81.6 | 0.73 |
| | | 37.0 | 3.68 | 0.124 | 107.1 | 0.95 |
| | | 42.0 | 3.68 | 0.196 | 133.1 | 1.34 |
| | | 47.0 | 3.68 | 0.348 | 165.9 | 1.83 |
| | | 52.0 | 3.68 | 0.521 | 168.9 | 1.57 |
| | | 57.0 | 3.68 | 0.715 | 136.8 | 1.32 |
| | | 62.0 | 3.68 | 0.790 | 113.1 | 1.14 |
| | | 67.0 | 3.59 | 0.858 | 83.6 | 0.92 |
| | | 72.0 | 3.59 | 0.913 | 57.0 | 0.68 |
| | | 77.0 | 3.59 | 0.935 | 44.2 | 1.89 |
| | | 82.0 | 3.59 | 0.951 | 36.5 | 0.55 |
| | | 87.0 | 3.59 | 0.965 | 27.7 | 0.53 |
| | | 92.0 | 3.59 | 0.976 | 20.2 | 0.47 |
| | | 97.0 | 3.59 | 0.980 | 16.5 | 0.50 |
| | | 102.0 | 3.59 | 0.982 | 13.9 | 0.47 |
| | | 107.0 | 3.68 | 0.989 | 9.9 | 0.33 |
| | | 112.0 | 3.68 | 0.990 | 8.1 | 0.41 |
| | | 117.0 | 3.59 | 0.992 | 6.9 | 0.40 |
| | | 122.0 | 3.59 | 0.995 | 4.8 | 0.11 |
| | | 127.0 | 3.68 | 0.995 | 4.0 | -- |
| | | 132.0 | 3.59 | 0.995 | 4.3 | -- |
| | | 132.0 | 3.68 | 0.997 | 2.9 | -- |
| | | 137.0 | 3.78 | 0.997 | 2.6 | -- |
| | | 142.0 | 3.59 | 0.998 | 1.8 | -- |
| | | 147.0 | 3.78 | 0.998 | 1.7 | -- |

| | | | | |
|---|---|---|---|---|
| 152.0 | 3.68 | 0.999 | 1.0 | -- |

## F.5 Experimental data for $d_C/h = 1.57$

| | |
|---|---|
| Location : | The University of Queensland (Australia) |
| Date : | April-June 2006 |
| Experiments by : | G. CAROSI |
| Data processing by: | G. CAROSI and H. CHANSON |
| Data analysis by : | H. CHANSON and G. CAROSI |
| Experiment characteristics : | Channel: width: 1.0 m, slope: 21.8º, h = 0.10 m, l = 0.25 m, 10 identical steps. Open channel with perspex sidewalls and smooth marine plywood staircase invert.<br>$Q_W$ = 0.1798 $m^3/s$, $d_C$ = 0.157 m, Re = 7.1 E+5 |
| Instrumentation : | Single-tip conductivity probe (∅ = 0.35 mm).<br>Scan rate: 20 kHz per probe sensor, Sampling duration: 45 sec. |
| Comments : | Inflow conditions : broad-crested weir.<br>Inception of free-surface aeration: between step edges 7 and 8. |

| Run | Step edge | y | C | F | Run | Step edge | y | C | F |
|---|---|---|---|---|---|---|---|---|---|
| | | mm | | Hz | | | mm | | Hz |
| 060404a | 8 | 1.0 | 0.004 | 3.8 | 060404b | 9 | 1.0 | 0.003 | 8.0 |
| | | 6.0 | 0.000 | 1.0 | | | 6.0 | 0.012 | 19.2 |
| | | 9.0 | 0.001 | 1.6 | | | 9.0 | 0.015 | 20.7 |
| | | 11.0 | 0.001 | 1.6 | | | 11.0 | 0.014 | 19.6 |
| | | 13.0 | 0.003 | 3.5 | | | 13.0 | 0.010 | 15.0 |
| | | 16.0 | 0.005 | 4.7 | | | 16.0 | 0.013 | 17.6 |
| | | 19.0 | 0.002 | 2.8 | | | 19.0 | 0.011 | 14.5 |
| | | 21.0 | 0.001 | 2.5 | | | 21.0 | 0.009 | 12.9 |
| | | 26.0 | 0.002 | 3.6 | | | 26.0 | 0.014 | 15.6 |
| | | 31.0 | 0.004 | 4.5 | | | 31.0 | 0.023 | 23.9 |
| | | 36.0 | 0.011 | 9.7 | | | 36.0 | 0.046 | 37.0 |
| | | 41.0 | 0.024 | 18.6 | | | 41.0 | 0.102 | 61.6 |
| | | 46.0 | 0.080 | 39.1 | | | 46.0 | 0.178 | 82.2 |
| | | 51.0 | 0.193 | 69.0 | | | 51.0 | 0.344 | 109.1 |
| | | 56.0 | 0.411 | 98.6 | | | 56.0 | 0.457 | 113.9 |
| | | 61.0 | 0.556 | 99.0 | | | 61.0 | 0.618 | 110.4 |
| | | 66.0 | 0.748 | 84.7 | | | 66.0 | 0.720 | 96.9 |
| | | 71.0 | 0.812 | 68.2 | | | 71.0 | 0.796 | 79.6 |
| | | 76.0 | 0.874 | 53.1 | | | 76.0 | 0.840 | 66.7 |
| | | 81.0 | 0.913 | 42.3 | | | 81.0 | 0.873 | 56.1 |
| | | 86.0 | 0.932 | 34.3 | | | 86.0 | 0.897 | 49.8 |
| | | 91.0 | 0.930 | 32.8 | | | 91.0 | 0.926 | 37.2 |
| | | 96.0 | 0.954 | 24.5 | | | 96.0 | 0.955 | 25.1 |
| | | 101.0 | 0.962 | 20.3 | | | 101.0 | 0.956 | 24.6 |
| | | 106.0 | 0.969 | 17.3 | | | 106.0 | 0.974 | 15.7 |
| | | 111.0 | 0.978 | 14.8 | | | 111.0 | 0.979 | 13.7 |
| | | 116.0 | 0.983 | 10.8 | | | 116.0 | 0.983 | 11.4 |
| | | 121.0 | 0.984 | 9.3 | | | 121.0 | 0.990 | 7.4 |
| | | 126.0 | 0.988 | 8.1 | | | 126.0 | 0.991 | 6.2 |
| | | 131.0 | 0.988 | 7.0 | | | 131.0 | 0.993 | 5.2 |
| | | 131.0 | 0.992 | 5.0 | | | 131.0 | 0.994 | 4.2 |
| | | 136.0 | 0.996 | 3.3 | | | 136.0 | 0.996 | 2.9 |
| | | 141.0 | 0.996 | 2.9 | | | 141.0 | 0.997 | 2.4 |

| | | | | | |
|---|---|---|---|---|---|
| 146.0 | 0.997 | 2.2 | 146.0 | 0.997 | 2.2 |
| 151.0 | 0.998 | 1.9 | 151.0 | 0.998 | 1.4 |

| Run | Step edge | y | C | F |
|---|---|---|---|---|
| | | mm | | Hz |
| 060404c | 10 | 1.0 | 0.002 | 7.3 |
| | | 6.0 | 0.006 | 13.5 |
| | | 9.0 | 0.007 | 15.1 |
| | | 11.0 | 0.007 | 13.8 |
| | | 13.0 | 0.007 | 14.9 |
| | | 16.0 | 0.009 | 17.6 |
| | | 19.0 | 0.010 | 18.6 |
| | | 21.0 | 0.013 | 21.7 |
| | | 26.0 | 0.013 | 20.4 |
| | | 31.0 | 0.020 | 27.2 |
| | | 36.0 | 0.044 | 43.6 |
| | | 41.0 | 0.077 | 61.0 |
| | | 46.0 | 0.121 | 82.5 |
| | | 51.0 | 0.222 | 108.9 |
| | | 56.0 | 0.417 | 135.2 |
| | | 61.0 | 0.564 | 131.7 |
| | | 66.0 | 0.687 | 116.1 |
| | | 71.0 | 0.773 | 96.7 |
| | | 76.0 | 0.840 | 74.4 |
| | | 81.0 | 0.880 | 61.0 |
| | | 86.0 | 0.907 | 49.0 |
| | | 91.0 | 0.925 | 44.2 |
| | | 96.0 | 0.950 | 30.1 |
| | | 101.0 | 0.958 | 27.1 |
| | | 106.0 | 0.972 | 20.1 |
| | | 111.0 | 0.979 | 14.5 |
| | | 116.0 | 0.980 | 13.8 |
| | | 121.0 | 0.986 | 10.1 |
| | | 126.0 | 0.988 | 8.1 |
| | | 131.0 | 0.992 | 6.2 |
| | | 131.0 | 0.994 | 4.6 |
| | | 136.0 | 0.995 | 4.0 |
| | | 141.0 | 0.995 | 3.8 |
| | | 146.0 | 0.996 | 2.6 |
| | | 151.0 | 0.997 | 2.3 |

# REFERENCES


AMADOR, A., SANCHEZ-JUNY, M., DOLZ, J., SANCHEZ-TEMBLEQUE, F., and PUERTAS, J. (2004a). "Velocity and Pressure Measurements in Skimming Flow in Stepped Spillways." *Proc. Intl Conf. on Hydraulics of Dams and River Structures*, Tehran, Iran, Balkema Publ., The Netherlands, F. YAZDANDOOST and J. ATTARI Ed., pp. 279-285.

AMADOR, A., VAN DER GRAAF, G., SANCHEZ-JUNY, M., DOLZ, J., SANCHEZ-TEMBLEQUE, F., and PUERTAS, J. (2004b). "Characterization of the Flow Field in a Stepped Spillway by PIV." *Proc. 12th Symp. Applications Laser to Fluid Mechanics*, Lisbon, Portugal, July 12-15, 10 pages.

AMADOR, A., SANCHEZ-JUNY, M., and DOLZ, J. (2006). "DPIV Study of the Turbulent Boundary Layer over V-shaped Cavities." *Proc. Intl Conf. Fluvial Hydraulics River Flow 2006*, Lisbon, Portugal, 6-8 Sept., Topic A1, R.M.L. FERREIRA, E.C.T.L. ALVES, J.G.A.B. LEAL, and A.H. CARDOSO Eds., Balkema Publ., Taylor & Francis Group, London, Vol. 2, pp. 1813-1821.

ANDRE, S., MANSO, P.A., SCHLEISS, A., and BOILLAT, J.L. (2003). "Hydraulic and Stability Criteria for the Rehabilitation of Appurtenant spillway Structures by Alternative Macro-roughness Concrete Linings." *Proc. 21st ICOLD Congress*, Montreal, Canada, Q. 82, R. 6, pp. 63-93.

ANDRE, S., BOILLAT, J.L., SCHLEISS, A.J., and MATOS, J. (2004). "Energy Dissipation and Hydrodynamic Forces of Aerated Flow over Macro-Roughness Linings for Overtopped Embankment Dams." *Proc. Intl Conf. on Hydraulics of Dams and River Structures*, Tehran, Iran, Balkema Publ., The Netherlands, pp. 189-196.

AUGIER, P. (1996). "Contribution à l'Etude et à la Modélisation Mécaniste-Statistique de la Distribution Spatiale des Apports d'Eau sous un Canon d'Irrigation: Application à la Caractérisation des Effets du Vent sur l'Uniformité d'Arrosage." ('Study and Modelling of the Spatial Distribution of Water Supply by an Irrigation Water Jet : Effect of the Wind on the Water supply Uniformity.') *Ph.D. thesis*, ENGREF, Montpellier, France, 247 pages (in French).

BaCaRa (1991). "Etude de la Dissipation d'Energie sur les Evacuateurs à Marches." ('Study of the Energy Dissipation on Stepped Spillways.') *Rapport d'Essais*, Projet National BaCaRa, CEMAGREF-SCP, Aix-en-Provence, France, Oct., 111 pages (in French).

BAKER, R. (1994). "Brushes Clough Wedge Block Spillway - Progress Report No. 3." *SCEL Project Report No. SJ542-4*, University of Salford, UK, Nov., 47 pages.

BARENBLATT, G.I. (1994). "Scaling, Phenomena in Fluid Mechanics. Inaugural Lecture Delivered before the University of Cambridge on 3 May 1993," *Cambridge University Press*, UK, 49 pages.

BARENBLATT, G.I. (1996). "Scaling, Self-Similarity, and Intermediate Asymptotics." *Cambridge University Press*, UK, 386 pages.

BOES, R.M. (2000a). "Zweiphasenstroömung und Energieumsetzung an Grosskaskaden." ('Two-Phase Flow and Energy Dissipation on Cascades.') *Ph.D. thesis*, VAW-ETH, Zürich, Switzerland (in German). (also *Mitteilungen der Versuchsanstalt fur Wasserbau, Hydrologie und Glaziologie*, ETH-Zurich, Switzerland, No. 166).

BOES, R.M. (2000b). "Scale Effects in Modelling Two-Phase Stepped Spillway Flow." *Intl Workshop on Hydraulics of Stepped Spillways*, Zürich, Switzerland, H.E. MINOR & W.H. HAGER Editors, Balkema Publ., pp. 53-60.

BROCCHINI, M., and PEREGRINE, D.H. (2001). "The Dynamics of Strong Turbulence at Free Surfaces. Part 1. Description." *Jl Fluid Mech.*, Vol. 449, pp. 225-254.

CHAMANI, M.R., and RAJARATNAM, N. (1994). "Jet Flow on Stepped Spillways." *Jl of Hyd. Engrg.*, ASCE, Vol. 120, No. 2, pp. 254-259.

CHAMANI, M.R., and RAJARATNAM, N. (1999). "Characteristics of Skimming Flow over Stepped Spillways." *Jl of Hyd. Engrg.*, ASCE, Vol. 125, No. 4, pp. 361-368. Discussion : Vol. 126, No. 11, pp. 860-872. Closure : Vol. 126, No. 11, pp. 872-873.

CHANSON, H. (1994a). "Hydraulics of Nappe Flow Regime above Stepped Chutes and Spillways." *Aust. Civil Engrg Trans.*, I.E.Aust., Vol. CE36, No. 1, Jan., pp. 69-76.

CHANSON, H. (1994b). "Hydraulics of Skimming Flows over Stepped Channels and Spillways." *Jl of Hyd. Res.*, IAHR, Vol. 32, No. 3, pp. 445-460. Discussion : Vol. 33, No. 3, pp. 414-419.

CHANSON, H. (1995a). "Hydraulic Design of Stepped Cascades, Channels, Weirs and Spillways." *Pergamon*, Oxford, UK, Jan., 292 pages (ISBN 0-08-041918-6).

CHANSON, H. (1995b). "Air Bubble Entrainment in Free-surface Turbulent Flows. Experimental Investigations." *Report CH46/95*, Dept. of Civil Engineering, University of Queensland, Australia, June, 368 pages (ISBN 0 86776 611 5).
CHANSON, H. (1997a). "Air Bubble Entrainment in Free-Surface Turbulent Shear Flows." *Academic Press*, London, UK, 401 pages (ISBN 0-12-168110-6).
CHANSON, H. (1997b). "Air Bubble Entrainment in Open Channels. Flow Structure and Bubble Size Distributions." *Intl Jl of Multiphase Flow*, Vol. 23, No. 1, pp. 193-203.
CHANSON, H. (1999a). "The Hydraulics of Open Channel Flows : An Introduction." *Edward Arnold*, London, UK, 512 pages (ISBN 0 340 74067 1).
CHANSON, H. (1999b). "Turbulent Open-Channel Flows : Drop-Generation and Self-Aeration. Discussion." *Jl of Hyd. Engrg.*, ASCE, Vol. 125, No. 6, pp. 668-670.
CHANSON, H. (2001a). "The Hydraulics of Stepped Chutes and Spillways." *Balkema*, Lisse, The Netherlands, 418 pages (ISBN 90 5809 352 2).
CHANSON, H. (2001b). "A Transition Flow Regime on Stepped Spillways ? The Facts." *Proc. 29th IAHR Congress*, Beijing, China, Theme D, Vol. 1, Tsinghua University Press, Beijing, G. LI Ed., pp. 490-498. (CD-ROM, *Tsinghua University Press*, ISBN 7-900637-10-9.)
CHANSON, H. (2002). "Air-Water Flow Measurements with Intrusive Phase-Detection Probes. Can we Improve their Interpretation ?." *Jl of Hyd. Engrg.*, ASCE, Vol. 128, No. 3, pp. 252-255.
CHANSON, H. (2004a). "The Hydraulics of Open Channel Flows : An Introduction." *Butterworth-Heinemann*, Oxford, UK, 2nd edition, 630 pages (ISBN 0 7506 5978 5).
CHANSON, H. (2004b). "Environmental Hydraulics of Open Channel Flows." *Elsevier Butterworth-Heinemann*, Oxford, UK, 483 pages (ISBN 0 7506 6165 8).
CHANSON, H. (2004c). "Drag Reduction in Skimming Flow on Stepped Spillways by Aeration." *Jl of Hyd. Research*, IAHR, Vol. 42, No. 3 , pp. 316-322 .
CHANSON, H. (2006a). "Air Bubble Entrainment in Hydraulic Jumps. Similitude and Scale Effects." *Report No. CH57/05*, Dept. of Civil Engineering, The University of Queensland, Brisbane, Australia, Jan., 119 pages (ISBN 1864998423).
CHANSON, H. (2006b). "Hydraulics of Skimming Flows on Stepped Chutes: the Effects of Inflow Conditions?" *Jl of Hyd. Res.*, IAHR, Vol. 44, No. 1, pp. 51-60.
CHANSON, H., AOKI, S., and HOQUE, A. (2002). "Similitude of Air Bubble Entrainment and Dispersion in Vertical Circular Plunging Jet Flows. An Experimental Study with Freshwater, Salty Freshwater and Seawater." *Coastal/Ocean Engineering Report*, No. COE02-1, Dept. of Architecture and Civil Eng., Toyohashi University of Technology, Japan, 94 pages.
CHANSON, H., AOKI, S., and HOQUE, A. (2006). "Bubble Entrainment and Dispersion in Plunging Jet Flows: Freshwater versus Seawater." *Jl of Coastal Research*, Vol. 22, No. 3, May, pp. 664-677.
CHANSON, H., and BRATTBERG, T. (1997). "Experimental Investigations of Air Bubble Entrainment in Developing Shear Layers." *Report CH48/97*, Dept. of Civil Engineering, University of Queensland, Australia, Oct., 309 pages (ISBN 0 86776 748 0).
CHANSON, H., and GONZALEZ, C.A. (2004). "Interactions between Free-surface, Free-stream Turbulence and Cavity Recirculation in Open Channel Flows: Measurements and Turbulence Manipulation." *Proc. 5th Intl Conf. on Multiphase Flow*, Yokohama, Japan, Y. MATSUMOTO, K. HISHIDA, A. TOMIYAMA, K. MISHIMA and S. HOSOKAWA editors, Paper 104, 14 pages (CD-ROM).
CHANSON, H., and GONZALEZ, C.A. (2005). "Physical Modelling and Scale Effects of Air-Water Flows on Stepped Spillways." *Journal of Zhejiang University SCIENCE*, Vol. 6A, No. 3, March, pp. 243-250.
CHANSON, H., and TOOMBES, L. (1997). "Flow Aeration at Stepped Cascades." *Research Report No. CE155*, Dept. of Civil Engineering, University of Queensland, Australia, June, 110 pages (ISBN 0 86776 730 8).
CHANSON, H., and TOOMBES, L. (2001). "Experimental Investigations of Air Entrainment in Transition and Skimming Flows down a Stepped Chute. Application to Embankment Overflow Stepped Spillways." *Research Report No. CE158*, Dept. of Civil Engineering, The University of Queensland, Brisbane, Australia, July, 74 pages (ISBN 1 864995297).
CHANSON, H., and TOOMBES, L. (2002a). "Air-Water Flows down Stepped chutes : Turbulence and Flow Structure Observations." *Intl Jl of Multiphase Flow*, Vol. 28, No. 11, pp. 1737-1761.
CHANSON, H., and TOOMBES, L. (2002b). "Energy Dissipation and Air Entrainment in a Stepped Storm Waterway: an Experimental Study." *Jl of Irrigation and Drainage Engrg.*, ASCE, Vol. 128, No. 5, pp. 305-315.

CHANSON, H., and TOOMBES, L. (2002c). "Experimental Study of Gas-Liquid Interfacial Properties in a Stepped Cascade Flow." *Environmental Fluid Mechanics*, Vol. 2, No. 3, pp. 241-263.
CHANSON, H., and TOOMBES, L. (2003). "Strong Interactions between Free-Surface Aeration and Turbulence in an Open Channel Flow." *Experimental Thermal and Fluid Science*, Vol. 27, No. 5, pp. 525-535.
CHANSON, H., and TOOMBES, L. (2004). "Hydraulics of Stepped Chutes: the Transition Flow." *Jl of Hyd. Res.*, IAHR, Vol. 42, No. 1, pp. 43-54.
CHANSON, H., YASUDA, Y., and OHTSU, I. (2002). "Flow Resistance in Skimming Flows and its Modelling." *Can Jl of Civ. Eng.*, Vol. 29, No. 6, pp. 809-819.
CROWE, C., SOMMERFIELD, M., and TSUJI, Y. (1998). "Multiphase Flows with Droplets and Particles." *CRC Press*, Boca Raton, USA, 471 pages.
CUMMINGS, P.D. (1996). "Aeration due to Breaking Waves." *Ph.D. thesis*, Dept. of Civil Engrg., University of Queensland, Australia.
EL-KAMASH, M.K., LOEWEN, M.R., and RAJARATNAM, N. (2005). "An Experimental Investigation of Jet Flow on a Stepped Chute." *Jl of Hyd. Res.*, IAHR, Vol. 43, No. 5, pp. 31-43.
FAVRE, A.J., GAVIGLIO, J.J., and DUMAS, R. (1957-58). "Further Space-Time Correlations of Velocity in a Turbulent Boundary Layer." *Jl of Fluid Mech.*, Vol. 3, pp. 344-356.
GONZALEZ, C.A. (2005). "An Experimental Study of Free-Surface Aeration on Embankment Stepped Chutes." *Ph.D. thesis*, Department of Civil Engineering, The University of Queensland, Brisbane, Australia, 240 pages.
GONZALEZ, C.A., and CHANSON, H. (2004). "Interactions between Cavity Flow and Main Stream Skimming Flows: an Experimental Study." *Can Jl of Civ. Eng.*, Vol. 31, No. 1, pp. 33-44.
GONZALEZ, C.A., and CHANSON, H. (2006). "Flow Characteristics of Skimming Flows in Stepped Channels. Discussion." *Jl of Hyd. Engrg.*, ASCE, Vol. 132, No. 5, pp. 537-539.
GONZALEZ, C.A., TAKAHASHI, M., and CHANSON, H. (2005). "Effects of Step Roughness in Skimming Flows: an Experimental Study." *Research Report No. CE160*, Dept. of Civil Engineering, The University of Queensland, Brisbane, Australia, July, 149 pages (ISBN 1864998105).
HAYES, M.H. (1996). "Statistical, Digital Signal Processing and Modeling." *John Wiley*, New York, USA.
HENDERSON, F.M. (1966). "Open Channel Flow." *MacMillan Company*, New York, USA.
HERRINGE, R.A., and DAVIS, M.R. (1974). "Detection of Instantaneous Phase Changes in Gas-Liquid Mixtures." *Jl. of Physics E: Scientific Instruments*, Vol. 7, pp. 807-812.
HONG, M., CARTELLIER, A., and HOPFINGER, E.J. (2004). "Characterization of Phase Detection Optical Probes for the Measurement of the Dispersed Phase Parameters in Sprays." *Intl Jl Multiphase Flow*, Vol. 30, pp. 615-648.
HOYT, J.W., and SELLIN, R.H.J. (1989). "Hydraulic Jump as 'Mixing Layer'." *Jl of Hyd. Engrg.*, ASCE, Vol. 115, No. 12, pp. 1607-1614.
HOYT, J.W., and TAYLOR, J.J. (1976). "Mechanism of Air Entrainment in a High Speed Water Jet." *Symp. IAHR/SHF*, March, Grenoble, France, pp. 329-335.
HOYT, J.W., and TAYLOR, J.J. (1977). "Turbulence Structure in a Water Jet Discharging in Air." *Physics of Fluids*, Vol. 20, No. 10, Pt. II, Oct., pp. S253-S257.
KADEM, N. (2005). "Atomisation du Jet d'un Canon d'Irrigation : Modèlisation Eulérienne et Validation." ('Atomisation of an Irrigation Water Jet: Eulerian Modelling and Validation.') *Ph.D. thesis*, CEMAGREF-LERMI & Unvi. Aix-Marseille II, Aix-en-Provence, France, 147 pages.
KAZEMIPOUR, A.K., and APELT, C.J. (1983). "Effects of Irregularity of Form on Energy Losses in Open Channel Flow." *Aust. Civil Engrg Trans.*, I.E.Aust., Vol. CE25, pp. 294-299.
KOBUS, H. (1984). "Local Air Entrainment and Detrainment." *Proc. Intl Symp. on Scale Effects in Modelling Hydraulic Structures*, IAHR, Esslingen, Germany.
KOKPINAR, M.A. (2005). "Flow over a Stepped Chute with and without Macro-Roughness Elements." Can. Jl of Civil Eng., Vol.. 31, No. 5, pp. 880-891.
LIN, J.C., and ROCKWELL, D. (2001). "Organized Oscillations of Initially Turbulent Flow past a Cavity." *AIAA Jl*, Vol. 39, No. 6, pp. 1139-1151.
MATOS, J. (2000). "Hydraulic Design of Stepped Spillways over RCC Dams." *Intl Workshop on Hydraulics of Stepped Spillways*, Zürich, Switzerland, H.E. MINOR & W.H. HAGER Editors, Balkema Publ., pp. 187-194.

MEIRELES, I., CABRITA, J., and MATOS, J. (2006). "Non-Aerated Skimming Flow Properties on Stepped Chutes over Small Embankment Dams." *Proc. Intl Junior Researcher and Engineer Workshop on Hydraulic Structures*, IAHR, Montemor-o-Novo, Portugal, 2-4 Sept. 2006.

MOUAZE, D., MURZYN, F., and CHAPLIN, J.R. (2005). "Free Surface Length Scale Estimation in Hydraulic Jumps." *Jl of Fluids Eng.*, Trans. ASME, Vol. 127, pp. 1191-1193.

MURAI, Y., OISHI, Y., TAKEDA, Y., and YAMAMOTO, F. (2006). "Turbulent Shear Stress Profiles in a Bubbly Channel Flow Assessed by Particle Tracing Velocimetry." *Experiments in Fluids*, Vol. 41, pp. 343-352.

MURILLO, R.E. (2006). "Experimental Study of the Development Flow Region on Stepped Chutes." *Ph.D. thesis*, Dept of Civil Eng., Univ. of Manitoba, Canada, 240 pages.

OHTSU, I., and YASUDA, Y. (1997). "Characteristics of Flow Conditions on Stepped Channels." *Proc. 27th IAHR Biennal Congress*, San Francisco, USA, Theme D, pp. 583-588.

OHTSU, I., YASUDA, Y., and TAKAHASHI, M. (2004). "Flow Characteristics of Skimming Flows in Stepped Channels." *Jl of Hyd. Engrg.*, ASCE, Vol. 130, No. 9, pp. 860-869. Discussion: Vol. 132, No. 5, pp. 527-542.

RAJARATNAM, N. (1976). "Turbulent Jets." *Elsevier Scientific*, Development in Water Science, 5, New York, USA.

RAJARATNAM, N. (1990). "Skimming Flow in Stepped Spillways." *Jl of Hyd. Engrg.*, ASCE, Vol. 116, No. 4, pp. 587-591. Discussion : Vol. 118, No. 1, pp. 111-114.

REIN, M. (1998). "Turbulent Open-Channel Flows : Drop-Generation and Self-Aeration." *Jl of Hyd. Engrg.*, ASCE, Vol. 124, No.1, pp. 98-102. Discussion : Vol. 125, No. 6, pp. 668-670.

RUFF, J.F., and FRIZELL, K.H. (1994). "Air Concentration Measurements in Highly-Turbulent Flow on a Steeply-Sloping Chute." *Proc. Hydraulic Engineering Conf.*, ASCE, Buffalo, USA, Vol. 2, pp. 999-1003.

SARPKAYA, T. (1996). "Vorticity, Free Surface and Surfactants." *Ann Rev. Fluid Mech.*, Vol. 28, pp. 83-128.

SCHLICHTING, H. (1979). "Boundary Layer Theory." *McGraw-Hill*, New York, USA, 7th edition.

SENE, K.J. (1984). "Aspects of Bubbly Two-Phase Flow." *Ph.D. thesis*, Trinity College, Cambridge, UK, Dec..

SHVAJNSHTEJN, A.M. (1999). "Stepped Spillways and Energy Dissipation." *Gidrotekhnicheskoe Stroitel'stvo*, No. 5, pp. 15-21 (in Russian). (Also Hydrotechnical Construction, Vol. 3, No. 5, 1999, pp. 275-282.)

TAKAHASHI, M., YASUDA, Y., and OHTSU, I (2005). "Effect of Reynolds Number on Characteristics of Skimming Flows in Stepped Channels." *Proc. 31th Biennial IAHR Congress*, Seoul, Korea, B.H. JUN, S.I. LEE, I.W. SEO and G.W. CHOI Editors, pp. 2880-2889.

TOOMBES, L. (2002). "Experimental Study of Air-Water Flow Properties on Low-Gradient Stepped Cascades." *Ph.D. thesis*, Dept of Civil Engineering, The University of Queensland.

WEGMANN, E. (1911). "The Design and Construction of Dams." *John Wiley & Sons*, New York, USA, 6th edition.

WOOD, I.R. (1991). "Air Entrainment in Free-Surface Flows." *IAHR Hydraulic Structures Design Manual No. 4*, Hydraulic Design Considerations, Balkema Publ., Rotterdam, The Netherlands, 149 pages.

WU, P.K., and FAETH, G.M. (1995). "Onset and End of Drop Formation along the Surface of Turbulent Liquid Jets in Still Gases." *Physics of Fluids*, Vol. 7, No. 11, pp. 2915-29-17.

WU, P.K., MIRANDA, R.F., and FAETH, G.M. (1995). "Effects of Initial Flow Conditions on Primary Breakup of Nonturbulent and Turbulent Round Liquid jets." *Atomization and Sprays*, Vol. 5, pp. 175-196.

YASUDA, Y., and CHANSON, H. (2003). "Micro- and Macro-scopic Study of Two-Phase Flow on a Stepped Chute." *Proc. 30th IAHR Biennial Congress*, Thessaloniki, Greece, J. GANOULIS and P. PRINOS Ed., Vol. D, pp. 695-702 .

YASUDA, Y., and OHTSU, I.O. (1999). "Flow Resistance of Skimming Flow in Stepped Channels." *Proc. 28th IAHR Congress*, Graz, Austria, Session B14, 6 pages.

INTERNET REFERENCES

| | |
|---|---|
| Photographs of stepped spillways | {http://www.uq.edu.au/~e2hchans/photo.html#Step_spillways} {http://www.iahrmedialibrary.net/} |
| Embankment overflow stepped spillways: earth dam spillways with precast concrete blocks | {http://www.uq.edu.au/~e2hchans/over_st.html} |
| Air entrainment on chute and stepped spillways | {http://www.uq.edu.au/~e2hchans/self_aer.html} |
| Gold Creek Dam and its Historical Stepped Spillway | {http://www.uq.edu.au/~e2hchans/gold_crk.html} |
| Timber crib weirs | {http://www.uq.edu.au/~e2hchans/tim_weir.html} |
| The Formal Water Garden | {http://www.uq.edu.au/~e2hchans/wat_gard.html} |

BIBLIOGRAPHIC REFERENCE OF THE REPORT CH59/06

The Hydraulic Model research report series CH is a refereed publication published by the Division of Civil Engineering at the University of Queensland, Brisbane, Australia.

The bibliographic reference of the present report is :

CAROSI, G., and CHANSON, H. (2006). "Air-Water Time and Length Scales in Skimming Flows on a Stepped Spillway. Application to the Spray Characterisation." *Report No. CH59/06*, Div. of Civil Engineering, The University of Queensland, Brisbane, Australia, July, 142 pages (ISBN 1864998601).

The Report CH59/06 is available, in the present form, as a PDF file on the Internet at EprintsUQ :

http://eprint.uq.edu.au/

It is listed in chronological order at :

http://eprint.uq.edu.au/view/person/Chanson,_Hubert.html

# HYDRAULIC MODEL RESEARCH REPORT CH

The Hydraulic Model Report CH series is published by the Division of Civil Engineering at the University of Queensland. Orders of any of the Hydraulic Model Reports should be addressed to the Departmental Secretary.

Departmental Secretary, Div. of Civil Engineering, The University of Queensland
Brisbane 4072, Australia - Tel.: (61 7) 3365 3619 - Fax : (61 7) 3365 4599
Url: http://www.eng.uq.edu.au/civil/ Email: hodciveng@uq.edu.au

| **Report CH** | **Unit price** | Quantity | **Total price** |
|---|---|---|---|
| CHANSON, H., TAKEUCHI, M, and TREVETHAN, M. (2006). "Using Turbidity and Acoustic Backscatter Intensity as Surrogate Measures of Suspended Sediment Concentration. Application to a Sub-Tropical Estuary (Eprapah Creek)." *Report No. CH60/06*, Div. of Civil Engineering, The University of Queensland, Brisbane, Australia, July (ISBN 1864998628). | AUD$60.00 | | |
| CAROSI, G., and CHANSON, H. (2006). "Air-Water Time and Length Scales in Skimming Flows on a Stepped Spillway. Application to the Spray Characterisation." *Report No. CH59/06*, Div. of Civil Engineering, The University of Queensland, Brisbane, Australia, July (ISBN 1864998601). | AUD$60.00 | | |
| TREVETHAN, M., CHANSON, H., and BROWN, R. (2006). "Two Series of Detailed Turbulence Measurements in a Small Sub-Tropical Estuarine System." *Report No. CH58/06*, Div. of Civil Engineering, The University of Queensland, Brisbane, Australia, Mar. (ISBN 1864998520). | AUD$60.00 | | |
| KOCH, C., and CHANSON, H. (2005). "An Experimental Study of Tidal Bores and Positive Surges: Hydrodynamics and Turbulence of the Bore Front." *Report No. CH56/05*, Dept. of Civil Engineering, The University of Queensland, Brisbane, Australia, July (ISBN 1864998245). | AUD$60.00 | | |
| CHANSON, H. (2005). "Applications of the Saint-Venant Equations and Method of Characteristics to the Dam Break Wave Problem." *Report No. CH55/05*, Dept. of Civil Engineering, The University of Queensland, Brisbane, Australia, May (ISBN 1864997966). | AUD$60.00 | | |
| CHANSON, H., COUSSOT, P., JARNY, S., and TOQUER, L. (2004). "A Study of Dam Break Wave of Thixotropic Fluid: Bentonite Surges down an Inclined plane." *Report No. CH54/04*, Dept. of Civil Engineering, The University of Queensland, Brisbane, Australia, June, 90 pages (ISBN 1864997710). | AUD$60.00 | | |
| CHANSON, H. (2003). "A Hydraulic, Environmental and Ecological Assessment of a Sub-tropical Stream in Eastern Australia: Eprapah Creek, Victoria Point QLD on 4 April 2003." *Report No. CH52/03*, Dept. of Civil Engineering, The University of Queensland, Brisbane, Australia, June, 189 pages (ISBN 1864997044). | AUD$90.00 | | |
| CHANSON, H. (2003). "Sudden Flood Release down a Stepped Cascade. Unsteady Air-Water Flow Measurements. Applications to Wave Run-up, Flash Flood and Dam Break Wave." *Report CH51/03*, Dept of Civil Eng., Univ. of Queensland, Brisbane, Australia, 142 pages (ISBN 1864996552). | AUD$60.00 | | |
| CHANSON, H,. (2002). "An Experimental Study of Roman Dropshaft Operation : Hydraulics, Two-Phase Flow, Acoustics." *Report CH50/02*, Dept of Civil Eng., Univ. of Queensland, Brisbane, Australia, 99 pages (ISBN 1864996544). | AUD$60.00 | | |
| CHANSON, H., and BRATTBERG, T. (1997). "Experimental Investigations of Air Bubble Entrainment in Developing Shear Layers." *Report CH48/97*, Dept. of Civil Engineering, University of Queensland, Australia, Oct., 309 pages (ISBN 0 86776 748 0). | AUD$90.00 | | |

| | | | |
|---|---|---|---|
| CHANSON, H. (1996). "Some Hydraulic Aspects during Overflow above Inflatable Flexible Membrane Dam." *Report CH47/96*, Dept. of Civil Engineering, University of Queensland, Australia, May, 60 pages (ISBN 0 86776 644 1). | AUD$60.00 | | |
| CHANSON, H. (1995). "Flow Characteristics of Undular Hydraulic Jumps. Comparison with Near-Critical Flows." *Report CH45/95*, Dept. of Civil Engineering, University of Queensland, Australia, June, 202 pages (ISBN 0 86776 612 3). | AUD$60.00 | | |
| CHANSON, H. (1995). "Air Bubble Entrainment in Free-surface Turbulent Flows. Experimental Investigations." *Report CH46/95*, Dept. of Civil Engineering, University of Queensland, Australia, June, 368 pages (ISBN 0 86776 611 5). | AUD$80.00 | | |
| CHANSON, H. (1994). "Hydraulic Design of Stepped Channels and Spillways." *Report CH43/94*, Dept. of Civil Engineering, University of Queensland, Australia, Feb., 169 pages (ISBN 0 86776 560 7). | AUD$60.00 | | |
| POSTAGE & HANDLING (per report) | AUD$10.00 | | |
| GRAND TOTAL | | | |

## OTHER HYDRAULIC RESEARCH REPORTS

| Reports/Theses | Unit price | Quantity | Total price |
|---|---|---|---|
| GONZALEZ, C.A. (2005). "An Experimental Study of Free-Surface Aeration on Embankment Stepped Chutes." *Ph.D. thesis*, Dept of Civil Engineering, The University of Queensland, Brisbane, Australia, 240 pages. | AUD$80.00 | | |
| TOOMBES, L. (2002). "Experimental Study of Air-Water Flow Properties on Low-Gradient Stepped Cascades." *Ph.D. thesis*, Dept of Civil Engineering, The University of Queensland, Brisbane, Australia. | AUD$120.00 | | |
| CHANSON, H. (1988). "A Study of Air Entrainment and Aeration Devices on a Spillway Model." *Ph.D. thesis*, University of Canterbury, New Zealand. | AUD$60.00 | | |
| POSTAGE & HANDLING (per report) | AUD$10.00 | | |
| GRAND TOTAL | | | |

## CIVIL ENGINEERING RESEARCH REPORT CE

The Civil Engineering Research Report CE series is published by the Division of Civil Engineering at the University of Queensland. Orders of any of the Civil Engineering Research Report CE should be addressed to the Departmental Secretary.

Departmental Secretary, Dept. of Civil Engineering, The University of Queensland
Brisbane 4072, Australia
Tel.: (61 7) 3365 3619 Fax : (61 7) 3365 4599
Url: http://www.eng.uq.edu.au/civil/ Email: hodciveng@uq.edu.au

| Recent Research Report CE | Unit price | Quantity | Total price |
|---|---|---|---|
| GONZALEZ, C.A., TAKAHASHI, M., and CHANSON, H. (2005). "Effects of Step Roughness in Skimming Flows: an Experimental Study." *Research Report No. CE160*, Dept. of Civil Engineering, The University of Queensland, Brisbane, Australia, July (ISBN 1864998105). | AUD$10.00 | | |

| | | | |
|---|---|---|---|
| CHANSON, H., and TOOMBES, L. (2001). "Experimental Investigations of Air Entrainment in Transition and Skimming Flows down a Stepped Chute. Application to Embankment Overflow Stepped Spillways." *Research Report No. CE158*, Dept. of Civil Engineering, The University of Queensland, Brisbane, Australia, July, 74 pages (ISBN 1 864995297). | AUD$10.00 | | |
| HANDLING (per order) | AUD$10.00 | | |
| GRAND TOTAL | | | |

Note: Prices include postages and processing.

**PAYMENT INFORMATION**

1- VISA Card

| | |
|---|---|
| Name on the card : | |
| Visa card number : | |
| Expiry date : | |
| Amount : | AUD$ ..... |

2- Cheque/remittance payable to : THE UNIVERSITY OF QUEENSLAND and crossed "Not Negotiable".

N.B. For overseas buyers, cheque payable in Australian Dollars drawn on an office in Australia of a bank operating in Australia, payable to: THE UNIVERSITY OF QUEENSLAND and crossed "Not Negotiable".

Orders of any Research Report should be addressed to the Departmental Secretary.

Departmental Secretary, Div. of Civil Engineering, The University of Queensland
Brisbane 4072, Australia - Tel.: (61 7) 3365 3619 - Fax : (61 7) 3365 4599
Url: http://www.eng.uq.edu.au/civil/ Email: hodciveng@uq.edu.au